Lepton flavor violation in the Littlest Higgs model with T-parity realizing an inverse seesaw

PhD Thesis

Author: Iván Pacheco Zamudio
Advisor: Dr. Pablo Roig Garcés

Department of Physics
Centro de Investigación y Estudios Avanzados del Instituto Politécnico Nacional

September 16, 2022

Agradecimientos

Agradecimientos a todos aquellos que estuvieron presente en este largo camino.

Introducción

El Modelo Estándar de física de partículas elementales es una de las teorías más exitosas creadas por el hombre, ésta logra explicar -en su mayoría- los fenómenos, procesos, interacciones que ocurren a nivel fundamental entre partículas y ha sido comprobado con gran precisión experimentalmente. Por ello existe un gran interés en hacer extensiones del modelo para encontrar una explicación a aquellos problemas que no pueden ser resueltos de forma satisfactoria con dicha teoría.

Una prueba importante del Modelo Estándar fue el hallazgo en 2012 por el LHC, de una partícula propuesta por Peter Higgs en 1964 mediante el llamado *Mecanismo de Higgs*, dicha partícula es nombrada en su honor Bosón de Higgs.

El Mecanismo de Higgs está estrechamente relacionado con el rompimiento de simetría electrodébil el cual se produce a una escala de energía $v = 246$ GeV, y se estima que la escala de energía de nueva física sea del orden de $\sim \mathcal{O}$ (TeV).

Se han propuesto diferentes modelos para tratar de explicar esta diferencia entre las escalas de energía, llamado *problema de jerarquía*, y estabilizar las contribuciones que existen de diagramas cuadráticamente divergentes a la masa del Higgs.

Little Higgs, es uno de los modelos desarrollados para abordar el problema descrito anteriormente. Modelos de tipo Little Higgs tienen como su principal característica común la propuesta de que el Higgs es un pseudo-bosón de Nambu-Goldstone originado -en este caso- por el rompimiento del grupo de simetría $SU(5)$ a una escala de energía $f \sim \mathcal{O}(\text{TeV})$. Dicha idea fue retomada por Arkani-Hamed, Cohen y Georgi quienes construyeron el primer modelo Little Higgs exitoso [1]. A partir de esto, se le han hecho varias extensiones al modelo Little Higgs y en esta tesis abordaremos una de ellas: *Modelo Littlest Higgs con T-paridad*.

Este modelo, abreviado LHT, tiene varias implicaciones fenomenológicas, por lo que nos propusimos estudiar las nuevas cotas a procesos de violación de sabor leptónico (LFV) por medio de interacciones de partículas propuestas que aparecen a una escala de energía de TeV's, además de introducir un mecanismo específico de los llamados See Saw para involucrar neutrinos de Majorana que no sólo aportarán a los procesos de LFV sino también a procesos de LNV. De esta manera, además, el problema de jerarquía se relaciona con la masa ínfima de los neutrinos y, posiblemente, con la explicación de la asimetría bariónica del Universo mediante leptogénesis.

La estructura de la tesis se describe a continuación: en el Capítulo 1, nombrado *Standard Model*, se explican los requisitos necesarios que debe cumplir la Lagrangiana del modelo estándar electrodébil tales como simetría de fase global y local. Sabemos que la Electrodinámica Cuántica es una teoría Abeliana, lo que implica que su mediador, el fotón, no interactúa consigo mismo, pero a diferencia de esto, en la teoría Electrodébil sus bosones de gauge, $W^{\pm}$ y Z^0, sí pueden interactuar entre ellos, lo que nos lleva a trabajar con una teoría no Abeliana. Por tanto es necesario conocer los campos de Yang-Mills, contenido del subcapítulo 1.1.3. En la segunda parte del Capítulo 1 se detalla el Modelo Glashow-Weinberg-Salam, introduciendo el Mecanismo de Higgs, y revisando cómo éste origina las

masas de los bosones de gauge y los fermiones. Para finalizar con este capítulo se muestra la forma de la Lagrangiana final del modelo, comentando brevemente cada una de sus partes constituyentes.

Como se mencionó anteriormente, las implicaciones del LHT aquí estudiadas son -fundamentalmente- de procesos de violación de sabor leptónico, por lo que se incluye un breve Capítulo 2 dedicado a LFV.

En el Capítulo 3 se desarrolla detalladamente el Modelo de Littlest Higgs con T-paridad. Aquí se explica cómo es el rompimiento de simetria $SU(5)/SO(5)$ y la parametrización de la matriz de Goldstones. Se introduce la T-paridad, que es una simetría Z_2, y la acción que tiene en los campos y Lagrangianas para hacer el modelo consistente. Se muestra como el grupo de gauge $[SU(2) \times U(1)]^2$, que se encuentra dentro del grupo $SU(5)$, se "romperá" al grupo del Modelo Estándar $SU(2)_L \times U(1)_Y$, dando así lugar a la aparición de nuevas partículas en un sector pesado: $W_H^{\pm}$, Z_H y A_H. Tras considerar efectos de EWSB, se recuperan los bosones de gauge conocidos: $W^{\pm}$, Z^0 y A. Se incluye el sector de fermiones, introduciendo los multipletes de $SU(5)$ que nos originan el sector pesado de fermiones junto con los fermiones del Modelo Estándar, y además se incluye el multiplete correspondiente a fermiones "espejo", los cuales son de vital importancia para el modelo.

En el Capítulo 4 se muestran las nuevas contribuciones a la amplitud por parte de los leptones T-odd (espejo) y partner provenientes de LHT para el proceso $\mu \to ee\bar{e}$ a nivel de diagramas de pingüino y caja. Una vez calculadas las amplitudes, en los Capítulos 5 y 6 se desarrolla minuciosamente el cálculo para los factores de forma de los diagramas de pingüino de γ y bosón Z y los factores de forma correspondientes a los diagramas de caja. LHT nos permite introducir un mecanismo para generar masas de neutrinos de tipo de Majorana. En el Capítulo 7 se introduce detalladamente el mecanismo de See Saw Inverso (ISS) para cumplir el objetivo de tener neutrinos de Majorana, así como las repercusiones en los procesos de LFV y LNV a través del cálculo de los factores de forma en los diagramas de pingüino y caja, ya que aparecen diagramas donde el número leptónico se viola por dos unidades. Veremos que al considerar neutrinos pesados de Majorana aparecerán nuevos acoplamientos como lo son los neutros de tipo $(\theta S \theta^{\dagger})_{\ell\ell'}$, los cuales tendrán un papel importante en el análisis numérico de estos procesos. Para el Capítulo 8 reservamos el análisis fenomenológico de los procesos descritos en el capítulo anterior, mostrando los valores representativos del modelo.

El decaimiento doble beta sin neutrinos es una de las pruebas más fuertes para la comprobación de la existencia de neutrinos de Majorana, por lo que en esta tesis también enfocamos parte de nuestro esfuerzo en calcular las predicciones de nuestro modelo a dicho proceso, esto puede ser encontrado en el Capítulo 9.

Finalmente, en el Capítulo 10, llevando nuestro modelo más allá para conseguir puebas más sólidas de autoconsistencia, se trabajó con decaimientos hadrónicos de tau (τ) donde se han calculado, por primera vez en el LHT, cotas para los branching ratios de $\tau \to \ell P, PP, V$ $(\ell = e, \mu)$, así como las masas esperadas de los fermiones T-odd, partner y neutrinos de Majorana, ángulos de mezcla para efectos de LFV y acoplamientos neutros $(\theta S \theta^{\dagger})_{\ell\ell'}$ lo cual nos permite validar la coincidencia con los resultados obtenidos en el Capítulo 8.

En el Capítulo 11 se escriben las conclusiones del trabajo de tesis. Se finaliza con nueve apéndices

donde se incluyen todas las herramientas usadas para el desarrollo de cálculos necesarios en la tesis.

Abstract

The Standard Model of particle physics is one of the most successful theories created by humans, it manages to explain basically all the phenomena, processes and interactions that occur at a fundamental level between particles and has been minutely verified by data experimentally obtained. Therefore, there is a great interest in making extensions of the model to find an explanation for those problems that cannot be solved satisfactorily with this theory.

An important test of SM was the discovery in 2012 by the LHC of a particle proposed by Peter Higgs in 1964 through the so-called *Higgs Mechanism*, that particle is named in his honor: Higgs Boson.

The Higgs Mechanism is closely related with the electroweak symmetry breaking (EWSB) which is produced at an energy scale $v = 246$ GeV, and it is estimated that the energy scale of new physics is of order $\sim \mathcal{O}(\text{TeV})$.

Several models have been proposed to attempt to explain this difference between the energy scales, called *hierarchy problem*, and to stabilize the contributions that exist from quadratically divergent diagrams correcting the Higgs mass.

Little Higgs is one class of models developed to address the problem described above. Little Higgs Models have as their main common feature the proposal that the Higgs is a pseudo-Nambu-Goldstone boson. In this particular case caused by the breaking of $SU(5)$ symmetry group at an energy scale $f \sim \mathcal{O}(\text{TeV})$. This idea was taken up by Arkani-Hamed, Cohen and Georgi who built the first successful Little Higgs model [1]. From this, several extensions have been made to the Little Higgs model and in this thesis we will address one of them: Littlest Higgs Model with T-parity.

This model, abbreviated LHT, has several scopes and one of which we set to study here, is that this model gives new contributions to lepton flavor violation (LFV) processes through interactions of particles that appear at energy scale of TeV's. In addition, a specific mechanism of the so-called See Saw is introduced to involve Majorana neutrinos that will contribute to LFV processes but also to LNV processes. In this way, the hierarchy problem is linked to understanding the tiny neutrino masses and, possibly, to generating the baryon asymmetry of the universe via leptogenesis.

The structure of the thesis is described below: in Chapter 1, named Standard Model, we explain the necessary requirements that the Lagrangian of the electroweak standard model must satisfy, such as global and local phase symmetry. We know that Quantum Electrodynamics is an Abelian theory, which implies that the mediator, the photon, does not self-interact, contrary to the Electroweak theory, whose gauge bosons, $W^{\pm}$ and Z^0, can interact with each other (and among themselves, in certain combinations), which leads us to work with a non-Abelian theory, so it is necessary to know Yang-Mills fields, content of subsection 1.1.3. For the second part of Chapter 1, the Glashow-Weinberg-Salam Model is detailed by introducing the Higgs Mechanism and how it gives rise to the masses of gauge bosons and fermions. We show the shape of the final Lagrangian of this model, commenting briefly each of its constituent parts.

As we mentioned previously, the scope of LHT reaches lepton flavor violation processes, so a brief Chapter 2 dedicated to LFV is included.

In Chapter 3 the Littlest Higgs Model with T-parity is developed in detail. We explain how is the symmetry breaking of $SU(5)/SO(5)$ and the parameterization of the Goldstones matrix. The T-parity is introduced, which is a Z_2 symmetry, and the action it has in the Lagrangian and fields to make the model consistent is displayed. We show how the gauge group $[SU(2)\times U(1)]^2$, that is within the $SU(5)$ group, will "break" to the Standard Model $SU(2)_L \times U(1)_Y$ group, and give rise to the appearance of new particles in a heavy sector: $W_H^{\pm}$, Z_H and A_H and how, after considering EWSB effects, we also recover the known gauge bosons: $W^{\pm}$, Z^0 and A. The fermion sector is also included, introducing the $SU(5)$ multiplets that will originate the heavy fermions sector as well as the Standard Model fermions, and also the multiplet corresponding to mirror fermions, that are vitally important for the model.

In Chapter 4 the new contributions to the amplitude by the T-odd (mirror) and partner leptons from LHT for the process $\mu \to ee\bar{e}$ are shown at the level of diagrams of penguin and box types. Once the amplitudes have been calculated, in Chapters 5 and 6 the calculation for the form factors of the penguin diagrams of γ and Z boson and form factors corresponding to the box diagrams are covered. LHT allows us to introduce a mechanism to generate neutrino masses of Majorana nature. In Chapter 7 the Inverse See Saw (ISS) mechanism is introduced in detail to meet the objective of having Majorana neutrinos as well as repercussions on the LFV and LNV processes through the calculation of the form factors from the penguin and box diagrams, since there are diagrams where the lepton number is violated by two units. We will see that when considering heavy Majorana neutrinos, new couplings will appear, such as the neutral couplings of type $(\theta S\theta^{\dagger})_{\ell\ell'}$, which will have an important role in the numerical analysis of these processes. For the Chapter 8 we reserve the phenomenological analysis of the processes described in the previous chapter showing representative values of the model.

Neutrinoless double beta decay is one of the strongest pieces of evidence for the possible existence of Majorana neutrinos, so in this thesis we also focus part of our effort on calculating the predictions of our model to this process, this can be found in Chapter 9.

Finally, in Chapter 10, taking our model further to get more solid evidence that everything is on the right track, we worked out -for the first time within the LHT- hadronic decays of tau (τ) where new bounds have been calculated for the branching ratios for $\tau \to \ell P, PP, V$ ($\ell = e, \mu$), as well as the expected masses of the T-odd fermions, partner and Majorana neutrinos, mixing angles for LFV effects and neutral couplings $(\theta S\theta^{\dagger})_{\ell\ell'}$, which altogether enables us to validate the coincidence with the results obtained in Chapter 8.

In Chapter 11 the conclusions of this thesis are written. Nine appendices are included, where all the tools used for the development of calculations are detailed.

Contents

List of Figures

List of Tables

1 Standard Model

Particle physics is the branch of physics which studies elementary particles and their properties. We can say that the elementary particles are the fundamental constituents of all objects in the universe. We mean by *elementary particles*: these are particles which do not have any substructure.

It's not easy to tell which particles are elementary. It's possible to say which particles are not elementary, if one knows of some experiment that shows substructure of the object. But no experiment can guarantee that a given object does not have any substructure. A new experiment might show substructure in an object that was earlier considered elementary. For instance, protons and neutrons came to be collectively called *nucleons* because they are the constituents of nuclei, and treated as elementary particles. A few decades later, new experiments indicated that the nucleons themselves have substructure. We now believe that they are made up of *quarks*, which are elementary particles like the electrons [2]. Thus the list of elementary particles changes with time. There is no guarantee that today's elementary particles would not turn out to be composite objects tomorrow.

The electron, the proton and the neutron are all examples of *fermions*, which have an intrinsic angular momentum, or *spin*, that is a half-integral multiple of the fundamental constant $\hbar$. In particular, all three of these have spin equal to $\frac{1}{2}\hbar$. The other alternative is to have spin in integral multiples of $\hbar$, and particles carrying such spin are called *bosons*.

The Standard Model (SM) constitutes one of the most successful achievements in modern physics. It provides a very elegant theoretical framework, which is able to describe the known experimental facts in particle physics with high precision [3].

According to this model, all matter is built from fermions: six *quarks* and six *leptons*. The leptons carry integral electric charge. The electron e with unit negative charge is familiar to everyone, and the other charged leptons are the *muon* μ and the *tau* τ, these are heavy versions of the electron. In modern terminology, we call the muon a particle of the second *generation*, and the tau belongs to the third generation.

In 1930, in order to explain the continuous spectrum of the electrons in nuclear beta decay, Pauli proposed that a neutral fermion was produced in such processes. Neutral fermions are collectively called *neutrinos*. A different flavour of charged lepton is paired with each flavour of neutrino, as indicated by the subscript: these are called the *electron-neutrino*(ν_e), *muon-neutrino*(ν_μ), and *tau-neutrino*(ν_τ). Summarizing, these neutrinos, along with the electron, the muon and the tau, form a class of elementary particles which are called *leptons*. There is another class of elementary particles which are called *quarks*. Unlike the leptons, no one has seen quarks in their free state. Quarks always appear in bound states. Bound states involving quarks are called *hadrons*. The quarks carry fractional charges, of $\frac{2}{3}e$ or $-\frac{1}{3}e$. For each of the various fundamental constituents, its symbol and the ratio of its electric charge $\mathcal{Q}$ to the elementary charge e of the electron are given in Table 1 [4].

Particle	Flavour			$\mathcal{Q}$
leptons	e	μ	τ	-1
	ν_e	ν_μ	ν_τ	0
quarks	u	c	t	$\frac{2}{3}$
	d	s	b	$-\frac{1}{3}$

Table 1: The fundamental fermions.

We have looked at the particles but the SM also comprises -extremely importantly- their interactions. The different interactions are described in quantum language in terms of the exchange of characteristic *bosons* (particles of integral spin) between the fermions constituents. These boson mediators are listed in Table 2.

Interaction	Mediator	Symbol	Number	Spin ($\hbar$)/Parity
Strong	Gluon	g	8	1^-
Electromagnetic	Photon	γ	1	1^-
Weak	W and Z bosons	$W^\pm, Z^0$	3	$1^-, 1^+$
Gravity	Graviton	G	1	2^+

Table 2: The boson mediators.

There are four kinds of fundamental interactions. The oldest known one is the gravitational interaction, known since the time of Newton in the 17th century. It is supposedly mediated by exchange of a spin 2 boson called *graviton*. Electricity and magnetism were unified into the electromagnetic theory, ans this is the second kind of interaction that we recognize to be fundamental and this interaction is mediated by *photon* exchange. The third one is the strong interaction, required to explain the stability of the atomic nuclei. The interquark force is mediated by a massless particle, the *gluon*. The last one is the weak interaction, needed to explain the phenomenon of beta radioactivity. The mediators of this interaction are the $W^\pm$ and Z^0 bosons, with masses of order 100 times the proton mass.

To indicate the relative magnitudes of the four types of interaction, the comparative strengths of the force between two protons when just in contact are very roughly as follows [4].

Strong	Electromagnetic	Weak	Gravity
1	10^{-2}	10^{-7}	10^{-39}

Table 3: Comparative strengths of the force between two protons.

In addition, the standard theory of electroweak interactions postulates that there is a spinless boson. It is called the *Higgs boson*. The discovery of the Higgs boson, announced on July 4th of 2012 by the CERN LHC collaborations ATLAS and CMS, marked the completion of the SM. This event can

be considered one of the greatest accomplishments of the High Energy Physics community. The Higgs mass value agrees quite well with the range preferred by the electroweak precision tests (EWPT), which confirms the success of the SM. Current measurements of its spin, parity, and couplings, also seem consistent with the SM. The fact that LHC has verified the linear realization of spontaneous symmetry breaking (SSB), as included in the SM, could also be taken as an indication that Nature likes scalars. [5].

The Standard Model was proposed in 1967, and the discovery of the Higgs boson was announced in 2012, i.e., a long 45 years later. It remained elusive for almost half a century. A big reason for the elusiveness of the Higgs boson is its coupling to fermions. The coupling of the Higgs boson to any fermion is proportional to the mass of the fermion, given by

$$h_f = \frac{\sqrt{2}m_f}{\upsilon} = \frac{gm_f}{\sqrt{2}M_W}, \tag{1}$$

with a vev $\upsilon = 246$ GeV. Our experimental detectors are made out particles in the first generation of fermions because they are constituents of stable material. The masses of the first generation fermions are much smaller compared to the masses of fermions in the other generations. For the electron, eq. (1) tell us that the coupling is of order 10^{-7}. With the up and the down quarks, the couplings are a little bigger, maybe an order to magnitude. This is the basic reason why the Higgs boson is hard to produce and to detect.

The mass of the Higgs boson is $M_H = 125.10 \pm 0.14$ GeV [6].

1.1 Gauge Invariance

1.1.1 Global phase symmetry

Consider the free Dirac Lagrangian

$$\mathcal{L}_0 = i\bar{\psi}\gamma^\mu\partial_\mu\psi - m\bar{\psi}\psi. \tag{2}$$

This Lagrangian is invariant under a change of phase of the field ψ. Suppose we change over to a new field

$$\psi'(x) = exp(-ieQ\theta)\psi(x), \tag{3}$$

where e, Q and θ are all real numbers, with different interpretations. The quantity e stands for a universal constant which sets up the scale of the phase, Q is a characteristic of the field ψ (quantum number) and θ is a variable which determines how large the phase is. Note that we have not changed the spacetime coordinates at all; the new field is defined in terms of the old field at the same spacetime point. Such symmetries are called *internal symmetries*.

Given the transformation from eq.(3), we show that

$$i\bar{\psi}'\gamma^\mu\partial_\mu\psi' - m\bar{\psi}'\psi' = i\bar{\psi}\gamma^\mu\partial_\mu\psi - m\bar{\psi}\psi. \tag{4}$$

Thus, the Lagrangian from eq.(2) is invariant under the transformation given from eq.(3). We can see that θ is independent of the spacetime coordinates, such that this transformation is called a *global symmetry*.

1.1.2 Local symmetry

Now we want to see what happens if the parameter depends on spacetime coordinates, $\theta = \theta(x)$. The derivative of $\psi'(x)$ is

$$\partial_\mu\psi'(x) = exp(-ieQ\theta)\left[\partial_\mu\psi(x) - ieQ(\partial_\mu\theta)\psi(x)\right]. \tag{5}$$

There is an extra term, involving the derivatives of θ. The Lagrangian from eq.(2) is not invariant under this local transformation. We obtain then

$$\mathcal{L}_0' - \mathcal{L}_0 = eQ(\partial_\mu\theta)\bar{\psi}(x)\gamma^\mu\psi(x). \tag{6}$$

Since we want the local symmetry, we would need to modify the original Lagrangian. So, instead of the Lagrangian from eq.(2), let us try

$$\mathcal{L} = i\bar{\psi}\gamma^\mu D_\mu\psi - m\bar{\psi}\psi, \tag{7}$$

where

$$D_\mu = \partial_\mu + ieQA_\mu, \tag{8}$$

bringing in a new A_μ. This D_μ is usually called the *covariant derivative*. The prescription of replacing ordinary derivatives by covariant derivatives is called *minimal substitution* [2].

The new Lagrangian must be invariant under the local symmetry, thus, under the local symmetry, A_μ changes to A'_μ such that

$$\mathcal{L}_0' - eQ\bar{\psi}'\gamma^\mu\psi' A'_\mu = \mathcal{L}_0 - eQ\bar{\psi}\gamma^\mu\psi A_\mu, \tag{9}$$

or

$$A'_\mu = A_\mu + \partial_\mu\theta. \tag{10}$$

We can thus identify A_μ with the photon field and conclude that, in the urge for making the global phase symmetry local, we have introduced the photon field in a natural form. If we are to regard this

new field as the physical photon field, we must add to the Lagrangian a term corresponding to its kinetic energy. Since the kinetic term must be invariant under eq.(10), it can only involve the gauge invariant field strength tensor

$$F_{\mu\nu} = \partial_\mu A_\nu - \partial_\nu A_\mu. \tag{11}$$

We are thus led to the Lagrangian of QED [7]

$$\mathcal{L} = \bar{\psi}(i\gamma^\mu \partial_\mu - m)\psi + e\bar{\psi}\gamma^\mu A_\mu \psi - \frac{1}{4}F_{\mu\nu}F^{\mu\nu}. \tag{12}$$

Note that the addition of a mass term $\frac{1}{2}m^2 A_\mu A^\mu$ is prohibited by gauge invariance. The gauge particle, the photon, must be massless, in agreement with experiment.

Local symmetries are also called *gauge symmetries*. Theories incorporating gauge symmetries are called *gauge theories*. The spin-1 particles which are necessary to keep the gauge invariance are called *gauge bosons*. QED is therefore a gauge theory, based on the gauge group $U(1)$. The gauge boson for QED is the photon.

1.1.3 Non-Abelian gauge symmetry: Yang-Mills fields

In 1954 Yang and Mills extended the gauge principle to non-Abelian symmetry. We are going to illustrate the construction for the simplest case of isospin $SU(2)$ [8].

Let the fermion field be an isospin doublet,

$$\psi = \begin{pmatrix} \psi_1 \\ \psi_2 \end{pmatrix}. \tag{13}$$

Under an $SU(2)$ transformation, we have

$$\psi(x) \to \psi'(x) = exp\left(\frac{-i\vec{\tau}\cdot\vec{\theta}}{2}\right)\psi(x), \tag{14}$$

where $\vec{\tau} = (\tau_1, \tau_2, \tau_3)$ are the Pauli matrices, satisfying

$$\left[\frac{\tau_i}{2}, \frac{\tau_j}{2}\right] = i\epsilon_{ijk}\frac{\tau_k}{2} \qquad i,j,k = 1,2,3, \tag{15}$$

and $\vec{\theta} = (\theta_1, \theta_2, \theta_3)$ are the $SU(2)$ transformation parameters. The free Lagrangian

$$\mathcal{L}_0 = \bar{\psi}(x)(i\gamma^\mu \partial_\mu - m)\psi(x), \tag{16}$$

is invariant under the global $SU(2)$ symmetry with $\{\theta_i\}_{i=1,2,3}$ being spacetime independent. However

under the local symmetry transformation

$$\psi(x) \to \psi'(x) = U(\theta)\psi(x), \tag{17}$$

with

$$U(\theta) = exp\left(\frac{-i\vec{\tau}\cdot\vec{\theta}(x)}{2}\right), \tag{18}$$

the free Lagrangian $\mathcal{L}_0$ is no longer invariant because the derivative term transforms as

$$\begin{aligned}\bar{\psi}(x)\partial_\mu\psi(x) \to \bar{\psi}'(x)\partial_\mu\psi'(x) =& \bar{\psi}(x)\partial_\mu\psi(x) \\ &+ \bar{\psi}(x)U^{-1}(\theta)\left[\partial_\mu U(\theta)\right]\psi(x).\end{aligned} \tag{19}$$

To construct a gauge invariant Lagrangian we follow a procedure similar to that of the Abelian case. We introduce the vector gauge field A^i_μ $(i = 1, 2, 3)$ (one for each group generator) to form the gauge covariant derivative through the minimal coupling

$$D_\mu\psi = \left(\partial_\mu - ig\frac{\vec{\tau}\cdot\vec{A}_\mu}{2}\right)\psi, \tag{20}$$

where g is the coupling constant. We want that $D_\mu\psi$ have the same transformation property as ψ itself

$$D_\mu\psi \to (D_\mu\psi)' = U(\theta)D_\mu\psi. \tag{21}$$

This implies that

$$\begin{aligned}&\left(\partial_\mu - ig\frac{\vec{\tau}\cdot\vec{A}'_\mu}{2}\right)(U(\theta)\psi) = U(\theta)\left(\partial_\mu - ig\frac{\vec{\tau}\cdot\vec{A}_\mu}{2}\right)\psi, \\ &\frac{\vec{\tau}\cdot\vec{A}'_\mu}{2} = U(\theta)\frac{\vec{\tau}\cdot\vec{A}_\mu}{2}U^{-1}(x) - \frac{i}{g}\left[\partial_\mu U(\theta)\right]U^{-1}(\theta),\end{aligned} \tag{22}$$

which defines the transformation law for the gauge fields. For an infinitesimal change $\vec{\theta}(x) \ll 1$,

$$\begin{aligned}\frac{\vec{\tau}\cdot\vec{A}'_\mu}{2} &= \frac{\vec{\tau}\cdot\vec{A}_\mu}{2} - i\theta^j A^k_\mu\left[\frac{\tau_j}{2}, \frac{\tau_k}{2}\right] - \frac{1}{g}\left(\frac{\vec{\tau}}{2}\cdot\partial_\mu\vec{\theta}\right) \\ &= \frac{\vec{\tau}\cdot\vec{A}_\mu}{2} + \frac{1}{2}\epsilon^{ijk}\tau^i\theta^j A^k_\mu - \frac{1}{g}\left(\frac{\vec{\tau}}{2}\cdot\partial_\mu\vec{\theta}\right),\end{aligned}$$

or

$$A^{i\prime}_\mu = A^i_\mu + \epsilon^{ijk}\theta^j A^k_\mu - \frac{1}{g}\partial_\mu\theta^i. \tag{23}$$

The second term is the transformation for a triplet representation under $SU(2)$. Thus the A^i_μs carry charge, in contrast to the Abelian gauge field.

To obtain the antisymmetric second-rank tensor of the gauge fields we can study the combination

$$[D_\mu, D_\nu]\,\psi \equiv ig\left(\frac{\tau^i}{2}F^i_{\mu\nu}\right)\psi, \tag{24}$$

with

$$\frac{\vec{\tau}\cdot\vec{F}_{\mu\nu}}{2} = \partial_\mu\frac{\vec{\tau}\cdot\vec{A}_\nu}{2} - \partial_\nu\frac{\vec{\tau}\cdot\vec{A}_\mu}{2} - ig\left[\frac{\vec{\tau}\cdot\vec{A}_\mu}{2}, \frac{\vec{\tau}\cdot\vec{A}_\nu}{2}\right], \tag{25}$$

where

$$F^i_{\mu\nu} = \partial_\mu A^i_\nu - \partial_\nu A^i_\mu + g\epsilon^{ijk}A^j_\mu A^k_\nu. \tag{26}$$

From the fact that $D_\mu\psi$ has the same gauge transformation property as ψ, we see that

$$([D_\mu, D_\nu]\,\psi)' = U(\theta)\,[D_\mu, D_\nu]\,\psi, \tag{27}$$

substituting eq.(24) on both sides from eq.(27), we have

$$\vec{\tau}\cdot\vec{F}'_{\mu\nu} = U(\theta)(\vec{\tau}\cdot\vec{F}_{\mu\nu})U^{-1}(\theta). \tag{28}$$

For the infinitesimal transformation $\theta_i \ll 1$, this translates into

$$F^{i\prime}_{\mu\nu} = F^i_{\mu\nu} + \epsilon^{ijk}\theta^j F^k_{\mu\nu}. \tag{29}$$

The $F^i_{\mu\nu}$ transforms nontrivially, however, the following product is gauge invariant

$$tr\left[(\vec{\tau}\cdot\vec{F}_{\mu\nu})(\vec{\tau}\cdot\vec{F}^{\mu\nu})\right] \propto F^i_{\mu\nu}F^{i\mu\nu}. \tag{30}$$

The complete gauge invariant Lagrangian which describes the interaction between gauge fields A^i_μ and $SU(2)$ doublet fields

$$\mathcal{L} = \bar{\psi}i\gamma^\mu D_\mu\psi - m\bar{\psi}\psi - \frac{1}{4}F^i_{\mu\nu}F^{i\mu\nu}, \tag{31}$$

where $F^i_{\mu\nu}$ is given by eq.(26) and $D_\mu\psi$ is given by eq.(20). The pure Yang-Mills term, $-\frac{1}{4}F^i_{\mu\nu}F^{i\mu\nu}$, contains factors that are trilinear and quadrilinear in A^i_μ, which correspond to self-couplings of non-Abelian gauge fields.

1.2 Standard Electroweak Theory - The Glashow-Weinberg-Salam Model

The SM is a gauge theory, based on the symmetry group $SU(3)_C \otimes SU(2)_L \otimes U(1)_Y$, which describes strong, weak and electromagnetic interactions, via the exchange of the corresponding spin-1 gauge fields: eight massless gluons and one massless photon, respectively , for the strong and electromagnetic interactions, and three massive bosons, $W^\pm$ and Z^0, for the weak interaction.

The gauge symmetry is broken by the vacuum, which triggers the SSB of the electroweak group

to the electromagnetic subgroup

$$SU(3)_C \otimes SU(2)_L \otimes U(1)_Y \xrightarrow{SSB} SU(3)_C \otimes U(1)_{QED}. \tag{32}$$

The SSB mechanism generates the masses of the weak gauge bosons, and gives rise to the appearance of a physical scalar particle in the model, the so-called Higgs. The fermion masses and mixings are also generated through the SSB [3].

1.2.1 Higgs mechanism

We start with a Lagrangian with a local $U(1)$ symmetry

$$\mathcal{L} = -\frac{1}{4}F_{\mu\nu}F^{\mu\nu} + (D^\mu\phi)^\dagger(D_\mu\phi) - \mu^2\phi^\dagger\phi - \lambda(\phi^\dagger\phi)^2, \tag{33}$$

where $\mu^2 < 0$. The gauge covariant derivative D_μ is defined by

$$D_\mu = \partial_\mu + ieA_\mu. \tag{34}$$

The covariant derivative from eq.(34) is different to eq.(8) one, the difference is a Q factor which is a characteristic of the field so we can omit it without to lose generality. Spontaneous symmetry breaking can occur if $\mu^2 < 0$, for which the minimum is obtained if

$$|\langle 0|\phi|0\rangle| = \frac{\upsilon}{\sqrt{2}}, \tag{35}$$

where

$$\upsilon = \sqrt{\frac{-\mu^2}{\lambda}}. \tag{36}$$

Only the magnitude of the vev is determined by the minimization condition. The phase can be arbitrary. Let us assume that the vacuum is where the phase value is zero, the vev of ϕ is $\frac{\upsilon}{\sqrt{2}}$. We can say that $\phi(x)$ can not be the quantum field in this case. We should write [9]

$$\phi(x) = \frac{1}{\sqrt{2}}(\upsilon + \eta(x) + i\zeta(x)), \tag{37}$$

where $\eta(x)$ and $\zeta(x)$ have zero vevs. Using eq.(37) in kinetic term from eq.(33)

$$(D^\mu\phi)^\dagger(D_\mu\phi) = \frac{1}{2}(\partial^\mu\eta)(\partial_\mu\eta) + \frac{1}{2}(\partial^\mu\zeta)(\partial_\mu\zeta) + e\upsilon A^\mu\partial_\mu\zeta + \frac{1}{2}e^2\upsilon^2 A_\mu A^\mu + \cdots. \tag{38}$$

We see that the $U(1)$ gauge boson has a mass term after the symmetry is broken, the mass is given by

$$M_A = e\upsilon. \tag{39}$$

Before we conclude that the gauge boson is massive, there is a problem to settle. There is a term $A^\mu \partial_\mu \zeta$ in eq.(38). Since it is quadratic in the fields, so it should be part of the free Lagrangian of the system. However, it contains two different fields, A^μ and ζ, involving a derivative. If it were written in terms of creation and annihilation operators, this would imply that we can have Feynman diagrams in which an A^μ changes into a ζ, without any other particle interacting with them, and vice versa.

The eq.(37) is not the only way that ϕ can be written in terms of quantum fields. Alternatively we could have written

$$\phi(x) = \frac{\upsilon + \eta(x)}{\sqrt{2}} e^{i\zeta(x)/\upsilon}. \tag{40}$$

If we keep only up to linear terms in quantum fields, this representation coincides with eq.(37). Here $\zeta(x)/\upsilon$ is the phase of the field ϕ, we know that any phase, even if it is a spacetime dependent one, it is irrelevant because of the local $U(1)$ symmetry. Explicitly, the Lagrangian from eq.(33) is invariant under the transformations

$$\begin{aligned} \phi(x) &\to \phi'(x) = e^{-ie\theta(x)}\phi(x), \\ A_\mu(x) &\to A'_\mu(x) = A_\mu(x) + \partial_\mu \theta(x). \end{aligned} \tag{41}$$

Therefore, given the representation of the field $\phi(x)$ as from eq.(40), we can always choose a new gauge through eq.(41). In particular, if we choose $\theta(x) = \zeta(x)/e\upsilon$, the gauge transformed fields are given by

$$\begin{aligned} \phi'(x) &= \frac{\upsilon + \eta(x)}{\sqrt{2}}, \\ A'(x) &= A_\mu(x) + \frac{1}{e\upsilon}\partial_\mu \zeta(x). \end{aligned} \tag{42}$$

If we substitute these primed fields instead of the unprimed fields, the $\zeta(x)$ field (would-be Goldstone boson) disappears altogether from the Lagrangian. This Lagrangian then contains physical fields only, and the gauge in which this takes place is called the *unitary gauge*.

1.2.2 Higgs boson multiplet

We introduce a scalar multiplet which is a doublet under the $SU(2)$ part of the gauge group, and write this as

$$\phi \begin{pmatrix} \phi^+ \\ \phi_0 \end{pmatrix} \; : \; \left(2, \frac{1}{2}\right). \tag{43}$$

The 2 indicates that it is a doublet of $SU(2)$, and we have normalized the $U(1)$ charge such that its value is $\frac{1}{2}$ for the multiplet ϕ.

The Lagrangian now contains terms involving ϕ as well. These are

$$\mathcal{L}_\phi = (D^\mu\phi)^\dagger(D_\mu\phi) - \mu^2\phi^\dagger\phi - \lambda(\phi^\dagger\phi)^2. \tag{44}$$

In general, when a multiplet transforms like an n-dimensional representation of $SU(2)$ and has a $U(1)$ quantum number Y, we should write

$$D_\mu = \partial_\mu + igT_a^{(n)}W_\mu^a + ig'YB_\mu, \tag{45}$$

where $T_a^{(n)}$ denote the generator of $SU(2)$ in the n-dimensional representation, and Y is the identity matrix times the hypercharge. For the doublet ϕ, the $SU(2)$ generators are $\tau_a/2$ (Pauli matrices) , and we can write

$$\begin{aligned} D_\mu\phi &= \left(\partial_\mu + ig\frac{\tau_a}{2}W_\mu^a + i\frac{g'}{2}B_\mu\right)\phi \\ &= \partial_\mu\begin{pmatrix}\phi^+\\ \phi_0\end{pmatrix} + \frac{i}{2\sqrt{2}}\begin{pmatrix} gW_\mu^3 + g'B_\mu & g(W_\mu^1 - iW_\mu^2)\\ g(W_\mu^1 + iW_\mu^2) & -gW_\mu^3 + g'B_\mu\end{pmatrix}\begin{pmatrix}\phi^+\\ \phi_0\end{pmatrix}. \end{aligned} \tag{46}$$

Let us now suppose that μ^2, the gauge symmetry will be spontaneously broken. The minimum for the scalar potential will be obtained for scalar field configurations given by

$$\phi_0 = \frac{\upsilon}{\sqrt{2}}\begin{pmatrix}0\\ 1\end{pmatrix}, \tag{47}$$

and $\upsilon = \sqrt{-\mu^2/\lambda}$. Any other vacuum satisfying eq.(47) can be reached from this by a global $SU(2)\times U(1)$ transformation. In this vacuum state, the generators T_1 and T_2 are no more part of the symmetry, since $\tau_{x,y}\phi_0 = (T_1 \pm iT_2)\phi_0 \neq 0$. The diagonal generators T_3 and the $U(1)$ generator Y do not annihilate the vacuum state either. However, we note that

$$\begin{pmatrix}1 & 0\\ 0 & 0\end{pmatrix}\begin{pmatrix}0\\ \upsilon/\sqrt{2}\end{pmatrix} = \begin{pmatrix}0\\ 0\end{pmatrix}. \tag{48}$$

Thus there is one diagonal generator which annihilates the vacuum. This is a linear combination of T_3 and Y, given by

$$Q = T_3 + Y \;:\; Q\phi_0 = 0. \tag{49}$$

The original gauge symmetry is therefore broken down to a $U(1)$ symmetry generated by Q. This is not the original $U(1)$ part of the symmetry group. As we have shown, its generator is actually a combination of an $SU(2)$ generator and the original $U(1)$ generator. To make this distinction, we will write the original symmetry from now as $SU(2)\times U(1)_Y$, whereas the remnant symmetry will be called $U(1)_Q$. This latter is in fact the electromagnetic gauge symmetry.

1.2.3 Gauge boson masses

Since ϕ_0 cannot be described by creation and annihilation operators, we can write

$$\phi(x) = \begin{pmatrix} \phi^+ \\ \frac{\upsilon + H(x) + i\zeta(x)}{\sqrt{2}} \end{pmatrix}, \tag{50}$$

where ϕ^+, H and ζ are all quantum fields with vanishing expectation values in the vacuum state. The gauge boson masses are identified by substituting the vacuum expectation value ϕ_0 for $\phi(x)$ in the Lagrangian from eq.(44). The relevant term from eq.(44) is

$$\begin{aligned} \left| \left(ig\frac{\tau_a}{2} W_\mu^a + i\frac{g'}{2} B_\mu \right) \phi_0 \right|^2 &= \frac{1}{8} \left| \begin{pmatrix} gW_\mu^3 + g'B_\mu & g(W_\mu^1 - iW_\mu^2) \\ g(W_\mu^1 + iW_\mu^2) & -gW_\mu^3 + g'B_\mu \end{pmatrix} \begin{pmatrix} 0 \\ \upsilon \end{pmatrix} \right|^2 \\ &= \frac{1}{8}\upsilon^2 g^2 \left[(W_\mu^1)^2 + (W_\mu^2)^2 \right] + \frac{1}{8}\upsilon^2 (g'B_\mu - gW_\mu^3)(g'B^\mu - gW^{3\mu}) \\ &= \left(\frac{1}{2}\upsilon g \right)^2 W_\mu^+ W^{-\mu} + \frac{1}{8}\upsilon^2 \begin{pmatrix} W_\mu^3 & B_\mu \end{pmatrix} \begin{pmatrix} g^2 & -gg' \\ -gg' & g'^2 \end{pmatrix} \begin{pmatrix} W^{3\mu} \\ B^\mu \end{pmatrix}, \end{aligned} \tag{51}$$

since $W^\pm = (W^1 \mp iW^2)/\sqrt{2}$. For any charged spin-1 field V_μ of mass M, the mass term in the Lagrangian is $MV_\mu^\dagger V^\mu$. Thus, the mass of the charged W boson is

$$M_W = \frac{1}{2}\upsilon g. \tag{52}$$

The remaining term is off-diagonal in the W_μ^3 and B_μ basis

$$\begin{aligned} \frac{1}{8}\upsilon^2 \left[g^2 (W_\mu^3)^2 - 2gg' W_\mu^3 B^\mu + g'^2 B_\mu^2 \right] =& \frac{1}{8}\upsilon^2 \left[gW_\mu^3 - g'B_\mu \right]^2 \\ &+ 0 \left[gW_\mu^3 + g'B_\mu \right]^2. \end{aligned} \tag{53}$$

One of the eigenvalues of the 2×2 matrix from eq.(51) is zero, we have included this term in eq.(53) with a combination of fields that is orthogonal to the combination given in the first term. Now, the physical fields Z_μ and A_μ diagonalize the mass matrix so that eq.(53) must be identified with

$$\frac{1}{2}M_Z^2 Z_\mu^2 + \frac{1}{2}M_A^2 A_\mu^2. \tag{54}$$

So, on normalizing the fields, we have [7]

$$\begin{aligned} A_\mu &= \frac{g'W_\mu^3 + gB_\mu}{\sqrt{g^2 + g'^2}} \quad \text{with } M_A = 0, \\ Z_\mu &= \frac{gW_\mu^3 - g'B_\mu}{\sqrt{g^2 + g'^2}} \quad \text{with } M_Z = \frac{1}{2}\upsilon\sqrt{g^2 + g'^2}. \end{aligned} \tag{55}$$

We can define the combinations

$$\begin{aligned} Z_\mu &= \cos\theta_W W_\mu^3 - \sin\theta_W B_\mu, \\ A_\mu &= \sin\theta_W W_\mu^3 + \cos\theta_W B_\mu, \end{aligned} \tag{56}$$

where θ_W is called the weak mixing, *'Weinberg' angle*, defined by

$$\frac{M_W}{M_Z} = \cos\theta_W \quad \text{or} \quad \frac{g'}{g} = \tan\theta_W. \tag{57}$$

The inequality $M_Z \neq M_W$ is due to the mixing between the W_μ^3 and B_μ fields. The mass eigenstates are then automatically a massless photon (A_μ) and a massive (Z_μ) field with $M_Z > M_W$.

1.2.4 Masses of the Fermions

An attractive feature of the SM is that the same Higgs doublet which generates $W^\pm$ and Z masses is also sufficient to give masses to the leptons and quarks. For example, to generate the electron mass, we include the following $SU(2) \times U(1)$ gauge invariant term in the Lagrangian

$$\mathcal{L} = -G_e \left[\begin{pmatrix} \bar{\nu}_e & \bar{e} \end{pmatrix}_L \begin{pmatrix} \phi^+ \\ \phi^0 \end{pmatrix} e_R + \bar{e}_R \begin{pmatrix} \phi^- & \bar{\phi}^0 \end{pmatrix}_L \begin{pmatrix} \nu_e \\ e \end{pmatrix}_L \right]. \tag{58}$$

The Higgs doublet has exactly the required $SU(2) \times U(1)$ quantum numbers to couple to $(\bar{e}_L e_R)$. We spontaneously break the symmetry and substitute

$$\phi = \sqrt{\frac{1}{2}} \begin{pmatrix} 0 \\ \upsilon + H(x) \end{pmatrix}, \tag{59}$$

into eq.(58). The neutral Higgs field $H(x)$ is the only remnant of the Higgs doublet, after the spontaneous breaking has taken place. On substitution of ϕ, the Lagrangian becomes

$$\mathcal{L} = -\frac{G_e}{\sqrt{2}}\upsilon(\bar{e}_L e_R + \bar{e}_R e_L) - \frac{G_e}{\sqrt{2}}(\bar{e}_L e_R + \bar{e}_R e_L)h. \tag{60}$$

We now choose G_e so that

$$m_e = \frac{G_e \upsilon}{\sqrt{2}}, \tag{61}$$

and hence generate the required electron mass,

$$\mathcal{L} = -m_e \bar{e} e - \frac{m_e}{\upsilon} \bar{e} e h. \tag{62}$$

Note however that, since G_e is arbitrary, the actual mass of the electron in not predicted.

The quark masses are generated in the same way. The only novel feature is that to generate a

mass for the upper member of a quark doublet, we must construct a new Higgs doublet from ϕ

$$\phi_c = i\tau_2\phi^* = \begin{pmatrix} -\bar{\phi}^0 \\ \phi^- \end{pmatrix} \xrightarrow{\text{breaking}} \sqrt{\frac{1}{2}} \begin{pmatrix} \upsilon + H(x) \\ 0 \end{pmatrix}. \tag{63}$$

Due to the special properties of $SU(2)$, ϕ_c transforms identically to ϕ. It can therefore be used to construct a gauge invariant contribution to the Lagrangian

$$\begin{aligned} \mathcal{L} &= -G_d \begin{pmatrix} \bar{u} & \bar{d} \end{pmatrix}_L \begin{pmatrix} \phi^+ \\ \phi^0 \end{pmatrix} d_R - G_u \begin{pmatrix} \bar{u} & \bar{d} \end{pmatrix}_L \begin{pmatrix} -\bar{\phi}^0 \\ \phi^- \end{pmatrix} u_R + \text{h.c.}, \\ &= -m_d \bar{d}d - m_u \bar{u}u - \frac{m_d}{\upsilon}\bar{d}dh - \frac{m_u}{\upsilon}\bar{u}uh. \end{aligned} \tag{64}$$

Here, we have just considered the $\begin{pmatrix} u & d \end{pmatrix}_L$ quark doublet. However, weak interactions operate on $\begin{pmatrix} u & d' \end{pmatrix}_L$, $\begin{pmatrix} c & s' \end{pmatrix}_L$,... doublets, where the primed states (mass eigenstates) are linear combinations of the flavor eigenstates. The quark Lagrangian is therefore of the form

$$\mathcal{L} = -G_d^{ij} \begin{pmatrix} \bar{u}_i & \bar{d}'_i \end{pmatrix}_L \begin{pmatrix} \phi^+ \\ \phi^0 \end{pmatrix} d_{jR} - G_u^{ij} \begin{pmatrix} \bar{u}_i & \bar{d}'_i \end{pmatrix}_L \begin{pmatrix} -\bar{\phi}^0 \\ \phi^- \end{pmatrix} u_{jR} + h.c., \tag{65}$$

with $i, j = 1, ..., N$, where N is the number of quarks doublets. We can rewrite the quark Lagrangian in diagonal form

$$\mathcal{L} = -m_d^i \bar{d}_i d_i \left(1 + \frac{h}{\upsilon}\right) - m_u^i \bar{u}_i u_i \left(1 + \frac{h}{\upsilon}\right). \tag{66}$$

1.2.5 The Final Lagrangian

To summarize the standard (Glashow-Weinberg-Salam) model, we gather together all the ingredients of the Lagrangian. The complete Lagrangian is given by Figure 1 [7].

$$\mathcal{L} = -\tfrac{1}{4}\mathbf{W}_{\mu\nu}\cdot\mathbf{W}^{\mu\nu} - \tfrac{1}{4}B_{\mu\nu}B^{\mu\nu}$$
{W ±, Z, γ kinetic energies and self-interactions}

$$+\bar{L}\gamma^{\mu}\left(i\partial_{\mu} - g\frac{1}{2}\boldsymbol{\tau}\cdot\mathbf{W}_{\mu} - g'\frac{Y}{2}B_{\mu}\right)L$$
$$+\bar{R}\gamma^{\mu}\left(i\partial_{\mu} - g'\frac{Y}{2}B_{\mu}\right)R$$
{lepton and quark kinetic energies and their interactions with W ±, Z, γ}

$$+\left|\left(i\partial_{\mu} - g\frac{1}{2}\boldsymbol{\tau}\cdot\mathbf{W}_{\mu} - g'\frac{Y}{2}B_{\mu}\right)\phi\right|^{2} - V(\phi)$$
{W ±, Z, γ, and Higgs masses and couplings}

$$-(G_1\bar{L}\phi R + G_2\bar{L}\phi_c R + \text{hermitian conjugate}).$$
{lepton and quark masses and coupling to Higgs}

Figure 1: The complete Lagrangian of the SM.

L denotes a left-handed fermion (lepton or quark) doublet, and R denotes a right-handed fermion singlet.

2 Lepton Flavor Violation (LFV)

Lepton mixing implies that the generational lepton numbers are not conserved. The most easy observables would be processes in which the initial and final states do not contain any neutrino. No such process has been observed so far.

Neutrino oscillations provide a clear evidence for lepton flavor violation (LFV) in the neutral sector, pointing out to physics beyond the Standard Model. However, no evidence of lepton flavor violating processes in the charged sector has been found despite the great experimental effort on searching for that violation [10].

LFV is absent in the SM with massless neutrinos. A minimal extension that includes right handed neutrinos allowing for small neutrino Dirac masses might allow LFV reactions such as $\mu \to e\gamma$ (though at an unobservable level). In the SM, particle masses are proportional to the strengths of the interactions between the particles and the Higgs bosons. Thus, the Dirac mass term like for example ν_e must be multiplied by some very small coupling strength such that his mass is at least $50,000$ times smaller than the mass of the electron. But the electron and the ν_e are part of the same weak doublet, and there seems to be no reason why they should have such enormously different interaction strengths with the Higgs boson [11].

We briefly review some processes which are expected, and discuss what sort of rates to expect for them.

2.1 Radiative decays

The muon might decay into the electron with the emission of a photon

$$\mu \to e + \gamma. \tag{67}$$

It cannot happen at the tree level. Figure 2 shows how the process might occur at the one-loop level, this diagram is one of three possible diagrams that contributes to the process.

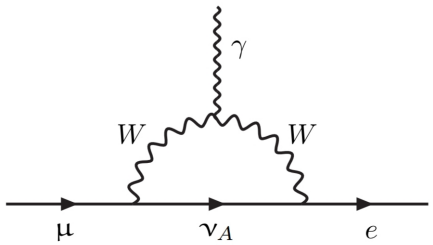

Figure 2: One-loop diagram for the process $\mu \to e + \gamma$.

Experimentally, only an upper bound is known for the branching ratio [6] of the process from eq.

(67)

$$\mathcal{B}(\mu \to e + \gamma) < 4.2 \times 10^{-13}. \tag{68}$$

For any acceptable value of neutrino masses, this branching ratio is well below 10^{-40}.

Processes like $\tau \to \mu + \gamma$ and $\tau \to e + \gamma$ are also expected to occur because of neutrino mixing [12–14]. They are also expected to be very suppressed for exactly the same reason.

2.1.1 Purely leptonic decays

We can also contemplate decay processes involving charged leptons and antileptons only

$$\mu^- \to e^- e^- e^+, \tag{69}$$

and its charge conjugate, as well as similar decays of the τ lepton where the final state can contain both muons and electrons. This process can occur at the one-loop level. One possible diagram is obtained by attaching an outgoing e^+e^- pair to the photon line of Figure 2 whereby the photon line itself becomes an internal virtual line. There are other possibilities shown in Figure 3.

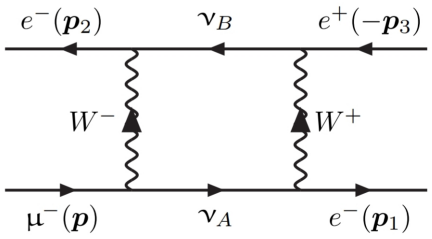

Figure 3: One-loop box diagram for the process $\mu \to 3e$.

The upper limit on the branching ratio for this process is given by [6]

$$\mathcal{B}(\mu \to 3e) < 1.0 \times 10^{-12}. \tag{70}$$

2.1.2 $\mu - e$ conversion in nuclei $\mu N \to eN$

Other experiments look for flavour transitions of charged leptons either in decays, like $\mu \to e\gamma$, or in bound states of a nucleus and a captured muon, usually referred to as $\mu - e$ conversion. Considerable theoretical and experimental effort has been dedicated to $\mu - e$ conversion [15]. This process will lead the limits on these transitions in the near future.

Muon-to-electron conversion is the spontaneous decay of a muon to an electron without the emission of neutrinos, within the Coulomb potential of an atomic nucleus: it is therefore only possible for negative muons.

Since no neutrinos are produced, muon-to-electron conversion is not a weak sM interaction: thus an observation of the process can only come from new physics.

The constraint of unchanged nucleus means that all the energy of the muon goes into the kinetic energy of the electron and the recoil of the parent nucleus, hence the signature of such a process is the presence of a monochromatic electron at an energy which is essentially the muon mass, corrected for the binding energy and nuclear recoil

$$E_e \approx m_\mu - B_\mu - E_r, \tag{71}$$

where $B_\mu \approx Z^2\alpha^2 m_\mu/2$ is the muon binding energy and $E_r \approx m_\mu^2/2m_N$ the nuclear recoil energy. There are many excellent articles motivating the search, such as Calibbi and Signorelli [16], de Gouvêa and Vogel [17], or Marciano et al. [18].

The Mu2e experiment will search for the charged-lepton flavor violating (CLFV) neutrino-less conversion of a negative muon into an electron in the field of a nucleus. The goal of the experiment is to improve the previous upper limit by four orders of magnitude and reach a SES (single event sensitivity) of 3×10^{-17} on the conversion rate, a 90% CL of 8×10^{-17}, and a 5σ discovery reach at 2×10^{-16}. We can see that this bound is more restrictive than the eqs.(68) and (70). The experiment will begin operations in 2022 [19].

3 Littlest Higgs Model with T-parity

3.1 The Model

The Littlest Higgs with T-parity (LHT) is a non-linear σ model based on the coset space $SU(5)/SO(5)$, where $SU(5)$ is the global symmetry, so guarantees 14 Nambu-Goldstone bosons. The global symmetry is broken by the vev of a 5×5 symmetric tensor. It is convenient to choose a basis in which the symmetric tensor is proportional to

$$\Sigma_0 = \begin{pmatrix} 0 & 0 & \mathbb{I} \\ 0 & 1 & 0 \\ \mathbb{I} & 0 & 0 \end{pmatrix}, \tag{72}$$

where $\mathbb{I}$ represents a unit 2×2 matrix. Here $\Sigma_0 = \langle \Sigma \rangle$ is the VEV of gauge field Σ. It transforms as $\Sigma \to U\Sigma U^T$ for $U \in SU(5)$.

The original SU(5) generators are shown in the Appendix A, but we are going to use a different representation of the Lie algebra of $SU(5)$. We introduce the matrix A [20]

$$A = \begin{pmatrix} \frac{1}{2}+\frac{i}{2} & 0 & 0 & \frac{1}{2}-\frac{i}{2} & 0 \\ 0 & \frac{1}{2}+\frac{i}{2} & 0 & 0 & \frac{1}{2}-\frac{i}{2} \\ 0 & 0 & 1 & 0 & 0 \\ \frac{1}{2}-\frac{i}{2} & 0 & 0 & \frac{1}{2}+\frac{i}{2} & 0 \\ 0 & \frac{1}{2}-\frac{i}{2} & 0 & 0 & \frac{1}{2}+\frac{i}{2} \end{pmatrix}, \tag{73}$$

where A satisfies $A^2 = \Sigma_0$ and $A^T = A$. We transform the usual matrix representantion of $SU(5)$ via the unitary transformation

$$\hat{\lambda}_a = A\lambda_a A^{-1} = \begin{pmatrix} \frac{1}{2}+\frac{i}{2} & 0 & 0 & \frac{1}{2}-\frac{i}{2} & 0 \\ 0 & \frac{1}{2}+\frac{i}{2} & 0 & 0 & \frac{1}{2}-\frac{i}{2} \\ 0 & 0 & 1 & 0 & 0 \\ \frac{1}{2}-\frac{i}{2} & 0 & 0 & \frac{1}{2}+\frac{i}{2} & 0 \\ 0 & \frac{1}{2}-\frac{i}{2} & 0 & 0 & \frac{1}{2}+\frac{i}{2} \end{pmatrix} \lambda_a \begin{pmatrix} \frac{1}{2}-\frac{i}{2} & 0 & 0 & \frac{1}{2}+\frac{i}{2} & 0 \\ 0 & \frac{1}{2}-\frac{i}{2} & 0 & 0 & \frac{1}{2}+\frac{i}{2} \\ 0 & 0 & 1 & 0 & 0 \\ \frac{1}{2}+\frac{i}{2} & 0 & 0 & \frac{1}{2}-\frac{i}{2} & 0 \\ 0 & \frac{1}{2}+\frac{i}{2} & 0 & 0 & \frac{1}{2}-\frac{i}{2} \end{pmatrix}, \tag{74}$$

with λ_a the generators of $SU(5)$.

With the new representation of $SU(5)$, the unbroken $SO(5)$ generators satisfy

$$\hat{T}_a\Sigma_0 + \Sigma_0\hat{T}_a^T = 0, \tag{75}$$

while the broken generators obey

$$\hat{X}_a\Sigma_0 - \Sigma_0\hat{X}_a^T = 0. \tag{76}$$

As usual, the Goldstone bosons are fluctuations about this background in the broken directions

$\Pi \equiv \pi^a \hat{X}^a$, and can be parameterized by the non-linear sigma model field

$$\Sigma(x) = e^{i\Pi/f}\Sigma_0 e^{i\Pi^T/f} = e^{2i\Pi/f}\Sigma_0, \tag{77}$$

where f is the effective NP scale. Thus the matrix of NGB may be written as

$$\Pi = \begin{pmatrix} \chi + \frac{\eta}{2\sqrt{5}} & \frac{h}{\sqrt{2}} & \phi \\ \frac{h^\dagger}{\sqrt{2}} & \frac{2\eta}{\sqrt{5}} & \frac{h^T}{\sqrt{2}} \\ \phi^\dagger & \frac{h^*}{\sqrt{2}} & \chi^T + \frac{\eta}{2\sqrt{5}} \end{pmatrix}. \tag{78}$$

Here $\chi = \chi^a\sigma^a/2$ with σ^a the three Pauli matrices, η is a real singlet, and they are the Goldstone bosons which are eaten to become the longitudinal modes of the partners of the SM gauge fields, $h = \begin{pmatrix} h^+ \\ h^0 \end{pmatrix}$ is the SM Higgs doublet and finally $\phi = \begin{pmatrix} -i\Phi^{++} & -i\frac{\Phi^+}{\sqrt{2}} \\ -i\frac{\Phi^+}{\sqrt{2}} & \frac{-\Phi^0+\Phi^P}{\sqrt{2}} \end{pmatrix}$ [21] is a complex $SU(2)_L$ triplet.

As χ is given by $\chi^a\sigma^a/2$, it has 3 degrees of freedom, η has only 1 degree of freedom, h has 4 ones and finally ϕ has 6 d.o.f. So together they add up to the desired 14 Goldstone bosons (in Section 7 all the Goldstone bosons are shown explicitly in Π matrix).

3.2 Gauge and Scalar Sector

Now we gauge a subgroup of the global symmetry, and we do this in such a way that each gauge coupling by itself preserves enough of the global symmetry to ensure that the Higgs doublet remains an exact NGB. The gauge group is taken to be $G_1 \times G_2 = [SU(2) \times U(1)]^2$, subgroup of the $SU(5)$ global symmetry.

$$\begin{array}{ccccc} SU(5) & \xrightarrow{f} & SO(5) & & \\ \bigcup & & \bigcup & & \\ [SU(2)\times U(1)]^2 & \xrightarrow{f} & SU(2)_w \times U(1)_Y & \xrightarrow{v_h} & U(1)_{\mathrm{EW}} \end{array}$$

Figure 4: The global SU(5) contains two copies of local $[SU(2) \times U(1)]^2$ that are diagonally broken to one copy $SU(2) \times U(1)$ contained in SO(5).

As we can see in Figure 4 [20], f is the energy scale where the symmetry breaking $[SU(2) \times U(1)]^2 \to SU(2)_W \times U(1)_Y$ occurs. The global symmetry breaking scale, f, is constrained on the order of a TeV.

The generators of the first $G_1 = SU(2) \times U(1)$ are embedded into $SU(5)$ as

$$Q_1^a = \begin{pmatrix} \sigma^a/2 & 0 \\ 0 & 0_{3\times 3} \end{pmatrix}, \qquad Y_1 = \mathrm{diag}(3,3,-2,-2,-2)/10, \tag{79}$$

while the generators of the second $SU(2) \times U(1)$ are given by

$$Q_2^a = \begin{pmatrix} 0_{3\times 3} & 0 \\ 0 & -\sigma^{a*}/2 \end{pmatrix}, \qquad Y_2 = \mathrm{diag}(2,2,2,-3,-3)/10. \tag{80}$$

The linear combination $Q_1^a + Q_2^a$ satisfies eq.(75), and generates the unbroken symmetry that we identify as $SU(2)_W$ of the SM. Now, the linear combination $Y_1 + Y_2$ satisfies eq.(75) too, and generates the unbroken symmetry that we identify as $U(1)_Y$. The orthogonal combinations are a subset of the broken generator, i.e., $\{Q_1^a - Q_2^a, Y_1 - Y_2\} \subset \{\hat{X}_a\}$. The vacuum breaks the $[SU(2) \times U(1)]^2$ gauge symmetry down to the diagonal subgroup, giving one set of $[SU(2) \times U(1)]$ gauge bosons masses of order of f, while the other set members are left massless at the scale f, and are identified as the $[SU(2)_L \times U(1)_Y]$ gauge fields of the SM.

T-parity is a natural symmetry of most little Higgs models (those that are product group models) where SM particles are even under this symmetry (T-even), while the new particles at the TeV scale are odd (T-odd). T-parity explicitly forbids any tree-level contributions from the heavy gauge bosons to the observables involving only SM particles as external states, as a result, the corrections to EWPO are generated exclusively at loop level. This implies that the constraints are generically weaker than in the Little Higgs models without this symmetry since the most serious constraints resulted from the tree-level corrections to EWPO throught to the exchange of heavy gauge bosons. In other words, when we introduced T-parity, we eliminate the tree-level electroweak precision constraints that the Littlest Higgs model has: because the external states in all experimentally tested processes are T-even, there is no T-odd state that can contribute to such processes at tree-level.

Using eqs.(75) and (76), a natural action of T-parity on the gauge fields is defined as

$$G_1 \leftrightarrow G_2, \tag{81}$$

its action on the gauge fields G_i exchanges the two gauge groups $SU(2)_i \times U(1)_i$. Then, T invariance requires that the gauge couplings associated to both factors are equal, leading to the Gauge Lagrangian

$$\mathcal{L}_G = \sum_{j=1}^{2} \left[-\frac{1}{2} Tr\left(\widetilde{W}_{j\mu\nu} \widetilde{W}_j^{\mu\nu} \right) - \frac{1}{4} B_{j\mu\nu} B_j^{\mu\nu} \right], \tag{82}$$

where

$$\widetilde{W}_{j\mu} = W_{j\mu}^a Q_j^a, \qquad \widetilde{W}_{j\mu\nu} = \partial_\mu \widetilde{W}_{j\nu} - \partial_\nu \widetilde{W}_{j\mu} - ig \left[\widetilde{W}_{j\mu}, \widetilde{W}_{j\nu} \right], \qquad B_{j\mu\nu} = \partial_\mu B_{j\nu} - \partial_\nu B_{j\mu}. \tag{83}$$

As mentioned earlier, the combination $\{Q_1^a + Q_2^a, Y_1 + Y_2\}$ generates the SM gauge group. The

SM gauge bosons are the T-even combinations multiplying the unbroken gauge generators,

$$W^{\pm} = \frac{1}{2}\left[\left(W_1^1 + W_2^1\right) \mp i\left(W_1^2 + W_2^2\right)\right], \qquad W^3 = \frac{W_1^3 + W_2^3}{\sqrt{2}}, \qquad B = \frac{B_1 + B_2}{\sqrt{2}}, \tag{84}$$

whereas the heavy gauge bosons are the T-odd combinations

$$W_H^{\pm} = \frac{1}{2}\left[\left(W_1^1 - W_2^1\right) \mp i\left(W_1^2 - W_2^2\right)\right], \qquad W_H^3 = \frac{W_1^3 - W_2^3}{\sqrt{2}}, \qquad B_H = \frac{B_1 - B_2}{\sqrt{2}}. \tag{85}$$

The eqs.(84) and (85) are computed in Appendix B.

Recalling that the heavy particles are T-odd and all SM particles are T-even, we have to impose an extra transformation rule for the scalar sector. In order to ensure that the SM Higgs doublet is T-even and the remaining Goldstone fields are T-odd, the T action on the scalar fields is defined as follows,

$$\Pi \xrightarrow{T} \hat{\Pi} = -\Omega\Pi\Omega, \qquad \Omega = \mathrm{diag}(-1,-1,1,-1,-1), \tag{86}$$

where Ω is an element of the center of the gauge group which commutes with Σ_0

$$\hat{\Pi} = \begin{pmatrix} -\chi - \frac{\eta}{2\sqrt{5}} & \frac{h}{\sqrt{2}} & -\phi \\ \frac{h^\dagger}{\sqrt{2}} & -\frac{2\eta}{\sqrt{5}} & \frac{h^T}{\sqrt{2}} \\ -\phi^\dagger & \frac{h^*}{\sqrt{2}} & -\chi^T - \frac{\eta}{2\sqrt{5}} \end{pmatrix}, \tag{87}$$

if we compared the eq.(87) with the eq.(78), we can see that the SM Higgs doublet keeps its parity.

Then,

$$\Sigma \xrightarrow{T} \widetilde{\Sigma} = \Sigma_0\Omega\Sigma^\dagger\Omega\Sigma_0. \tag{88}$$

We know that $\Sigma = e^{2i\Pi/f}\Sigma_0$, and since χ and η are the Goldstone bosons which are eaten to become the longitudinal modes of the partners of the SM gauge fields, we have

$$\Pi = \begin{pmatrix} 0 & \frac{h}{\sqrt{2}} & \phi \\ \frac{h^\dagger}{\sqrt{2}} & 0 & \frac{h^T}{\sqrt{2}} \\ \phi^\dagger & \frac{h^*}{\sqrt{2}} & 0 \end{pmatrix}, \tag{89}$$

expanding Σ until order of $\frac{1}{f^2}$

$$\begin{aligned} \Sigma &= \left(\mathbb{I} + \frac{2i}{f}\Pi - \frac{2}{f^2}\Pi^2 + \dots\right)\Sigma_0 \\ &= \Sigma_0 + \frac{2i}{f}\begin{pmatrix} \phi & \frac{h}{\sqrt{2}} & 0 \\ \frac{h^\dagger}{\sqrt{2}} & 0 & \frac{h^T}{\sqrt{2}} \\ 0 & \frac{h^*}{\sqrt{2}} & \phi^\dagger \end{pmatrix} - \frac{1}{f^2}\begin{pmatrix} h^T h & \sqrt{2}\phi h^* & h^\dagger h + 2\phi\phi^\dagger \\ \sqrt{2}h^\dagger\phi & 2h^T h^* & \sqrt{2}h^T\phi^\dagger \\ 2\phi^\dagger\phi + h^T h^* & \sqrt{2}\phi^\dagger h & h^\dagger h^* \end{pmatrix} + \mathcal{O}\left(\frac{1}{f^3}\right). \end{aligned} \tag{90}$$

Now, including the EWSB, the vacuum expectation values of h and ϕ are [20]

$$\langle h\rangle_0 = \frac{1}{\sqrt{2}}\begin{pmatrix} 0 \\ \upsilon_h \end{pmatrix}, \qquad \langle \phi\rangle_0 = \begin{pmatrix} 0 & 0 \\ 0 & 0 \end{pmatrix}, \tag{91}$$

where $\upsilon_h = 246$ GeV is the EWSB scale and h is the physical Higgs field. Thus, considering the eq.(91), the eq.(89) transforms as

$$\Pi = \frac{1}{\sqrt{2}}\begin{pmatrix} 0 & 0 & 0 & 0 & 0 \\ 0 & 0 & \upsilon_h & 0 & 0 \\ 0 & \upsilon_h & 0 & 0 & \upsilon_h \\ 0 & 0 & 0 & 0 & 0 \\ 0 & 0 & \upsilon_h & 0 & 0 \end{pmatrix}. \tag{92}$$

Then, including the EWSB effects, the vev of the Σ field has the form [22]

$$\Sigma = \exp\left\{\frac{i\sqrt{2}}{f}\begin{pmatrix} 0 & 0 & 0 & 0 & 0 \\ 0 & 0 & \upsilon_h & 0 & 0 \\ 0 & \upsilon_h & 0 & 0 & \upsilon_h \\ 0 & 0 & 0 & 0 & 0 \\ 0 & 0 & \upsilon_h & 0 & 0 \end{pmatrix}\right\}\Sigma_0 = \begin{pmatrix} 0 & 0 & 0 & 1 & 0 \\ 0 & -\frac{1}{2}(1-c_\upsilon) & \frac{i}{\sqrt{2}}s_\upsilon & 0 & \frac{1}{2}(1+c_\upsilon) \\ 0 & \frac{i}{\sqrt{2}}s_\upsilon & c_\upsilon & 0 & \frac{i}{\sqrt{2}}s_\upsilon \\ 1 & 0 & 0 & 0 & 0 \\ 0 & \frac{1}{2}(1+c_\upsilon) & \frac{i}{\sqrt{2}}s_\upsilon & 0 & -\frac{1}{2}(1-c_\upsilon) \end{pmatrix}, \tag{93}$$

where

$$s_{\upsilon_h} = \sin\left(\frac{\sqrt{2}\upsilon_h}{f}\right), \qquad c_{\upsilon_h} = \cos\left(\frac{\sqrt{2}\upsilon_h}{f}\right). \tag{94}$$

The scalar Lagrangian of the gauged theory is obtained from the non-linear σ model field Σ in the Littlest Higgs

$$\mathcal{L}_S = \frac{f^2}{8}Tr[(\mathcal{D}_\mu\Sigma)(\mathcal{D}^\mu\Sigma)^\dagger], \tag{95}$$

where

$$\mathcal{D}_\mu\Sigma = \partial_\mu\Sigma - i\sum_{j=1}^{2}\left[g_j W_j^a\left(Q_j^a\Sigma + \Sigma Q_j^{aT}\right) + g_j' B_j\left(Y_j\Sigma + \Sigma Y_j^T\right)\right]. \tag{96}$$

In the above equation, the Q_j and Y_j are the gauged generators, W_j^a and B_j are the $SU(2)_j$ and $U(1)_j$ gauge fields, respectively, and g_j and g_j' are the corresponding coupling constants. We know that the T-parity exchanges the two gauge groups as we can see from eq.(81), i.e., under this T-parity the gauge bosons and the $[SU(2)\times U(1)]_j$ generators change as

$$W_1^a \leftrightarrow W_2^a, \qquad B_1 \leftrightarrow B_2, \qquad Q_1^a \leftrightarrow Q_2^a, \qquad Y_1 \leftrightarrow Y_2. \tag{97}$$

Because the Lagrangian $\mathcal{L}_S$ is T-even, from the eqs.(96) and (97) it is easy to see that

$$g_1 = g_2 = \sqrt{2} g_W, \qquad g_1' = g_2' = \sqrt{2} g', \tag{98}$$

where g_W is the $SU(2)_W$ coupling constant and g' is the $U(1)_Y$ coupling constant.

Then, the eq.(96) looks as

$$\mathcal{D}_\mu \Sigma = \partial_\mu \Sigma - i\sqrt{2} \sum_{j=1}^{2} \left[g_W W_j^a \left(Q_j^a \Sigma + \Sigma Q_j^{aT} \right) + g' B_j \left(Y_j \Sigma + \Sigma Y_j^T \right) \right]. \tag{99}$$

Under T-parity, the relevant term for calculating the mass of gauge bosons is

$$\left| -i\sqrt{2} \sum_{j=1}^{2} \left[g_W W_j^a \left(Q_j^a \widetilde{\Sigma} + \widetilde{\Sigma} Q_j^{aT} \right) + g' B_j \left(Y_j \widetilde{\Sigma} + \widetilde{\Sigma} Y_j^T \right) \right] \right|^2. \tag{100}$$

We have, to lowest order, $\widetilde{\Sigma} = \Sigma_0$, in the gauge sector before EWSB, there is a linear combination of gauge bosons that acquire a mass of order f, from eq.(100)

$$\begin{aligned} \begin{pmatrix} W_L^a \\ W_H^a \end{pmatrix} &= \frac{1}{\sqrt{2}} \begin{pmatrix} 1 & 1 \\ 1 & -1 \end{pmatrix} \begin{pmatrix} W_1^a \\ W_2^a \end{pmatrix}, \\ \begin{pmatrix} B_L \\ B_H \end{pmatrix} &= \frac{1}{\sqrt{2}} \begin{pmatrix} 1 & 1 \\ 1 & -1 \end{pmatrix} \begin{pmatrix} B_1 \\ B_2 \end{pmatrix}. \end{aligned} \tag{101}$$

From eq.(101) we see the SM light gauge bosons are W_L^a and B_L. At this stage, they are massless and T-even, while the heavy gauge bosons are W_H^a and B_H, they are T-odd and massive. After high energy symmetry breaking, their masses are [23]

$$M_{W_H^a} = g_W f, \qquad M_{B_H} = \frac{g' f}{\sqrt{5}}. \tag{102}$$

In Appendix C, we computed the masses of gauge bosons.

Now, considering the EWSB effects of order $(v_h/f)^2$, the Σ field according to eq.(93) is

$$\Sigma = \begin{pmatrix} 0 & 0 & 0 & 1 & 0 \\ 0 & -\epsilon^2/2 & -i\epsilon & 0 & 1-\epsilon^2/2 \\ 0 & i\epsilon & 1-\epsilon^2 & 0 & i\epsilon \\ 1 & 0 & 0 & 0 & 0 \\ 0 & 1-\epsilon^2/2 & i\epsilon & 0 & -\epsilon^2/2 \end{pmatrix}, \tag{103}$$

with $\epsilon = \frac{v_h}{f}$.

When we include the EWSB effects, the LHT model must reproduce the SM gauge bosons, i.e.,

$W^{\pm}$, Z and A bosons have to appear. Moreover, the masses of the heavy sector will have small corrections of order $\frac{v^2}{f^2}$.

We are separating explicitly the third components, W_1^3 and W_2^3, which is convenient, because in the Scalar Lagrangian of order $\frac{v^2}{f^2}$, this component has a different transformation. Now, we split W_1^a and W_2^a, $a = 1, 2$.

The Scalar Lagrangian, with EWSB effects is explicitly

$$\begin{aligned}
\mathcal{L}_S = & \frac{f^2 g_W^2}{4}\left[-\frac{\epsilon^4}{6}W_1^a W_2^a + \epsilon^2 W_1^a W_2^a + (W_1^a - W_2^a)^2\right] \\
& + \frac{f^2 g_W^2}{4}\left[\frac{\epsilon^4}{8}\left(\left(W_1^3 - W_2^3\right)^2 - \frac{1}{4}W_1^3 W_2^3\right) + \epsilon^2 W_1^3 W_2^3 + \left(W_1^3 - W_2^3\right)^2\right] \\
& + \frac{f^2 g'^2}{4}\left[\epsilon^4\left(\frac{1}{8}\left(B_1^2 + B_2^2\right) - \frac{5}{12}B_1 B_2\right) + \epsilon^2 B_1 B_2 + \frac{1}{5}\left(B_1 - B_2\right)^2\right] \\
& + \frac{f^2 g_W g'}{4}\left[\frac{\epsilon^4}{4}\left(-\left(W_1^3 - W_2^3\right)\left(B_1 - B_2\right) + \frac{2}{3}\left(B_1 W_2^3 + B_2 W_1^3\right)\right) - \epsilon^2\left(B_1 W_2^3 + B_2 W_1^3\right)\right].
\end{aligned} \tag{104}$$

Also we are considering the crossed terms of W_j and B_j in the Scalar Lagrangian. We can see in the Scalar Lagrangian, the terms W_j^3 are separated explicitly of the terms W_1^1, W_1^2, W_2^1 and W_2^2, moreover W_j^3 is the only component of W_1^a and W_2^a that mixes with the B_j bosons.

Finally, the Scalar Lagrangian for the light and heavy gauge bosons sector is

$$\begin{aligned}
\mathcal{L}_S = & \frac{1}{2}\left[\frac{g_W^2 v_h^2}{4}\left(1 - \frac{v_h^2}{6f^2}\right)\right] W_L^+ W_L^- \\
& + \frac{1}{2}\left[f^2 g_W^2\left(1 - \frac{v_h^2}{4f^2}\right)\right] W_H^+ W_H^- \\
& + \frac{1}{2}\left[f^2 g_W^2\left(1 - \frac{v_h^2}{4f^2}\right)\right] (Z_H)^2 \\
& + \frac{1}{2}\left[\frac{f^2 g'^2}{5}\left(1 - \frac{5v_h^2}{4f^2}\right)\right] (A_H)^2 \\
& + \frac{1}{2}\left[\frac{g_W^2 v_h^2}{4\cos^2\theta_W}\left(1 - \frac{v_h^2}{6f^2}\right)\right] Z_L^2.
\end{aligned} \tag{105}$$

The light gauge sector includes the $W_L^{\pm}$, Z_L, and A_L bosons, that we identify as the SM gauge bosons with masses

$$\begin{aligned}
M_{W_L^{\pm}} &= \frac{g_W v_h}{2}\left(1 - \frac{v_h^2}{6f^2}\right)^{1/2} \approx \frac{g_W v_h}{2}\left(1 - \frac{v_h^2}{12f^2}\right), \\
M_{Z_L} &= \frac{g_W v_h}{2\cos\theta_H}\left(1 - \frac{v_h^2}{6f^2}\right)^{1/2} = \frac{M_{W_L^{\pm}}}{\cos\theta_W}, \\
M_{A_L} &= 0,
\end{aligned} \tag{106}$$

and the mass of the heavy bosons are

$$\begin{aligned} M_{W_H^\pm} = M_{Z_H} &= fg_W \left(1 - \frac{v_h^2}{4f^2}\right)^{1/2} \approx fg_W \left(1 - \frac{v_h^2}{8f^2}\right), \\ M_{A_H} &= \frac{fg'}{\sqrt{5}} \left(1 - \frac{5v_h^2}{4f^2}\right)^{1/2} \approx \frac{fg'}{\sqrt{5}} \left(1 - \frac{5v_h^2}{8f^2}\right). \end{aligned} \tag{107}$$

In Appendix C, we show the process to obtain their masses.

3.3 Fermion Sector

The LHT must implemented in the fermion sector, too. We would like to introduce SM fermions that transform linearly under the gauge symmetries to avoid large contributions to four fermion operators that would require the scale f to be large. As we have seen before, T-parity exchanges $SU(2)_1$ and $SU(2)_2$, so one must introduce two doublets ψ_1, and ψ_2, which transform linearly under $SU(2)_1$ and $SU(2)_2$ respectively, i.e., for each SM $SU(2)_L$ doublet, a doublet under $SU(2)_1$ and one under $SU(2)_2$ are introduced. The T-even combination is associated with the SM $SU(2)_L$ doublet while the T-odd combination is given a mass of order the breaking scale f.

For each lepton/quark doublet, embedding is possible in incomplete representations Ψ_1, Ψ_2 of the global $SU(5)$ symmetry. An additional set of fermions forming a T-odd $SO(5)$ multiplet Ψ_R, which is right-handed and transforms non-linearly under the full $SU(5)$, is introduced to give mass to the extra fermions; the field content can be expressed as follows [22, 24]

$$\Psi_1 = \begin{pmatrix} \psi_1 \\ 0 \\ 0 \end{pmatrix}, \qquad \Psi_2 = \begin{pmatrix} 0 \\ 0 \\ \psi_2 \end{pmatrix}, \qquad \Psi_R = \begin{pmatrix} \tilde{\psi}_R^c \\ \chi_R \\ \psi_R \end{pmatrix}, \tag{108}$$

with χ_R is a lepton singlet and ψ_i for each SM left-handed lepton doublet is [25]

$$\psi_{i(R)} = -i\sigma^2 l_{iL(R)} = -i\sigma^2 \begin{pmatrix} \nu_{iL(R)} \\ \ell_{iL(R)} \end{pmatrix}, \qquad i = 1, 2, \tag{109}$$

and for left-handed quarks doublet [24]

$$\psi_{i(R)} = -i\sigma^2 q_{i(R)} = -i\sigma^2 \begin{pmatrix} u_{iL(R)} \\ d_{iL(R)} \end{pmatrix}, \qquad i = 1, 2. \tag{110}$$

Also $\tilde{\psi}_R^c$ has the form as the eqs. (109) and (110), with the difference that there are right-handed and heavy fermions: ℓ_{HR}, u_{HR}, and d_{HR}. The extra doublet ψ_R, is assumed to be heavy enough to agree with EWPD, is T-odd as desired, and the gauge singlet χ_R completes the $SO(5)$ representation.

These fields transform under $SU(5)$ as follows

$$\Psi_1 \to V^*\Psi_1, \qquad \Psi_2 \to V\Psi_2, \qquad \Psi_R \to U\Psi_R, \tag{111}$$

where $U = \exp\left(iu^a\left(\Pi, V\right)T^a\right)$ [26] belongs to the unbroken $SO(5)$ and is a non-linear representation of the $SU(5)$, the function u^a depends on the Goldstone fields Π and the $SU(5)$ rotation V in a non-linear way.

Under the action of T-parity on the multiplets, one has

$$\Psi_1 \leftrightarrow \Omega\Sigma_0\Psi_2, \qquad \Psi_R \to \Omega\Psi_R. \tag{112}$$

We desire that Ψ interacted with other fields which obey linear transformations laws, so we introduce a field $\xi = exp\left(i\Pi/f\right)$. In terms of ξ the field Σ can be expressed as $\Sigma = \xi^2\Sigma_0$, and from the linear transformation of Σ, we have that, by action of T-parity,

$$\xi \xrightarrow{T} \Omega\xi^\dagger\Omega, \tag{113}$$

with invariance under global transformation,

$$\Sigma = \xi^2\Sigma_0 \to V\Sigma V^T, \qquad \xi \to V\xi U^\dagger = U\xi\Sigma_0 V^T\Sigma_0. \tag{114}$$

Recalling that the T-even combination of ψ_1 and ψ_2 are the SM electroweak lepton and quark doublets, while T-odd combination is given a Dirac mass of order $\mathcal{O}(f)$ with the $\tilde{\psi}^c$ through the following non-linear Yukawa Lagrangian

$$\begin{aligned}\mathcal{L}_{Y_H} &= -\kappa f\left(\overline{\Psi}_2\xi + \overline{\Psi}_1\Sigma_0\xi^\dagger\right)\Psi_R - \kappa_2\overline{\Psi_L}\Psi_R - M\overline{\Psi_L^\chi}\Psi_R + \text{h.c.} \\ &= -\kappa f\left(\overline{\Psi}_2\xi + \overline{\Psi}_1\Sigma_0\xi^\dagger\right)\Psi_R - \kappa_2\overline{\tilde{\psi}_L^c}\tilde{\psi}_R^c - M\overline{\chi_L}\chi_R + \text{h.c.}\end{aligned} \tag{115}$$

where we included two incomplete $SO(5)$ multiplets, defined as [23, 27, 51]

$$\Psi_L = \begin{pmatrix} \tilde{\psi}_L^c \\ 0 \\ 0 \end{pmatrix}, \quad \Psi_L^\chi = \begin{pmatrix} 0 \\ \chi_L \\ 0 \end{pmatrix}, \quad \text{with } \Psi_L \xrightarrow{T} \Omega\Psi_L, \text{ and } \Psi_L^\chi \xrightarrow{T} \Omega\Psi_L^\chi. \tag{116}$$

Since we want to calculate first the mass of order $\mathcal{O}(f)$ we can approach $\xi = \exp(i\Pi/f) \approx \mathbb{I}$, then

$$\begin{aligned}
\mathcal{L}_{Y_H} &= -\kappa f \left(\bar{\Psi}_2 \xi + \bar{\Psi}_1 \Sigma_0 \xi^\dagger\right) \Psi_R \\
&\approx -\kappa f \left(\bar{\Psi}_2 + \bar{\Psi}_1 \Sigma_0\right) \Psi_R \\
&= -\kappa f \left(\begin{pmatrix} 0 & 0 & \bar{\psi}_2 \end{pmatrix} + \begin{pmatrix} \bar{\psi}_1 & 0 & 0 \end{pmatrix} \begin{pmatrix} 0 & 0 & 1 \\ 0 & 1 & 0 \\ 1 & 0 & 0 \end{pmatrix} \right) \Psi_R \\
&= -\kappa f \begin{pmatrix} 0 & 0 & \bar{\psi}_2 + \bar{\psi}_1 \end{pmatrix} \begin{pmatrix} \tilde{\psi}^c_R \\ \chi_R \\ \psi_R \end{pmatrix} \\
&= -\kappa f \left(\bar{\psi}_1 + \bar{\psi}_2\right) \tilde{\psi}^c_R,
\end{aligned} \tag{117}$$

we defined the T-odd combination as

$$\psi_H = \frac{1}{\sqrt{2}} \left(\psi_1 + \psi_2\right), \tag{118}$$

and the T-even combination given by

$$\psi_{SM} = \frac{1}{\sqrt{2}} \left(\psi_1 - \psi_2\right). \tag{119}$$

Then,

$$\mathcal{L}_{Y_H} = \sqrt{2}\kappa_1 f \bar{\psi}_H \tilde{\psi}_R + \kappa_2 \Psi^T_R \Psi_R + h.c. \tag{120}$$

As we can see from the eq. (120), the Yukawa Lagrangian gives a Dirac mass $M_- = \sqrt{2}\kappa_1 f$ to the T-odd combination ψ_H, together with $\tilde{\psi}^c_R$, and a mass κ_2 to the Dirac pair from Φ_R. The T-even combination ψ_{SM} remains massless and is identified with the SM lepton or quark doublet.

If now we consider EWSM effects of order $(v_h/f)^2$ the field ξ is

$$\xi \approx \begin{pmatrix} 1 & 0 & 0 & 0 & 0 \\ 0 & 1 - \frac{v_h^2}{8f^2} & \frac{iv_h}{2f} & 0 & -\frac{v_h^2}{8f^2} \\ 0 & \frac{iv_h}{2f} & 1 - \frac{v_h^2}{4f^2} & 0 & \frac{iv_h}{2f} \\ 0 & 0 & 0 & 1 & 0 \\ 0 & -\frac{v_h^2}{8f^2} & \frac{iv_h}{2f} & 0 & 1 - \frac{v_h^2}{8f^2} \end{pmatrix}, \tag{121}$$

and considering as $\tilde{\psi}^c_R = -i\sigma^2\tilde{q}^c_L$ and $\tilde{q}^c_L = \begin{pmatrix} \tilde{u}^c_L & \tilde{d}^c_L \end{pmatrix}^T$, then

$$\Psi_1 = \begin{pmatrix} -d_{1L} \\ u_{1L} \\ 0 \\ 0 \\ 0 \end{pmatrix}, \qquad \Psi_2 = \begin{pmatrix} 0 \\ 0 \\ 0 \\ -d_{2L} \\ u_{2L} \end{pmatrix}, \qquad \Psi_R = \begin{pmatrix} -\tilde{d}^c_R \\ \tilde{u}^c_R \\ \chi_R \\ -d^c_L \\ u^c_L \end{pmatrix}, \tag{122}$$

thus, introducing the above matrix and these multiplets in the Yukawa Lagrangian we have among other terms

$$\mathcal{L}_{Y_H} = \kappa_1 f d^c_L \left(\bar{d}_{1L} + \bar{d}_{2L}\right) + \kappa_1 f u^c_L \left(\bar{u}_{1L} + \bar{u}_{2L}\right)\left(1 - \frac{v_h^2}{8f^2}\right) - \kappa_1 f u^c_R \left(\bar{u}_{1L} + \bar{u}_{2L}\right) + \cdots, \tag{123}$$

defining the T-odd combinations as

$$u_H = \frac{1}{\sqrt{2}}\left(u_{1L} + u_{2L}\right), \qquad d_H = \frac{1}{\sqrt{2}}\left(d_{1L} + d_{2L}\right), \tag{124}$$

the Yukawa Lagrangian is written as

$$\mathcal{L}_{Y_H} = \sqrt{2}\kappa_1 f \bar{d}_H d^c_L + \sqrt{2}\kappa_1 f \bar{u}_H u^c_L \left(1 - \frac{v_h^2}{8f^2}\right) - \sqrt{2}\kappa_1 f u^c_R u_H + \cdots. \tag{125}$$

After EWSB, a small mass splitting between the T-odd up and down-type quarks is induced, and their masses are [28]

$$\begin{aligned} m_{u_H} &= \sqrt{2}\kappa_1 f\left(1 - \frac{v_h^2}{8f^2}\right), \\ m_{d_H} &= \sqrt{2}\kappa_1 f. \end{aligned} \tag{126}$$

The Yukawa Lagrangian $\mathcal{L}_{Y_H}$ fixes the transformation properties of the heavy fermions including their gauge couplings, even more, the non-linear couplings of the right-handed heavy fermions are fixed to be [29] (we change the signs of the second line from eq.(127) and the covariant derivative from eq.(128) in order to obtain the SM couplings)

$$\begin{aligned} \mathcal{L}_{Y_H} &= i\overline{\Psi}_1\gamma^\mu D^*_\mu \Psi_1 + i\overline{\Psi}_2\gamma^\mu D_\mu \Psi_2 \\ &\quad + i\overline{\Psi}^c_R\gamma^\mu\left(\partial\mu - \frac{1}{2}\xi^\dagger\left(D_\mu\xi\right) - \frac{1}{2}\xi\left(\Sigma_0 D^*_\mu \Sigma_0 \xi^\dagger\right)\right)\Psi^c_R \\ &\quad + \Psi^c_R \to \Psi^c_L, \end{aligned} \tag{127}$$

with the covariant derivative defined as

$$D_\mu = \partial_\mu - \sqrt{2}ig_W \left(W_{1\mu}^a Q_1^a + W_{2\mu}^a Q_2^a\right) - \sqrt{2}ig' \left(Y_1 B_{1\mu} + Y_2 B_{2\mu}\right). \tag{128}$$

In order to assign the proper SM hypercharge $y = -1$ to the charged right-handed leptons ℓ_R, which are SU(5) singlets and T-even, the corresponding gauge and T-invariant Lagrangian is similar to the SM one

$$\mathcal{L}'_F = i\bar{\ell}_R \gamma^\mu \left(\partial_\mu + ig' y B_\mu\right) \ell_R. \tag{129}$$

3.4 Top Sector

In order to avoid dangerous contributions to the Higgs mass from one loop quadratic divergences, the third generation Yukawa sector must be modified. The Ψ_1 and Ψ_2 multiplets for the third generation must be completed to representations of the $SU(3)_1$ (upper-left corner) and $SU(3)_2$ (lower-right corner) subgroups of $SU(5)$. These multiplets are (we change the notation $U_{Li} \to t'_{Li}$ and $U_{Ri} \to t'_{Ri}$) [22]

$$Q_1 = \begin{pmatrix} q_1 \\ t'_{L1} \\ 0 \end{pmatrix}, \qquad Q_2 = \begin{pmatrix} 0 \\ t'_{L2} \\ q_2 \end{pmatrix}, \tag{130}$$

they obey the same transformation laws under T-parity and the SU(5) symmetry as Ψ_1 and Ψ_2. The quark doublets are embedded such that

$$q_i = -\sigma^2 \begin{pmatrix} u_{Li} \\ b_{Li} \end{pmatrix}. \tag{131}$$

In addition to the SM right-handed top quark field u_{3R}, which is assumed to be T-even, the model contains two $SU(2)_L$-singlet fermions t'_{R1} and t'_{R2} of hypercharge 2/3, which transform under T-parity as

$$t'_{R1} \leftrightarrow -t'_{R2}. \tag{132}$$

The top Yukawa couplings arise from the Lagrangian of the form

$$\begin{aligned} \mathcal{L}_t =& \frac{1}{2\sqrt{2}} \lambda_1 f \epsilon_{ijk} \epsilon_{xy} \left[\left(\overline{Q}_1\right)_i \left(\Sigma\right)_{jx} \left(\Sigma\right)_{ky} - \left(\overline{Q}_2 \Sigma_0\right)_i \left(\tilde{\Sigma}\right)_{jx} \left(\tilde{\Sigma}\right)_{ky}\right] u_{3R} \\ &+ \lambda_2 f \left(\overline{t}'_{L1} t'_{R1} + \overline{t}'_{L2} t'_{R2}\right) + h.c.\,, \end{aligned} \tag{133}$$

where $\tilde{\Sigma} = \Sigma_0 \Omega \Sigma^\dagger \Omega \Sigma_0$, is the image of Σ under T-parity and the indices $i, j = 1, 2, 3$ and $x, y = 4, 5$.

The T-parity eigenstates are

$$q_{\pm} = \frac{1}{\sqrt{2}}\left(q_1 \mp q_2\right), \qquad t'_{L\pm} = \frac{1}{\sqrt{2}}\left(t'_{L1} \mp t'_{L2}\right), \qquad t'_{R\pm} = \frac{1}{\sqrt{2}}\left(t'_{R1} \mp t'_{R2}\right). \tag{134}$$

Thus, the Lagrangian is

$$\mathcal{L}_t = \lambda_1 f\left(\frac{1}{2}\left(1+c_\upsilon\right)\overline{t}'_{L+} + \frac{s_\upsilon}{\sqrt{2}}\bar{u}_{L+}\right)u_{3R} + \lambda_2 f\left(\overline{t}'_{L+}t'_{R+} + \overline{t}'_{L-}t'_{R-}\right) + h.c. \tag{135}$$

The T-odd states t'_{L-} and t'_{R-} combine to form a Dirac fermion T_-, with mass $M_{T_-} = \lambda_2 f$.
We can see that the T-odd top sector does not mix with the T-even heavy and the T-even SM top quark. The mass terms for the T-even states are diagonalized by [22]

$$t_L = \cos\beta u_{L+} - \sin\beta t'_{L+}, \qquad t_R = \cos\alpha u_{3R} - \sin\alpha t'_{R+}, \tag{136}$$

$$T_{L+} = \sin\beta u_{L+} + \cos\beta t'_{L+}, \qquad T_{R+} = \sin\alpha u_{3R} + \cos\alpha t'_{R+}, \tag{137}$$

where t is identified with the SM top and T_+ is its T-even heavy partner.

The masses of the two T-even Dirac fermios to leading order in (υ_h/f) [22] read

$$m_t = \frac{\lambda_1\lambda_2\upsilon_h}{\sqrt{\lambda_1^2+\lambda_2^2}}, \qquad m_{T_+} = \sqrt{\lambda_1^2+\lambda_2^2}f. \tag{138}$$

As the Yukawa couplings of the other SM quarks are small, there is no need to introduce additional heavy partners to cancel their quadratically divergent contribution of the Higgs mass. Then the Yukawa coupling for the other up-type and down-type fermions is given by

$$\begin{aligned}
\mathcal{L}_{up} &= -\frac{1}{2\sqrt{2}}\lambda_u f\epsilon_{ijk}\epsilon_{xy}\left[\left(\overline{Q}_1\right)_i\left(\Sigma\right)_{jx}\left(\Sigma\right)_{ky} - \left(\overline{Q}_2\Sigma_0\right)_i\left(\tilde{\Sigma}\right)_{jx}\left(\tilde{\Sigma}\right)_{ky}\right]u_R + h.c.,\\
\mathcal{L}_{down} &= \frac{i\lambda_d}{2\sqrt{2}}f\epsilon_{ij}\epsilon_{xyz}\left[\left(\overline{\Psi}_2\right)_x\left(\Sigma\right)_{iy}\left(\Sigma\right)_{jz}X - \left(\overline{\Psi}_1\Sigma_0\right)_x\left(\tilde{\Sigma}\right)_{iy}\left(\tilde{\Sigma}\right)_{jz}\tilde{X}\right]d_R + h.c.,
\end{aligned} \tag{139}$$

and their masses are [24]

$$\begin{aligned}
m_u^i &= \lambda_u^i\upsilon_h\left(1 - \frac{\upsilon_h^2}{3f^2}\right),\\
m_d^j &= \lambda_d^j\upsilon_h\left(1 - \frac{\upsilon_h^2}{12f^2}\right),
\end{aligned} \tag{140}$$

with $i = 1, 2$ and $j = 1, 2, 3$.

4 Generic New Physics contributions to LFV processes

As we know, the SM contributions to the LFV processes like $\mu \to e\gamma$ and $\mu \to ee\overline{e}$ are negligible since they are proportional to the observed neutrino masses [13, 14, 30–32]. Nevertheless, the new LHT contributions shall be considered and they will generally give branching ratios only slightly below than current upper limits. One expects that the dominant contributions come from the exchange of the new vector bosons and heavy fermions required to realize the discrete symmetry T that allows the Littlest Higgs Model to remain viable with a typical mass scale accessible to LHC. In this section we will discuss generic contributions to the LFV processes that will be studied in this Ph. D. Thesis. The following material was published in the article [33].
Two types of diagrams contribute to $\mu \to ee\overline{e}$ [1], which are shown in Figure 5. In the diagrams of

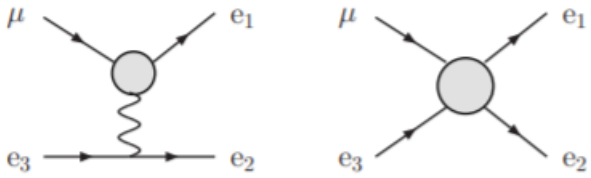

Figure 5: Generic penguin and box diagrams for $\mu \to ee\overline{e}$.

penguin type the exchanged vector boson can be a γ or a Z but not a heavy vector boson because the coupling is forbidden by T-parity. The amplitude for this process also receives contributions from box diagrams. The total amplitude for $\mu(p) \to e(p_1)e(p_2)\overline{e}(p_3)$ can be written [25]

$$\mathcal{M} = \mathcal{M}_{\gamma-penguin} + \mathcal{M}_{Z-penguin} + \mathcal{M}_{box}, \tag{141}$$

with

$$\begin{aligned}\mathcal{M}_{\gamma-penguin} = \frac{e^2}{Q^2}\overline{u}(p_1)[Q^2\gamma^\mu(A_1^L P_L + A_1^R P_R) + m_\mu i\sigma^{\mu\nu}Q_\nu(A_2^L P_L + A_2^R P_R)]u(p) \\ \times \overline{u}(p_2)\gamma_\mu \upsilon(p_3) - (p_1 \leftrightarrow p_2),\end{aligned} \tag{142}$$

$$\begin{aligned}\mathcal{M}_{Z-penguin} = \frac{e^2}{M_Z^2}\overline{u}(p_1)[\gamma^\mu(F_L P_L + F_R P_R)]u(p)\overline{u}(p_2)[\gamma_\mu(Z_L^e P_L + Z_R^e P_R)]\upsilon(p_3) \\ - (p_1 \leftrightarrow p_2),\end{aligned} \tag{143}$$

[1] We do not discuss in detail $\mu \to e\gamma$ or $Z \to \mu\bar{e}$, which can be seen as building blocks of the $\mu \to ee\bar{e}$ decays.

$$
\begin{aligned}
\mathcal{M}_{box} &= e^2 B_1^L [\overline{u}(p_1)\gamma^\mu P_L u(p)][\overline{u}(p_2)\gamma_\mu P_L \upsilon(p_3)] \\
&+ e^2 B_1^R [\overline{u}(p_1)\gamma^\mu P_R u(p)][\overline{u}(p_2)\gamma_\mu P_R \upsilon(p_3)] \\
&+ e^2 B_2^L \{[\overline{u}(p_1)\gamma^\mu P_L u(p)][\overline{u}(p_2)\gamma_\mu P_R \upsilon(p_3)] - (p_1 \leftrightarrow p_2)\} \\
&+ e^2 B_2^R \{[\overline{u}(p_1)\gamma^\mu P_R u(p)][\overline{u}(p_2)\gamma_\mu P_L \upsilon(p_3)] - (p_1 \leftrightarrow p_2)\} \\
&+ e^2 B_3^L \{[\overline{u}(p_1) P_L u(p)][\overline{u}(p_2) P_L \upsilon(p_3)] - (p_1 \leftrightarrow p_2)\} \\
&+ e^2 B_3^R \{[\overline{u}(p_1) P_R u(p)][\overline{u}(p_2) P_R \upsilon(p_3)] - (p_1 \leftrightarrow p_2)\} \\
&+ e^2 B_4^L \{[\overline{u}(p_1)\sigma^{\mu\nu} P_L u(p)][\overline{u}(p_2)\sigma_{\mu\nu} P_L \upsilon(p_3)] - (p_1 \leftrightarrow p_2)\} \\
&+ e^2 B_4^R \{[\overline{u}(p_1)\sigma^{\mu\nu} P_R u(p)][\overline{u}(p_2)\sigma_{\mu\nu} P_R \upsilon(p_3)] - (p_1 \leftrightarrow p_2)\}.
\end{aligned}
\tag{144}
$$

We have defined new vertex form factors in the penguin amplitudes

$$
A_1^{L,R} = F_{L,R}^\gamma / Q^2, \quad A_2^{L,R} = (F_M^\gamma \pm i F_E^\gamma)/m_\mu, \quad F_{L,R} = -F_{L,R}^Z,
\tag{145}
$$

and used that $Q^2 \ll M_Z^2$ in Eq. (143). $Z_{L,R}^e$ are the corresponding Z couplings to the electron in the SM. The dipole form factors $F_{M,E}^Z$ are dropped from the amplitude because their contributions are effectively suppressed by a factor $m_\mu^2/M_{W_H}^2$. Then, the total width can be written as [25]

$$
\begin{aligned}
\Gamma(\mu \to ee\bar{e}) = \frac{\alpha^2 m_\mu^5}{32\pi} \Big[& |A_1^L|^2 + |A_1^R|^2 - 2(A_1^L A_2^{R*} + A_2^L A_1^{R*} + h.c.) \\
&+ (|A_2^L|^2 + |A_2^R|^2)\left(\frac{16}{3}\ln\frac{m_\mu}{m_e} - \frac{22}{3}\right) + \frac{1}{6}(|B_1^L|^2 + |B_1^R|^2) + \frac{1}{3}(|B_2^L|^2 + |B_2^R|^2) \\
&+ \frac{1}{24}(|B_3^L|^2 + |B_3^R|^2) + 6(|B_4^L|^2 + |B_4^R|^2) - \frac{1}{2}(B_3^L B_4^{L*} + B_3^R B_4^{R*} + h.c.) \\
&+ \frac{1}{3}(A_1^L B_1^{L*} + A_1^R B_1^{R*} + A_1^L B_2^{L*} + A_1^R B_2^{R*} + h.c.) \\
&- \frac{2}{3}(A_2^R B_1^{L*} + A_2^L B_1^{R*} + A_2^L B_2^{R*} + A_2^R B_2^{L*} + h.c.) \\
&+ \frac{1}{3}\Big\{2(|F_{LL}|^2 + |F_{RR}|^2) + |F_{LR}|^2 + |F_{RL}|^2 \\
&+ (B_1^L F_{LL}^* + B_1^R F_{RR}^* + B_2^L F_{LR}^* + B_2^R F_{RL}^* + h.c.) + 2(A_1^L F_{LL}^* + A_1^R F_{RR}^* + h.c.) \\
&+ (A_1^L F_{LR}^* + A_1^R F_{RL}^* + h.c.) - 4(A_2^R F_{LL}^* + A_2^L F_{RR}^* + h.c.) \\
&- 2(A_2^L F_{RL}^* + A_2^R F_{LR}^* + h.c.) \Big\} \Big].
\end{aligned}
\tag{146}
$$

We are going to develop each term of the total amplitude explicitly.

4.1 $\mathcal{M}_{\gamma-penguin}$ contribution

The total amplitude is given by Eq. (141)

$$\mathcal{M} = \mathcal{M}_{\gamma-penguin} + \mathcal{M}_{Z-penguin} + \mathcal{M}_{box},$$

so, the total width is

$$\begin{aligned}\Gamma(\mu \to ee\overline{e}) = &|\mathcal{M}_{\gamma-penguin}|^2 + |\mathcal{M}_{Z-penguin}|^2 + |\mathcal{M}_{box}|^2 \\ &+ \mathcal{M}_{\gamma-penguin}\mathcal{M}^{\dagger}_{Z-penguin} + \mathcal{M}_{\gamma-penguin}\mathcal{M}^{\dagger}_{box} + \mathcal{M}_{Z-penguin}\mathcal{M}^{\dagger}_{box} + h.c.\end{aligned} \tag{147}$$

From the Eq. (142), writing the second term explicitly

$$\begin{aligned}\mathcal{M}_{\gamma-penguin} = &\frac{e^2}{Q^2}\overline{u}(p_1)[Q^2\gamma^{\mu}(A_1^L P_L + A_1^R P_R) + m_{\mu} i\sigma^{\mu\nu}Q_{\nu}(A_2^L P_L + A_2^R P_R)]u(p) \times \overline{u}(p_2)\gamma_{\mu}\upsilon(p_3) \\ &- (p_1 \leftrightarrow p_2),\end{aligned} \tag{148}$$

where Q and R are the vector bosons momenta entering the vertex. They are defined as $Q = p - p_1$, and $R = p - p_2$. $|\mathcal{M}_{\gamma-penguin}|^2$ has terms whose behaviors are $\frac{1}{Q^2}$, $\frac{1}{R^2}$, $\frac{1}{Q^2R^2}$, $\frac{1}{Q^4}$, and $\frac{1}{R^4}$. We will study them in two parts: the first three of them do not have any problems and their computation is direct, but in the last ones we need to proceed carefully because they are divergent.
Then, we can write $|\mathcal{M}_{\gamma-penguin}|^2$ as follows

$$|\mathcal{M}_{\gamma-penguin}|^2 = \Lambda_1\left(\frac{1}{Q^2}, \frac{1}{R^2}\right) + \Lambda_2\left(\frac{1}{Q^2R^2}, \frac{1}{Q^4}, \frac{1}{R^4}\right). \tag{149}$$

Although Λ_1 depends on $\frac{1}{Q^2}$ and $\frac{1}{R^2}$, it is possible to remove them if we consider $m_e = 0$. Hence, $Q^2 = 2(p_2 \cdot p_3)$ and $R^2 = 2(p_1 \cdot p_3)$. Developing Λ_1 we obtain

$$\begin{aligned}\Lambda_1 = &16e^4\left(|A_1^L|^2 + |A_1^R|^2\right)[4(p\cdot p_3)(p_1\cdot p_2) + (p\cdot p_2)(p_1\cdot p_3) + (p\cdot p_1)(p_2\cdot p_3)] \\ &- 8e^4 m_{\mu}^2\left(A_2^R A_1^{L*} + A_1^L A_2^{R*} + A_2^L A_1^{R*} + A_1^R A_2^{L*}\right)[4(p_1\cdot p_2) + (p_1\cdot p_3) + (p_2\cdot p_3)].\end{aligned} \tag{150}$$

Λ_2 is expressed as the sum of three contributions

$$\Lambda_2\left(\frac{1}{Q^2R^2}, \frac{1}{Q^4}, \frac{1}{R^4}\right) = \Lambda_{21}\left(\frac{1}{Q^4}\right) + \Lambda_{22}\left(\frac{1}{R^4}\right) + \Lambda_{23}\left(\frac{1}{Q^2R^2}\right). \tag{151}$$

Λ_2 is more difficult than Λ_1, since if we consider $m_e = 0$, Λ_2 is divergent, then now we must take massive electrons. The first term of the Eq. (151) is

$$\begin{aligned}\Lambda_{21} = 16\frac{m_\mu^2 e^4}{Q^4}\left(|A_2^L|^2+|A_2^R|^2\right)\left[m_e^2\left(2(p\cdot p_3)(p_1\cdot p_3)-(p\cdot p_1)(p_2\cdot p_3)\right)+2(p\cdot p_2)(p_1\cdot p_2)\right] \\ -(p\cdot p_1)m_e^4+2(p_2\cdot p_3)\left[(p\cdot p_2)(p_1\cdot p_2)+(p\cdot p_3)(p_1\cdot p_3)\right],\end{aligned} \tag{152}$$

here, as $Q = p - p_1$ is comparable with m_e since the photon is massless, $e(p_1)$ is considered massless too and the $e(p_2)\overline{e}(p_3)$ pair is massive. The same happens to Λ_{22}, because we just change $(p_1 \leftrightarrow p_2)$

$$\begin{aligned}\Lambda_{22} = 16\frac{m_\mu^2 e^4}{R^4}\left(|A_2^L|^2+|A_2^R|^2\right)\left[m_e^2\left(2(p\cdot p_3)(p_2\cdot p_3)-(p\cdot p_2)(p_1\cdot p_3)\right)+2(p\cdot p_1)(p_1\cdot p_2)\right] \\ -(p\cdot p_2)m_e^4+2(p_1\cdot p_3)\left[(p\cdot p_1)(p_1\cdot p_2)+(p\cdot p_3)(p_2\cdot p_3)\right].\end{aligned} \tag{153}$$

In Λ_{23} the term $\frac{1}{Q^2R^2}$ appears, so it is necessary to consider now $e(p_1)$,$e(p_2)$ massless and $\overline{e}(p_3)$ massive

$$\begin{aligned}\Lambda_{23} = 4\frac{m_\mu^2 e^4}{Q^2R^2}\left(|A_2^L|^2+|A_2^R|^2\right)\left(-8(p\cdot p_3)(p_1\cdot p_2)^2+8(p\cdot p_2)(p_1\cdot p_3)(p_1\cdot p_2)+8(p\cdot p_1)(p_2\cdot p_3)(p_1\cdot p_2)\right. \\ \left.+m_e^2\left[4(p\cdot p_1)(p_1\cdot p_2)-4(p\cdot p_2)(p_1\cdot p_2)-5(p\cdot p_3)(p_1\cdot p_2)+(p\cdot p_2)(p_1\cdot p_3)+(p\cdot p_1)(p_2\cdot p_3)\right]\right).\end{aligned} \tag{154}$$

The photon penguin contribution to the $\mu \to 3e$ decay width is given by

$$\Gamma_{\gamma-penguin} = \frac{1}{2m_\mu}\int\frac{d^3p_1}{(2\pi)^3 2E_1}\int\frac{d^3p_2}{(2\pi)^3 2E_2}\int\frac{d^3p_3}{(2\pi)^3 2E_3}(2\pi)^4\delta^{(4)}(p-p_1-p_2-p_3)\times\frac{1}{2}\times\frac{1}{2}\sum_{spin}|\mathcal{M}_{\gamma-penguin}|^2. \tag{155}$$

We have added 1/2 twice explicitly, one comes from the two indistinguishable electrons in the final state, and the other one because the initial state is a muon, with two possible polarizations.
Before starting, an important tool that will help us for analyzing the photon penguin contribution to the $\mu \to 3e$ decay width is to solve the next type of integral

$$\Delta = \frac{e^4}{8(2\pi)^5 m_\mu}\int\frac{d^3p_j}{2E_j}\int\frac{d^3p_k}{2E_k}\int\frac{d^3p_l}{2E_l}\delta^{(4)}(p_i-p_j-p_k-p_l)\times G(p_i\cdot p_j)(p_k\cdot p_l), \quad i\neq j\neq k\neq l, \tag{156}$$

where G is a constant and the e^4 factor is extracted from the $|\mathcal{M}_{\gamma-penguin}|^2$.
For this integral we are assuming that $m_e = 0$ and taking the particular case

$$p_i = p, \quad p_j = p_3, \quad p_k = p_1, \quad p_l = p_2\,, \tag{157}$$

with

$$p^2 = m_\mu^2, \quad p_1^2 = p_2^2 = p_3^2 = 0. \tag{158}$$

Then

$$\Delta = \frac{Ge^4}{8(2\pi)^5 m_\mu} \int \frac{d^3p_1}{2E_1} \int \frac{d^3p_2}{2E_2} \int \frac{d^3p_3}{2E_3} \delta^{(4)}(p - p_1 - p_2 - p_3) \times (p \cdot p_3)(p_1 \cdot p_2), \tag{159}$$

making $q = p - p_2 = p_1 + p_3$, we can write (159) as

$$\Delta = G \int \frac{d^3p_2}{2E_2} p^\lambda p_2^\sigma I_{\lambda\sigma}(q), \tag{160}$$

with

$$I_{\lambda\sigma}(q) = \int \frac{d^3p_1}{2E_1} \int \frac{d^3p_3}{2E_3} \delta^{(4)}(q - p_1 - p_3) p_{1\sigma} p_{3\lambda}, \tag{161}$$

$I_{\lambda\sigma}$ is a rank-2 tensor and can depend only on the 4-vector q. So the most general form for $I_{\lambda\sigma}$ can be written as [9]

$$I_{\lambda\sigma}(q) = Aq^2 g_{\lambda\sigma} + Bq_\lambda q_\sigma. \tag{162}$$

Multiplying by $g^{\lambda\sigma}$ the Eqs. (161) and (162) and matching them

$$(4A + B)q^2 = \int \frac{d^3p_1}{2E_1} \int \frac{d^3p_3}{2E_3} \delta^{(4)}(q - p_1 - p_3)(p_1 \cdot p_3). \tag{163}$$

Now contracting the two equations with $q^\lambda q^\sigma$, and as $p_1^2 = p_3^2 = 0$

$$(A + B)q^4 = \int \frac{d^3p_1}{2E_1} \int \frac{d^3p_3}{2E_3} \delta^{(4)}(q - p_1 - p_3)(p_1 \cdot p_3)^2. \tag{164}$$

Eqs. (163) and (164) have Lorentz invariant quantities on both sides, so we can choose any frame for evaluating these integrals. The convenient frame is COM, where

$$p - p_2 = 0 = p_1 + p_3, \tag{165}$$

since $m_e = 0$,

$$E_1 = E_3 = |\vec{p_1}| = |\vec{p_3}| = k, \tag{166}$$

$$(p_1 \cdot p_3)_{COM} = k^2 - \vec{p_1} \cdot \vec{p_3} = k^2 + |\vec{p_1}|^2 = k^2 + k^2 = 2k^2. \tag{167}$$

Thus, (163) can be written

$$\begin{aligned}(4A+B)q^2_{COM} &= \int \frac{d^3p_1}{2E_1}\int \frac{d^3p_3}{2E_3}\delta^{(4)}(q-p_1-p_3)(p_1\cdot p_3)_{COM}\\ &= \int \frac{d^3p_1}{2k}\int \frac{d^3p_3}{2k}\delta(q_0-2k)\delta^{(3)}(\vec{q}-\vec{p_1}-\vec{p_3})2k^2\\ &= \int \frac{d^3p_1}{2}\delta(q_0-2k)\\ &= \frac{1}{4}\int k^2 dk d\Omega\delta(\frac{q_0}{2}-k)\\ &= \frac{\pi q_0^2}{4},\end{aligned} \tag{168}$$

in the COM frame $q=(q_0,\vec{0})$, then $q^2_{COM}=q_0^2$, in (168)

$$4A+B=\frac{\pi}{4}. \tag{169}$$

For (164)

$$\begin{aligned}(A+B)q^4_{COM} &= \int \frac{d^3p_1}{2E_1}\int \frac{d^3p_3}{2E_3}\delta^{(4)}(q-p_1-p_3)(p_1\cdot p_3)^2_{COM}\\ &= \frac{1}{2}\int k^4 dk d\Omega\delta(\frac{q_0}{2}-k)\\ &= \frac{\pi q_0^4}{8},\end{aligned} \tag{170}$$

thus,

$$A+B=\frac{\pi}{8}, \tag{171}$$

solving the system of equations (169) and (171) we obtain $A=\frac{\pi}{24}$ and $B=\frac{\pi}{12}$, substituting them in (162)

$$I_{\lambda\sigma}(q)=\frac{\pi}{24}(q^2 g_{\lambda\sigma}+2q_\lambda q_\sigma). \tag{172}$$

The Eq. (160) takes the shape

$$\begin{aligned}\Delta &= \frac{\pi}{24}G\int \frac{d^3p_2}{2E_2}p^\lambda p_2^\sigma(q^2 g_{\lambda\sigma}+2q_\lambda q_\sigma)\\ &= \frac{\pi}{24}G\int \frac{d^3p_2}{2E_2}(q^2(p\cdot p_2)+2(p\cdot q)(p_2\cdot q)), \qquad q\equiv p-p_2\\ &= \frac{\pi}{24}G\int \frac{d^3p_2}{2E_2}((p^2+p_2^2-2p\cdot p_2)(p\cdot p_2)+2(p^2-p\cdot p_2)(p\cdot p_2-p_2^2)),\end{aligned} \tag{173}$$

in the muon rest system

$$p=(m_\mu,\vec{0}) \qquad \text{and} \qquad p_2=(E_2,\vec{p}_2), \tag{174}$$

thus,

$$p \cdot p_2 = m_\mu E_2, \quad p_2^2 = 0, \quad p^2 = m_\mu^2, \tag{175}$$

so (173) results

$$\begin{aligned}\Delta &= \frac{\pi}{24} G \int \frac{d^3p_2}{2E_2}((m_\mu^2 - 2m_\mu E_2)m_\mu E_2 + 2(m_\mu^2 - m_\mu E_2)m_\mu E_2) \\ &= \frac{\pi}{24} G \int \frac{d^3p_2}{2E_2}(3m_\mu - 4E_2)m_\mu^2 E_2 \\ &= \frac{4m_\mu^2\pi^2}{48} G \int_0^{m_\mu/2} dE_2(3m_\mu E_2^2 - 4E_2^3).\end{aligned} \tag{176}$$

The limits have been chosen as follows: the lower limit of the electron energy $e(p_2)$ can certainly be zero if the $e(p_1)\overline{e}(p_3)$ pair carries the entire energy. The upper limit is obtained when the $e(p_1)\overline{e}(p_3)$ pair is emitted in the same direction, opposite to the direction of the electron $e(p_2)$. In this case $p_2 = p_1 + p_3$, it implies that $E_2 = E_1 + E_3$ and we are considering that $m_e = 0$. Furthermore, $m_\mu = E_1 + E_2 + E_3$ by conservation of energy, then substituting it in the above relation we obtain $E_2 = m_\mu/2$.
Integrating the Eq. (176), we obtain

$$\Delta = \frac{\alpha^2 m_\mu^5}{3072\pi} G. \tag{177}$$

Another type of integral which will be of aid is

$$\Omega = \frac{e^4}{8(2\pi)^5 m_\mu} \int \frac{d^3p_j}{2E_j} \int \frac{d^3p_k}{2E_k} \int \frac{d^3p_l}{2E_l} \delta^{(4)}(p_i - p_j - p_k - p_l) \times G(p_j \cdot p_k), \quad i \neq j \neq k \neq l, \tag{178}$$

where G is a constant. We solve the case $p_i = p$, $p_j = p_1$, $p_k = p_2$, and $p_l = p_3$ and p_1, p_2, p_3 satisfy that $p_1^2 = p_2^2 = p_3^2 = 0$. Then

$$\Omega = \frac{Ge^4}{64(2\pi)^5 m_\mu} \int \frac{d^3p_1}{|\vec{p}_1|} \int \frac{d^3p_2}{|\vec{p}_2|} \int \frac{d^3p_3}{|\vec{p}_3|} \delta^{(4)}(p - p_1 - p_2 - p_3)(p_1 \cdot p_2). \tag{179}$$

Integrating on $\vec{p}_3$

$$\Omega = \frac{Ge^4}{64(2\pi)^5 m_\mu} \int \frac{d^3p_1}{|\vec{p}_1|} \int \frac{d^3p_2}{|\vec{p}_2|} \frac{1}{|\vec{p}_1 + \vec{p}_2|} \delta(m_\mu - |\vec{p}_1| - |\vec{p}_2| - |\vec{p}_1 + \vec{p}_2|)(p_1 \cdot p_2). \tag{180}$$

Defining u as follows

$$u \equiv \sqrt{|\vec{p}_1|^2 + |\vec{p}_2|^2 + 2|\vec{p}_1||\vec{p}_2| cos\theta}, \tag{181}$$

and

$$d^3p_2 = 2\pi \frac{u}{|\vec{p}_1|} |\vec{p}_2| d|\vec{p}_2| du, \tag{182}$$

substituting last two equations in (180)

$$\Omega = \frac{Ge^4}{64(2\pi)^4 m_\mu}\int \frac{d^3p_1}{|\vec{p}_1|^2}\int d|\vec{p}_2| du \delta(m_\mu - |\vec{p}_1| - |\vec{p}_2| - u)(p_1 \cdot p_2). \tag{183}$$

We have that $p = (m_\mu, 0)$ amd $p = p_1 + p_2 + p_3$, then

$$p_1 \cdot p_2 = \frac{m_\mu^2}{2} - m_\mu |\vec{p}_3|. \tag{184}$$

The limits for $|\vec{p}_2|$ are calculated from Eq. (181), since

$$u_\pm = ||\vec{p}_1| \pm |\vec{p}_2||, \tag{185}$$

therefore

$$\frac{m_\mu}{2} - |\vec{p}_1| \leq |\vec{p}_2| \leq \frac{m_\mu}{2} \quad \text{and} \quad |\vec{p}_1| \leq \frac{m_\mu}{2}. \tag{186}$$

As $d^3p_1 = 4\pi|\vec{p}_1|^2 d|\vec{p}_1|$, and evaluating the integral on u the Eq. (183) is transformed in

$$\Omega = \frac{\pi G}{16(2\pi)^4 m_\mu}\int_0^{m_\mu/2} d|\vec{p}_1| \int_{m_\mu/2-|\vec{p}_1|}^{m_\mu/2} d|\vec{p}_2| \left(-\frac{1}{2}m_\mu^2 + m_\mu|\vec{p}_1| + m_\mu|\vec{p}_2|\right), \tag{187}$$

finally we obtain

$$\Omega = \frac{\alpha^2 m_\mu^3}{768\pi} G. \tag{188}$$

So, from the Eqs. (177) and (188) we can get the contribution to the width of the photon due to the term $\Lambda_1\left(\frac{1}{Q^2}, \frac{1}{R^2}\right)$

$$\Gamma_{\Lambda_1} = \frac{\alpha^2 m_\mu^5}{32\pi}\left[\left(|A_1^L|^2 + |A_1^R|^2\right) - 2\left(A_2^R A_1^{L*} + A_1^L A_2^{R*} + A_2^L A_1^{R*} + A_1^R A_2^{L*}\right)\right]. \tag{189}$$

Now we are going to analyze the contribution of the $\Lambda_2\left(\frac{1}{Q^2R^2}, \frac{1}{Q^4}, \frac{1}{R^4}\right)$ term. In this case, we have that

$$p = (m_\mu, 0),\ p_1 = (|\vec{p}_1|, \vec{p}_1),\quad p_2 = (|\vec{p}_2|, \vec{p}_2),\quad p_1 = (E_3, \vec{p}_3), \tag{190}$$

then

$$\begin{aligned}\Gamma_{\Lambda_2} &= \frac{1}{8m_\mu}\int \frac{d^3p_1}{(2\pi)^3 2|\vec{p}_1|}\int \frac{d^3p_2}{(2\pi)^3 2|\vec{p}_2|}\int \frac{d^3p_3}{(2\pi)^3 2E_3}(2\pi)^4\delta^{(4)}(p - p_1 - p_2 - p_3)\Lambda_2\left(\frac{1}{Q^2R^2}, \frac{1}{Q^4}, \frac{1}{R^4}\right) \\ &= \frac{1}{8m_\mu}\int \frac{d^3p_1}{(2\pi)^3 2|\vec{p}_1|}\int \frac{d^3p_2}{(2\pi)^3 2|\vec{p}_2|}\int \frac{d^3p_3}{(2\pi)^3 2E_3}(2\pi)^4\delta^{(4)}(p - p_1 - p_2 - p_3)\left(\Lambda_{21} + \Lambda_{22} + \Lambda_{23}\right).\end{aligned} \tag{191}$$

We integrate first the Λ_{21} term. In this case $e(p_1)$ is massless and $e(p_2)\overline{e}(p_3)$ are massive.

$$\Gamma_{\Lambda_{21}} = \frac{e^4 m_\mu (|A_2^L|^2 + |A_2^R|^2)}{4(2\pi)^5} \int \frac{d^3p_1}{|\vec{p}_1|} \int \frac{d^3p_2}{E_2} \int \frac{d^3p_3}{E_3} \delta^{(4)}(p - p_1 - p_2 - p_3) \times G_{21}, \tag{192}$$

where

$$G_{21} = \frac{1}{(m_\mu - 2|\vec{p}_1|)^2} \left[\frac{m_\mu^3}{2}(E_2 + E_3) - 2m_\mu^2 E_2 E_3 + m_\mu |\vec{p}_1| \left(-\frac{m_e^2}{2} - m_\mu (E_2 + E_3) + 4E_2 E_3 \right) + m_e^2 |\vec{p}_1|^2 \right]. \tag{193}$$

Integrating on p_3

$$\Gamma_{\Lambda_{21}} = \frac{e^4 m_\mu (|A_2^L|^2 + |A_2^R|^2)}{4(2\pi)^5} \int \frac{d^3p_1}{|\vec{p}_1|} \int \frac{d^3p_2}{E_2} \frac{1}{E_3} \delta(m_\mu - |\vec{p}_1| - E_2 - E_3) \times G_{21}, \tag{194}$$

with $\vec{p}_3^2 = (\vec{p}_1 + \vec{p}_2)^2$, then

$$E_3 = \sqrt{|\vec{p}_1 + \vec{p}_2|^2 + m_e^2} = \sqrt{|\vec{p}_1|^2 + |\vec{p}_2|^2 + 2|\vec{p}_1||\vec{p}_2| cos\theta + m_e^2} \equiv u \tag{195}$$

also we have that

$$d^3p_1 = 2\pi \frac{u|\vec{p}_1|}{|\vec{p}_2|} d|\vec{p}_1| du, \tag{196}$$

hence,

$$\Gamma_{\Lambda_{21}} = \frac{e^4 m_\mu (|A_2^L|^2 + |A_2^R|^2)}{4(2\pi)^5} \int \frac{d^3p_2}{|\vec{p}_2| E_2} \int d|\vec{p}_1| du \delta(m_\mu - |\vec{p}_1| - E_2 - u) \times G_{21}|_{E_3 = u}. \tag{197}$$

The integration on u allows us to define the limits for $|\vec{p}_1|$. These limits are given by

$$\frac{m_\mu(m_\mu - 2E_2)}{2(m_\mu - E_2 + \sqrt{E_2^2 - m_e^2})} \leq |\vec{p}_1| \leq \frac{m_\mu(m_\mu - 2E_2)}{2(m_\mu - E_2 - \sqrt{E_2^2 - m_e^2})}. \tag{198}$$

Considering $d^3p_2 = 4\pi E_2 |\vec{p}_2| dE_2$ and the limits for E_2 as $(E_2)_{min} = m_e$ and $(E_2)_{max} = m_\mu/2$

$$\Gamma_{\Lambda_{21}} = \frac{e^4 m_\mu (|A_2^L|^2 + |A_2^R|^2)}{4(2\pi)^5} \int_{m_e}^{m_\mu/2} dE_2 \int_{|\vec{p}_1|_-}^{|\vec{p}_1|_+} d|\vec{p}_1| \times G_{21}|_{u = m_\mu - |\vec{p}_1| - E_2}. \tag{199}$$

The integral (199) is solved by using Mathematica 10.0 [34].

$\Gamma_{\Lambda_{22}}$ is completely identical to $\Gamma_{\Lambda_{21}}$ because we just change $(p_1 \leftrightarrow p_2)$ the physical argument is the same.

Now, we work with the last term

$$\begin{aligned}\Gamma_{\Lambda_{23}} &= \frac{1}{8m_\mu}\int\frac{d^3p_1}{(2\pi)^3 2|\vec{p}_1|}\int\frac{d^3p_2}{(2\pi)^3 2|\vec{p}_2|}\int\frac{d^3p_3}{(2\pi)^3 2E_3}(2\pi)^4\delta^{(4)}(p-p_1-p_2-p_3)\times\Lambda_{23}\\ &= \frac{e^4(|A_2^L|^2+|A_2^R|^2)}{16(2\pi)^5}\int\frac{d^3p_1}{|\vec{p}_1|}\int\frac{d^3p_2}{|\vec{p}_2|}\int\frac{d^3p_3}{E_3}\delta^{(4)}(p-p_1-p_2-p_3)\times\bigstar\end{aligned} \tag{200}$$

where

$$\begin{aligned}\bigstar = &\frac{1}{(m_\mu-2|\vec{p}_1|)(m_\mu-2|\vec{p}_2|)}\left[-8E_3\left(A^2-2Am_\mu E_3+m_\mu^2E_3^2\right)\right.\\ &+8|\vec{p}_2|\left(AB-Bm_\mu E_3+m_\mu|\vec{p}_2|(m_\mu E_3-A)\right)++8|\vec{p}_1|\left(AB-Bm_\mu E_3+m_\mu|\vec{p}_1|(m_\mu E_3-A)\right)\\ &\left.+m_e^2(|\vec{p}_1|(4A-4m_\mu E_3+B)-m_\mu|\vec{p}_1|^2+|\vec{p}_2|(-4A-+4m_\mu E_3+B)-m_\mu|\vec{p}_2|^2-5AE_3+5m_\mu E_3^2)\right],\end{aligned} \tag{201}$$

and $A=\frac{m_\mu^2+m_e^2}{2}$ and $B=\frac{m_\mu^2-m_e^2}{2}$.
Integrating on p_3

$$\Gamma_{\Lambda_{23}} = \frac{e^4(|A_2^L|^2+|A_2^R|^2)}{16(2\pi)^5}\int\frac{d^3p_1}{|\vec{p}_1|}\int\frac{d^3p_2}{|\vec{p}_2|}\frac{1}{E_3}\delta(m_\mu-|\vec{p}_1|-|\vec{p}_2|-E_3)\times\bigstar, \tag{202}$$

with $|\vec{p}_3|^2=|\vec{p}_1+\vec{p}_2|^2$, defining as

$$E_3=\sqrt{|\vec{p}_1+\vec{p}_2|^2+m_e^2}=\sqrt{|\vec{p}_1|^2+|\vec{p}_2|^2+2|\vec{p}_1||\vec{p}_2|cos\theta+m_e^2}\equiv u, \tag{203}$$

$$d^3p_2 = 2\pi\frac{u|\vec{p}_2|}{|\vec{p}_1|}d|\vec{p}_2|du, \tag{204}$$

the Eq. (202) transforms to

$$\Gamma_{\Lambda_{23}} = \frac{e^4(|A_2^L|^2+|A_2^R|^2)}{16(2\pi)^4}\int\frac{d^3p_1}{|\vec{p}_1|^2}\int d|\vec{p}_2|du\delta(m_\mu-|\vec{p}_1|-|\vec{p}_2|-u)\times\bigstar|_{E_3=u}. \tag{205}$$

From the Eq. (233) we can see that $u_\pm=\sqrt{|\vec{p}_1+\vec{p}_1|^2+m_e^2}$, therefore

$$\frac{m_\mu^2-m_e^2-2m_\mu|\vec{p}_1|}{2m_\mu}\leq|\vec{p}_2|\leq\frac{m_\mu^2-m_e^2-2m_\mu|\vec{p}_1|}{2(m_\mu-2|\vec{p}_1|)}, \tag{206}$$

substituting $d^3p_1=4\pi|\vec{p}_1|^2d|\vec{p}_1|$ and the limits for $|\vec{p}_1|$ are $(|\vec{p}_1|)_{min}=0$ and $(|\vec{p}_1|)_{max}=\frac{m_\mu^2-m_e^2}{2m_\mu}$ in the Eq. (205)

$$\Gamma_{\Lambda_{23}} = \frac{\pi e^4(|A_2^L|^2+|A_2^R|^2)}{4(2\pi)^4}\int_0^{\frac{m_\mu^2-m_e^2}{2m_\mu}}d|\vec{p}_1|\int_{|\vec{p}_2|_-}^{|\vec{p}_2|_+}d|\vec{p}_2|\times\bigstar|_{u=m_\mu-|\vec{p}_1|-|\vec{p}_2|}. \tag{207}$$

The last integral was evaluated by Mathematica 10.0 [34].
Therefore, the total value of the contribution of Γ_{Λ_2} is given by Eqs. (199) and (207)

$$\Gamma_{\Lambda_2} = \Gamma_{\Lambda_{21}} + \Gamma_{\Lambda_{22}} + \Gamma_{\Lambda_{23}}, \tag{208}$$

omitting terms $\sim \mathcal{O}(m_e)$, we obtain

$$\Gamma_{\Lambda_2} = \frac{\alpha^2 m_\mu^5}{32\pi}(|A_2^L|^2 + |A_2^R|^2)\left(\frac{16}{3}\ \ln\left(\frac{m_\mu}{m_e}\right) - \frac{26}{3}\right). \tag{209}$$

Finally the total contribution of $|\mathcal{M}_{\gamma-penguin}|$ is given by Eqs. (189) and (209)

$$\begin{aligned}\Gamma_{\gamma-penguin} = \frac{\alpha^2 m_\mu^5}{32\pi}\Big[&|A_1^L|^2 + |A_1^R|^2 - 2\left(A_1^L A_2^{R*} + A_2^L A_1^{R*} + h.c.\right)\\ &+(|A_2^L|^2 + |A_2^R|^2)\left(\frac{16}{3}\ \ln\left(\frac{m_\mu}{m_e}\right) - \frac{26}{3}\right)\Big]\end{aligned} \tag{210}$$

In [25] the authors report the following result

$$\begin{aligned}\Gamma_{\gamma-penguin} = \frac{\alpha^2 m_\mu^5}{32\pi}\Big[&|A_1^L|^2 + |A_1^R|^2 - 2\left(A_1^L A_2^{R*} + A_2^L A_1^{R*} + h.c.\right)\\ &+(|A_2^L|^2 + |A_2^R|^2)\left(\frac{16}{3}\ \ln\left(\frac{m_\mu}{m_e}\right) - \frac{22}{3}\right)\Big],\end{aligned} \tag{211}$$

we realize that our results differ by 4/3 since we obtained 26/3 and in their result appears 22/3, it is important to say that it is not really significant because the dominant term is the logarithm and we have the same coefficient in that term [2].

4.2 $\mathcal{M}_{Z-penguin}$ contribution

Now we analyze the Z-penguin contribution to the $\mu \to 3e$ decay width. From Eq. (143) the Z-penguin contribution is written as

$$\begin{aligned}\mathcal{M}_{Z-penguin} = &\frac{e^2}{M_Z^2}\overline{u}(p_1)[\gamma^\mu(F_L P_L + F_R P_R)]u(p)\overline{u}(p_2)[\gamma_\mu(Z_L^e P_L + Z_R^e P_R)]\upsilon(p_3)\\ &-(p_1 \leftrightarrow p_2),\end{aligned}$$

[2] We have nevertheless verified, using FORM [35], the correct coefficient of $\frac{22}{3}$.

in this case we shall consider $m_e = 0$ because $m_e \ll m_\mu$. Hence,

$$\begin{aligned}|\mathcal{M}_{Z-penguin}|^2 = \frac{e^4}{M_Z^4}\,\big[&64(|F_L|^2|Z_L^e|^2 + |F_R|^2|Z_R^e|^2)(p\cdot p_3)(p_1\cdot p_2)\\ &+ 16(|F_L|^2|Z_R^e|^2 + |F_R|^2|Z_L^e|^2)(p\cdot p_1)(p_2\cdot p_3)\\ &+ 16(|F_L|^2|Z_R^e|^2 + |F_R|^2|Z_L^e|^2)(p\cdot p_2)(p_1\cdot p_3)\,\big]\,.\end{aligned} \tag{212}$$

So, $\Gamma_{Z-penguin}$ is given by

$$\Gamma_{Z-penguin} = \frac{1}{2m_\mu}\int\frac{d^3p_1}{(2\pi)^3 2E_1}\int\frac{d^3p_2}{(2\pi)^3 2E_2}\int\frac{d^3p_3}{(2\pi)^3 2E_3}(2\pi)^4\delta^{(4)}(p-p_1-p_2-p_3)\times\frac{1}{4}\sum_{spin}|\mathcal{M}_{Z-penguin}|^2. \tag{213}$$

Substituting the Eq. (212) in (213) the first term is

$$\Lambda_1 = G\int\frac{d^3p_1}{2E_1}\int\frac{d^3p_2}{2E_2}\int\frac{d^3p_3}{2E_3}\delta^{(4)}(p-p_1-p_2-p_3)\times(p\cdot p_3)(p_1\cdot p_2), \tag{214}$$

where G is

$$G = \frac{8e^4}{(2\pi)^5 m_\mu M_Z^4}(|F_L|^2|Z_L^e|^2 + |F_R|^2|Z_R^e|^2). \tag{215}$$

We recall that we have resolved this kind of integral before in Eq. (177), in this case G is given by Eq. (215), therefore

$$\Lambda_1 = \frac{\alpha^2 m_\mu^5}{48\pi}(|F_{LL}|^2 + |F_{RR}|^2), \tag{216}$$

where we have defined the following expressions

$$F_{LL} = \frac{F_L Z_L^e}{M_Z^2},\quad F_{LR} = \frac{F_L Z_R^e}{M_Z^2},\quad F_{RL} = \frac{F_R Z_L^e}{M_Z^2},\quad F_{RR} = \frac{F_R Z_R^e}{M_Z^2}. \tag{217}$$

The second term in the Eq. (213) is

$$\begin{aligned}\Lambda_2 = \frac{e^4}{8(2\pi)^5 m_\mu M_Z^4}\int\frac{d^3p_1}{2E_1}\int\frac{d^3p_2}{2E_2}\int\frac{d^3p_3}{2E_3}&(2\pi)^4\delta^{(4)}(p-p_1-p_2-p_3)\\ &\times 16(|F_L|^2|Z_R^e|^2 + |F_R|^2|Z_L^e|^2)(p\cdot p_1)(p_2\cdot p_3),\end{aligned} \tag{218}$$

using the Eq. (177) again, we obtain

$$\Lambda_2 = \frac{\alpha^2 m_\mu^5}{192\pi}(|F_{LR}|^2 + |F_{RL}|^2). \tag{219}$$

The last one in Eq. (213) is

$$\Lambda_3 = \frac{e^4}{8(2\pi)^5 m_\mu M_Z^4}\int\frac{d^3p_1}{2E_1}\int\frac{d^3p_2}{2E_2}\int\frac{d^3p_3}{2E_3}(2\pi)^4\delta^{(4)}(p-p_1-p_2-p_3) \times 16(|F_L|^2|Z_R^e|^2+|F_R|^2|Z_L^e|^2)(p\cdot p_2)(p_1\cdot p_3), \tag{220}$$

thus,

$$\Lambda_3 = \frac{\alpha^2 m_\mu^5}{192\pi}(|F_{LR}|^2+|F_{RL}|^2). \tag{221}$$

We sum the Eqs. (216), (219) and (221) to obtain the total contribution of Z-penguin

$$\Gamma_{Z-penguin} = \frac{\alpha^2 m_\mu^5}{32\pi}\left[\frac{1}{3}\left\{2(|F_{LL}|^2+|F_{RR}|^2)+|F_{LR}|^2+|F_{RL}|^2\right\}\right]. \tag{222}$$

4.3 $\mathcal{M}_{box}$ contribution

This contribution is given by Eq. (144)

$$\begin{aligned}
\mathcal{M}_{box} &= e^2 B_1^L[\overline{u}(p_1)\gamma^\mu P_L u(p)][\overline{u}(p_2)\gamma_\mu P_L \upsilon(p_3)] \\
&+ e^2 B_1^R[\overline{u}(p_1)\gamma^\mu P_R u(p)][\overline{u}(p_2)\gamma_\mu P_R \upsilon(p_3)] \\
&+ e^2 B_2^L\{[\overline{u}(p_1)\gamma^\mu P_L u(p)][\overline{u}(p_2)\gamma_\mu P_R \upsilon(p_3)] - (p_1\leftrightarrow p_2)\} \\
&+ e^2 B_2^R\{[\overline{u}(p_1)\gamma^\mu P_R u(p)][\overline{u}(p_2)\gamma_\mu P_L \upsilon(p_3)] - (p_1\leftrightarrow p_2)\} \\
&+ e^2 B_3^L\{[\overline{u}(p_1) P_L u(p)][\overline{u}(p_2) P_L \upsilon(p_3)] - (p_1\leftrightarrow p_2)\} \\
&+ e^2 B_3^R\{[\overline{u}(p_1) P_R u(p)][\overline{u}(p_2) P_R \upsilon(p_3)] - (p_1\leftrightarrow p_2)\} \\
&+ e^2 B_4^L\{[\overline{u}(p_1)\sigma^{\mu\nu} P_L u(p)][\overline{u}(p_2)\sigma_{\mu\nu} P_L \upsilon(p_3)] - (p_1\leftrightarrow p_2)\} \\
&+ e^2 B_4^R\{[\overline{u}(p_1)\sigma^{\mu\nu} P_R u(p)][\overline{u}(p_2)\sigma_{\mu\nu} P_R \upsilon(p_3)] - (p_1\leftrightarrow p_2)\}.
\end{aligned}$$

With aid of FeynCalc 9.2.0 [36] from the equation above we obtain

$$\begin{aligned}
|\mathcal{M}_{box}|^2 = 4e^2\big[&4(|B_1^L|^2+|B_1^R|^2)+(|B_3^L|^2+|B_3^R|^2)+144(|B_4^L|^2+|B_4^R|^2) \\
&-12(B_3^L B_4^{L*}+B_3^R B_4^{R*}+B_4^L B_3^{L*}+B_4^R B_3^{R*})\big](p\cdot p_3)(p_1\cdot p_2) \\
&+16e^2(|B_2^L|^2+|B_2^R|^2)\left[(p\cdot p_2)(p_1\cdot p_3)+(p\cdot p_1)(p_2\cdot p_3)\right].
\end{aligned} \tag{223}$$

We can see that in the Eq. (223) the only contributing integrals are shown in the Eq. (156), therefore the result is given by Eq. (177). According to the above, the contribution of $\mathcal{M}_{box}$ is

$$\begin{aligned}
\Gamma_{box} = \frac{\alpha^2 m_\mu^5}{32\pi}\Big[&\frac{1}{6}(|B_1^L|^2+|B_1^R|^2)+\frac{1}{3}(|B_2^L|^2+|B_2^R|^2)+\frac{1}{24}(|B_3^L|^2+|B_3^R|^2) \\
&+6(|B_4^L|^2+|B_4^R|^2)-\frac{1}{2}(B_3^L B_4^{L*}+B_3^R B_4^{R*}+h.c.)\Big].
\end{aligned} \tag{224}$$

4.4 $\mathcal{M}_{\gamma-penguin}\mathcal{M}^{\dagger}_{Z-penguin}$ contribution

We recall the total width has interference terms like

$$\mathcal{M}_{\gamma-penguin}\mathcal{M}^{\dagger}_{Z-penguin} + h.c. \tag{225}$$

Since $m_e \ll M_Z$, in the interference $\mathcal{M}_{\gamma-penguin}\mathcal{M}^{\dagger}_{Z-penguin}$ we will consider $m_e = 0$.
Then

$$\begin{aligned}\mathcal{M}_{Z-penguin}\mathcal{M}^{\dagger}_{\gamma-penguin} &= 64e^4(F_{LL}A_1^{L*} + F_{RR}A_1^{R*})(p\cdot p_3)(p_1\cdot p_2)\\ &+ 16e^4(F_{LR}A_1^{L*} + F_{RL}A_1^{R*})\left[(p\cdot p_2)(p_1\cdot p_3) + (p\cdot p_1)(p_2\cdot p_3)\right]\\ &- 32e^4m_\mu^2(F_{RR}A_2^{L*} + F_{LL}A_2^{R*})(p_1\cdot p_2)\\ &- 8e^4m_\mu^2(F_{RL}A_2^{L*} + F_{LR}A_2^{R*})\left[(p_2\cdot p_3) + (p_1\cdot p_3)\right].\end{aligned} \tag{226}$$

The result of this interference is obtained through the Eqs. (177) and (188) that we have computed previously, just redefining the constants adequately. Hence

$$\begin{aligned}\Gamma_{Z-\gamma^\dagger} = \frac{\alpha^2 m_\mu^5}{32\pi}\Big[\frac{1}{3}\big(&2(F_{LL}A_1^{L*} + F_{RR}A_1^{R*}) + (F_{LR}A_1^{L*} + F_{RL}A_1^{R*})\\ &-4(F_{RR}A_2^{L*} + F_{LL}A_2^{R*}) - 2(F_{RR}A_2^{L*} + F_{LL}A_2^{R*})\big)\Big].\end{aligned} \tag{227}$$

As $\mathcal{M}_{Z-penguin}\mathcal{M}^{\dagger}_{\gamma-penguin}$ is the hermitian conjugate of $\mathcal{M}_{\gamma-penguin}\mathcal{M}^{\dagger}_{Z-penguin}$, the total contribution to the $\mu \to 3e$ decay width of this interference is given by

$$\begin{aligned}\Gamma_{(\gamma-Z)-interference} = \frac{\alpha^2 m_\mu^5}{32\pi}\Big[\frac{1}{3}\big(&2(A_1^L F_{LL}^* + A_1^R F_{RR}^* + h.c.) + (A_1^L F_{LR}^* + A_1^R F_{RL}^* + h.c.)\\ &-4(A_2^R F_{LL}^* + A_2^L F_{RR}^* + h.c.) - 2(A_2^L F_{RL}^* + A_2^R F_{LR}^* + h.c.)\big)\Big].\end{aligned} \tag{228}$$

4.5 $\mathcal{M}_{\gamma-penguin}\mathcal{M}^{\dagger}_{box}$ contribution

Now, we are going to analyze the interference between γ-penguin and box diagrams, which is given by

$$\begin{aligned}\mathcal{M}_{box}\mathcal{M}^{\dagger}_{\gamma-penguin} &= 32e^4(A_1^L B_1^{L*} + A_1^R B_1^{R*})(p\cdot p_3)(p_1\cdot p_2)\\ &+ 16e^4(A_1^L B_2^{L*} + A_1^R B_2^{R*})\left[(p\cdot p_2)(p_1\cdot p_3) + (p\cdot p_1)(p_2\cdot p_3)\right]\\ &- 16e^4m_\mu^2(A_2^L B_1^{R*} + A_2^R B_1^{L*})(p_1\cdot p_2)\\ &- 8e^4m_\mu^2(A_2^L B_2^{R*} + A_2^R B_2^{L*})\left[(p_2\cdot p_3) + (p_1\cdot p_3)\right].\end{aligned} \tag{229}$$

Taking the results of the Eqs. (177) and (188), the contribution of the equation above is

$$\begin{aligned}\Gamma_{box-\gamma^\dagger} = \frac{\alpha^2 m_\mu^5}{32\pi}\Bigg[&\frac{1}{3}\left(A_1^L B_1^{L*} + A_1^R B_1^{R*} + A_1^L B_2^{L*} + A_1^R B_2^{R*}\right)\\ &-\frac{2}{3}\left(A_2^L B_1^{R*} + A_2^R B_1^{L*} + A_2^L B_2^{R*} + A_2^R B_2^{L*}\right)\Bigg].\end{aligned} \tag{230}$$

Also we need to add the hermitian conjugate of $\mathcal{M}_{box}\mathcal{M}^\dagger_{\gamma-penguin}$, therefore, the total contribution is

$$\begin{aligned}\Gamma_{(\gamma-box)-interference} = \frac{\alpha^2 m_\mu^5}{32\pi}\Bigg[&\frac{1}{3}\left(A_1^L B_1^{L*} + A_1^R B_1^{R*} + A_1^L B_2^{L*} + A_1^R B_2^{R*} + h.c.\right)\\ &-\frac{2}{3}\left(A_2^L B_1^{R*} + A_2^R B_1^{L*} + A_2^L B_2^{R*} + A_2^R B_2^{L*} + h.c.\right)\Bigg].\end{aligned} \tag{231}$$

4.6 $\mathcal{M}_{Z-penguin}\mathcal{M}^\dagger_{box}$ contribution

Finally, we are going to compute the last contribution to the $\mu \to 3e$ decay width which is given by

$$\begin{aligned}\mathcal{M}_{Z-penguin}\mathcal{M}^\dagger_{box} =& e^4\left\{32F_{LL}B_1^{L*}(p\cdot p_3)(p_1\cdot p_2) + 32F_{RR}B_1^{R*}(p\cdot p_3)(p_1\cdot p_2)\right.\\ &+16F_{LR}B_2^{L*}\left[(p\cdot p_2)(p_1\cdot p_3)+(p\cdot p_1)(p_2\cdot p_3)\right]\\ &\left.+16F_{RL}B_2^{R*}\left[(p\cdot p_2)(p_1\cdot p_3)+(p\cdot p_1)(p_2\cdot p_3)\right]\right\}.\end{aligned} \tag{232}$$

With the results of the Eqs. (177) and (188), we have that

$$\begin{aligned}\Gamma_{Z-box^\dagger} &= \frac{\alpha^2 m_\mu^5}{96\pi}\left(B_1^{L*}F_{LL} + B_1^{R*}F_{RR} + B_2^{L*}F_{LR} + B_2^{R*}F_{RL}\right)\\ &= \frac{\alpha^2 m_\mu^5}{32\pi}\left[\frac{1}{3}\left(B_1^{L*}F_{LL} + B_1^{R*}F_{RR} + B_2^{L*}F_{LR} + B_2^{R*}F_{RL}\right)\right].\end{aligned} \tag{233}$$

The total contribution of the interference between Z-penguin and box diagrams needs the addition of the hermitian conjugate term, $M_{box}M^\dagger_{Z-penguin}$, hence

$$\Gamma_{(Z-box)-interference} = \frac{\alpha^2 m_\mu^5}{32\pi}\left[\frac{1}{3}\left(B_1^L F_{LL}^* + B_1^R F_{RR}^* + B_2^L F_{LR}^* + B_2^R F_{RL}^* + h.c.\right)\right]. \tag{234}$$

5 Extracting Form Factors from the $\mu \to e\gamma$ Amplitude in the LHT

Most general structure of the $\mu \to e\gamma$ amplitude for on-shell fermions f_{ij} can be written in terms of six form factors [25]

$$i\Gamma^{\mu}(p_1,p_2) = ie\left[\gamma^{\mu}\left(F_L^V P_L + F_R^V P_R\right) + (iF_M^V + F_E^V\gamma_5)\sigma^{\mu\nu}Q_{\nu} + (iF_S^V + F_P^V\gamma_5)Q^{\mu}\right], \tag{235}$$

with $P_{R,L} = \frac{1}{2}(1 \pm \gamma_5)$ and $Q = p_2 - p_1$ the vector boson momentum entering the vertex.
The development is done in the 't Hooft-Feynman ($\xi = 1$) gauge. We are going to consider in the $\mu \to e\gamma$ decay that the photon is on-shell and then only the dipole form factors $F_{M,E}^{\gamma}$ contribute. Furthermore, the electron mass is neglected ($m_e \approx 0$). We show below the topologies of the diagrams that contribute to the $\mu \to e\gamma$ decay [37].

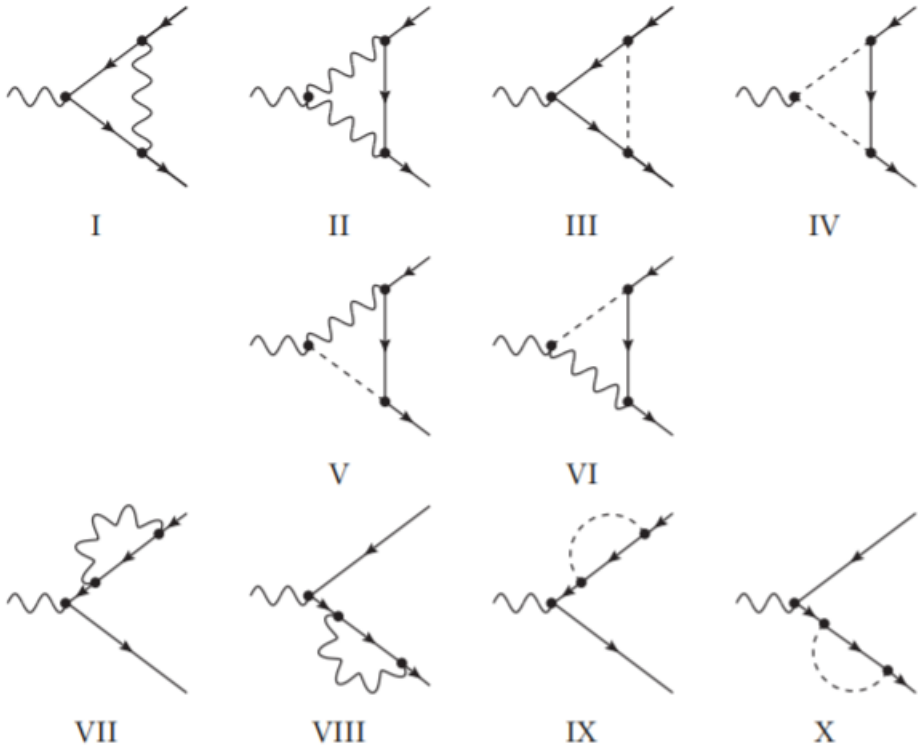

Figure 6: Topologies of the diagrams that contribute to the processes $\gamma, Z \to \bar{\ell}\ell'$.

We can write the two-body decays $\ell \to \ell'\gamma$, $Z \to \bar{\ell}\ell'$, and $h \to \bar{\ell}\ell'$ in terms of three-point form factors with the generic form [37],

$$\begin{aligned}\mathcal{F}_3 = &\sum_i V_{\ell' i}^{\dagger} V_{i\ell} F_3(m_{\ell_{Hi}}, ...) \\ &+ \sum_{i,j,k} V_{\ell' i}^{\dagger} \frac{m_{\ell_{Hi}}}{M_{W_H}} W_{ij}^{\dagger} W_{jk} \frac{m_{\ell_{Hk}}}{M_{W_H}} V_{k\ell} G_3(m_{\bar{\nu}_j^c}, ...),\end{aligned} \tag{236}$$

where $V_{i\ell}$ are the matrix elements of the 3×3 unitary mixing matrix parametrizing the misalignment between the SM left-handed charged leptons ℓ with the heavy mirror ones ℓ_H. The W_{jk} are the matrix elements of the 3×3 unitary mixing matrix parametrizing the misalignment between the mirror leptons and their partners $\bar{\ell}^c$ in the $SO(5)$ (right-handed) multiplets.
We write down the Feynman rules that we need for computing each diagram in LHT model [25]:

$$\begin{aligned}
[V_\mu FF] &= ie\gamma^\mu(g_L P_L + g_R P_R),\\
[SFF] &= ie(c_L P_L + c_R P_R),\\
[V_\mu S(p_1)S(p_2)] &= ieG(p_1-p_2)^\mu,\\
[SV_\mu V_\nu] &= ieK g^{\mu\nu},\\
[V_\mu(p_1)V_\nu(p_2)V_\rho(p_3)] &= ieJ\left[g^{\mu\nu}(p_2-p_1)^\rho + g^{\nu\rho}(p_3-p_2)^\mu + g^{\mu\rho}(p_1-p_3)^\nu\right].
\end{aligned} \tag{237}$$

$V_\mu FF$	g_L	g_R
$\gamma \bar{f}^i_H f^j_H$	$-Q_f\delta_{ij}$	$-Q_f\delta_{ij}$
$Z_H \bar{\ell}^i_H \ell^j$	$-\left(\frac{1}{2s_W} + \frac{x_H}{10c_W}\frac{v^2}{f^2}\right)V^{ij}_{H\ell}$	0
$Z_H \bar{\nu}^i_H \nu^j_H$	$\frac{1}{2s_W c_W}\delta_{ij}$	$\frac{1}{2s_W c_W}\left(1-\frac{v^2}{4f^2}\right)\delta_{ij}$
$A_H \bar{\ell}^i_H \ell^j$	$\left(\frac{1}{10c_W} - \frac{x_H}{2s_W}\frac{v^2}{f^2}\right)V^{ij}_{H\ell}$	0
$Z_H \bar{\ell}^i_H \ell^j_H$	$\frac{1}{2s_W c_W}\left(-1+2s^2_W\right)\delta_{ij}$	$\frac{1}{2s_W c_W}\left(-1+2s^2_W\right)\delta_{ij}$
$W^+_H \bar{\nu}^i_H \ell^j$	$\frac{1}{\sqrt{2}s_W}V^{ij}_{H\ell}$	0

Table 4: Fermion couplings to gauge bosons.

SFF	c_L	c_R
$\omega^0 \bar{\ell}^i_H \ell^j$	$\frac{i}{2s_W}\frac{m_{\ell^i_H}}{M_{Z_H}}\left[1+\frac{v^2}{f^2}\left(-\frac{1}{4}+x_H\frac{c_W}{s_W}\right)\right]V^{ij}_{H\ell}$	$-\frac{i}{2s_W}\frac{m_{\ell^i}}{M_{Z_H}}V^{ij}_{H\ell}$
$\eta \bar{\ell}^i_H \ell^j$	$\frac{i}{10c_W}\frac{m_{\ell^i_H}}{M_{A_H}}\left[1-\frac{v^2}{f^2}\left(\frac{5}{4}+x_H\frac{s_W}{c_W}\right)\right]V^{ij}_{H\ell}$	$-\frac{i}{10c_W}\frac{m_{\ell^i}}{M_{A_H}}V^{ij}_{H\ell}$
$\omega^+ \bar{\nu}^i_H \ell^j$	$-\frac{i}{\sqrt{2}s_W}\frac{m_{\nu^i_H}}{M_{W_H}}V^{ij}_{H\ell}$	$\frac{i}{\sqrt{2}s_W}\frac{m_{\ell^i}}{M_{W_H}}V^{ij}_{H\ell}$

Table 5: Fermion couplings to Goldstone boson.

SVV	K
$\omega^\pm W^\mp_H \gamma$	$\pm iM_{W_H}$
$\omega^\pm W^\mp_H Z$	$\mp iM_{W_H}\frac{c_W}{s_W}\left(1-\frac{v^2}{4f^2c^2_W}\right)$

Table 6: Heavy and SM gauge bosons couplings to Goldstone boson.

VSS	G
$\gamma\omega^{\pm}\omega^{\mp}$	∓ 1
$Z\omega^{\pm}\omega^{\mp}$	$\pm\frac{c_W}{s_W}\left(1-\frac{v^2}{8f^2c_W^2}\right)$

Table 7: Goldstone boson couplings to SM gauge boson.

VVV	J
$\gamma W_H^+ W_H^-$	-1
$Z W_H^+ W_H^-$	$\frac{c_W}{s_W}$

Table 8: Triple heavy and SM gauge bosons couplings.

5.1 Diagrams exchanging Z_H

The diagrams that contribute to the $\mu \to e\gamma$ decay exchanging Z_H are given by the topologies (I) and (III). We have to recall that the field ω^0 is eaten by the heavy gauge boson Z_H.
We can write the amplitude of the next diagram which is shown in the Figure 7 as

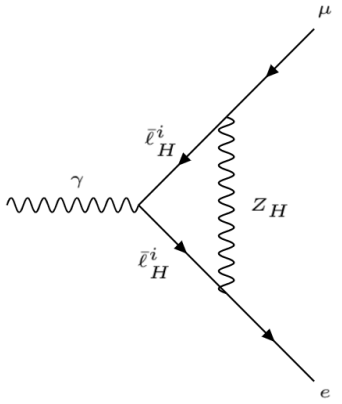

Figure 7: Diagram exchanging Z_H (Topology I).

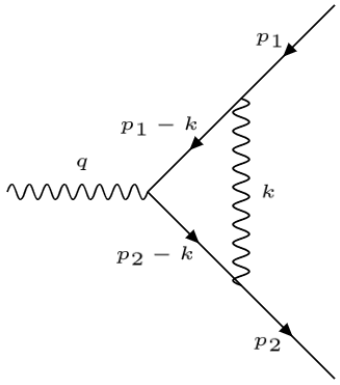

Figure 8: Diagram of momenta for Z_H exchange.

$$i\Gamma^{\mu} = \frac{\alpha_W}{32\pi}\sum_i V_{H\ell}^{ie*}V_{H\ell}^{i\mu}\int\frac{d^4k}{(2\pi)^4}\frac{\gamma^{\alpha}P_L(\not{p}_2-\not{k}+M_2)\gamma^{\mu}(\not{p}_1-\not{k}+M_2)\gamma^{\beta}P_L g_{\beta\alpha}}{(k^2-M_1^2+i\epsilon)((p_1-k)^2-M_2^2+i\epsilon)((p_2-k)^2-M_2^2+i\epsilon)}, \quad (238)$$

where $q = p_2 - p_1$, $M_1 = M_{Z_H}$, $M_2 = m_{\ell_H^i}$ and $\alpha_W \equiv \frac{\alpha}{s_W^2}$.
Now, we analyse the self-energy diagrams.

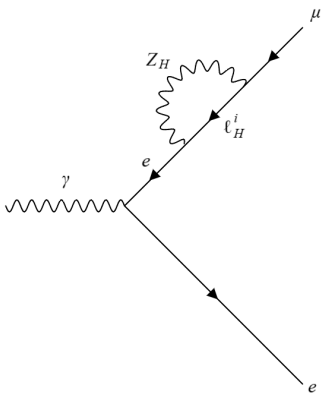

Figure 9: Self-energy diagram (Topology VII).

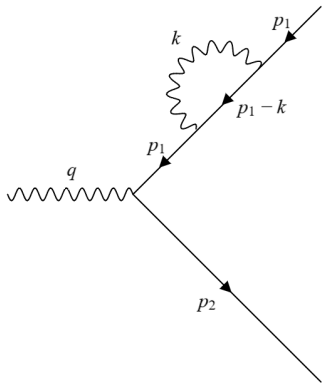

Figure 10: Diagram of momenta for self-energy diagram.

The amplitude of the diagram shown in the Figure 9 is

$$i\Gamma^{\mu} = \frac{\alpha_W}{32\pi} \sum_i V_{H\ell}^{ie*} V_{H\ell}^{i\mu} \int \frac{d^4k}{(2\pi)^4} \frac{\gamma^{\mu} \not{p}_1 \gamma^{\beta} P_L (\not{p}_1 - \not{k} + M_2) \gamma^{\alpha} P_L g_{\alpha,\beta}}{(p_1^2 + i\epsilon)(k^2 - M_1^2 + i\epsilon)((p_1 - k)^2 - M_2^2 + i\epsilon)}. \tag{239}$$

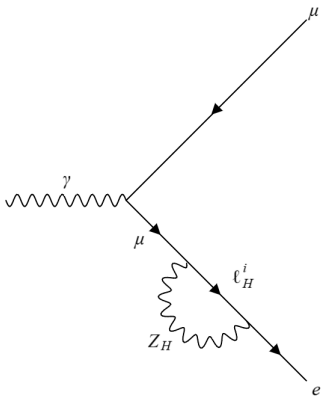

Figure 11: Self-energy diagram (Topology VIII).

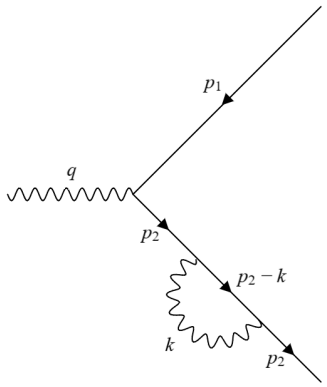

Figure 12: Diagram of momenta for self-energy diagram.

The amplitude corresponding to the Figure 11 is

$$i\Gamma^{\mu} = \frac{\alpha_W}{32\pi} \sum_i V_{H\ell}^{ie*} V_{H\ell}^{i\mu} \int \frac{d^4k}{(2\pi)^4} \frac{\gamma^{\alpha} P_L (\not{p}_2 - \not{k} + M_2) \gamma^{\beta} P_L (\not{p}_2 + m_{\mu}) \gamma^{\mu} g_{\alpha,\beta}}{(k^2 - M_1^2 + i\epsilon)(p_2^2 - m_{\mu}^2 + i\epsilon)((p_2 - k)^2 - M_2^2 + i\epsilon)}. \tag{240}$$

Considering the contribution of each one of the diagrams above we obtain that the form factor $F_M^{\gamma}|_{Z_H}$

is given by [25] (loop function are given the in the appendices)

$$I: \quad F_M^\gamma|_{Z_H} = -iF_E^\gamma|_{Z_H} = \frac{\alpha_W}{16\pi} m_\mu \sum_i V_{H\ell}^{ie*} V_{H\ell}^{i\mu} \left[C_0 + 3C_1 + \frac{3}{2} C_{11} \right]. \tag{241}$$

We are going to compute next the contributions of the diagrams exchanging an ω^0 boson.

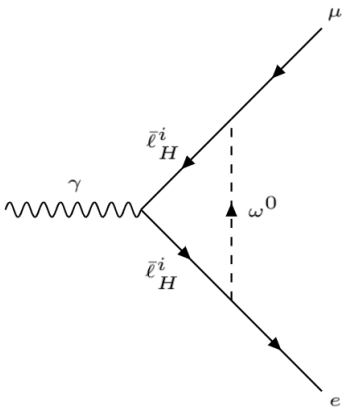

Figure 13: Diagram with an ω^0 boson exchange (Topology III).

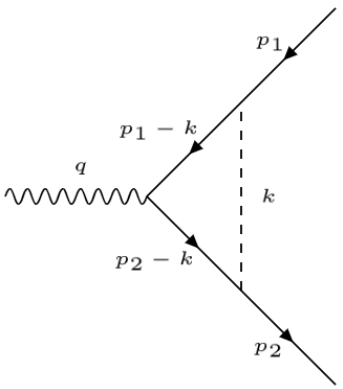

Figure 14: Diagram of momenta for ω^0 exchange.

The amplitud of the diagram corresponding to the Figure 13, omitting the $\frac{v^2}{f^2}$-suppressed terms in the Feynman rules, is given by

$$i\Gamma^\mu = \frac{\alpha_W}{32\pi} \sum_i V_{H\ell}^{ie*} V_{H\ell}^{i\mu} y_i \int \frac{d^4k}{(2\pi)^4} \frac{P_R(\not{p}_2 - \not{k} + M_2)\gamma^\mu(\not{p}_1 - \not{k} + M_2)(M_2 P_L - m_\mu P_R)}{(k^2 - M_1^2 + i\epsilon)((p_1 - k)^2 - M_2^2 + i\epsilon)((p_2 - k)^2 - M_2^2 + i\epsilon)}, \tag{242}$$

where $y_i = \frac{M_2^2}{M_1^2}$.
Now, we will develop the self-energy diagrams for ω^0.

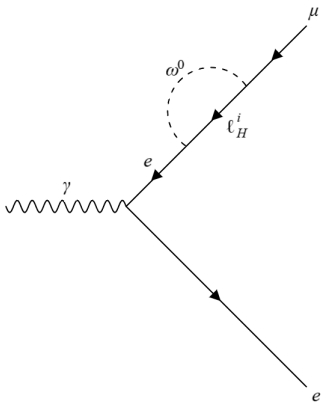

Figure 15: Self-energy diagram exchanging a ω^0 boson (Topology IX).

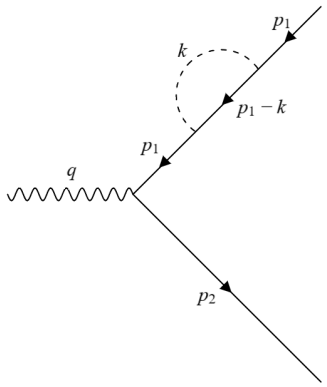

Figure 16: Diagram of momenta for self-energy diagram exchanging an ω^0.

The amplitude of the diagram shown in the Figure 15 is

$$i\Gamma^{\mu} = \frac{\alpha_W}{32\pi}\sum_i V_{H\ell}^{ie*}V_{H\ell}^{i\mu}y_i\int\frac{d^4k}{(2\pi)^4}\frac{\gamma^{\mu}\not{p}_1 P_R(\not{p}_1-\not{k}+M_2)(M_2P_L-m_{\mu}P_R)}{(p_1^2+i\epsilon)(k^2-M_1^2+i\epsilon)((p_1-k)^2-M_2^2+i\epsilon)}. \tag{243}$$

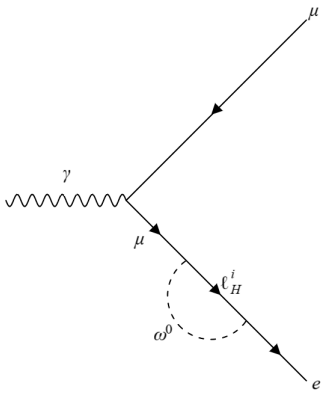

Figure 17: Self-energy diagram (Topology X).

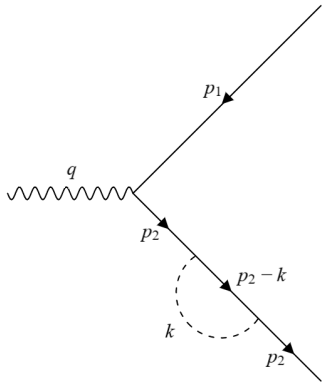

Figure 18: Diagram of momenta for self-energy diagram exchanging an ω^0.

The amplitude corresponding to the Figure 17 is

$$i\Gamma^{\mu} = \frac{\alpha_W}{32\pi}\sum_i V_{H\ell}^{ie*}V_{H\ell}^{i\mu}y_i\int\frac{d^4k}{(2\pi)^4}\frac{P_R(\not{p}_2-\not{k}+M_2)(M_2P_L-m_{\mu}P_R)(\not{p}_2+m_{\mu})\gamma^{\mu}}{(k^2-M_1^2+i\epsilon)(p_2^2-m_{\mu}^2+i\epsilon)((p_2-k)^2-M_2^2+i\epsilon)}. \tag{244}$$

Adding the contributions of the 3 diagrams above, the ω^0 contributions to the form factors yields [25]

$$III: \quad F_M^\gamma|_{Z_H} = -iF_E^\gamma|_{Z_H} = -\frac{\alpha_W}{32\pi} m_\mu \sum_i V_{H\ell}^{ie*} V_{H\ell}^{i\mu} y_i \left[C_1 - \frac{3}{2}C_{11}\right]. \tag{245}$$

The total contribution for the form factor is the sum of the eqs. (241) and (245) [25]

$$\text{Total}: \quad F_M^\gamma|_{Z_H} = -iF_E^\gamma|_{Z_H} = \frac{\alpha_W}{16\pi}\frac{m_\mu}{M_{W_H}^2} \sum_i V_{H\ell}^{ie*} V_{H\ell}^{i\mu} F_Z(y_i), \tag{246}$$

where

$$\begin{aligned} F_Z(x) &= M_1^2 \left[C_0 + 3C_1 + \frac{3}{2}C_{11} - \frac{x}{2}\left(C_1 - \frac{3}{2}C_{11}\right)\right] \\ &= -\frac{1}{3} + \frac{2x + 5x^2 - x^3}{8(1-x)^3} + \frac{3x^2}{4(1-x)^4} \ln\ x, \end{aligned} \tag{247}$$

The integrals were developed with aid of Package-X [38].
During the process of calculating the integrals the muon mass must be considered $m_\mu \neq 0$, otherwise the self-energy diagrams will be undetermined. Finally, we just take the terms which are proportional to the muon mass m_μ.

5.2 Diagrams exchanging A_H

This contribution can be obtained from diagrams with Z_H, replacing Z_H by A_H. It is convenient to introduce the mass ratio

$$y_i' = a y_i, \quad a = \frac{M_{W_H}^2}{M_{A_H}^2} = \frac{5c_W^2}{s_W^2}. \tag{248}$$

Then,

$$\begin{aligned} F_M^\gamma|_{A_H} = -iF_E^\gamma|_{A_H} &= \frac{\alpha_W}{16\pi}\frac{m_\mu}{M_{A_H}^2}\frac{1}{25}\frac{s_W^2}{c_W^2}\sum_i V_{H\ell}^{ie*} V_{H\ell}^{i\mu} F_Z(y_i') \\ &= \frac{\alpha_W}{16\pi}\frac{m_\mu}{M_{W_H}^2}\frac{1}{5}\sum_i V_{H\ell}^{ie*} V_{H\ell}^{i\mu} F_Z(y_i'), \end{aligned} \tag{249}$$

in agreement with [25].

5.3 Diagrams exchanging W_H

The diagrams that contribute to the $\mu \to e\gamma$ decay width are given by the Topologies II, IV, V and VI. We are going to show the development of the diagram given by the topology IV.
The Feynman rules that we need to write the amplitudes are given in the Apendix B.2 in [25].

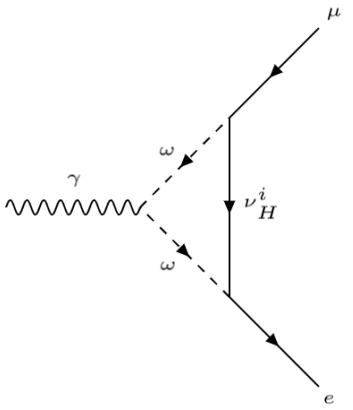

Figure 19: Diagram corresponding to Topology IV.

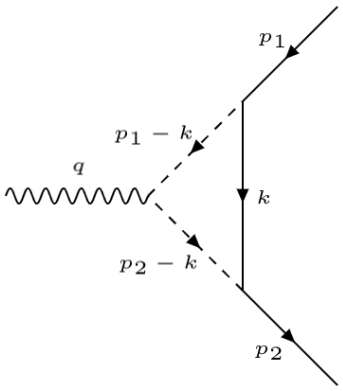

Figure 20: Diagram of momenta in Topology IV.

Taking $M_1 = M_{W_H}$ and $M_2 = m_{\nu_H^i}$ and introducing the mass ratio

$$y_i = \frac{m_{H_i}^2}{M_{W_H}^2}, \tag{250}$$

with $m_{H_i} \equiv m_{\ell_H^i} \simeq m_{\nu_H^i}$, the amplitude associated with the Figure 19 reads

$$i\Gamma^\mu = -\frac{\alpha_W}{16\pi} \sum_i V_{H\ell}^{ie*} V_{H\ell}^{i\mu}\, y_i \int \frac{d^4k}{(2\pi)^4} \frac{P_R(\not{k} + M_2)(M_2 P_L - m_\mu P_R)(p_1 + p_2 - 2k)^\mu}{(k^2 - M_2^2 + i\epsilon)((p_1 - k)^2 - M_1^2 + i\epsilon)((p_2 - k)^2 - M_1^2 + i\epsilon)}. \tag{251}$$

The self-energy type diagrams are given by the Figures 21 and 23.

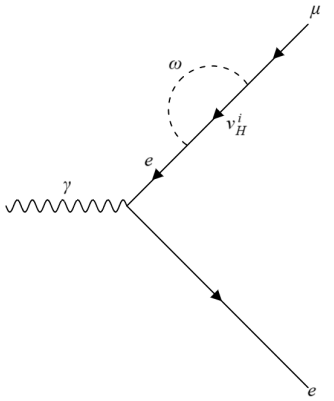

Figure 21: Diagram corresponding to Topology IX.

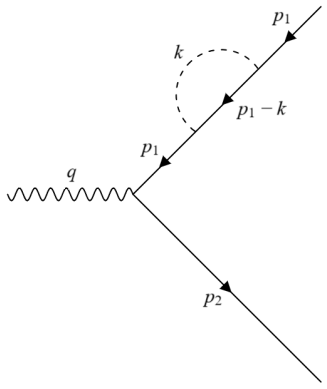

Figure 22: Diagram of momenta in Topology IX.

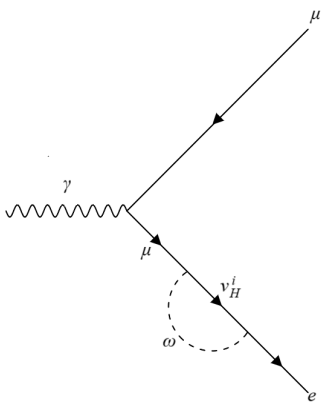

Figure 23: Diagram corresponding to Topology X.

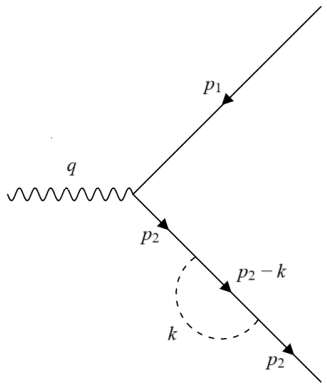

Figure 24: Diagram of momenta in Topology X.

The amplitudes are given respectively by

$$i\Gamma^{\mu} = -\frac{\alpha_W}{16\pi}\sum_i V_{H\ell}^{ie*}V_{H\ell}^{i\mu}\, y_i \int \frac{d^4k}{(2\pi)^4}\frac{\gamma^{\mu}\not{p}_1 P_R(\not{p}_1 - \not{k} + M_2)(M_2 P_L - m_\mu P_R)}{(p_1^2+i\epsilon)(k^2-M_1^2+i\epsilon)((p_1-k)^2-M_2^2+i\epsilon)}, \tag{252}$$

$$i\Gamma^{\mu} = -\frac{\alpha_W}{16\pi}\sum_i V_{H\ell}^{ie*}V_{H\ell}^{i\mu}\, y_i \int \frac{d^4k}{(2\pi)^4}\frac{(M_2 P_L - m_\mu P_R)(\not{p}_2 - \not{k} + M_2)P_R(\not{p}_2 + m_\mu)\gamma^{\mu}}{(k^2-M_1^2+i\epsilon)(p_2^2-m_\mu^2+i\epsilon)((p_2-k)^2-M_2^2+i\epsilon)}. \tag{253}$$

From the eqs. (251), (252) and (253) we obtain

$$IV: \quad F_M^{\gamma}|_{M_{W_H}} = -iF_E^{\gamma}|_{M_{W_H}} = -\frac{\alpha_W}{16\pi}m_\mu \sum_i V_{H\ell}^{ie*}V_{H\ell}^{i\mu} y_i \left[\overline{C}_0 + 3\overline{C}_1 + \frac{3}{2}\overline{C}_{11}\right]. \tag{254}$$

This result is in agreement with [25].
For the other contributions we have that [25]

$$II: \quad F_M^{\gamma}|_{W_H} = -iF_E^{\gamma}|_{W_H} = -\frac{\alpha_W}{16\pi}m_\mu \sum_i V_{H\ell}^{ie*}V_{H\ell}^{i\mu}\left[3\overline{C}_{11} - \overline{C}_1\right], \tag{255}$$

$$V: \quad F_M^{\gamma}|_{W_H} = -iF_E^{\gamma}|_{W_H} = 0, \tag{256}$$

$$VI: \quad F_M^{\gamma}|_{W_H} = -iF_E^{\gamma}|_{W_H} = \frac{\alpha_W}{16\pi}m_\mu \sum_i V_{H\ell}^{ie*}V_{H\ell}^{i\mu}\,\overline{C}_1, \tag{257}$$

$$\text{Total}: \quad F_M^{\gamma}|_{W_H} = -iF_E^{\gamma}|_{W_H} = \frac{\alpha_W}{16\pi}\frac{m_\mu}{M_{W_H}^2}\sum_i V_{H\ell}^{ie*}V_{H\ell}^{i\mu}F_W(y_i), \tag{258}$$

where

$$\begin{aligned} F_W(x) &= M_1^2 \left[2\overline{C}_1 - 3\overline{C}_{11} - x\left(\overline{C}_0 + 3\overline{C}_1 + \frac{3}{2}\overline{C}_{11}\right)\right] \\ &= \frac{5}{6} - \frac{3x - 15x^2 - 6x^3}{12(1-x)^3} + \frac{3x^3}{2(1-x)^4}\ln\ x. \end{aligned} \tag{259}$$

SM contributions mediated by W bosons are negligible due to the tiny neutrino masses.
Something that is interesting about the above results is they are similar to the SM contributions with massive neutrinos, if we consider W instead of W_H, ν^i instead of ν_H^i and $V_{PMNS}^\dagger$ instead of $V_{H\ell}$, and since the neutrino mass in tiny in SM, $x_i = m_{\nu_i}^2/M_W^2 \ll 1$, the eq. (259) reduces to

$$F_W(x) \to \frac{5}{6} - \frac{x}{4} + \mathcal{O}(x^2), \tag{260}$$

so that we recover SM result bounded by neutrino oscillation experiments:

$$\mathcal{B}(\mu \to e\gamma)_{SM} = \frac{3\alpha}{32\pi}|\sum_i V_{PMNS}^{ei} V_{PMNS}^{\mu i *} x_i|^2 \lesssim 10^{-54}. \tag{261}$$

5.4 Contributions from partner leptons $\bar{\ell}^c = (\bar{\nu}^c, \bar{\ell}^c)$

The contributions from partner leptons $\bar{\ell}^c = (\bar{\nu}^c, \bar{\ell}^c)$ only involve topologies III, IV, IX and X in the Figure 6 because they do not couple to one T-odd gauge boson and a SM charged lepton.
The scalar triplet Φ contributes to the process $\mu \to e\gamma$, the corresponding diagrams can be obtained replacing $W_H^\pm$ by $\Phi^\pm$ and Z_H, A_H by Φ^0 and Φ^P.
We are going to develop the next diagram

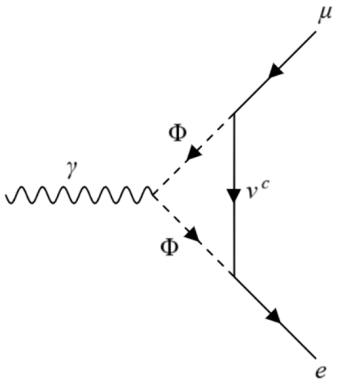

Figure 25: Diagram exchanging a Φ boson.

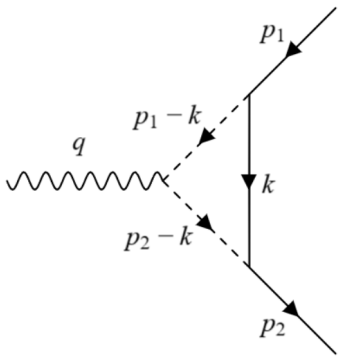

Figure 26: Diagram of momenta for Φ exchange.

The Feynman rules what we need are

SFF	c_L	c_R
$\Phi^+\overline{\overline{\nu}_i^c}\ell^j$	$W_{ik}\frac{m_{\ell_{Hk}}}{\sqrt{2}f}V_{kj}$	0

Table 9: Partner lepton Scalar-Fermion-Fermion coupling [29].

$S(p_1)S(p_2)V_\mu$	G
$\Phi^+\Phi^-\gamma$	-1

Table 10: Partner lepton Scalar-Scalar-Vector coupling [37].

Then, the amplitude corresponding to the Figure 25 is

$$i\Gamma^\mu = \sum_{i,j,k} V^\dagger_{\ell' i}\frac{m_{\ell_{Hi}}}{M_{W_H}}W^\dagger_{ij}W_{jk}\frac{m_{\ell_{Hk}}}{M_{W_H}}V_{k\ell}\int\frac{d^4k}{(2\pi)^4}\frac{P_R(\not{k}+M_2)P_L(p_1+p_2-2k)^\mu}{(k^2-M_2^2+i\epsilon)[(p_1-k)^2-M_1^2+i\epsilon][(p_2-k)^2-M_1^2+i\epsilon]}, \tag{262}$$

hence,

$$IV: \quad F_M^\gamma|_{\bar{\nu}^c} = -iF_E^\gamma|_{\bar{\nu}^c} = \sum_{i,j,k} V^\dagger_{\ell' i}\frac{m_{\ell_{Hi}}}{M_{W_H}}W^\dagger_{ij}W_{jk}\frac{m_{\ell_{Hk}}}{M_{W_H}}V_{k\ell}\frac{\alpha_W}{16\pi}\frac{m_\mu}{M_\Phi^2}\left[\overline{C}_1+\frac{3}{2}\overline{C}_{11}\right], \tag{263}$$

according with the Appendix A for the Three-Point Functions, we have that

$$F_M^{\bar{\nu^c}}(x) = \left[\overline{C}_1+\frac{3}{2}\overline{C}_{11}\right] = \frac{-1+5x+2x^2}{12(1-x)^3}+\frac{x^2}{2(1-x)^4}\ \ln x, \tag{264}$$

where $x = \frac{m^2_{\nu^c_j}}{M_\Phi^2}$. This result is in agreement with [37].
Similarly for the contribution to $\bar{\ell}^c$ we obtain [37]

$$III: \quad F_M^\gamma|_{\bar{\ell}^c} = -iF_E^\gamma|_{\bar{\ell}^c} = \sum_{i,j,k} V^\dagger_{\ell' i}\frac{m_{\ell_{Hi}}}{M_{W_H}}W^\dagger_{ij}W_{jk}\frac{m_{\ell_{Hk}}}{M_{W_H}}V_{k\ell}\frac{\alpha_W}{16\pi}\frac{m_\mu}{M_\Phi^2}F_M^{\bar{\ell^c}}\left(\frac{m^2_{\nu^c_j}}{M_\Phi^2}\right), \tag{265}$$

with

$$F_M^{\bar{\ell^c}}(x) = \frac{-4+5x+5x^2}{6(1-x)^3}-\frac{x(1-2x)}{(1-x)^4}\ \ln x. \tag{266}$$

Observing the form factors above $F_M^{W,A/Z,\bar{\nu},\bar{\ell}}$, they are finite and depend just on the ratio of the particle masses in the loop.
We know that $m_{\nu_{Hi}} = m_{\ell_{Hi}}(1-v^2/8f^2) \approx m_{\ell_{Hi}}$, $M^2_{W_H} = M^2_{Z_H} = 5M^2_{A_H}(1+v^2/f^2)/t^2_W \approx 5M^2_{A_H}/t^2_W$ where we have neglected terms suppressed by v^2/f^2 factors, while the masses of $\overline{\nu}_i$ and $\overline{\ell}_i$ are the same, therefore in the form factors their own v^2/f^2 corrections can be neglected. Since we are considering $\overline{\nu}_i$ and $\overline{\ell}_i$ have the same mass, it means that the different components of the same $SU(2)_L$ multiplet

are degenerate when substituted in $F_M^{W,A/Z,\bar{\nu},\bar{\ell}}$. For the case of the electroweak triplet Φ, we consider the same argument.

6 Extracting Form Factors from the $\mu \to ee\bar{e}$ Amplitude in the LHT

This process can be studied like a $\ell \to \ell'\bar{\ell}'\ell'$ decay which involves photon and Z penguin diagrams as well as box contributions.
The amplitude can be written as follows [37]

$$i\Gamma^{\mu}_{\gamma}(p_\ell, p_{\ell'}) = ie\{\left[iF^{\gamma}_{M}(Q^2) + F^{\gamma}_{E}(Q^2)\gamma_5\right]\sigma^{\mu\nu}Q_\nu + F^{\gamma}_{L}(Q^2)\gamma^{\mu}P_L\}, \tag{267}$$

with $Q_\nu = (p_{\ell'} - p_\ell)_\nu$. In our case $\ell \to \mu$ and $\ell' \to e$ therefore the corresponding right-handed vector form factor vanishes ($m_e \approx 0$). Due the constraints of LHT only photon and Z penguin diagrams contribute, since A_H and Z_H do not couple to two ordinary fermions, as required by T-parity conservation.

6.1 The $\gamma-$penguin contributions

The form factors F^{γ}_{M} and F^{γ}_{E} have the same expressions (247, 249, 259, 264, 266) as for an on-shell photon, since terms of order Q^2 can be neglected [25]. We are going to show the contributions to F^{γ}_{L}, which are proportional to $Q^2 \sim m^2_\mu$ as expected.
The form factor $F^{\gamma}_{L}|_{Z_H}$ contribution is given by the following diagrams

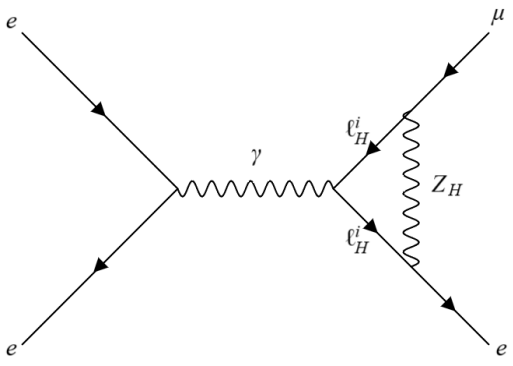

Figure 27: Penguin diagram exchanging Z_H gauge boson.

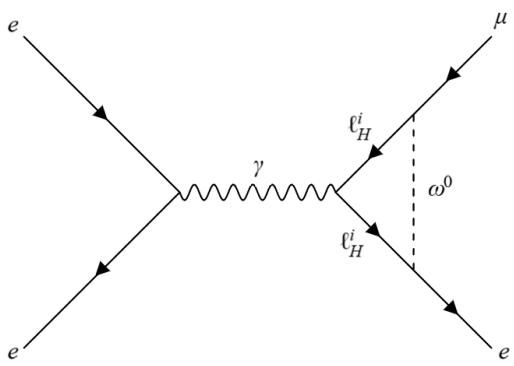

Figure 28: Penguin diagram exchanging ω^0 Goldstone boson.

and we also need to consider their self-energy diagrams, which contribute to F^{V}_{L} in this process.
The amplitude of the diagrams above can be written as

$$\mathcal{M} \sim L^{\lambda}_{\mu e} \times \ell_{e\bar{e}\lambda}, \tag{268}$$

where $\ell^{\lambda}_{e\bar{e}} = ie\bar{u}(p_3)\gamma^{\lambda}v(p_4)$ is independent of the loop integration whereas the relevant part for the latter is given by the effective $Z_H\mu e$ transition as follows

$$L^{\lambda}_{\mu e} = \bar{u}(p_2)\Gamma^{\lambda}_{\gamma}(p_2, p_1)u(p_1). \tag{269}$$

Therefore, $\Gamma^{\lambda}_{\gamma}(p_2, p_1)$, for diagram 27 is given by eq. (238)

$$i\Gamma^{\mu} = \frac{\alpha_W}{32\pi}\sum_i V^{ie*}_{H\ell}V^{i\mu}_{H\ell}\int \frac{d^4k}{(2\pi)^4}\frac{\gamma^{\alpha}P_L(\not{p}_2 - \not{k} + M_2)\gamma^{\mu}(\not{p}_1 - \not{k} + M_2)\gamma^{\beta}P_L g_{\beta\alpha}}{(k^2 - M_1^2 + i\epsilon)((p_1-k)^2 - M_2^2 + i\epsilon)((p_2-k)^2 - M_2^2 + i\epsilon)},$$

and self-energy diagrams are given by eqs. (239) and (240).
Now, $\Gamma^{\lambda}_{\gamma}(p_2, p_1)$ corresponding to diagram 28 is given by eq. (242)

$$i\Gamma^{\mu} = \frac{\alpha_W}{32\pi}\sum_i V^{ie*}_{H\ell}V^{i\mu}_{H\ell}y_i\int \frac{d^4k}{(2\pi)^4}\frac{P_R(\not{p}_2 - \not{k} + M_2)\gamma^{\mu}(\not{p}_1 - \not{k} + M_2)(M_2P_L - m_{\mu}P_R)}{(k^2 - M_1^2 + i\epsilon)((p_1-k)^2 - M_2^2 + i\epsilon)((p_2-k)^2 - M_2^2 + i\epsilon)},$$

and self-energy diagrams are determined by eqs. (243) and (244).
With aid of Package-X [38] and the *Projector* command, we add the contributions of the two topologies above, therefore, the form factor $F_L^{\gamma}|_{Z_H}$ is

$$\begin{aligned} F_L^{\gamma}|_{Z_H} &= \frac{\alpha_W}{4\pi}\sum_i V^{ie*}_{H\ell}V^{i\mu}_{H\ell}G_Z(y_i) \\ &= \frac{\alpha_W}{4\pi}\frac{Q^2}{M^2_{W_H}}\sum_i V^{ie*}_{H\ell}V^{i\mu}_{H\ell}G^{(1)}_Z(y_i), \end{aligned} \tag{270}$$

with [25] [37]

$$\begin{aligned} G_Z(y_i) &= \left(1+\frac{x}{2}\right)\left(-\frac{1}{4} + \frac{1}{2}\overline{B}_1 + C_{00} - \frac{x}{2}M_1^2C_0\right) - \left(\frac{1}{2}C_0 + C_1 + \frac{1}{8}(2+x)C_{11}\right)Q^2, \\ &= \frac{Q^2}{M_1^2}G^{(1)}_Z(x) + \mathcal{O}\left(\frac{Q^4}{M_1^4}\right), \end{aligned} \tag{271}$$

$$G^{(1)}_Z(x) = \frac{1}{36} + \frac{x(18-11x-x^2)}{48(1-x)^3} - \frac{4-16x+9x^2}{24(1-x)^4}\ln x, \tag{272}$$

where $M_1 = M_{Z_H}$ and $M_2 = m_{\ell^i_H}$.
Similarly, the form factor of A_H is obtained just replacing Z_H by A_H and y_i by $y'_i = 5c_W^2y_i/s_W^2$, hence [25] [37]

$$F_L^{\gamma}|_{A_H} = \frac{\alpha_W}{4\pi}\frac{Q^2}{M^2_{W_H}}\frac{1}{5}\sum_i V^{ie*}_{H\ell}V^{i\mu}_{H\ell}G^{(1)}_Z(y'_i). \tag{273}$$

Now, the contributions of diagrams with W_H are given by the topologies II, IV, V, and VI, yielding

$$\begin{aligned} F_L^{\gamma}|_{W_H} &= \frac{\alpha_W}{4\pi}\sum_i V^{ie*}_{H\ell}V^{i\mu}_{H\ell}G_W(y_i) \\ &= \frac{\alpha_W}{4\pi}\frac{Q^2}{M^2_{W_H}}\sum_i V^{ie*}_{H\ell}V^{i\mu}_{H\ell}G^{(1)}_W(y_i), \end{aligned} \tag{274}$$

with [25] [37]

$$\begin{aligned} G_W(x) &= -\frac{1}{2} + \overline{B}_1 + 6\overline{C}_{00} + x\left(\frac{1}{2}\overline{B}_1 + \overline{C}_{00} - M_1^2\overline{C}_0\right) - \left(2\overline{C}_1 + \frac{1}{2}\overline{C}_{11}\right)Q^2 \\ &= \Delta_\epsilon - \ln\frac{M_1^2}{\mu^2} + \frac{Q^2}{M_1^2}G_W^{(1)}(x) + \mathcal{O}\left(\frac{Q^4}{M_1^4}\right), \end{aligned} \tag{275}$$

$$G_W^{(1)}(x) = -\frac{5}{18} + \frac{x(12+x-7x^2)}{24(1-x)^3} + \frac{x^2(12-10x+x^2)}{12(1-x)^4}\ln x. \tag{276}$$

Due to the unitarity of the mixing matrix, the x-independent terms in $G_W(x)$ drop out (including the ultraviolet divergence). After considering the explicit expressions of $\overline{B}$ and $\overline{C}$ functions shown in the Appendices E and F, we obtain the eq.(276). The SM prediction is obtained by replacing W_H by W, ν_H^i by ν^i and $V_{H\ell}$ by $V_{PMNS}^\dagger$.
The new contributions due to $F_L^\gamma|_{\overline{\nu}^c,\overline{\ell}^c}$ are given by [37]

$$F_L^\gamma|_{\overline{\nu}^c,\overline{\ell}^c} = \frac{\alpha_W}{4\pi}\frac{Q^2}{M_\Phi^2}\sum_{ijk} V_{\ell' i}^\dagger \frac{m_{\ell_{Hi}}}{M_{W_H}} W_{ij}^\dagger W_{jk} \frac{m_{\ell_{Hk}}}{M_{W_H}} V_{k\ell}\left(G_{\overline{\nu}^c}^{(1)}(x) + G_{\overline{\ell}^c}^{(1)}(x)\right), \tag{277}$$

with

$$\begin{aligned} G_{\overline{\nu}^c}(x) &= -\overline{B}_1 - 2\overline{C}_{00} = \frac{Q^2}{M_\Phi^2}G_{\overline{\nu}^c}^{(1)}(x) \\ G_{\overline{\nu}^c}^{(1)}(x) &= \frac{2-7x+11x^2}{72(1-x)^3} + \frac{x^3}{12(1-x)^4}\ln x, \end{aligned} \tag{278}$$

and

$$G_{\overline{\ell}^c}^{(1)}(x) = \frac{20-43x+29x^2}{36(1-x)^3} + \frac{2-3x+2x^3}{6(1-x)^4}\ln x. \tag{279}$$

6.2 The $Z-$penguin contributions

Z penguins diagrams involve a Z boson propagator which for small momentum transfer processes is proportional to M_Z^{-2}. The dipole form factors $F_{M,E}^Z$, which are chirality flipping and hence proportional to the muon mass, can be neglected as compared to F_L^Z. This is in contrast with the $\gamma-$penguin, for which $QF_{M,E}^\gamma(\sim QF_{M,E}^Z) \sim Q^2/M_{W_H}^2 \lessapprox m_\mu^2/M_{W_H}^2 \sim F_L^\gamma$, to be compared with $F_L^Z \sim 1$. This justifies neglecting $F_{M,E}^Z$ in the Z-penguin (143) [25].
Thus, at leading order the $Z\bar{\ell}\ell'$ vertex reduces to

$$i\Gamma_Z^\mu(p_\ell, p_{\ell'}) = ieF_L^Z(Q^2)\gamma^\nu P_L. \tag{280}$$

Taking $M_1 = M_{W_H}$, $M_2 = m_{Hi}$ and $y_i = m_{Hi}^2/M_{W_H}^2$, and using the unitarity of $V_{H\ell}$ we obtain [25] [37]

$$F_L^Z = F_L^Z|_{W_H} + F_L^Z|_{A_H} + F_L^Z|_{Z_H} + F_L^Z|_{\overline{\nu}^c} + F_L^Z|_{\overline{\ell}^c}, \tag{281}$$

where,

$$\begin{aligned}
F_L^Z|_{W_H} &= \frac{\alpha_W}{8\pi c_W s_W}\sum_i V_{H\ell}^{ie*}V_{H\ell}^{i\mu}\left[-2c_W^2\left(-\frac{1}{2}+\overline{B}_1+6\overline{C}_{00}-y_iM_1^2\overline{C}_0\right)-y_ic_W^2\left(\overline{B}_1+2\overline{C}_{00}\right)\right.\\
&\qquad\left.+2(1+\frac{y_i}{2})\left(\frac{1}{2}\overline{B}_1+C_{00}-\frac{1}{2}y_iM_1^2C_0\right)+\frac{v^2}{f^2}\frac{y_i}{16}\left[1+4\left(\overline{C}_{00}-C_{00}+M_1^2\left(C_0-2\overline{C}_0\right)\right)\right]\right]\\
&= \frac{\alpha_W}{8\pi c_W s_W}\sum_i V_{H\ell}^{ie*}V_{H\ell}^{i\mu}\left[-2c_W^2\left(\Delta_\epsilon-\ln\frac{M_1^2}{\mu^2}\right)+\frac{v^2}{f^2}\frac{y_i}{8}H_W(y_i)\right]\\
&= \frac{\alpha_W}{8\pi c_W s_W}\sum_i V_{H\ell}^{ie*}V_{H\ell}^{i\mu}\frac{v^2}{f^2}\frac{y_i}{8}H_L^{W(0)}(y_i),\\
F_L^Z|_{Z_H} &= \frac{\alpha_W}{8\pi c_W s_W}\sum_i V_{H\ell}^{ie*}V_{H\ell}^{i\mu}(1-2c_W^2)\left(-\frac{1}{4}+\frac{1}{2}\overline{B}_1+C_{00}-\frac{1}{2}y_iM_{Z_H}^2C_0\right)\\
&\qquad\times\left[\left(1+\frac{y_i}{2}\right)-\frac{v^2}{f^2}\left(\frac{y_i}{4}+\left(\frac{c_W}{s_W}y_i-\frac{2s_W}{5c_W}\right)x_H\right)\right]=0,\\
F_L^Z|_{A_H} &= \frac{\alpha_W}{8\pi c_W s_W}\sum_i V_{H\ell}^{ie*}V_{H\ell}^{i\mu}(1-2c_W^2)\left(-\frac{1}{4}+\frac{1}{2}\overline{B}_1+C_{00}-\frac{1}{2}y_i'M_{A_H}^2C_0\right)\\
&\qquad\times\frac{1}{25}\frac{s_W^2}{c_W^2}\left[\left(1+\frac{y_i'}{2}\right)-\frac{v^2}{f^2}\left(\frac{5}{4}y_i'+\left(\frac{s_W}{c_W}y_i'+10\frac{c_W}{s_W}\right)x_H\right)\right]=0,
\end{aligned}$$

$$F_L^Z|_{\overline{\nu}^c}+F_L^Z|_{\overline{\ell}^c} = \frac{\alpha_W}{8\pi s_W c_W}\sum_{ijk}V_{\ell' i}^\dagger\frac{m_{\ell_{Hi}}}{M_{W_H}}W_{ij}^\dagger W_{jk}\frac{m_{\ell_{Hk}}}{M_{W_H}}V_{k\ell}\frac{Q^2}{M_\Phi^2}\left[H_L^{\overline{\nu}^c}\left(\frac{m_{\overline{\nu}_j^c}^2}{M_\Phi^2}\right)+(1-2c_W^2)H_L^{\overline{\ell}^c}\left(\frac{m_{\overline{\nu}_j^c}^2}{M_\Phi^2}\right)\right]=0,$$

with

$$\begin{aligned}
H_L^{W(0)}(x) &= \frac{6-x}{1-x}+\frac{2+3x}{(1-x)^2}\ln x,\\
H_L^{\overline{\nu}^c}(x) &= \frac{1}{2}F_L^{\overline{\ell}^c}(x)-2c_W^2F_L^{\overline{\nu}^c}(x),\\
H_L^{\overline{\ell}^c}(x) &= F_L^{\overline{\ell}^c}(x).
\end{aligned}\tag{282}$$

The eqs.(278) and (279) have been renamed as $F_L^{\overline{\nu}^c}$ and $F_L^{\overline{\ell}^c}$, respectively. The only term that contributes to three body lepton decays is $H_L^{W(0)}$, which comes from the diagrams with W_H and it is proportional to v^2/f^2. The other terms are negligible as long as $Q^2 \ll v^2$.

6.3 Box diagrams

In the $\mu \to ee\overline{e}$ process there are eight different kinds of box diagrams, which are shown in Figure 29.

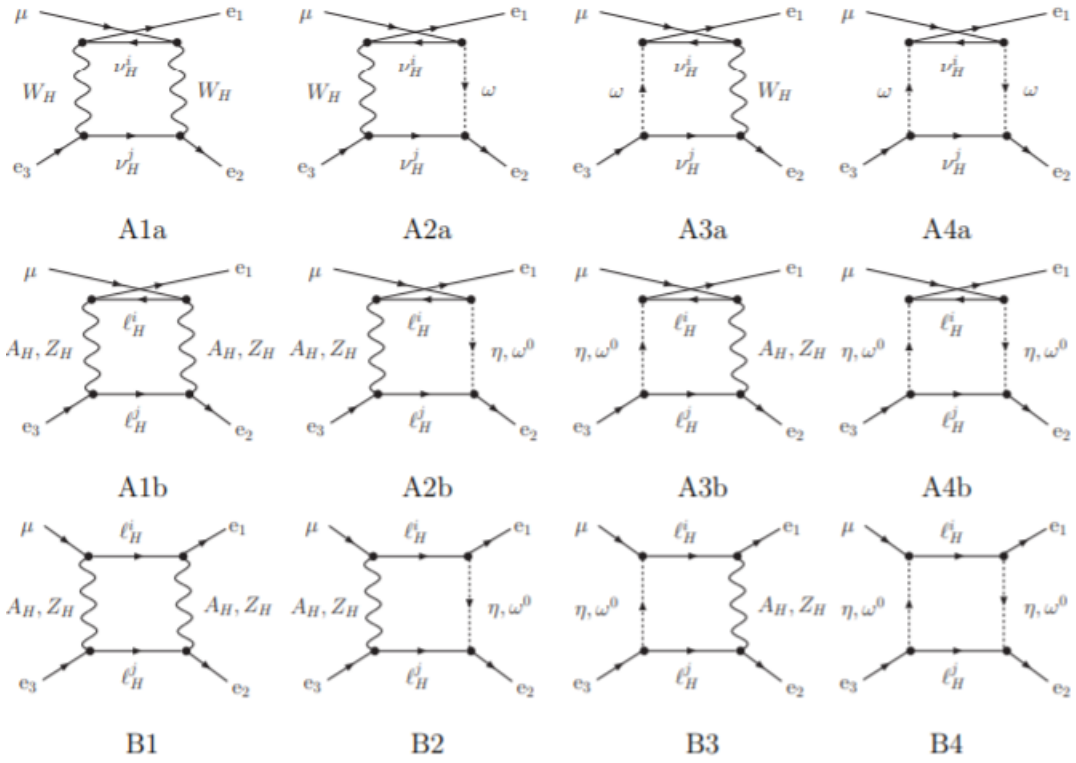

Figure 29: Box diagrams corresponding to $\mu \to ee\overline{e}$ process in the LHT model [25].

As we can see, these diagrams are classified in two types: A and B. Type A diagrams are crossed diagrams with the two outgoing leptons. In the limit of zero external momenta (all internal masses are much larger than the muon mass) all of them have the same form, being proportional to a scalar integral over the internal momentum q. The amplitude due to box diagrams is given by

$$\mathcal{M}_{box}^{\ell \to \ell'_1 \overline{\ell'}_2 \ell'_3} = e^2 B_L(0) \overline{u}(p_1) \gamma^\mu P_L u(p_\ell) \overline{u}(p_3) \gamma_\mu P_L v(p_2). \tag{283}$$

Thus, all box form factors except B_1^L, which appears in the eqs. (144) and (283), vanish. We use the Fierz identity

$$\langle 1|\gamma^\mu P_L|2\rangle\langle 3|\gamma_\mu P_L|4\rangle = -\langle 3|\gamma^\mu P_L|2\rangle\langle 1|\gamma_\mu P_L|4\rangle. \tag{284}$$

The whole $B_1^L(0)$ form factor is written as follows

$$B_1^L(0) = B_1^L(W_H, W_H) + B_1^L(Z_H, Z_H) + B_1^L(A_H, A_H) + B_1^L(A_H, Z_H) + B_1^L(\Phi, \Phi). \tag{285}$$

In [25] we can find the generic expressions for the contributions from diagrams of types A and B

$$\begin{aligned} A: \quad B_1^L = 2\frac{\alpha}{4\pi}\sum_{ij}\Bigg[&\left(g_{L1}^{ie*}g_{L2}^{i\mu}g_{L1}^{je}g_{L2}^{je*}+\frac{1}{4}c_{L1}^{ie*}c_{L2}^{i\mu}c_{L1}^{je}c_{L2}^{je*}\right)\widetilde{D}_0(M_1^2,M_2^2,m_{Hi}^2,m_{Hj}^2)\\ &-\left(g_{L1}^{ie*}c_{L2}^{i\mu}g_{L1}^{je}c_{L2}^{je*}+c_{L1}^{ie*}g_{L2}^{i\mu}c_{L1}^{je}g_{L2}^{je*}\right)m_{Hi}m_{Hj}D_0(M_1^2,M_2^2,m_{Hi}^2,m_{Hj}^2)\Bigg], \end{aligned} \tag{286}$$

$$\begin{aligned} B: \quad B_1^L = 2\frac{\alpha}{4\pi}\sum_{ij}\Bigg[&-\left(4g_{L2}^{ie*}g_{L1}^{i\mu}g_{L1}^{je}g_{L2}^{je*}+\frac{1}{4}c_{L2}^{ie*}c_{L1}^{i\mu}c_{L1}^{je}c_{L2}^{je*}\right)\widetilde{D}_0(M_1^2,M_2^2,m_{Hi}^2,m_{Hj}^2)\\ &+\left(g_{L2}^{ie*}c_{L1}^{i\mu}c_{L1}^{je}g_{L2}^{je*}+c_{L2}^{ie*}g_{L1}^{i\mu}g_{L1}^{je}c_{L2}^{je*}\right)m_{Hi}m_{Hj}D_0(M_1^2,M_2^2,m_{Hi}^2,m_{Hj}^2)\Bigg]. \end{aligned} \tag{287}$$

We just need to replace the vertex coefficients given by the Feynman rules from Table 4 to 10.
We are going to show the development of the diagrams with W_H, where we just write the numerator and omit the ie factor:

A1:

$$\begin{aligned} &\frac{1}{4s_W^4}\sum_{ij}V_{H\ell}^{ie*}V_{H\ell}^{i\mu}|V_{H\ell}^{je}|^2\langle p_1|\gamma^\mu P_L(-\not{q}+m_{\nu_H^i})\gamma^\nu P_L|p\rangle\langle p_2|\gamma^\beta P_L(-\not{q}+m_{\nu_H^j})\gamma^\alpha P_L|p_3\rangle g_{\alpha\mu}g_{\beta\nu}\\ &\quad=...\langle p_1|\gamma^\mu P_L(-\not{q}+m_{\nu_H^i})\gamma^\nu P_L|p\rangle\langle p_2|\gamma_\nu P_L(-\not{q}+m_{\nu_H^j})\gamma_\mu P_L|p_3\rangle\\ &\quad=...4q^2\langle p_1|\gamma^\mu P_L|p\rangle\langle p_2|\gamma_\mu P_L|p_3\rangle, \end{aligned} \tag{288}$$

then, the result of the diagram A1 with W_H is given by

$$\frac{q^2}{s_W^4}\sum_{ij}V_{H\ell}^{ie*}V_{H\ell}^{i\mu}|V_{H\ell}^{je}|^2\langle p_1|\gamma^\mu P_L|p\rangle\langle p_2|\gamma_\mu P_L|p_3\rangle. \tag{289}$$

A2:

$$\begin{aligned} -\frac{1}{4s_W^4M_{W_H}^2}m_{\nu_H^i}m_{\nu_H^j}\sum_{ij}&V_{H\ell}^{ie*}V_{H\ell}^{i\mu}|V_{H\ell}^{je}|^2\langle p_1|\gamma^\mu P_L(-\not{q}+m_{\nu_H^i})P_L|p\rangle\langle p_2|P_R(-\not{q}+m_{\nu_H^j})\gamma^\alpha P_L|p_3\rangle g_{\alpha\mu}\\ &=...\langle p_1|\gamma^\mu P_L(-\not{q}+m_{\nu_H^i})P_L|p\rangle\langle p_2|P_R(-\not{q}+m_{\nu_H^j})\gamma_\mu P_L|p_3\rangle\\ &=...m_{\nu_H^i}m_{\nu_H^j}\langle p_1|\gamma^\mu P_L|p\rangle\langle p_2|\gamma_\mu P_L|p_3\rangle, \end{aligned} \tag{290}$$

thus,

$$-\frac{1}{4s_W^4M_{W_H}^2}m_{\nu_H^i}^2m_{\nu_H^j}^2\sum_{ij}V_{H\ell}^{ie*}V_{H\ell}^{i\mu}|V_{H\ell}^{je}|^2\langle p_1|\gamma^\mu P_L|p\rangle\langle p_2|\gamma_\mu P_L|p_3\rangle. \tag{291}$$

A3:

$$\begin{aligned}-\frac{1}{4s_W^4 M_{W_H}^2} m_{\nu_H^i} m_{\nu_H^j} \sum_{ij} V_{H\ell}^{ie*} V_{H\ell}^{i\mu} |V_{H\ell}^{je}|^2 \langle p_1|P_R(-\not{q} + m_{\nu_H^i})\gamma^\mu P_L|p\rangle \langle p_2|\gamma^\alpha P_L(-\not{q} + m_{\nu_H^j})P_L|p_3\rangle g_{\alpha\mu} \\ = ...\langle p_1|P_R(-\not{q} + m_{\nu_H^i})\gamma^\mu P_L|p\rangle \langle p_2|\gamma_\mu P_L(-\not{q} + m_{\nu_H^j})P_L|p_3\rangle \\ = ... m_{\nu_H^i} m_{\nu_H^j} \langle p_1|\gamma^\mu P_L|p\rangle \langle p_2|\gamma_\mu P_L|p_3\rangle,\end{aligned} \tag{292}$$

hence,

$$-\frac{1}{4s_W^4 M_{W_H}^2} m_{\nu_H^i}^2 m_{\nu_H^j}^2 \sum_{ij} V_{H\ell}^{ie*} V_{H\ell}^{i\mu} |V_{H\ell}^{je}|^2 \langle p_1|\gamma^\mu P_L|p\rangle \langle p_2|\gamma_\mu P_L|p_3\rangle. \tag{293}$$

A4:

$$\begin{aligned}\frac{1}{4s_W^4 M_{W_H}^4} m_{\nu_H^i}^2 m_{\nu_H^j}^2 \sum_{ij} V_{H\ell}^{ie*} V_{H\ell}^{i\mu} |V_{H\ell}^{je}|^2 \langle p_1|P_R(-\not{q} + m_{\nu_H^i})P_L|p\rangle \langle p_2|P_R(-\not{q} + m_{\nu_H^j})P_L|p_3\rangle \\ = ... q^2 \langle p_1|\gamma^\mu P_L|p\rangle \langle p_2|\gamma_\mu P_L|p_3\rangle,\end{aligned} \tag{294}$$

therefore,

$$\frac{q^2}{4s_W^4 M_{W_H}^4} m_{\nu_H^i}^2 m_{\nu_H^j}^2 \sum_{ij} V_{H\ell}^{ie*} V_{H\ell}^{i\mu} |V_{H\ell}^{je}|^2 \langle p_1|\gamma^\mu P_L|p\rangle \langle p_2|\gamma_\mu P_L|p_3\rangle. \tag{295}$$

Adding all the contributions above and using the functions of the Appendix F, we obtain

$$B_1^L(W_H, W_H) = \frac{\alpha}{2\pi} \frac{1}{4s_W^4} \frac{1}{M_W^2} \frac{v^2}{4f^2} \sum_{ij} \chi_{ij} \left[\left(1 + \frac{1}{4} y_i y_j\right) \widetilde{d}_0(y_i, y_j) - 2 y_i y_j d_0(y_i, y_j) \right], \tag{296}$$

with $\chi_{ij} = V_{H\ell}^{ie*} V_{H\ell}^{i\mu} |V_{H\ell}^{je}|^2$ and we have used that $M_W^2/M_{W_H}^2 = v^2/4f^2$.
Now, we are going to show the development of the diagrams with Z_H. Here, we have omitted the v^2/f^2 contribution from the Feynman rules.

A1:

$$\begin{aligned}\frac{1}{16 s_W^4} \sum_{ij} \chi_{ij} \langle p_1|\gamma^\mu P_L(-\not{q} + m_{\ell_H^i})\gamma^\nu P_L|p\rangle \langle p_2|\gamma^\beta P_L(-\not{q} + m_{\ell_H^j})\gamma^\alpha P_L|p_3\rangle g_{\alpha\mu} g_{\beta\nu} \\ = ... 4q^2 \langle p_1|\gamma^\mu P_L|p\rangle \langle p_2|\gamma_\mu P_L|p_3\rangle\end{aligned} \tag{297}$$

then,

$$\frac{q^2}{4s_W^4} \sum_{ij} \chi_{ij} \langle p_1|\gamma^\mu P_L|p\rangle \langle p_2|\gamma_\mu P_L|p_3\rangle. \tag{298}$$

A2:

$$-\frac{1}{16s_W^4 M_{Z_H}^2} m_{\ell_H^i} m_{\ell_H^j} \sum_{ij} \chi_{ij} \langle p_1|\gamma^\mu P_L(-\not{q} + m_{\ell_H^i}) P_L|p\rangle \langle p_2|P_R(-\not{q} + m_{\ell_H^j})\gamma^\alpha P_L|p_3\rangle g_{\alpha\mu} \\ = ... m_{\ell_H^i} m_{\ell_H^j} \langle p_1|\gamma^\mu P_L|p\rangle \langle p_2|\gamma_\mu P_L|p_3\rangle, \tag{299}$$

thus,

$$-\frac{1}{16s_W^4 M_{Z_H}^2} m_{\ell_H^i}^2 m_{\ell_H^j}^2 \sum_{ij} \chi_{ij} \langle p_1|\gamma^\mu P_L|p\rangle \langle p_2|\gamma_\mu P_L|p_3\rangle. \tag{300}$$

A3:

$$-\frac{1}{16s_W^4 M_{Z_H}^2} m_{\ell_H^i} m_{\ell_H^j} \sum_{ij} \chi_{ij} \langle p_1|P_R(-\not{q} + m_{\ell_H^i})\gamma^\mu P_L|p\rangle \langle p_2|\gamma^\alpha P_L(-\not{q} + m_{\ell_H^j}) P_L|p_3\rangle g_{\alpha\mu} \\ = ... m_{\ell_H^i} m_{\ell_H^j} \langle p_1|\gamma^\mu P_L|p\rangle \langle p_2|\gamma_\mu P_L|p_3\rangle, \tag{301}$$

hence,

$$-\frac{1}{16s_W^4 M_{Z_H}^2} m_{\ell_H^i}^2 m_{\ell_H^j}^2 \sum_{ij} \chi_{ij} \langle p_1|\gamma^\mu P_L|p\rangle \langle p_2|\gamma_\mu P_L|p_3\rangle. \tag{302}$$

A4:

$$\frac{1}{16s_W^4 M_{Z_H}^4} m_{\ell_H^i}^2 m_{\ell_H^j}^2 \sum_{ij} \chi_{ij} \langle p_1|P_R(-\not{q} + m_{\ell_H^i}) P_L|p\rangle \langle p_2|P_R(-\not{q} + m_{\ell_H^j}) P_L|p_3\rangle \\ = ... q^2 \langle p_1|\gamma^\mu P_L|p\rangle \langle p_2|\gamma_\mu P_L|p_3\rangle, \tag{303}$$

therefore,

$$\frac{q^2}{16s_W^4 M_{Z_H}^4} m_{\ell_H^i}^2 m_{\ell_H^j}^2 \sum_{ij} \chi_{ij} \langle p_1|\gamma^\mu P_L|p\rangle \langle p_2|\gamma_\mu P_L|p_3\rangle. \tag{304}$$

B1:

$$\frac{1}{16s_W^4} \sum_{ij} \chi_{ij} \langle p_1|\gamma^\mu P_L(\not{q} + m_{\ell_H^i})\gamma^\nu P_L|p\rangle \langle p_2|\gamma^\beta P_L(-\not{q} + m_{\ell_H^j})\gamma^\alpha P_L|p_3\rangle g_{\alpha\mu} g_{\beta\nu} \\ = ... - 4q^2 \langle p_1|\gamma^\mu P_L|p\rangle \langle p_2|\gamma_\mu P_L|p_3\rangle \tag{305}$$

then,

$$-\frac{q^2}{4s_W^4} \sum_{ij} \chi_{ij} \langle p_1|\gamma^\mu P_L|p\rangle \langle p_2|\gamma_\mu P_L|p_3\rangle. \tag{306}$$

B2:

$$\frac{1}{16s_W^4 M_{Z_H}^2} m_{\ell_H^i} m_{\ell_H^j} \sum_{ij} \chi_{ij} \langle p_1|P_R(\not{q} + m_{\ell_H^i})\gamma^\mu P_L|p\rangle \langle p_2|P_R(-\not{q} + m_{\ell_H^j})\gamma^\alpha P_L|p_3\rangle g_{\alpha\mu} \\ = ... m_{\ell_H^i} m_{\ell_H^j} \langle p_1|\gamma^\mu P_L|p\rangle \langle p_2|\gamma_\mu P_L|p_3\rangle, \tag{307}$$

thus,

$$\frac{1}{16s_W^4 M_{Z_H}^2} m_{\ell_H^i}^2 m_{\ell_H^j}^2 \sum_{ij} \chi_{ij} \langle p_1|\gamma^\mu P_L|p\rangle\langle p_2|\gamma_\mu P_L|p_3\rangle. \tag{308}$$

B3:

$$\begin{aligned}\frac{1}{16s_W^4 M_{Z_H}^2} m_{\ell_H^i} m_{\ell_H^j} \sum_{ij} \chi_{ij} \langle p_1|\gamma^\mu P_L(\not{q} + m_{\ell_H^i})P_L|p\rangle\langle p_2|\gamma^\alpha P_L(-\not{q} + m_{\ell_H^j})P_L|p_3\rangle g_{\alpha\mu} \\ = ... m_{\ell_H^i} m_{\ell_H^j} \langle p_1|\gamma^\mu P_L|p\rangle\langle p_2|\gamma_\mu P_L|p_3\rangle,\end{aligned} \tag{309}$$

hence,

$$\frac{1}{16s_W^4 M_{Z_H}^2} m_{\ell_H^i}^2 m_{\ell_H^j}^2 \sum_{ij} \chi_{ij} \langle p_1|\gamma^\mu P_L|p\rangle\langle p_2|\gamma_\mu P_L|p_3\rangle. \tag{310}$$

B4:

$$\begin{aligned}\frac{1}{16s_W^4 M_{Z_H}^4} m_{\ell_H^i}^2 m_{\ell_H^j}^2 \sum_{ij} \chi_{ij} \langle p_1|P_R(\not{q} + m_{\ell_H^i})P_L|p\rangle\langle p_2|P_R(-\not{q} + m_{\ell_H^j})P_L|p_3\rangle \\ = ... - q^2 \langle p_1|\gamma^\mu P_L|p\rangle\langle p_2|\gamma_\mu P_L|p_3\rangle,\end{aligned} \tag{311}$$

therefore,

$$-\frac{q^2}{16s_W^4 M_{Z_H}^4} m_{\ell_H^i}^2 m_{\ell_H^j}^2 \sum_{ij} \chi_{ij} \langle p_1|\gamma^\mu P_L|p\rangle\langle p_2|\gamma_\mu P_L|p_3\rangle. \tag{312}$$

From the contributions above we obtain [25] [37]

$$B_1^L(Z_H, Z_H) = \frac{\alpha}{2\pi}\frac{1}{16s_W^4}\frac{1}{M_W^2}\frac{v^2}{4f^2}\sum_{ij}\chi_{ij}\left[-3\widetilde{d}_0(y_i, y_j)\right], \tag{313}$$

where $M_{W_H} \approx M_{Z_H}$.
It is important to note that in [25] the numerators for B2 and B3 are misspelled.
The others form factors are given by [25] [37]

$$B_1^L(A_H, A_H) = \frac{\alpha}{2\pi}\frac{1}{16s_W^4}\frac{1}{M_W^2}\frac{v^2}{4f^2}\sum_{ij}\chi_{ij}\left[-\frac{3}{50a}\widetilde{d}_0(y_i', y_j')\right], \tag{314}$$

$$B_1^L(A_H, Z_H) = \frac{\alpha}{2\pi}\frac{1}{16s_W^4}\frac{1}{M_W^2}\frac{v^2}{4f^2}\sum_{ij}\chi_{ij}\left[-\frac{3}{5}\frac{M_{A_H}^2}{M_{W_H}^2}\widetilde{d}_0(y_i', y_j', a)\right], \tag{315}$$

$$B_1^L(\Phi, \Phi) = \frac{\alpha}{2\pi}\frac{1}{16s_W^4}\frac{1}{M_\Phi^2}\sum_{ij}\chi_{ij}\widetilde{d}_0\left(\frac{m_{\bar{\nu}_i^c}^2}{M_\Phi^2}, \frac{m_{\bar{\nu}_j^c}^2}{M_\Phi^2}\right), \tag{316}$$

where $y_i' = m_{\ell_{Hi}}^2/M_{A_H}^2$ and $a = M_{W_H}^2/M_{A_H}^2$. The new contributions from the partner leptons $\bar{\nu}^c$ and $\bar{\ell}^c$ are equal (neglecting small mass differences within the scalar triplet Φ components) and included

in $B_1^L(\Phi, \Phi)$.

7 Neutrino masses in the LHT and new contributions to LFV processes

The LHT is a non-linear σ model based on the coset space $SU(5)/SO(5)$, with the $SU(5)$ global symmetry broken by the vacuum expectation value (VEV) giving rise to 14 NG bosons [25]

$$\Pi = \begin{pmatrix} -\omega^0/2 - \eta/\sqrt{20} & -\omega^+/\sqrt{2} & -i\pi^+/\sqrt{2} & -i\Phi^{++} & -i\frac{\Phi^+}{\sqrt{2}} \\ -\omega^-/2 & \omega^0/2 - \eta/\sqrt{20} & \frac{\upsilon_h + h + i\pi^0}{2} & -i\Phi^+/\sqrt{2} & \frac{-i\Phi^0 + \Phi^P}{\sqrt{2}} \\ -i\pi^-/\sqrt{2} & \left(\upsilon_h + h - i\pi^0\right)/2 & \sqrt{\frac{4}{5}}\eta & -i\pi^+/\sqrt{2} & \left(\upsilon_h + h + i\pi^0\right)/2 \\ i\Phi^{--} & i\frac{\Phi^-}{\sqrt{2}} & i\pi^-/\sqrt{2} & -\omega^0/2 - \eta/\sqrt{20} & -\omega^-/\sqrt{2} \\ i\frac{\Phi^-}{\sqrt{2}} & \frac{i\Phi^0 + \Phi^P}{\sqrt{2}} & \frac{\upsilon_h + h - i\pi^0}{2} & -\omega^+/\sqrt{2} & \omega^0/2 - \eta/\sqrt{20} \end{pmatrix}, \tag{317}$$

which decomposes into the SM Higgs doublet $(-i\pi^+/\sqrt{2}, (\upsilon + h + i\pi^0)/2)^T$, a complex $SU(2)_L$ triplet Φ, and the longitudinal modes of the heavy gauge fields $\omega^\pm$, ω^0 and η. They act on the fundamental representation of the unbroken subgroup multiplying by $\xi = e^{i\Pi/f}$. The action of T–parity is defined to make T–odd all but the SM Higgs doublet.

In the fermion sector each SM lepton doublet $l_L = (\nu_L \ \ell_L)^T$ is doubled introducing two incomplete quintuplets (σ^2 is the second Pauli matrix)

$$\Psi_1 = \begin{pmatrix} -i\sigma^2 l_{1L} \\ 0 \\ 0 \end{pmatrix}, \quad \Psi_2 = \begin{pmatrix} 0 \\ 0 \\ -i\sigma^2 l_{2L} \end{pmatrix}. \tag{318}$$

The action of T-parity on the LH leptons is then defined to be

$$\Psi_1 \longleftrightarrow \Omega\Sigma_0\Psi_2, \tag{319}$$

with

$$\Omega = diag(-1,-1,1,-1,-1), \quad \Sigma_0 = \begin{pmatrix} 0 & 0 & \mathbf{1}_{2\times 2} \\ 0 & 1 & 0 \\ \mathbf{1}_{2\times 2} & 0 & 0 \end{pmatrix}. \tag{320}$$

This discrete symmetry is implemented in the fermion sector duplicating the SM doublet $l_L = (l_{1L} - l_{2L})/\sqrt{2}$, corresponding to the T-even combination $(\Psi_1 + \Omega\Sigma_0\Psi_2)/\sqrt{2}$, that remains light, with an extra heavy mirror doublet $l_{HL} = (\nu_{HL} \ \ell_{HL})^T = (l_{1L} + l_{2L})/\sqrt{2}$ obtained from the T-odd orthogonal combination $(\Psi_1 - \Omega\Sigma_0\Psi_2)/\sqrt{2}$. This extra doublet per family will get its mass combining with a RH

doublet l_{HR} (eigenvector of T) in an $SO(5)$ multiplet Ψ_R,

$$\Psi_R = \begin{pmatrix} \tilde{\psi}^c_R \\ \chi_R \\ -i\sigma^2 l_{HR} \end{pmatrix}, \quad \Psi_R \xrightarrow{T} \Omega\Psi_R, \tag{321}$$

the superscript (^{c}) denotes a partner lepton field, not to be confused with charge conjugation. The non-linear Yukawa coupling generating this large mass $\sim f$ reads [39]

$$\mathcal{L}_{Y_H} = -\kappa f \left(\overline{\Psi}_2\xi + \overline{\Psi}_1\Sigma_0\xi^\dagger\right)\Psi_R - \kappa_2\overline{\Psi_L}\Psi_R - M\overline{\Psi^\chi_L}\Psi_R + \text{h.c.}, \tag{322}$$

where $\xi = e^{i\Pi/f}$, the first term preserves the global symmetry for $\xi \to V\xi U^\dagger$. While the second one is its T-transformed once the T-transformed of Ψ_R is fixed to be $\Omega\Psi_R$.
Approaching $\xi = \exp(i\Pi/f) \approx \mathbb{I}$, then

$$\mathcal{L}_{Y_H} = -\kappa f \left(\overline{\Psi}_2\xi + \overline{\Psi}_1\Sigma_0\xi^\dagger\right)\Psi_R + h.c. \approx \sqrt{2}\kappa f\ \overline{\psi}_{HL}\psi_{HR} - \kappa_2\overline{\tilde{\psi}^c_L}\tilde{\psi}^c_R - M\overline{\chi_L}\chi_R, \tag{323}$$

with $\psi_{HR} = -i\sigma^2 l_{HR}$. This Lagrangian gives a vector-like mass $\sqrt{2}\kappa f$ to ν_H.
The lepton singlets χ_R must also get a large (vector–like) mass by combining with a LH singlet χ_L through a direct mass term without further couplings to the Higgs. Thus, its mass term is written (which matches with eq. (323))

$$\mathcal{L}_M = -M\overline{\chi}_L\chi_R + h.c.. \tag{324}$$

χ_L is an $SU(5)$ singlet and it is therefore nature to include a small Majorana mass for it. Once LN is assumed to be only broken by small Majorana masses μ in the heavy LH neutral sector,

$$\mathcal{L}_\mu = -\frac{\mu}{2}\overline{\chi^c_L}\chi_L + h.c., \tag{325}$$

the resulting (T-even) neutrino mass matrix reduces to the inverse see-saw one [39]:

$$\mathcal{L}^\nu_M = -\frac{1}{2}\left(\overline{\nu^c_l}\ \overline{\chi_R}\ \overline{\chi^c_L}\right)\mathcal{M}^{T-even}_\nu \begin{pmatrix} \nu_L \\ \chi^c_R \\ \chi_L \end{pmatrix} + h.c., \tag{326}$$

where

$$\mathcal{M}^{T-even}_\nu = \begin{pmatrix} 0 & i\kappa^* f sin\left(\frac{v}{\sqrt{2}f}\right) & 0 \\ i\kappa^\dagger f sin\left(\frac{v}{\sqrt{2}f}\right) & 0 & M^\dagger \\ 0 & M^* & \mu \end{pmatrix}, \tag{327}$$

with each entry standing for a 3×3 matrix to take into account the 3 lepton families. The κ entries are given by the Yukawa Lagrangian in eq. (322) and M stands for the direct heavy Dirac mass matrix

from eq. (324), and μ is the mass matrix of small Majorana masses in eq.(325).
On considering the hierarchy $\mu << \kappa f << M$ (inverse see-saw), the mass eigenvalues for M are ~ 10 TeV, of the order of $4\pi f$ with $f \sim TeV$, as required by current EWPD if we assume the κ eigenvalues to be order 1 [3]. On the contrary, the μ eigenvalues shall be much smaller than the GeV.
Let $\mathcal{U}$ be a unitary transformation that diagonalizes $\mathcal{M}$ and transforms the states $(\nu_L \ \Psi_L)$ to the mass states $\left(\nu_L^l \ \Psi_L^h\right)$, light and heavy (quasi-Dirac) neutrinos, l and h, respectively

$$\mathcal{U}^\dagger \begin{pmatrix} \nu_L \\ \Psi_L \end{pmatrix} = \begin{pmatrix} \nu_L^l \\ \Psi_L^h \end{pmatrix}, \quad \text{with} \quad \Psi_L = \begin{pmatrix} \chi_R^c \\ \chi_L \end{pmatrix}. \tag{328}$$

The matrix $\mathcal{U}$ can be written as [41] [42]

$$\mathcal{U} = \begin{pmatrix} \sqrt{1-\mathcal{B}\mathcal{B}^\dagger} & \mathcal{B} \\ -\mathcal{B}^\dagger & \sqrt{1-\mathcal{B}^\dagger\mathcal{B}} \end{pmatrix}, \tag{329}$$

such that U satisfies

$$\mathcal{U}^T \mathcal{M} \mathcal{U} = \begin{pmatrix} \mathcal{M}_\nu^l & 0_{3\times 6} \\ 0_{6\times 3} & \mathcal{M}_\chi^h \end{pmatrix}, \tag{330}$$

where we can see $\mathcal{U}$ decouples the heavy from the light neutrino fields. $\mathcal{B}$ is a complex 3×3 matrix and we consider that

$$\sqrt{1-\mathcal{B}\mathcal{B}^\dagger} \approx 1 - \frac{1}{2}\mathcal{B}\mathcal{B}^\dagger - \frac{1}{8}\mathcal{B}\mathcal{B}^\dagger\mathcal{B}\mathcal{B}^\dagger - \cdots - \frac{\Gamma\left(-\frac{1}{2}+n\right)}{n!\Gamma\left(-\frac{1}{2}\right)}\left(\mathcal{B}\mathcal{B}^\dagger\right)^n - \cdots, \tag{331}$$

in our case we will just admit terms of the order $\mathcal{B}\mathcal{B}^\dagger$.
In order to diagonalize the $\mathcal{M}$ matrix, we can rewrite it defining the next matrices:

$$M_D = \begin{pmatrix} i\kappa^\dagger f \sin\left(\frac{v}{\sqrt{2}f}\right) \\ 0 \end{pmatrix}, \quad M_R = \begin{pmatrix} 0 & M^\dagger \\ M^* & \mu \end{pmatrix}, \tag{332}$$

hence,

$$\mathcal{M}_\nu^{T-even} = \begin{pmatrix} 0 & M_D^T \\ M_D & M_R \end{pmatrix}. \tag{333}$$

According to [41] a first approximation in $\mathcal{B}$ is

$$\mathcal{B}^* = M_D^T M_R^{-1} \rightarrow \mathcal{B} = M_D^\dagger \left(M_R^{-1}\right)^* = \left(if\sin\left(\frac{v}{\sqrt{2}f}\right)\kappa M^{-1}\mu^*(M^T)^{-1} \quad -if\sin\left(\frac{v}{\sqrt{2}f}\right)\kappa M^{-1}\right). \tag{334}$$

[3] We have considered lighter, O(4 TeV), Majorana neutrino masses in ref. [40].

Therefore, computing the eq. (331)

$$\sqrt{1-\mathcal{B}\mathcal{B}^\dagger} \approx 1 - \frac{1}{2}\mathcal{B}\mathcal{B}^\dagger \approx 1 - \frac{1}{2}\theta\theta^\dagger, \tag{335}$$

where we have omitted terms of the order of μ because of $\mu << \kappa f << M$ and we redefine $\mathcal{B} \to \Theta$

$$\Theta = \begin{pmatrix} -\theta\mu^*(M^T)^{-1} & \theta \end{pmatrix}, \quad \text{with} \quad \theta = -if\sin\left(\frac{v}{\sqrt{2}f}\right)\kappa M^{-1}, \tag{336}$$

we can see Θ is a 3×6 matrix and θ is a 3×3 matrix in agreement with [39, 43]. So that, the $\mathcal{U}$ matrix is written as

$$\mathcal{U} = \begin{pmatrix} 1-\frac{1}{2}\Theta\Theta^\dagger & \Theta \\ -\Theta^\dagger & 1-\frac{1}{2}\Theta^\dagger\Theta \end{pmatrix}, \tag{337}$$

then, we have that the $\mathcal{M}_\nu^l$ and $\mathcal{M}_\chi^h$ matrices in the eq. (330) are given by [39, 41–43]

$$(\mathcal{M}_\nu^l)_{ij} = -(M_D^T M_R^{-1} M_D)_{ij} = \theta_{ik}^*\mu_{kl}\theta_{jl}^\dagger, \qquad \mathcal{M}_\chi^h = M_R, \tag{338}$$

we have assumed without loss of generality that the χ mass matrix, M, is diagonal and positive definite. The diagonalized (Majorana) mass terms of eq. (328) thus read

$$\mathcal{L}_M^\nu = -\frac{1}{2}\left(\sum_{i=1}^{3}(\mathcal{M}_\nu^l)_i\overline{\nu_{Li}^l}\nu_{Ri}^l + \sum_{j=4}^{9}(\mathcal{M}_\chi^h)_j\overline{\Psi_{Lj}^h}\Psi_{Rj}^h\right). \tag{339}$$

We notice $\mathcal{M}_\nu^l$ is a 3×3 matrix and $\mathcal{M}_\chi^h$ is a 6×6 matrix. We can work in the basis where the charged lepton mass matrix is diagonal

$$\mathcal{M}_\nu^l = U_{PMNS}^*\mathcal{D}_\nu^l U_{PMNS}^\dagger, \tag{340}$$

from eq. (338),

$$\mu = (\theta^*)^{-1}U_{PMNS}^*\mathcal{D}_\nu^l U_{PMNS}^\dagger(\theta^\dagger)^{-1}, \tag{341}$$

where U_{PMNS} in the Pontecorvo-Maki-Nakagawa-Sakata matrix and $\mathcal{D}_\nu^l$ the diagonal neutrino mass matrix.

Applying explicitly $\mathcal{U}^\dagger$ in the eq. (328)

$$\begin{pmatrix} 1-\frac{1}{2}\Theta\Theta^\dagger & -\Theta \\ \Theta^\dagger & 1-\frac{1}{2}\Theta^\dagger\Theta \end{pmatrix}\begin{pmatrix} \nu_L \\ \Psi_L \end{pmatrix} = \begin{pmatrix} \nu_L^l \\ \Psi_L^h \end{pmatrix}, \tag{342}$$

due to the eq. (340) the light and heavy eigenstates are (mixing relations between flavor and mass eigenstates)

$$\begin{aligned}\sum_{j=1}^{3}(U_{PMNS})_{ij}\nu_{Lj}^{l} &= \sum_{j=1}^{3}[\mathbf{1}_{3\times3} - \frac{1}{2}(\Theta\Theta^{\dagger})]_{ij}\nu_{Lj} - \sum_{j=4}^{9}\Theta_{ij}\Psi_{Lj}, \\ \Psi_{Li}^{h} &= \sum_{j=4}^{9}[\mathbf{1}_{6\times6} - \frac{1}{2}(\Theta^{\dagger}\Theta)]_{ij}\Psi_{Lj} + \sum_{j=1}^{3}\Theta_{ij}^{\dagger}\nu_{Lj},\end{aligned} \tag{343}$$

where Θ matrix elements give the mixing between light and heavy (quasi-Dirac) neutrinos to leading order.

Let Φ be a flavor eigenstate composed by

$$\Phi_L = \mathcal{U}\begin{pmatrix}\nu_L^l \\ \Psi_L^h\end{pmatrix}, \tag{344}$$

thus, in terms of the mass eigenstates from the eq. (343) the SM charged current is modified as follows

$$\begin{aligned}\mathcal{L}_W &= \frac{g}{\sqrt{2}}W_{\mu}^{+}\sum_{i=1}^{9}\sum_{j=1}^{3}\overline{\Phi_{Li}}\gamma^{\mu}\ell_{Lj} \\ &= \frac{g}{\sqrt{2}}W_{\mu}^{+}\sum_{j=1}^{3}\left(\sum_{i=1}^{3}\{U_{PMNS}^{\dagger}[\mathbf{1}_{3\times3} - \frac{1}{2}(\Theta\Theta^{\dagger})]\}_{ij}\overline{\nu_{Li}^{l}} + \sum_{i=4}^{9}\Theta_{ij}^{\dagger}\overline{\Psi_{Li}^{h}}\right)\gamma^{\mu}\ell_{Lj},\end{aligned} \tag{345}$$

we can separate the Lagrangian above in two parts each one fixing the coupling between the SM leptons and the light and heavy quasi Dirac neutrinos, respectively,

$$\begin{aligned}\mathcal{L}_W^{l} &= \frac{g}{\sqrt{2}}W_{\mu}^{+}\sum_{j=1}^{3}\sum_{i=1}^{3}\overline{\nu_i^l}W_{ij}\gamma^{\mu}P_L\ell_j + h.c., \quad \text{with} \quad W_{ij} = \{U_{PMNS}^{\dagger}[\mathbf{1}_{3\times3} - \frac{1}{2}(\Theta\Theta^{\dagger})]\}_{ij}, \\ \mathcal{L}_W^{lh} &= \frac{g}{\sqrt{2}}W_{\mu}^{+}\sum_{j=1}^{3}\sum_{i=4}^{9}\overline{\Psi_i^h}\Theta_{ij}^{\dagger}\gamma^{\mu}P_L\ell_j + h.c..\end{aligned} \tag{346}$$

The SM neutral current is written as

$$\mathcal{L}_Z = \frac{g}{2cos\theta_W}Z_{\mu}\sum_{j=1}^{9}\sum_{i=1}^{9}\overline{\nu_{Li}}\gamma^{\mu}\nu_{Lj}, \tag{347}$$

we consider just the first order approximation to $\Theta\Theta^\dagger$ matrix and write down the light and heavy neutral currents,

$$\begin{aligned}
\mathcal{L}_Z^l &= \frac{g}{2cos\theta_W} Z_\mu \sum_{j=1}^{3}\sum_{i=1}^{3} \overline{\nu_i^l} X_{ij} \gamma^\mu P_L \nu_j^l, \quad \text{with} \quad X_{ij} = \{U_{PMNS}^\dagger [\mathbf{1}_{3\times 3} - (\Theta\Theta^\dagger)] U_{PMNS}\}_{ij}, \\
\mathcal{L}_Z^{lh} &= \frac{g}{2cos\theta_W} Z_\mu \sum_{j=1}^{3}\sum_{i=4}^{9} \overline{\Psi_i^h} (\Theta^\dagger U_{PMNS})_{ij} \gamma^\mu P_L \nu_j^l + h.c.. \\
\mathcal{L}_Z^h &= \frac{g}{2cos\theta_W} Z_\mu \sum_{j=1}^{3}\sum_{i=4}^{9} \overline{\Psi_i^h} (\Theta^\dagger \Theta)_{ij} \gamma^\mu P_L \Psi_j^h.
\end{aligned} \tag{348}$$

Now, we do not consider the μ term ($\mu \ll \kappa f \ll M$) in the Θ matrix, $\Theta = (0_{3\times 3} \quad \theta)$. Therefore, the eigenstates in the eq. (343) transform as [39]

$$\begin{aligned}
\sum_{j=1}^{3} (U_{PMNS})_{ij} \nu_{Lj}^l &= \sum_{j=1}^{3} [\mathbf{1}_{3\times 3} - \frac{1}{2}(\theta\theta^\dagger)]_{ij} \nu_{Lj} - \sum_{j=7}^{9} \theta_{ij} \chi_{Lj}, \\
\chi_{Li}^h &= \sum_{j=7}^{9} [\mathbf{1}_{3\times 3} - \frac{1}{2}(\theta^\dagger\theta)]_{ij} \chi_{Lj} + \sum_{j=1}^{3} \theta_{ij}^\dagger \nu_{Lj},
\end{aligned} \tag{349}$$

hence, the Lagrangians from eqs. (346) and (348) read

$$\begin{aligned}
\mathcal{L}_W^l &= \frac{g}{\sqrt{2}} W_\mu^+ \sum_{i,j=1}^{3} \overline{\nu_i^l} W_{ij} \gamma^\mu P_L \ell_j + h.c., \quad \text{with} \quad W_{ij} = \sum_{k=1}^{3} (U_{PMNS}^\dagger)_{ik} [\mathbf{1}_{3\times 3} - \frac{1}{2}(\theta\theta^\dagger)]_{kj}, \\
\mathcal{L}_W^{lh} &= \frac{g}{\sqrt{2}} W_\mu^+ \sum_{i,j=1}^{3} \overline{\chi_i^h} \theta_{ij}^\dagger \gamma^\mu P_L \ell_j + h.c..
\end{aligned} \tag{350}$$

and

$$\begin{aligned}
\mathcal{L}_Z^l &= \frac{g}{2\cos\theta_W} Z_\mu \sum_{i,j=1}^{3} \overline{\nu_i^l} \gamma^\mu (X_{ij} P_L - X_{ij}^\dagger P_R) \nu_j^l, \quad \text{with} \quad X_{ij} = \sum_{k=1}^{3} \left(U_{PMNS}^\dagger [\mathbf{1}_{3\times 3} - (\theta\theta^\dagger)] \right)_{ik} (U_{PMNS})_{kj}, \\
\mathcal{L}_Z^{lh} &= \frac{g}{2cos\theta_W} Z_\mu \sum_{i,j=1}^{3} \overline{\chi_i^h} \gamma^\mu (Y_{ij} P_L - Y_{ij}^\dagger P_R) \nu_j^l + h.c., \quad \text{with} \quad Y_{ij} = \sum_{k=1}^{3} \theta_{ik}^\dagger (U_{PMNS})_{kj}, \\
\mathcal{L}_Z^h &= \frac{g}{2\cos\theta_W} Z_\mu \sum_{i,j=1}^{3} \overline{\chi_i^h} \gamma^\mu (S_{ij} P_L - S_{ij}^\dagger P_R) \chi_j^h, \quad \text{with} \quad S_{ij} = \sum_{k=1}^{3} \theta_{ik}^\dagger \theta_{kj}.
\end{aligned} \tag{351}$$

where the dimension of the square W and X mixing matrices is 3×3. If we compare our charged-current and neutral-current interactions from eqs. (350) and (351) with the SM ones, we observe that

they differ by the presence of the θ matrix which is a consequence of introducing Majorana neutrinos. We can define the B_{ij} and C_{ij} matrices according to SM charged and neutral currents [44]

$$B_{ij} = \sum_{k=1}^{3} U_{ik}\mathcal{U}^{\dagger}_{kj} \quad \text{and} \quad C_{ij} = \sum_{k=1}^{3} \mathcal{U}_{ki}\mathcal{U}^{\dagger}_{kj}, \tag{352}$$

where B mixing matrix is 3×9, whereas C is a 9×9 matrix.

All LHT particles extended with Majorana neutrinos are collected in Table 12.

Particle Content of LHT with Majorana neutrinos	
Nambu–Goldstone bosons	
SM Higgs	$\left(-i\pi^+/\sqrt{2},\ (v+h+i\pi^0)/2\right)$
Longitudinal modes of the heavy gauge fields	$\omega^{\pm}, \omega^0, \eta$
Complex $SU(2)_L$ triplet	$\begin{pmatrix} i\Phi^{--} & i\Phi^-/\sqrt{2} \\ i\Phi^-/\sqrt{2} & (i\Phi^0+\Phi^P)/\sqrt{2} \end{pmatrix}$
Gauge bosons	
SM gauge bosons (T-even)	$\{W_L^{\pm}, Z_L, \gamma\}$
Heavy gauge bosons (T-odd)	$\{W_H^{\pm}, Z_H, A_H\}$
Fermions (i = 1,2,3)	
SM Fermions (T-even)	$\{\ell_L^i, \nu_L^i, u_L^i, d_L^i\}$
Mirror/Heavy/T-odd Fermions	$\{\ell_H^i, \nu_H^i, u_H^i, d_H^i\}$
Partner Fermions	$\{\ell_i^c, \nu_i^c, u_i^c, d_i^c\}$
Majorana neutrinos ($i = 1, 2, 3$)	
Heavy Majorana neutrinos	χ_{Li}^h

Table 11: The full content of particles of LHT with Majorana neutrinos.

We give the corresponding Feynman rules for the interaction vertices from the eqs. (350) and (351), we adopt the convention Feynman rule $= -i\mathcal{L}$.

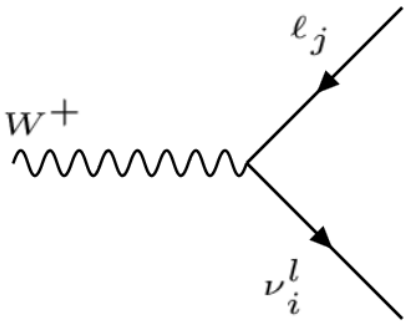

Figure 30: $-i\frac{g}{\sqrt{2}}W_\mu^+ W_{ij}\gamma^\mu P_L$.

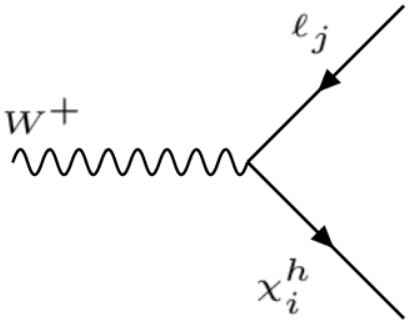

Figure 31: $-i\frac{g}{\sqrt{2}}W_\mu^+ \theta_{ij}^\dagger \gamma^\mu P_L$.

Particle Content of LHT with Majorana neutrinos	
Nambu–Goldstone bosons	
SM Higgs	$\left(-i\pi^+/\sqrt{2},\ (v+h+i\pi^0)/2\right)$
Longitudinal modes of the heavy gauge fields	$\omega^\pm, \omega^0, \eta$
Complex $SU(2)_L$ triplet	$\begin{pmatrix} i\Phi^{--} & i\Phi^-/\sqrt{2} \\ i\Phi^-/\sqrt{2} & (i\Phi^0+\Phi^P)/\sqrt{2} \end{pmatrix}$
Gauge bosons	
SM gauge bosons (T-even)	$\{W_L^\pm, Z_L, \gamma\}$
Heavy gauge bosons (T-odd)	$\{W_H^\pm, Z_H, A_H\}$
Fermions (i = 1,2,3)	
SM Fermions (T-even)	$\{\ell_L^i, \nu_L^i, u_L^i, d_L^i\}$
Mirror/Heavy/T-odd Fermions	$\{\ell_H^i, \nu_H^i, u_H^i, d_H^i\}$
Partner Fermions	$\{\ell_i^c, \nu_i^c, u_i^c, d_i^c\}$
Majorana neutrinos ($i = 1, 2, 3$)	
Heavy Majorana neutrinos	χ_{Li}^h

Table 12: The full content of particles of LHT with Majorana neutrinos.

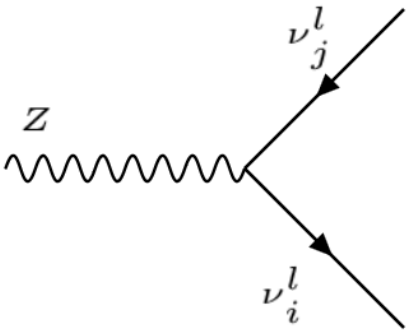

Figure 32: $-i\frac{g}{2\cos\theta_W}X_{ij}\gamma^\mu P_L$.

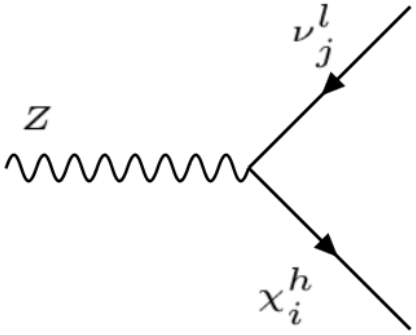

Figure 33: $-i\frac{g}{2\cos\theta_W}(\theta^\dagger U_{PMNS})_{ij}\gamma^\mu P_L$.

We calculate the box form factors of the amplitude for $\ell \to \ell'\ell''\bar{\ell}'''$ that receives contributions from the diagrams shown in Figures 35 and 36.

We recall from eq. (283) that the amplitude due to box diagrams is given by

$$\mathcal{M}_{box}^{\ell\to\ell'\ell''\bar{\ell}'''} = e^2 F_B \overline{u}(p_{\ell'})\gamma^\mu P_L u(p_\ell)\overline{u}(p_{\ell''})\gamma_\mu P_L \upsilon(p_{\ell'''}), \tag{353}$$

where F_B is the form factor. Because of the Fierz identity from eq. (284) all the box diagrams can be reduced to the form of the equation above.

The contributions of the diagrams in Figure 35 are the same as those of eq.(296) except for constants.

$$F_B^{\nu_i^l\nu_j^l} = \frac{\alpha_W}{16\pi M_W^2 s_W^2}\sum_{i,j=1}^{3}\{W_{\ell i}W_{\ell' i}^\dagger W_{\ell'' j}W_{\ell''' j}^\dagger + (\ell' \leftrightarrow \ell'')\} f_B^l(y_i, y_j), \tag{354}$$

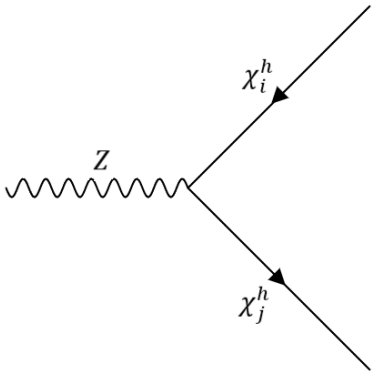

Figure 34:
$-i\frac{g}{2\cos\theta_W}(\theta^\dagger\theta)_{ij}\gamma^\mu P_L$.

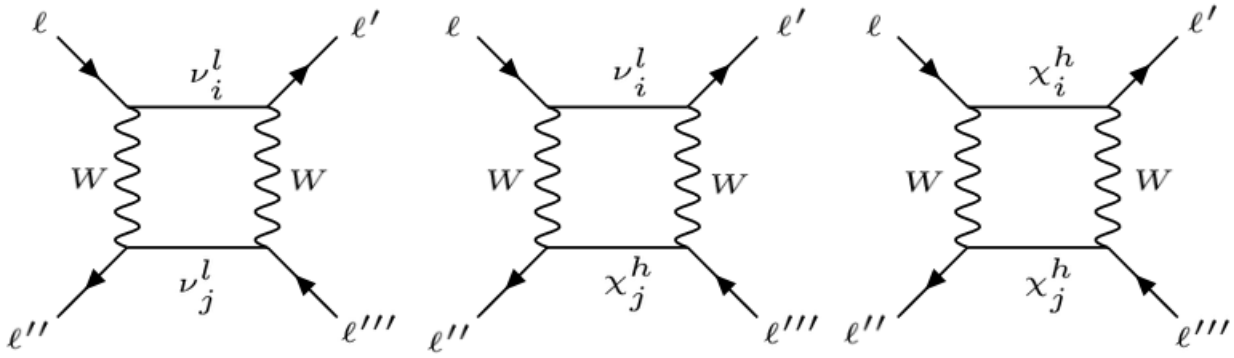

Figure 35: Box diagrams contributing to $\ell \to \ell'\ell''\bar{\ell}'''$.

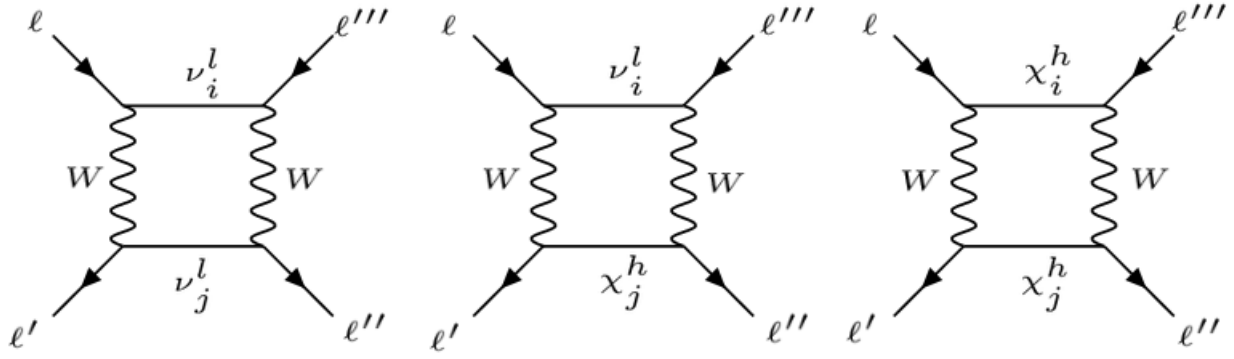

Figure 36: Explicit LNV contributions are introduced by these diagrams.

$$F_B^{\nu_i^l \chi_j^h} = \frac{\alpha_W}{16\pi M_W^2 s_W^2} \sum_{i,j=1}^{3} \{W_{\ell i} W^\dagger_{\ell' i} \theta^\dagger_{\ell''' j} \theta_{\ell'' j} + (\ell' \leftrightarrow \ell'')\} f_B^{lh}(y_i, x_j), \tag{355}$$

$$F_B^{\chi_i^h \chi_j^h} = \frac{\alpha_W}{16\pi M_W^2 s_W^2} \sum_{i,j=1}^{3} \{\theta^\dagger_{\ell i}\theta_{\ell' i}\theta^\dagger_{\ell'' j}\theta_{\ell'' j} + (\ell' \leftrightarrow \ell'')\} f_B^h(x_i, x_j), \tag{356}$$

with

$$\begin{aligned} f_B^l(y_i, y_j) &= \left(1 + \frac{1}{4} y_i y_j\right) \bar{d}_0(y_i, y_j) - 2 y_i y_j d_0(y_i, y_j), \\ f_B^{lh}(y_i, x_j) &= \left(1 + \frac{1}{4} \frac{y_i}{x_j}\right) \bar{d}_0^{lh}(y_i, x_j) - 2 \frac{y_i}{x_j} d_0^{lh}(y_i, x_j), \\ f_B^h(x_i, x_j) &= \left(1 + \frac{1}{4} \frac{1}{x_i x_j}\right) \bar{d}_0^h(x_i, x_j) - 2 \frac{1}{x_i x_j} d_0^h(x_i, x_j), \end{aligned} \tag{357}$$

where $y_i = \frac{m_i^2}{M_W^2}$ and $x_j = \frac{M_W^2}{M_j^2}$. We have defined the above functions in the Appendix G.
Calculating the LNV diagrams is more complicated than the first ones, we show the Feynman rules for fermionic vertices [45–47] between a scalar and fermionic fields, where,

$$\Gamma_i' = C\Gamma_i^T C^T = \eta_i \Gamma_i, \tag{358}$$

and,

$$\eta_i = \begin{cases} 1 & \text{if } \Gamma_i = 1, i\gamma_5, \gamma_\mu\gamma_5 \\ -1 & \text{if } \Gamma_i = \gamma_\nu, \sigma_{\mu\nu} \end{cases}, \tag{359}$$

with Φ, a scalar or vector field and λ, Ψ Majorana and Dirac fermion fields respectively. Notice that in our case the interactions we have are $V_\mu FF$, because we were able to fix the Feynman rules from eqs. (350) and (351), the Feynman rules for SFF can immediately be obtained since longitudinal component of W boson is equivalent to a scalar (Goldstone).
We use this convention in the Feynman Rules [45, 46], because we can proceed without involving the C matrices explicitly in the calculation (the physical observables do not depend on the representation in the Dirac space). Besides, this convention allows us to use Dirac propagators even for Majorana fermions.
We will use the next properties

$$\langle a|\gamma_\alpha P_R|b\rangle\langle c|\gamma^\alpha P_L|d\rangle = 2\langle a|P_L|d\rangle\langle c|P_R|b\rangle, \tag{360}$$

$$\langle a|\gamma^\mu\gamma^\nu P_L|b\rangle\langle c|\gamma_\mu\gamma_\nu P_R|d\rangle = 4\langle a|P_L|b\rangle\langle c|P_R|d\rangle, \tag{361}$$

$$u(p) = C\hat{v}^T(p), \quad u^T(p) = \hat{v}(p)C^T, \tag{362}$$

$$v(p) = C\hat{u}^T(p), \quad v^T(p) = \hat{u}(p)C^T, \tag{363}$$

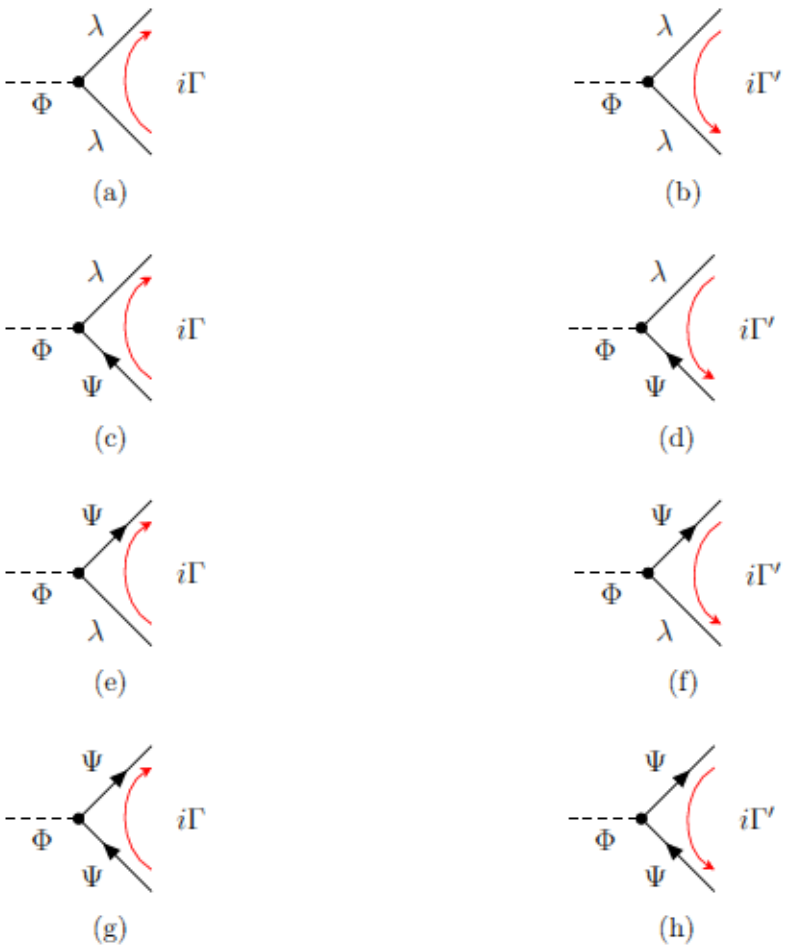

Figure 37: The Feynman rules for fermionic vertices.

$$C^T = C^{-1} = -C, \quad C P_L^T C^T = P_L, \quad C(\gamma_\alpha P_L)^T C^T = -\gamma_\alpha P_R. \tag{364}$$

Then, we develop the left diagram in Figure 36

$$\begin{aligned}
&\hat{u}(p_{\ell'''}) \left[\Gamma'(\not{q} + m_i)\Gamma\right] u(p_\ell) \hat{u}(p_{\ell''}) \left[\Gamma(-\not{q} + m_j)\Gamma'\right] v(p_{\ell'}) \\
&= \hat{u}(p_{\ell'''}) \left[\gamma^\mu P_R(\not{q} + m_i)\gamma^\nu P_L\right] u(p_\ell) \hat{u}(p_{\ell''}) \left[\gamma_\mu P_L(-\not{q} + m_j)\gamma_\nu P_R\right] v(p_{\ell'}) \\
&= m_i m_j \hat{u}(p_{\ell'''}) \left[\gamma^\mu \gamma^\nu P_L\right] u(p_\ell) \hat{u}(p_{\ell''}) \left[\gamma_\mu \gamma_\nu P_R\right] v(p_{\ell'}) \\
&= 4 m_i m_j \left[\hat{u}(p_{\ell'''}) P_L u(p_\ell)\right] \left[\hat{u}(p_{\ell''}) P_R v(p_{\ell'})\right], \text{ where we have used eq.(361).}
\end{aligned} \tag{365}$$

Taking the first fermion chain and transposing

$$\begin{aligned}[\hat{u}(p_{\ell'''})P_L u(p_\ell)] &= u^T(p_\ell)P_L^T\hat{u}^T(p_{\ell'''}) \\ &= \hat{v}(p_\ell)C^T P_L^T C^T v(p_{\ell'''}) \text{ using eqs.(362) and (363)} \\ &= -\hat{v}(p_\ell)P_L v(p_{\ell'''}) \text{ using eq.(364)},\end{aligned} \tag{366}$$

hence,

$$\begin{aligned}[\hat{u}(p_{\ell'''})P_L u(p_\ell)]\,[\hat{u}(p_{\ell''})P_R v(p_{\ell'})] &= -\hat{v}(p_\ell)P_L v(p_{\ell'''})\hat{u}(p_{\ell''})P_R v(p_{\ell'}) \\ &= -\frac{1}{2}\,[\hat{v}(p_\ell)\gamma_\mu P_R v(p_{\ell'})]\,[\hat{u}(p_{\ell''})\gamma^\mu P_L v(p_{\ell'''})]\,, \text{ using eq.(360)} \\ &= -\frac{1}{2}\left[v^T(p_{\ell'})(\gamma_\mu P_R)^T\hat{v}^T(p_\ell)\right][\hat{u}(p_{\ell''})\gamma^\mu P_L v(p_{\ell'''})]\,, \text{ applying the T} \\ &= +\frac{1}{2}\left[\hat{u}(p_{\ell'})C(\gamma_\mu P_R)^T C^T\hat{u}(p_\ell)\right][\hat{u}(p_{\ell''})\gamma^\mu P_L v(p_{\ell'''})] \\ &= -\frac{1}{2}\,[\hat{u}(p_{\ell'})\gamma_\mu P_L\hat{u}(p_\ell)]\,[\hat{u}(p_{\ell''})\gamma^\mu P_L v(p_{\ell'''})]\,.\end{aligned} \tag{367}$$

Therefore, the eq. (365) reads as

$$-2m_i m_j\,[\hat{u}(p_{\ell'})\gamma_\mu P_L\hat{u}(p_\ell)]\,[\hat{u}(p_{\ell''})\gamma^\mu P_L v(p_{\ell'''})]\,. \tag{368}$$

Taking all the constants from the Feynamn rules (eqs. (350) and (351)), and considering the contribution of $(\ell' \leftrightarrow \ell'')$ we have

$$\mathcal{M}_{(1)} = -\frac{\alpha_W}{16\pi M_W^2 s_W^2}\sum_{i,j}^{3} W_{\ell i}W^\dagger_{\ell' j}W_{\ell''' i}W^\dagger_{\ell'' j}\left(4\sqrt{y_i y_j}\,d_0(y_i,y_j)\right). \tag{369}$$

We have to consider the contributions of type $A2a$, $A3a$ and $A4a$, as shown in Figure 29, but now applied to LNV.
We know $\mathcal{M}_{A2a} = \mathcal{M}_{A3a}$, thus

$$\begin{aligned}&-\frac{m_i}{M_W}\frac{m_j}{M_W}\,\hat{u}(p_{\ell'''})\left[P_L(\not{q}+m_i)\gamma^\mu P_L\right]u(p_\ell)\hat{u}(p_{\ell''})\left[P_R(-\not{q}+m_j)\gamma_{\frac{m_j}{M_W}u}P_R\right]v(p_{\ell'}) \\ &= -q^2\frac{m_i}{M_W}\frac{m_j}{M_W}\,[\hat{u}(p_{\ell'''})P_L u(p_\ell)]\,[\hat{u}(p_{\ell''})P_R v(p_{\ell'})] \\ &= \frac{1}{2}q^2\frac{m_i}{M_W}\frac{m_j}{M_W}\,[\hat{u}(p_{\ell'})\gamma_\mu P_L\hat{u}(p_\ell)]\,[\hat{u}(p_{\ell''})\gamma^\mu P_L v(p_{\ell'''})]\,, \text{ using eq.(367)},\end{aligned} \tag{370}$$

hence the $A2a$ and $A3a$ amplitudes read

$$\mathcal{M}_{A2a} = \mathcal{M}_{A2a} = \frac{\alpha_W}{16\pi M_W^2 s_W^2} \sum_{i,j}^{3} W_{\ell i} W^{\dagger}_{\ell' j} W_{\ell''' i} W^{\dagger}_{\ell'' j} \left(\sqrt{y_i y_j}\, \tilde{d}_0(y_i, y_j) \right). \tag{371}$$

Finally, the $A4a$ amplitude for Majorana neutrinos is given by

$$\begin{aligned} &\frac{m_i^2}{M_W^2}\frac{m_j^2}{M_W^2}\ \hat{u}(p_{\ell'''}) \left[P_L(\not{q} + m_i)P_L\right] u(p_\ell) \hat{u}(p_{\ell''}) \left[P_R(-\not{q} + m_j)P_R\right] v(p_{\ell'}) \\ &= \frac{m_i^3}{M_W^2}\frac{m_j^3}{M_W^2} \left[\hat{u}(p_{\ell'''})P_L u(p_\ell)\right] \left[\hat{u}(p_{\ell''})P_R v(p_{\ell'})\right] \\ &= -\frac{1}{2}\frac{m_i^3}{M_W^2}\frac{m_j^3}{M_W^2} \left[\hat{u}(p_{\ell'})\gamma_\mu P_L \hat{u}(p_\ell)\right] \left[\hat{u}(p_{\ell''})\gamma^\mu P_L v(p_{\ell'''})\right], \text{ using eq.(367)}, \end{aligned} \tag{372}$$

therefore,

$$\mathcal{M}_{(A4a)} = -\frac{\alpha_W}{16\pi M_W^2 s_W^2} \sum_{i,j}^{3} W_{\ell i} W^{\dagger}_{\ell' j} W_{\ell''' i} W^{\dagger}_{\ell'' j} \left((y_i y_j)^{3/2} d_0(y_i, y_j) \right). \tag{373}$$

The whole contribution of left diagram in Figure 36 is given by

$$\begin{aligned} F_{B-LNV}^{\nu_i^l \nu_j^l} &= \mathcal{M}_{(1)} + \mathcal{M}_{(A2a)} + \mathcal{M}_{(A3a)} + \mathcal{M}_{(A4a)} \\ &= \frac{\alpha_W}{16\pi M_W^2 s_W^2} \sum_{i,j}^{3} W_{\ell i} W^{\dagger}_{\ell' j} W_{\ell''' i} W^{\dagger}_{\ell'' j} f_B^{l-LNV}(y_i, y_j). \end{aligned} \tag{374}$$

where,

$$\begin{aligned} f_B^{l-LNV}(y_i, y_j) &= \sqrt{y_i y_j} \left(2\tilde{d}_0(y_i, y_j) - (4 + y_i y_j) d_0(y_i, y_j) \right), \\ f_B^{lh-LNV}(y_i, x_j) &= \frac{1}{\sqrt{x_i x_j}} \left(2\tilde{d}_0^{lh}(y_i, x_j) - \left(4 + \frac{1}{x_i x_j}\right) d_0^{lh}(y_i, x_j) \right), \\ f_B^{h-LNV}(x_i, x_j) &= \frac{1}{\sqrt{x_i x_j}} \left(2\tilde{d}_0^{h}(x_i, x_j) - \left(4 + \frac{1}{x_i x_j}\right) d_0^{h}(x_i, x_j) \right), \end{aligned} \tag{375}$$

with $y_i = m_i^2/M_W^2$, m_i standing for the mass of light neutrinos; $x_j = M_W^2/M_j^2$, M_j standing for the mass of heavy neutrinos. We have added the $f_B^{(lh,h)-LNV}(z_i, z_j)$ functions as they will be used in the following equations.

The contributions of the center and right diagrams in Figure 36 are written as follows

$$F_{B-LNV}^{\nu_i^l \chi_j^h} = \frac{\alpha_W}{16\pi M_W^2 s_W^2} \sum_{i=1}^{3} \sum_{j=7}^{9} W_{\ell i} \theta_{\ell' j} W_{\ell''' i} \theta_{\ell'' j} f_B^{lh-LNV}(y_i, x_j), \tag{376}$$

$$F_{B-LNV}^{\chi_i^h\chi_j^h} = \frac{\alpha_W}{16\pi M_W^2 s_W^2}\sum_{i,j=7}^{9}\theta^\dagger_{\ell i}\theta_{\ell' j}\theta^\dagger_{\ell''' i}\theta_{\ell'' j} f_B^{h-LNV}(x_i,x_j). \tag{377}$$

Consequently, the complete F_B form factor from eq.(353) is given by the eqs.(354), (355), (356), (374), (376) and (377)

$$F_B = F_B^{\nu_i^l\nu_j^l} + F_B^{\nu_i^l\chi_j^h} + F_B^{\chi_i^h\chi_j^h} + F_{B-LNV}^{\nu_i^l\nu_j^l} + F_{B-LNV}^{\nu_i^l\chi_j^h} + F_{B-LNV}^{\chi_i^h\chi_j^h}. \tag{378}$$

7.1 Bounds on LFV processes

We present various LFV processes in this section: $\ell \to \ell'\gamma$ and $\ell \to \ell'\ell''\bar{\ell}'''$, where the last one has three possible channels that are shown in Table 13 [48] [4].

Type	Flavor	$\ell \to \ell'\ell''\bar{\ell}'''$		
1	$\ell \neq \ell' = \ell'' = \ell'''$	$\mu \to ee\bar{e}$	$\tau \to ee\bar{e}$	$\tau \to \mu\mu\bar{\mu}$
2	$\ell \neq \ell' \neq \ell'' = \ell'''$		$\tau \to e\mu\bar{\mu}$	$\tau \to \mu e\bar{e}$
3	$\ell \neq \ell' = \ell'' \neq \ell'''$		$\tau \to ee\bar{\mu}$	$\tau \to \mu\mu\bar{e}$

Table 13: Three diferent decay channels of the $\ell \to \ell'\ell''\bar{\ell}'''$ processes.

All of them involve the effective interaction of a neutral vector boson with a pair of on-shell fermions, through a loop with Majorana neutrinos.
The effective $V\ell\ell'$ vertices ($\ell \neq \ell'$) are written in terms of the following form factor [37]

$$\begin{aligned} i\Gamma_\gamma^\mu(p_\ell, p_{\ell'}) &= ie\{\left[iF_M^\gamma(Q^2) + F_E^\gamma(Q^2)\gamma_5\right]\sigma^{\mu\nu}Q_\nu + F_L^\gamma(Q^2)\gamma^\mu P_L\}, \\ i\Gamma_Z^\gamma(p_\ell, p_{\ell'}) &= ieF_L^Z(Q^2)\gamma^\mu P_L, \end{aligned} \tag{379}$$

with $Q_\nu = (p_{\ell'} - p_\ell)_\nu$ is the momentum of the V boson.

7.1.1 $\ell \to \ell'\gamma$ decays

In order to constrain the elements of the θ matrix in LFV processes such as $\mu \to e\gamma$, $\tau \to e\gamma$ and $\tau \to \mu\gamma$ decays we are going to compute the contributions coming from light-heavy neutrinos using 't Hooft-Feynman gauge.
Gauge invariance reduces the $\ell \to \ell'\gamma$ vertex for an on-shell photon to a dipole transition,

$$i\Gamma_\gamma^\mu(p_\ell, p_{\ell'}) = ie\left[iF_M^\gamma(Q^2) + F_E^\gamma(Q^2)\gamma_5\right]\sigma^{\mu\nu}Q_\nu, \tag{380}$$

[4] We do not consider $H \to \bar{\ell}\ell$, since it does not enter as a relevant building block of the studied processes, and it is necessarily below current and near future sensitivities [49]. This is a general feature of LH models [50–52].

where $Q_\nu = (p_{\ell'} - p_\ell)_\nu$. Neglecting $m_{\ell'} \ll m_\ell$

$$\Gamma(\ell \to \ell'\gamma) = \frac{\alpha}{2} m_\ell^3 (|F_M^\gamma|^2 + |F_E^\gamma|^2). \tag{381}$$

The form factor is written as follows

$$F_M^\gamma = U_{\ell' j} U_{\ell j}^* \frac{\alpha_W}{16\pi} \frac{m_\ell}{M_W^2} F_M^\chi(x), \tag{382}$$

with $x = \frac{M_W^2}{M_j^2}$ and $U_{\ell' j} U_{\ell j}^*$ are the vertex interactions.
Because of $F_M^\gamma = -iF_E^\gamma$, and the branching ratios for these types of processes are obtained dividing by the SM decay width

$$\Gamma(\ell_j \to \ell_i \nu_j \bar{\nu}_i) = \frac{G_F^2 m_{\ell_j}^5}{192\pi^3}, \tag{383}$$

where G_F is the Fermi constant, hence

$$\mathrm{Br}(\ell \to \ell'\gamma) = \frac{3\alpha}{2\pi} \left| U_{\ell' j} U_{\ell j}^* F_M^\chi(x) \right|^2. \tag{384}$$

The active (light) neutrino contribution is analogous to the SM one, we just replace U_{PMNS} by W due to Feynman rule from the eq. (350). We notice W matrix has the SM contribution which is U_{PMNS} matrix and also it has a "correction" coming from introducing heavy neutrinos, given by $\theta\theta^\dagger$ term.
The Feynman diagrams are given by topologies II, IV, V and VI shown in the Figure 6. For active neutrinos $m_{\nu_i^l} \ll M_W$, then the $F_M^\nu(x)$ function from the eq.(382), defining $x = \frac{m_{\nu_i}^2}{M_W^2}$, reads [25]

$$\begin{aligned} F_M^\nu(x) &= \frac{10 - 33x + 45x^2 - 4x^3}{12(1-x)^3} + \frac{3x^3}{2(1-x)^4} \ln x \\ &= \frac{5}{6} - \frac{3x - 15x^2 - 6x^3}{12(1-x)^3} + \frac{3x^3}{2(1-x)^4} \ln x, \end{aligned} \tag{385}$$

and considering $x \ll 1$, it behaves as

$$F_M^\nu(x) \to \frac{5}{6} - \frac{x}{4} + \mathcal{O}(x^2). \tag{386}$$

Therefore, the branching ratio of $\mu \to e\gamma$ due to active neutrinos is

$$\mathrm{Br}(\mu \to e\gamma) = \frac{3\alpha}{2\pi} \left| W_{ej} W_{\mu j}^\dagger F_M^\nu(y) \right|^2. \tag{387}$$

Now, we are going to discuss the contribution of heavy neutrinos. For the $\mu \to e\gamma$ decay, the form factors will be similar to the Subsection 2.3, since the topologies II, IV, V and VI are involved with this type of neutrinos as well. For the $\mu \to e\gamma$ decay, the $F_M^\chi(x)$ function is given by

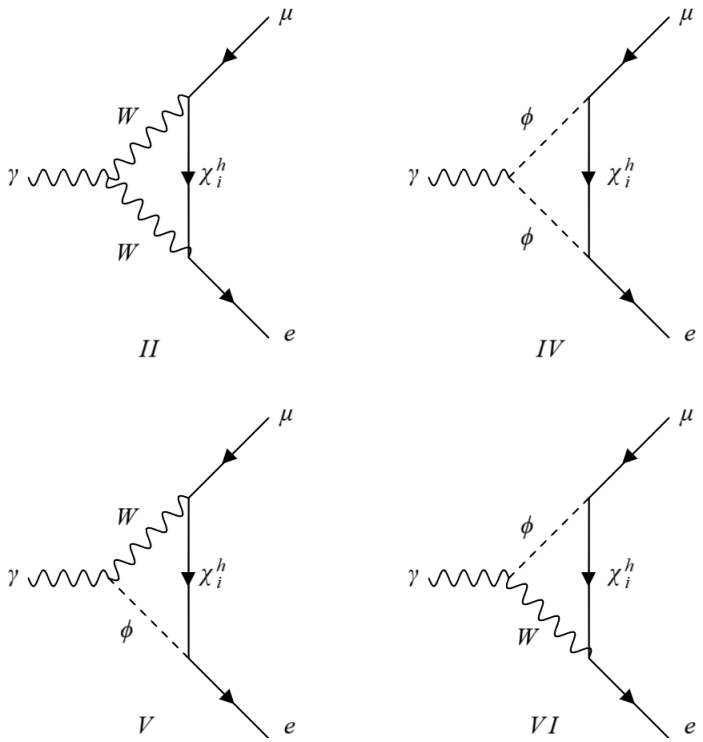

Figure 38: Feynman diagrams involved in the $\mu \to e\gamma$ decay considering heavy neutrinos. We have to take into account the self-energy diagrams, additionally. ϕ are the would-be Goldstones absorbed by W boson.

$$\begin{aligned} F_M^{\chi^h}(x) &= \frac{-10x^3+33x^2-45x+4}{12(1-x)^3} + \frac{3x}{2(1-x)^4}\ln x \\ &= \frac{1}{3} - \frac{2x^3-7x^2+11x}{4(1-x)^3} + \frac{3x}{2(1-x)^4}\ln x, \end{aligned} \tag{388}$$

with $x = \frac{M_W^2}{M_j^2}$ and M_j is the mass of χ_L^h. Considering $M_M^2 \ll M_j^2$ $(x \to 0)$,

$$F_M^{\chi^h}(x) \to \frac{1}{3} - \frac{11x}{4} + \mathcal{O}(x^2). \tag{389}$$

Hence, the contribution to the branching ratio from heavy neutrinos χ_L^h is written as

$$\mathrm{Br}(\mu \to e\gamma) = \frac{3\alpha}{2\pi}\left|\theta_{ej}\theta_{\mu j}^{\dagger} F_M^{\chi}(x)\right|^2. \tag{390}$$

It is important to note that the contribution to the $\mathrm{Br}(\mu \to e\gamma)$ coming from ν_H neutrinos we have computed in the eq. (258) behaves as

$$\mathrm{Br}(\mu \to e\gamma) = \frac{3\alpha}{2\pi}\left|\frac{M_W^2}{M_{W_H}^2} V_{H\ell}^{ie*} V_{H\ell}^{i\mu} F_W(x)\right|^2, \tag{391}$$

where $x = \frac{m_{Hi}^2}{M_{W_H}^2}$. Using $\frac{M_W^2}{M_{W_H}^2} = \frac{v^2}{4f^2}$, the equation above can be written as

$$\mathrm{Br}(\mu \to e\gamma) = \frac{3\alpha}{2\pi}\left|\frac{v^2}{4f^2}V_{H\ell}^{ie*}V_{H\ell}^{i\mu}F_W(x)\right|^2, \tag{392}$$

however, this contribution is neglected because of $v^2/4f^2 << 1$ term.
Summing the contributions from eqs. (387) and (390) yields the complete branching ratio to $\mu \to e\gamma$ decay

$$\mathrm{Br}(\mu \to e\gamma) = \frac{3\alpha}{2\pi}\left|\theta_{ej}\theta_{\mu j}^{\dagger}F_M^{\chi}(x) + W_{ej}W_{\mu j}^{\dagger}F_M^{\nu}(y)\right|^2, \tag{393}$$

with $x = \frac{M_W^2}{M_j^2}$, $y = \frac{m_{\nu_i}^2}{M_W^2}$ and W_{ij} matrix is given by the eq. (350).
Taking the approximations from the eqs. (386) and (389), we obtain

$$\begin{aligned}\mathrm{Br}(\mu \to e\gamma) \approx & \frac{3\alpha}{2\pi}\left|\left(\frac{1}{3} - \frac{11x}{4}\right)\theta_{ej}\theta_{\mu j}^{\dagger} + \left(\frac{5}{6} - \frac{y}{4}\right)(U_{PMNS}^{\dagger})_{ej}(U_{PMNS})_{\mu j}\right. \\ & \left. + \left(\frac{y}{8} - \frac{5}{12}\right)\left((U_{PMNS}^{\dagger})_{ej}(\theta\theta^{\dagger}U_{PMNS})_{\mu j} + (U_{PMNS}^{\dagger}\theta\theta^{\dagger})_{ej}(U_{PMNS})_{\mu j}\right)\right|^2,\end{aligned} \tag{394}$$

as the sum on the repeated index is understood, the PMNS matrix satisfies [53]

$$\sum_i U_{\alpha i}U_{\beta i}^{*} = \delta_{\alpha\beta} \quad (\alpha, \beta = e, \mu, \tau), \qquad UU^{\dagger} = U^{\dagger}U = \mathbf{1}, \tag{395}$$

therefore the second term is canceled and considering the leading terms

$$\begin{aligned}\mathrm{Br}(\mu \to e\gamma) &\approx \frac{3\alpha}{2\pi}\left|\frac{1}{3}\theta_{ej}\theta_{\mu j}^{\dagger} - \frac{5}{6}\theta_{ej}\theta_{\mu j}^{\dagger}\right|^2 \\ &\approx \frac{3\alpha}{8\pi}\left|\theta_{ej}\theta_{\mu j}^{\dagger}\right|^2.\end{aligned} \tag{396}$$

We know that $Br(\mu \to e\gamma) < 4.2 \times 10^{-13}$ (at 90% C.L.) [6, 39], hence

$$\left|\theta_{ej}\theta_{\mu j}^{\dagger}\right| < 0.14 \times 10^{-4}. \tag{397}$$

For τ decays the SM branching ratio (eq.(383)) must be corrected multiplying by 0.17 to take into account other possible decay channels [25], therefore

$$\mathrm{Br}(\tau \to e\gamma) = (0.17)\frac{3\alpha}{2\pi}\left|\theta_{ej}\theta_{\tau j}^{\dagger}F_M^{\chi}(x) + W_{ej}W_{\tau j}^{*}F_M^{\nu}(y)\right|^2, \tag{398}$$

taking the value of $\mathrm{Br}(\tau \to e\gamma) < 3.3 \times 10^{-8}$ (at 90% C.L.) [6, 39] and the same consideration on $x \to 0$ and $y \to 0$ yield

$$\mathrm{Br}(\tau \to e\gamma) \approx (0.17)\frac{3\alpha}{8\pi}|\theta_{ej}\theta_{\tau j}^{*}|^2, \tag{399}$$

$$|\theta_{ej}\theta^{\dagger}_{\tau j}| < 0.95 \times 10^{-2}, \tag{400}$$

Finally, for $\text{BR}(\tau \to \mu\gamma) < 4.4 \times 10^{-8}$ (at 90% C.L.) [6, 39]

$$\begin{aligned} \text{Br}(\tau \to \mu\gamma) &= (0.17)\frac{3\alpha}{2\pi}\left|\theta_{\mu j}\theta^{\dagger}_{\tau j}F^{\chi}_{M}(x) + W_{\mu j}W^{*}_{\tau j}F^{\nu}_{M}(y)\right|^2 \\ &\approx (0.17)\frac{3\alpha}{8\pi}|\theta_{\mu j}\theta^{*}_{\tau j}|^2, \end{aligned} \tag{401}$$

therefore,

$$|\theta_{\mu j}\theta^{\dagger}_{\tau j}| < 0.011. \tag{402}$$

We notice that our result from the eq. (397) matches with the reported one in the Table 1 of [39] but the results from the eqs. (400) and (402) do not. For tau decays in [39] the 0.17 factor is missing.

7.1.2 Type I: $\ell \to \ell'\ell''\bar{\ell}'''$ with $\ell \neq \ell' = \ell'' = \ell'''$

The $\mathcal{M}^{\ell\to\ell'\ell'\bar{\ell}'}$ amplitude for decays Type I gets contributions from γ and Z penguins diagrams, and it also receives contributions from box diagrams. All theses diagrams are similar to those shown in Section 6, where we replace W_H by W, Z_H by Z and ν_H by ν^l and χ^h, which are Majorana neutrinos. Therefore, we can write the whole $\ell \to \ell'\ell'\bar{\ell}'$ amplitude as

$$\mathcal{M}^{\ell\to\ell'\ell'\bar{\ell}'} = \mathcal{M}^{\ell\to\ell'\ell'\bar{\ell}'}_{\gamma} + \mathcal{M}^{\ell\to\ell'\ell'\bar{\ell}'}_{Z} + \mathcal{M}^{\ell\to\ell'\ell'\bar{\ell}'}_{box}, \tag{403}$$

where each amplitude is defined as follows [37]

$$\begin{aligned} \mathcal{M}^{\ell\to\ell'_1\ell'_2\bar{\ell}'_3}_{\gamma} =& \overline{u}(p_1)e\left[iF^{\gamma}_{M}(0)2P_R\sigma^{\mu\nu}(p_1-p_\ell)_\nu + F^{\gamma}_{L}((p_1-p_\ell)^2)\gamma^\mu P_L\right]u(p_\ell) \\ &\times \frac{1}{(p_1-p_\ell)^2}\overline{u}(p_3)\gamma_\mu e v(p_2) - (p_1 \leftrightarrow p_3), \\ \mathcal{M}^{\ell\to\ell'_1\ell'_2\bar{\ell}'_3}_{Z} =& \overline{u}(p_1)\left(-eF^{Z}_{L}(0)\right)\gamma^\mu P_L u(p_\ell)\frac{1}{M^2_Z}\overline{u}(p_3)\gamma_\mu\left(g^Z_L P_L + g^Z_R P_R\right)v(p_2) \\ &- (p_1 \leftrightarrow p_3), \\ \mathcal{M}^{\ell\to\ell'_1\ell'_2\bar{\ell}'_3}_{box} =& e^2 B_L(0)\overline{u}(p_1)\gamma^\mu P_L u(p_\ell)\overline{u}(p_3)\gamma_\mu P_L v(p_2), \end{aligned} \tag{404}$$

where $F^{\gamma}_{E} = iF^{\gamma}_{M}$. The photon magnetic and Z left-handed vector form factors, $F^{\gamma}_{M}(0)$ and $F^{Z}_{L}(0)$ respectively, are evaluated at $Q^2 = (p_1 - p_\ell)^2 = 0$ because their leading terms are momentum independent for small momentum transfer $Q^2 \sim m^2_\ell$ whereas the photon left-handed vector form factor, $F^{\gamma}_{L}\left((p_1-p_\ell)^2\right)$, is linear in Q^2.

The form factors F^{γ}_{M} and F^{γ}_{E} have the the same expressions than the eqs.(386) and (389), where we have supposed $m_{\nu^l_i} \ll M_W$, and $M_M \ll M_j$ with $m_{\nu^l_i}$ and M_j the mass of light and heavy Majorana

neutrinos, respectively. So, the complete F_M^γ is given by

$$F_M^\gamma = F_M^{\nu^l} + F_M^{\chi^h} = \frac{\alpha_W}{16\pi}\frac{m_\ell}{M_W^2}\sum_{j=1}^{3}\left(W_{\ell' j}W_{\ell j}^\dagger F_M^{\nu^l}(x) + \theta_{\ell' j}\theta_{\ell j}^\dagger F_M^{\chi^h}(y)\right), \tag{405}$$

with $x = \frac{m_\nu^2}{M_W^2}$ and $y = \frac{M_W^2}{M_j^2}$.
The F_L^γ form factor is obtained from the diagrams in the Figure 38, it is given by

$$F_L^\gamma = F_L^{\nu^l} + F_L^{\chi^h} = \frac{\alpha_W}{8\pi M_W^2}\sum_{i}^{3}\left(W_{\ell' j}W_{\ell j}^\dagger F_L^{\nu^l}(x) + \theta_{\ell' j}\theta_{\ell j}^\dagger F_L^{\chi^h}(y)\right), \tag{406}$$

where

$$\begin{aligned} F_L^{\nu^l}(x) &= 2M_W^2\Delta_\epsilon + Q^2\left(\frac{x^2(12-10x+x^2)\ln x}{6(1-x)^4} - \frac{7x^3-x^2-12x}{12(1-x)^3} - \frac{5}{9}\right), \\ F_L^{\chi^h}(y) &= 2M_W^2\Delta_\epsilon + Q^2\left(-\frac{(12y^2-10y+1)\ln y}{6(1-y)^4} + \frac{20y^3-96y^2+57y+1}{36(1-y)^3}\right), \end{aligned} \tag{407}$$

with $\Delta_\epsilon = \frac{1}{\epsilon} - \gamma_E + \ln(4\pi) + \ln\left(\frac{\mu^2}{M_W^2}\right)$ which regulates the ultraviolet divergence in $4-2\epsilon$ dimensions is canceled by unitarity of mixing matrices.

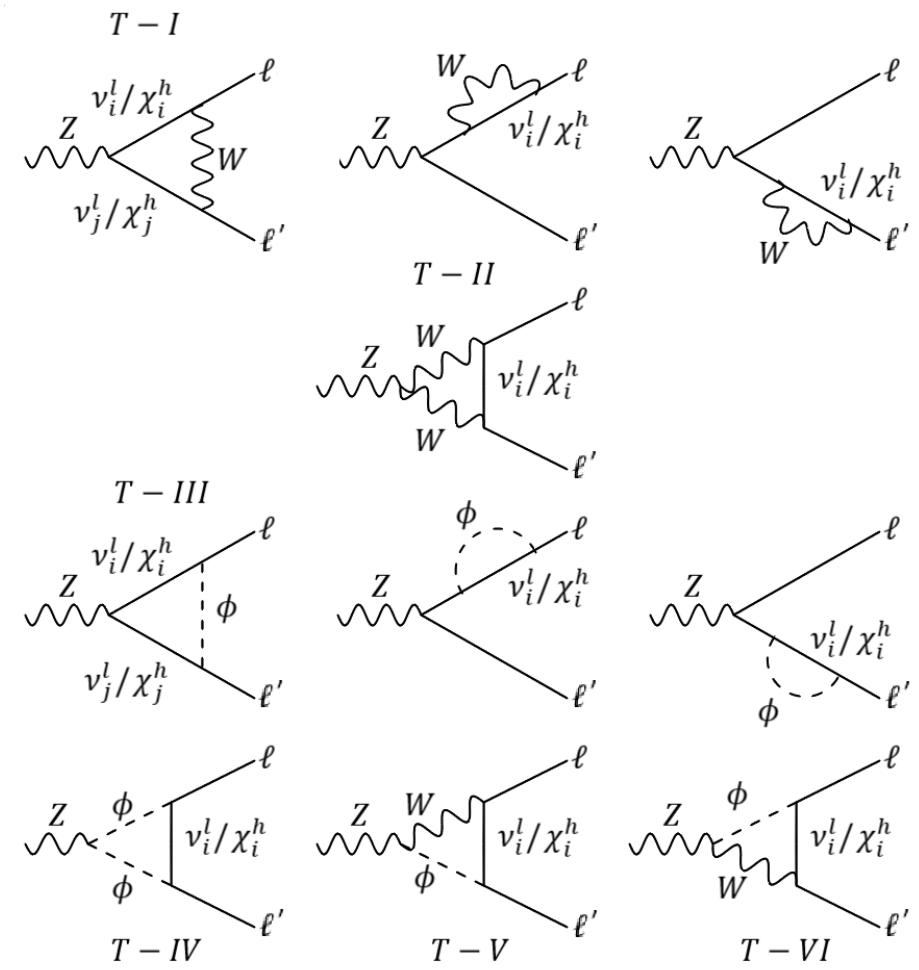

Figure 39: Z penguins diagrams that contribute to the decay. Diagrams corresponding to $T-I$ and $T-III$ allow to mix light and heavy Majorana neutrinos.

We take into account Z penguin diagrams that are shown in Figure 39 that involve purely light neutrinos, a mixing of light and heavy neutrinos, and diagrams in which only heavy neutrinos appear. We calculate the one-loop contributions in the Feynman ´t Hoof gauge, therefore, we also take in account the diagrams of the would-be-Goldstone fields. The form factor from ν^l-diagrams in Figure 39 is given by

$$F_L^{Z-\nu^l}(Q^2) = \frac{\alpha_W}{8\pi c_W s_W}\sum_{i,j=1}^{3}\Big[W_{\ell' i}W_{\ell i}^{\dagger}F^l(x_i;Q^2) + W_{\ell' j}X_{ji}W_{\ell i}^{\dagger}\left(G^l(x_i,x_j;Q^2)+\sqrt{x_i x_j}H^l(x_i,x_j;Q^2)\right)\Big], \tag{408}$$

(we have used that $X_{ji} = X_{ji}^\dagger$ from eq. (351)), where

$$\begin{aligned}
F^l(x_i;Q^2) &= -2c_W^2\left[Q^2(\overline{C}_1+\overline{C}_2+\overline{C}_{12})+6\overline{C}_{00}-1\right]-(1-2s_W^2)x_i\overline{C}_{00}-2s_W^2x_iM_W^2\overline{C}_0\\
&\quad-\frac{1}{2}(1-2s_W^2)\left[(2+x_i)\overline{B}_1+1\right],\\
G^l(x_i,x_j;Q^2) &= -Q^2(C_0+C_1+C_2+C_{12})+2C_{00}-1-\frac{1}{2}x_ix_jM_W^2C_0,\\
H^l(x_i,x_j;Q^2) &= M_W^2C_0+\frac{1}{2}Q^2C_{12}-C_{00}+\frac{1}{4}.
\end{aligned} \tag{409}$$

We see a difference in $Z\bar{\nu}_i\nu_j$ vertex in this process: if the neutrinos were SM neutrinos, the $Z\bar{\nu}_i\nu_j$ vertex would be $\sim\delta_{ij}$. In this case, the neutrinos have a Majorana nature, so their $Z\bar{\nu_i^l}\nu_j^l$ interaction is given by X_{ij} matrix, which is shown in eq. (351).
Analytic expressions for the above functions in the low Q^2 limit can be given by

$$\begin{aligned}
F^l(x_i;0) &= -\left(\frac{5}{2}-2s_W^2\right)\Delta_\epsilon+\frac{5x_i^2\,\ln x_i}{2(x_i-1)^2}-\frac{5x_i}{2(x_i-1)}+\frac{1}{4},\\
G^l(x_i,x_j;0) &= \frac{1}{2}\left(\Delta_\epsilon-\frac{1}{2}\right)+\frac{1}{2(x_i-x_j)}\left(\frac{(x_j-1)x_i^2\,\ln x_i}{x_i-1}-\frac{(x_i-1)x_j^2\,\ln x_j}{x_j-1}\right),\\
H^l(x_i,x_j;0) &= -\frac{1}{4}\left(\Delta_\epsilon+\frac{1}{2}\right)+\frac{1}{4(x_i-x_j)}\left(\frac{x_i(x_i-4)\,\ln x_i}{x_i-1}-\frac{x_j(x_j-4)\,\ln x_j}{x_j-1}\right).
\end{aligned} \tag{410}$$

with $x_{i,j} = m_{i,j}^2/M_W^2$, m_i are the light neutrino masses. The contribution from $\nu^l\chi^h-$diagrams in Figure 39 is written as

$$\begin{aligned}
F_L^{Z-\nu^l\chi^h}(Q^2) = \frac{\alpha_W}{8\pi c_W s_W}\sum_{i,j=1}^{3}\Bigg[&\theta_{\ell'j}W_{\ell i}^\dagger\left(Y_{ji}G_1^{lh}(x_i,y_j;Q^2)+Y_{ji}^\dagger\sqrt{\frac{x_i}{y_j}}H_1^{lh}(x_i,y_j;Q^2)\right)\\
&+W_{\ell'j}\theta_{\ell i}^\dagger\left(Y_{ji}^\dagger G_2^{lh}(x_j,y_i;Q^2)+Y_{ji}\sqrt{\frac{x_j}{y_i}}H_2^{lh}(x_j,y_i;Q^2)\right)\Bigg],
\end{aligned} \tag{411}$$

where

$$\begin{aligned}
G_1^{lh}(x_i,y_j;Q^2) &= -Q^2(C_0+C_1+C_2+C_{12})+2C_{00}-1-\frac{1}{2}\frac{x_i}{y_j}M_W^2C_0,\\
H_1^{lh}(x_i,y_j;Q^2) &= M_W^2C_0+\frac{1}{2}Q^2C_{12}-C_{00}+\frac{1}{4},\\
G_2^{lh}(x_j,y_i;Q^2) &= -Q^2(C_0+C_1+C_2+C_{12})+2C_{00}-1-\frac{1}{2}\frac{x_j}{y_i}M_W^2C_0,\\
H_2^{lh}(x_j,y_i;Q^2) &= M_W^2C_0+\frac{1}{2}Q^2C_{12}-C_{00}+\frac{1}{4},
\end{aligned} \tag{412}$$

and their analytic expressions are

$$\begin{aligned}
G_1^{lh}(x_i,y_j;0) &= G^l(x_i,x_j;0) \quad \text{with} \quad \left(x_j \to \frac{1}{y_j}\right), \\
H_1^{lh}(x_i,y_j;0) &= H^l(x_i,x_j;0) \quad \text{with} \quad \left(x_j \to \frac{1}{y_j}\right), \\
G_2^{lh}(x_j,y_i;0) &= G^l(x_i,x_j;0) \quad \text{with} \quad \left(x_i \to \frac{1}{y_i}\right), \\
H_2^{lh}(x_j,y_i;0) &= H^l(x_i,x_j;0) \quad \text{with} \quad \left(x_i \to \frac{1}{y_i}\right),
\end{aligned} \tag{413}$$

with $x_{i,j} = m_{i,j}^2/M_W^2$, $y_{i,j} = M_W^2/M_{i,j}^2$, being m_i and $M_{i,j}$ the light and heavy neutrinos masses, respectively.
The $F_L^{Z-\chi^h}$ form factor, which stands for the contribution from χ^h-diagrams, yields

$$\begin{aligned}
F_L^{Z-\chi^h}(Q^2) = \frac{\alpha_W}{8\pi c_W s_W} \sum_{i,j=1}^{3} \Big[& \theta_{\ell' i}\theta_{\ell i}^\dagger F^h(y_i;Q^2) \\
& + \theta_{\ell' j} S_{ji} \theta_{\ell i}^\dagger \left(G^h(y_i,y_j;Q^2) + \frac{1}{\sqrt{y_i y_j}} H^h(y_i,y_j;Q^2) \right) \Big],
\end{aligned} \tag{414}$$

($S_{ji} = S_{ji}^\dagger$ from the eq.(351)) where

$$\begin{aligned}
F^h(y_i;Q^2) &= -2c_W^2 \left[Q^2(\overline{C}_1 + \overline{C}_2 + \overline{C}_{12}) + 6\overline{C}_{00} - 1 \right] - (1-2s_W^2)\frac{1}{y_i}\overline{C}_{00} - 2s_W^2 \frac{1}{y_i} M_W^2 \overline{C}_0 \\
&\quad - \frac{1}{2}(1-2s_W^2)\left[(2+\frac{1}{y_i})\overline{B}_1 + 1 \right], \\
G^h(y_i,y_j;Q^2) &= -Q^2(C_0 + C_1 + C_2 + C_{12}) + 2C_{00} - 1 - \frac{1}{2}\frac{1}{y_i y_j} M_W^2 C_0, \\
H^h(y_i,y_j;Q^2) &= M_W^2 C_0 + \frac{1}{2}Q^2 C_{12} - C_{00} + \frac{1}{4},
\end{aligned} \tag{415}$$

where $y_{i,j} = M_W^2/M_{i,j}^2$, $M_{i,j}$ are the heavy neutrino masses. Analytic expressions for the functions F^h, G^h, and H^h in the low Q^2 limit are written as

$$\begin{aligned}
F^h(y_i;0) &= -\left(\frac{5}{2} - 2s_W^2\right)\Delta_\epsilon - \frac{5\ \ln y_i}{2(1-y_i)^2} - \frac{5}{2(1-y_i)} + \frac{1}{4}, \\
G^h(y_i,y_j;0) &= \frac{1}{2}\left(\Delta_\epsilon - \frac{1}{2}\right) + \frac{1}{2(y_j-y_i)}\left(-\frac{(1-y_j)\ \ln y_i}{(1-y_i)} + \frac{(1-y_i)\ \ln y_j}{(1-y_j)} \right), \\
H^h(y_i,y_j;0) &= -\frac{1}{4}\left(\Delta_\epsilon + \frac{1}{2}\right) + \frac{1}{4(y_j-y_i)}\left(-\frac{(1-4y_i)y_j\ \ln y_i}{(1-y_i)} + \frac{(1-4y_j)y_i\ \ln y_j}{(1-y_j)} \right).
\end{aligned} \tag{416}$$

The ultraviolet divergences (Δ_ϵ) cancel in (410), (413) and (416) using the following properties of the

mixing matrices [44, 48]

$$\begin{aligned}
&\sum_{k=1}^{9} B_{ik}B_{jk}^{\dagger} = \delta_{ij}, \quad \sum_{k=1}^{3} B_{ki}^{\dagger}B_{kj} = \sum_{k=1}^{9} C_{ik}C_{jk}^{\dagger} = C_{ij}\,, \\
&\sum_{k=1}^{9} B_{ik}C_{kj} = B_{ij}, \\
&\sum_{k=1}^{9} m_{\Phi_k} C_{ik}C_{jk} = \sum_{k=1}^{9} m_{\Phi_k} B_{ik}C_{kj}^{\dagger} = \sum_{k=1}^{3} m_{\Phi_k} B_{ik}B_{jk}^{\dagger} = 0.
\end{aligned} \tag{417}$$

The box diagrams are computed in eqs. (354), (355) and (356) by replacing the $\ell\ell'\ell''\ell'''$ flavor factor by $\ell\ell'\ell'\ell'$. In this case there are no LNV vertices.
After integrating the three-body phase space the decay width reads [37]

$$\begin{aligned}
\Gamma(\ell \to \ell'\overline{\ell'}\ell') = \frac{\alpha^2 m_\ell^5}{96\pi}\Bigg[&3|A_L|^2 + 2|A_R|^2\left(8\,\ln\frac{m_\ell}{m_{\ell'}} - 13\right) + 2|F_{LL}|^2 + |F_{LR}|^2 + \frac{1}{2}|B_L|^2 \\
&- (6A_L A_R^* - (A_L - 2A_R)(2F_{LL}^* + F_{LR}^* + B_L^*) - F_{LL}B_L^* + \text{h.c.})\Bigg]\,,
\end{aligned} \tag{418}$$

where we have defined

$$A_L = \frac{F_L^\gamma}{Q^2}, \quad A_R = \frac{2F_M^\gamma(0)}{m_\ell}, \quad F_{LL} = -\frac{g_L F_L^Z(0)}{eM_Z^2}, \quad F_{LR} = -\frac{g_R F_L^Z(0)}{eM_Z^2}, \quad B_L = B_L(0), \tag{419}$$

with $g_{L,R}$ the corresponding Z couplings to the charged lepton ℓ'.

7.1.3 Type II: $\ell \to \ell'\ell''\bar{\ell}'''$ with $\ell \neq \ell' \neq \ell'' = \ell'''$

This process can be expressed like $\ell \to \ell'\ell''\overline{\ell''}$ since $\ell'' = \ell'''$.
The difference between processes Type I and Type II is that there are no crossed penguin diagram contributions in the last one. This is due to $\ell''\overline{\ell''}$ coming from through pair production. Two gauge boson LFV transitions would be needed for swapping ℓ' and ℓ''. This is the reason why the $\ell(p_\ell) \to \ell'(p_1)\overline{\ell''}(p_2)\ell''(p_3)$ amplitude $\mathcal{M}^{\ell\to\ell'_1\overline{\ell''}_2\ell''_3}$ has no $p_1 \leftrightarrow p_2$ term in eq.(404). Nevertheless, there are additional diagrams for the box contributions at this order for swapping ℓ' and ℓ''. The box contributions are calculated in eqs. (354), (355) and (356), the additional contributions are considered once the flavor factors with $\ell\ell'\ell''\ell'''$ are replaced by the appropriate ones with $\ell\ell'\ell''\ell''$. Furthermore, there is no symmetry factor of 1/2 in the phase space integration needed to obtain the decay width because all three final leptons are distinguishable. The final decay width can be written as [37]

$$\begin{aligned}
\Gamma(\ell \to \ell'\overline{\ell''}\ell'') = \frac{\alpha^2 m_\ell^5}{96\pi}\Bigg[&2|A_L|^2 + 4|A_R|^2\left(4\,\ln\frac{m_\ell}{m_{\ell''}} - 7\right) + |F_{LL}|^2 + |F_{LR}|^2 + |B_L|^2 \\
&- \left(4A_L A_R^* - (A_L - 2A_R)\left(F_{LL}^* + F_{LR}^* + \frac{B_L^*}{2}\right) - F_{LL}\frac{B_L^*}{2} + \text{h.c.}\right)\Bigg]\,,
\end{aligned} \tag{420}$$

with the same definitions as in eq. (414).

7.1.4 Type III: $\ell \to \ell'\ell''\bar{\ell}'''$ with $\ell \neq \ell' = \ell'' \neq \ell'''$

We are going to analyze $\ell \to \ell'\ell''\bar{\ell}'''$ decays with the ($\ell \neq \ell' = \ell'' \neq \ell'''$) condition, hence these processes just have box contributions.
Recalling that the eqs.(354), (355), (356), (374), (376) and (377) yield the complete F_B form factor from eq.(353)

$$F_B = F_B^{\nu_i^l \nu_j^l} + F_B^{\nu_i^l \chi_j^h} + F_B^{\chi_i^h \chi_j^h} + F_{B-LNV}^{\nu_i^l \nu_j^l} + F_{B-LNV}^{\nu_i^l \chi_j^h} + F_{B-LNV}^{\chi_i^h \chi_j^h}. \tag{421}$$

$$\begin{aligned}
F_B^{\nu_i^l \nu_j^l} &= \frac{\alpha_W}{16\pi M_W^2 s_W^2} \sum_{i,j=1}^{3} \{W_{\ell i} W^\dagger_{\ell' i} W_{\ell''' j} W^\dagger_{\ell'' j} + (\ell' \leftrightarrow \ell'')\} f_B^l(y_i, y_j), \\
F_B^{\nu_i^l \chi_j^h} &= \frac{\alpha_W}{16\pi M_W^2 s_W^2} \sum_{i,j=1}^{3} \{W_{\ell i} W^\dagger_{\ell' i} \theta^\dagger_{\ell''' j} \theta_{\ell'' j} + (\ell' \leftrightarrow \ell'')\} f_B^{lh}(y_i, x_j), \\
F_B^{\chi_i^h \chi_j^h} &= \frac{\alpha_W}{16\pi M_W^2 s_W^2} \sum_{i,j=1}^{3} \{\theta^\dagger_{\ell i} \theta_{\ell' i} \theta^\dagger_{\ell''' j} \theta_{\ell'' j} + (\ell' \leftrightarrow \ell'')\} f_B^h(x_i, x_j), \\
F_{B-LNV}^{\nu_i^l \nu_j^l} &= \frac{\alpha_W}{16\pi M_W^2 s_W^2} \sum_{i,j=1}^{3} W_{\ell i} W^\dagger_{\ell' j} W_{\ell''' i} W^\dagger_{\ell'' j} f_B^{l-LNV}(y_i, y_j), \\
F_{B-LNV}^{\nu_i^l \chi_j^h} &= \frac{\alpha_W}{16\pi M_W^2 s_W^2} \sum_{i,j=1}^{3} W_{\ell i} \theta_{\ell' j} W_{\ell''' i} \theta_{\ell'' j} f_B^{lh-LNV}(y_i, x_j), \\
F_{B-LNV}^{\chi_i^h \chi_j^h} &= \frac{\alpha_W}{16\pi M_W^2 s_W^2} \sum_{i,j=1}^{3} \theta^\dagger_{\ell i} \theta_{\ell' j} \theta^\dagger_{\ell''' i} \theta_{\ell'' j} f_B^{h-LNV}(x_i, x_j),
\end{aligned} \tag{422}$$

where the $f_B^{(l,lh,h)}(z_i, z_j)$ and $f_B^{(l,lh,h)-LNV}(z_i, z_j)$ functions are shown in the Appendix G.
The $F_B^{\nu_i^l \nu_j^l}$ form factor just involves active neutrinos, therefore, $y_i, y_j \to 0$ ($m_i, m_j \ll M_W$) which implies

$$f_B^l(y_i, y_j)\Big|_{y_i, y_j \to 0} \approx -\left[1 + (y_j + y_i)\left(1 + \ln y_j\right)\right], \tag{423}$$

therefore,

$$F_B^{\nu_i^l \nu_j^l} \approx -\frac{\alpha_W}{16\pi M_W^2 s_W^2} \sum_{i,j=1}^{3} \{W_{\ell i} W^\dagger_{\ell' i} W_{\ell''' j} W^\dagger_{\ell'' j} + (\ell' \leftrightarrow \ell'')\} \left[1 + (y_j + y_i)\left(1 + \ln y_j\right)\right]. \tag{424}$$

The $F_B^{\nu_i^l \chi_j^h}$ form factor involves a mixing of active and heavy neutrinos, due to their masses satisfying $m_i \ll M_W \ll m_j$, respectively. We have that $y_i, x_j \to 0$

$$f_B^{lh}(y_i, x_j)\Big|_{y_i, x_j \to 0} \approx x_j(1 + \ln x_j) + \frac{1}{4} y_i(\ln x_j - 7). \tag{425}$$

Hence,

$$F_B^{\nu_i^l \chi_j^h} \approx \frac{\alpha_W}{16\pi M_W^2 s_W^2} \sum_{i=1}^{3} \sum_{j=7}^{9} \{W_{\ell i} W^*_{\ell' i} \theta^\dagger_{\ell''' j} \theta_{\ell'' j} + (\ell' \leftrightarrow \ell'')\} \left[x_j(1 + \ln x_j) + \frac{1}{4} y_i(\ln x_j - 7) \right]. \tag{426}$$

The $F_B^{\chi_i \chi_j}$ form factor appears from the interaction of two heavy neutrinos, then we need to analyze the behavior of the f_B^h function with $M_W \ll M_i, M_j$. Therefore,

$$\begin{aligned} f_B^h(x_i, x_j)|_{x_i, x_j \to 0} \approx x_i \Bigg[\left(\frac{1}{2x_j} - 3 \right) \frac{1}{2x_j} \ln\left(\frac{x_i}{x_j} \right) + \ln x_i + \frac{9}{4} \ln x_j + x_j \left(3 \ln x_j + \frac{3}{4} \right) + \frac{7}{4} \Bigg] \\ + \frac{1}{4x_j} \ln\left(\frac{x_i}{x_j} \right) + \frac{1}{4} (6 \ln x_j + 7) + \frac{1}{4} x_j (13 \ln x_j + 7), \end{aligned} \tag{427}$$

we have assumed heavy neutrinos are not degenerate but they may be of the same order of magnitude ($m_i \sim m_j$). If the x_i/x_j ratio approached 1 much faster than $1/x_j$ diverges, we could get rid of the $\frac{1}{x_j} \ln\left(\frac{x_i}{x_j}\right)$ term, otherwise this one is divergent.

For the f_B^{l-LNV} considering $y_i, y_j \to 0$ we obtain

$$f_B^{l-LNV}(y_i, y_j)\Big|_{y_i, y_j \to 0} \approx 2\sqrt{y_i y_j}(1 + 2 \ln y_j), \tag{428}$$

which yields

$$F_{B-LNV}^{\nu_i^l \nu_j^l} = \frac{\alpha_W}{16\pi M_W^2 s_W^2} \sum_{i,j}^{3} \{W_{\ell i} W^\dagger_{\ell' j} W_{\ell''' i} W^\dagger_{\ell'' j}\} \left[2\sqrt{y_i y_j}(1 + 2 \ln y_j) \right]. \tag{429}$$

For the f_B^{lh-LNV} the considerations what we make are $y_i, x_j \to 0$, then

$$f_B^{lh-LNV}(y_i, x_j)\Big|_{y_i, x_j \to 0} \approx 2\sqrt{y_i x_j}(\ln x_j - 1), \tag{430}$$

therefore

$$F_{B-LNV}^{\nu_i^l \chi_j^h} \approx \frac{\alpha_W}{32\pi M_W^2 s_W^2} \sum_{i=1}^{3} \sum_{j=7}^{9} \{W_{\ell i} \theta_{\ell' j} W_{\ell''' i} \theta_{\ell'' j}\} \left[2\sqrt{y_i x_j}(\ln x_j - 1) \right]. \tag{431}$$

Finally, for $F_{B-LNV}^{\chi_i^l \chi_j^l}$ if $x_i, x_j \to 0$, the f_B^{h-LNV} behaves as

$$f_B^{h-LNV}(x_i,x_j)\Big|_{x_i,x_j\to 0} \approx \sqrt{\frac{x_i}{x_j^3}}\ln\left(\frac{x_j}{x_i}\right) + \sqrt{\frac{x_i}{x_j}}(2\,\ln x_i + 1) + 3\sqrt{x_i x_j}(\ln x_j + 1) + \frac{1}{\sqrt{x_i x_j}}(\ln x_j + 1) + \sqrt{\frac{x_j}{x_i}}(2\,\ln x_j + 1). \tag{432}$$

We naively observe that we have a perturbative unitarity issue with the functions from the eqs. (427) and (432) when $x_{i,j} \to 0$ that it is equivalent to consider $m_{i,j} \to \infty$, but we must understand that infinity (∞) is an unphysical value. Then, in order to not violate perturbative unitarity, the heavy neutrino masses $m_{i,j}$ can not to exceed an upper limit which makes the (427) and (432) functions not divergent. Thus, all form factors from (422) are finite.

Due to this process has no penguin contributions, the total decay width for $\ell \to \ell'\ell''\bar{\ell}'''$ is given by

$$\Gamma(\ell \to \ell'\ell''\bar{\ell}''') = \frac{\alpha^2 m_\ell^5}{192\pi}\left|F_B\right|^2, \tag{433}$$

Then, the branching ratio is written down as follows

$$
\begin{aligned}
\mathrm{Br}(\ell \to \ell'\ell''\bar{\ell}''') &= \frac{\alpha_W^2}{128\pi^2}\,|F_B|^2 \\
&= \frac{\alpha_W^2}{128\pi^2}\left|F_B^{\nu_i^l\nu_j^l} + F_B^{\nu_i^l\chi_j^h} + F_B^{\chi_i^h\chi_j^h} + F_{B-LNV}^{\nu_i^l\nu_j^l} + F_{B-LNV}^{\nu_i^l\chi_j^h} + F_{B-LNV}^{\chi_i^h\chi_j^h}\right|^2 \\
&= \frac{\alpha_W^2}{128\pi^2}\left|-\sum_{i,j=1}^{3}\left\{W_{\ell i}W^{\dagger}_{\ell' i}W_{\ell''' j}W^{\dagger}_{\ell'' j} + (\ell' \leftrightarrow \ell'')\right\}\left[1 + (y_j + y_i)\,(1 + \ln y_j)\right]\right. \\
&+ \sum_{i=1}^{3}\sum_{j=7}^{9}\left\{W_{\ell i}W^{*}_{\ell' i}\theta^{\dagger}_{\ell''' j}\theta_{\ell'' j} + (\ell' \leftrightarrow \ell'')\right\}\left[x_j(1+\ln x_j) + \frac{1}{4}y_i(\ln x_j - 7)\right] \\
&+ \sum_{i,j=7}^{9}\left\{\theta^{\dagger}_{\ell i}\theta_{\ell' i}\theta^{\dagger}_{\ell''' j}\theta_{\ell'' j} + (\ell' \leftrightarrow \ell'')\right\}\left[\left(\frac{1}{2x_j} - 3\right)\frac{x_i}{2x_j}\,\ln\left(\frac{x_i}{x_j}\right) + x_i \ln x_i + \frac{9}{4}x_i \ln x_j\right. \\
&\left. + x_i x_j\left(3\,\ln x_j + \frac{3}{4}\right) + \frac{7}{4}x_i + \frac{1}{4x_j}\ln\left(\frac{x_i}{x_j}\right) + \frac{1}{4}\,(6\,\ln x_j + 7) + \frac{1}{4}x_j\,(13\,\ln x_j + 7)\right] \\
&+ \sum_{i,j}^{3}\left\{W_{\ell i}W^{\dagger}_{\ell' j}W_{\ell''' i}W^{\dagger}_{\ell'' j}\right\}\left[2\sqrt{y_i y_j}(1 + 2\,\ln y_j)\right] \\
&+ \sum_{i=1}^{3}\sum_{j=7}^{9}\left\{W_{\ell i}\theta_{\ell' j}W_{\ell''' i}\theta_{\ell'' j}\right\}\left[2\sqrt{y_i x_j}(\ln x_j - 1)\right] \\
&+ \sum_{i,j=7}^{9}\left\{\theta^{\dagger}_{\ell i}\theta_{\ell' j}\theta^{\dagger}_{\ell''' i}\theta_{\ell'' j}\right\}\left[\sqrt{\frac{x_i}{x_j^3}}\ln\left(\frac{x_j}{x_i}\right) + \sqrt{\frac{x_i}{x_j}}(2\,\ln x_i + 1) + 3\sqrt{x_i x_j}(\ln x_j + 1)\right. \\
&\left.\left. + \frac{1}{\sqrt{x_i x_j}}(\ln x_j + 1) + \sqrt{\frac{x_j}{x_i}}(2\,\ln x_j + 1)\right]\right|^2,
\end{aligned}
\tag{434}
$$

in the equation above we are considering $y \to 0$ and $x \to 0$, where the y variable is corresponding to active neutrinos and x variable stands for heavy neutrinos. The masses of active neutrinos are of the order of $\mathcal{O}(\mathrm{eV})$, while we assume that the masses of heavy neutrinos are of the order of $\mathcal{O}(\mathrm{TeV})$, and the well-known mass of W boson is of the order of $\mathcal{O}(100\mathrm{GeV})$, therefore the y variable approaches zero faster than the x variable does. This ensures that the $\frac{1}{4}y_i\,(\ln x_j - 7)$ and $2\sqrt{y_i x_j}(\ln x_j - 1)$ terms

are finite. Hence, the branching ratio at leading order behaves as

$$\begin{aligned}\mathrm{Br}(\ell\to\ell'\ell''\bar{\ell}''') = \frac{\alpha_W^2}{128\pi^2}\Bigg|&-\sum_{i,j=1}^{3}\{W_{\ell i}W^\dagger_{\ell' i}W_{\ell''' j}W^\dagger_{\ell'' j}+(\ell'\leftrightarrow\ell'')\}\\&+\sum_{i,j=7}^{9}\{\theta^\dagger_{\ell i}\theta_{\ell' i}\theta^\dagger_{\ell''' j}\theta_{\ell'' j}+(\ell'\leftrightarrow\ell'')\}\left[\left(\frac{1}{2x_j}-3\right)\frac{x_i}{2x_j}\,\ln\left(\frac{x_i}{x_j}\right)+\frac{1}{4x_j}\ln\left(\frac{x_i}{x_j}\right)\right.\\&\left.+\frac{1}{4}\,(6\,\ln x_j+7)\right]+\sum_{i,j=7}^{9}\{\theta^\dagger_{\ell i}\theta_{\ell' j}\theta^\dagger_{\ell''' i}\theta_{\ell'' j}\}\left[\sqrt{\frac{x_i}{x_j^3}}\ln\left(\frac{x_j}{x_i}\right)+\sqrt{\frac{x_i}{x_j}}(2\,\ln x_i+1)\right.\\&\left.+\frac{1}{\sqrt{x_i x_j}}(\ln x_j+1)+\sqrt{\frac{x_j}{x_i}}(2\,\ln x_j+1)\right]\Bigg|^2,\end{aligned}\tag{435}$$

From the definition of W_{ij} matrix (350), we can reduce the following terms

$$\begin{aligned}W_{\ell i}W^\dagger_{\ell' i}W_{\ell''' j}W^\dagger_{\ell'' j} &= \delta_{\ell\ell'}\delta_{\ell'''\ell''}-\delta_{\ell\ell'}\theta_{\ell''' j}\theta^\dagger_{\ell'' j}-\delta_{\ell'''\ell''}\theta_{\ell i}\theta^\dagger_{\ell' i}+\theta_{\ell i}\theta^\dagger_{\ell' i}\theta_{\ell''' j}\theta^\dagger_{\ell'' j},\\ W_{\ell i}W^\dagger_{\ell'' i}W_{\ell''' j}W^\dagger_{\ell' j} &= \delta_{\ell\ell''}\delta_{\ell'''\ell'}-\delta_{\ell\ell''}\theta_{\ell''' j}\theta^\dagger_{\ell' j}-\delta_{\ell'''\ell'}\theta_{\ell i}\theta^\dagger_{\ell'' i}+\theta_{\ell i}\theta^\dagger_{\ell'' i}\theta_{\ell''' j}\theta^\dagger_{\ell' j},\end{aligned}\tag{436}$$

therefore (the sum on the repeated index is understood), the branching ratio looks as follows

$$\begin{aligned}\mathrm{Br}(\ell\to\ell'\ell''\bar{\ell}''') = \frac{\alpha_W^2}{128\pi^2}\Bigg|&-\{\delta_{\ell\ell'}\delta_{\ell'''\ell''}-\delta_{\ell\ell'}\theta_{\ell''' j}\theta^\dagger_{\ell'' j}-\delta_{\ell'''\ell''}\theta_{\ell i}\theta^\dagger_{\ell' i}+\theta_{\ell i}\theta^\dagger_{\ell' i}\theta_{\ell''' j}\theta^\dagger_{\ell'' j}\\&+\delta_{\ell\ell''}\delta_{\ell'''\ell'}-\delta_{\ell\ell''}\theta_{\ell''' j}\theta^\dagger_{\ell' j}-\delta_{\ell'''\ell'}\theta_{\ell i}\theta^\dagger_{\ell'' i}+\theta_{\ell i}\theta^\dagger_{\ell'' i}\theta_{\ell''' j}\theta^\dagger_{\ell' j}\}\\&+\{\theta^\dagger_{\ell i}\theta_{\ell' i}\theta^\dagger_{\ell''' j}\theta_{\ell'' j}+\theta^\dagger_{\ell i}\theta_{\ell'' i}\theta^\dagger_{\ell''' j}\theta_{\ell' j}\}\left[\left(\frac{1}{2x_j}-3\right)\frac{x_i}{2x_j}\,\ln\left(\frac{x_i}{x_j}\right)+\frac{1}{4x_j}\ln\left(\frac{x_i}{x_j}\right)\right.\\&\left.+\frac{1}{4}\,(6\,\ln x_j+7)\right]+\{\theta^\dagger_{\ell i}\theta_{\ell' j}\theta^\dagger_{\ell''' i}\theta_{\ell'' j}\}\left[\sqrt{\frac{x_i}{x_j^3}}\ln\left(\frac{x_j}{x_i}\right)+\sqrt{\frac{x_i}{x_j}}(2\,\ln x_i+1)\right.\\&\left.+\frac{1}{\sqrt{x_i x_j}}(\ln x_j+1)+\sqrt{\frac{x_j}{x_i}}(2\,\ln x_j+1)\right]\Bigg|^2,\end{aligned}\tag{437}$$

as the process that we are analyzing satisfies ($\ell\neq\ell'=\ell''\neq\ell'''$), hence

$$\begin{aligned}\mathrm{Br}(\ell\to\ell'\ell''\bar{\ell}''') = \frac{\alpha_W^2}{128\pi^2}\Bigg|&-\{\theta_{\ell i}\theta^\dagger_{\ell' i}\theta_{\ell''' j}\theta^\dagger_{\ell'' j}+(\ell'\leftrightarrow\ell'')\}\\&+\{\theta^\dagger_{\ell i}\theta_{\ell' i}\theta^\dagger_{\ell''' j}\theta_{\ell'' j}+(\ell'\leftrightarrow\ell'')\}\left[\left(\frac{1}{2x_j}-3\right)\frac{x_i}{2x_j}\,\ln\left(\frac{x_i}{x_j}\right)+\frac{1}{4x_j}\ln\left(\frac{x_i}{x_j}\right)\right.\\&\left.+\frac{1}{4}\,(6\,\ln x_j+7)\right]+\{\theta^\dagger_{\ell i}\theta_{\ell' j}\theta^\dagger_{\ell''' i}\theta_{\ell'' j}\}\left[\sqrt{\frac{x_i}{x_j^3}}\ln\left(\frac{x_j}{x_i}\right)+\sqrt{\frac{x_i}{x_j}}(2\,\ln x_i+1)\right.\\&\left.+\frac{1}{\sqrt{x_i x_j}}(\ln x_j+1)+\sqrt{\frac{x_j}{x_i}}(2\,\ln x_j+1)\right]\Bigg|^2.\end{aligned}\tag{438}$$

Now, we are going to consider the $\tau \to ee\bar{\mu}$ and $\tau \to \mu\mu\bar{e}$ processes which yield [6]

$$\begin{aligned}\mathrm{Br}(\tau \to ee\bar{\mu}) = (0.17)\frac{\alpha_W^2}{128\pi^2}\Bigg|&-2\theta_{\tau i}\theta^\dagger_{ei}\theta_{\mu j}\theta^\dagger_{ej} + 2\theta^\dagger_{\tau i}\theta_{ei}\theta^\dagger_{\mu j}\theta_{ej}\left[\left(\frac{1}{2x_j}-3\right)\frac{x_i}{2x_j}\,\ln\left(\frac{x_i}{x_j}\right)+\frac{1}{4x_j}\ln\left(\frac{x_i}{x_j}\right)\right.\\ &\left.+\frac{1}{4}\left(6\,\ln x_j+7\right)\right]+\theta^\dagger_{\tau i}\theta_{ej}\theta^\dagger_{\mu i}\theta_{ej}\left[\sqrt{\frac{x_i}{x_j^3}}\ln\left(\frac{x_j}{x_i}\right)+\sqrt{\frac{x_i}{x_j}}(2\,\ln x_i+1)\right.\\ &\left.+\frac{1}{\sqrt{x_i x_j}}(\ln x_j+1)+\sqrt{\frac{x_j}{x_i}}(2\,\ln x_j+1)\right]\Bigg|^2 < 1.5\times 10^{-8}(\mathrm{C.L}=90\%),\end{aligned} \tag{439}$$

$$\begin{aligned}\mathrm{Br}(\tau \to \mu\mu\bar{e}) = (0.17)\frac{\alpha_W^2}{128\pi^2}\Bigg|&-2\theta_{\tau i}\theta^\dagger_{\mu i}\theta_{ej}\theta^\dagger_{\mu j} + 2\theta^\dagger_{\tau i}\theta_{\mu i}\theta^\dagger_{ej}\theta_{\mu j}\left[\left(\frac{1}{2x_j}-3\right)\frac{x_i}{2x_j}\,\ln\left(\frac{x_i}{x_j}\right)+\frac{1}{4x_j}\ln\left(\frac{x_i}{x_j}\right)\right.\\ &\left.+\frac{1}{4}\left(6\,\ln x_j+7\right)\right]+\theta^\dagger_{\tau i}\theta_{\mu j}\theta^\dagger_{ei}\theta_{\mu j}\left[\sqrt{\frac{x_i}{x_j^3}}\ln\left(\frac{x_j}{x_i}\right)+\sqrt{\frac{x_i}{x_j}}(2\,\ln x_i+1)\right.\\ &\left.+\frac{1}{\sqrt{x_i x_j}}(\ln x_j+1)+\sqrt{\frac{x_j}{x_i}}(2\,\ln x_j+1)\right]\Bigg|^2 < 1.7\times 10^{-8}(\mathrm{C.L}=90\%),\end{aligned} \tag{440}$$

with $i,j=1,2,3$. The 0.17 factor is because we need to take into account other possible decay channels for the tau. Notice all contributions of diagrams with explicit lepton number violating (LNV) vertices come from θ matrix defined by the interactions from (350) due to introducing Majorana neutrinos.

7.2 Contributions to $Z \to \bar{\ell}\ell'$ decays

At leading order the $Z \to \bar{\ell}\ell'$ vertex reduces to

$$i\Gamma^\mu_Z(p_\ell, p_{\ell'}) = ieF_L^Z(Q^2)\gamma^\mu P_L. \tag{441}$$

We work in the approximation of zero light neutrino masses. Therefore, only diagrams with heavy neutrinos contribute to this process. In this type of decay we have that $Q^2 = M_Z^2$, so the Z width is written as follows

$$\Gamma(Z \to \bar{\ell}\ell') = \frac{\alpha}{3}M_Z|F_L^Z(M_Z^2)|^2, \tag{442}$$

where the $F_L^Z(M_Z^2)$ form factor is given by

$$F_L^Z(M_Z^2) = F_L^{Z-\chi^h}(y_i, y_j; M_Z^2). \tag{443}$$

The $F_L^{Z-\chi^h}$ form factor receives 10 contributions from the Figure 39

$$F_L^{Z-\chi^h} = \frac{\alpha_W}{8\pi c_W s_W}\sum_{a=1}^{10} F_Z^{(a)} \tag{444}$$

where the form factors of the different diagrams are:

Topology I

$$F_Z^{(1)} = \theta_{\ell' j}\theta_{\ell i}^{\dagger}\left(-S_{ji}\left[M_Z^2(C_0+C_1+C_2+C_{12})-2C_{00}+1\right]+S_{ji}^{\dagger}\sqrt{\frac{1}{y_i y_j}}M_W^2 C_0\right), \tag{445}$$

where $C_{00,0,1,2,12} \equiv C_{00,0,1,2,12}(0, M_Z^2, 0; M_i, M_j, M_W)$;

Topology II

$$F_Z^{(2)} = -2c_W^2\theta_{\ell' j}\theta_{\ell i}^{\dagger}\left(M_Z^2\left[C_1+C_2+C_{12}\right]+6C_{00}-1\right), \tag{446}$$

where $C_{00,1,2,12} \equiv C_{00,1,2,12}(0, M_Z^2, 0; M_i, M_W, M_W)$;

Topology III

$$F_Z^{(3)} = \frac{1}{2}\theta_{\ell' j}\theta_{\ell i}^{\dagger}\left(-S_{ji}\frac{1}{y_i y_j}M_W^2 C_0+S_{ji}^{\dagger}\sqrt{\frac{1}{y_i y_j}}\left[M_Z^2 C_{12}-2C_{00}+\frac{1}{2}\right]\right), \tag{447}$$

where $C_{00,0,12} \equiv C_{00,0,12}(0, M_Z^2, 0; M_i, M_j, M_W)$;

Topology IV

$$F_Z^{(4)} = -(1-2s_W^2)\theta_{\ell' j}\theta_{\ell i}^{\dagger}\frac{1}{y_i}C_{00}, \tag{448}$$

where $C_{00} \equiv C_{00}(0, M_Z^2, 0; M_i, M_W, M_W)$;

Topology V and VI

$$F_Z^{(5)} + F_Z^{(6)} = -2s_W^2\theta_{\ell' j}\theta_{\ell i}^{\dagger}\frac{1}{y_i}M_W^2 C_0, \tag{449}$$

where $C_0 \equiv C_0(0, M_Z^2, 0; M_i, M_W, M_W)$;

Self-energy diagrams

$$F_Z^{(7)} + F_Z^{(8)} + F_Z^{(9)} + F_Z^{(10)} = -\frac{1}{2}(1-2s_W^2)\theta_{\ell' j}\theta_{\ell i}^{\dagger}\left[\left(2+\frac{1}{y_i}\right)B_1+1\right], \tag{450}$$

where $B_1 \equiv B_1(0; M_i, M_W)$. In all these expressions we have defined $y_{i,j} = M_W^2/M_{i,j}^2$, being $M_{i,j}$ the heavy neutrino masses. The form factors above are in agreement with [54], we have different signs in the eqs. (446) and (450). Writing the 10 form factors above in a compact way we obtain a similar

expressions from the eqs. (414), (415), and (416).

$$F_L^Z(M_Z^2) = \frac{\alpha_W}{8\pi c_W s_W}\sum_{i,j=1}^{3}\Big[\theta_{\ell' i}\theta^\dagger_{\ell i}F^h(y_i;M_Z^2) + \theta_{\ell' j}S_{ji}\theta^\dagger_{\ell i}\left(G^h(y_i,y_j;M_Z^2)+\frac{1}{\sqrt{y_i y_j}}H^h(y_i,y_j;M_Z^2)\right)\Big], \tag{451}$$

where

$$\begin{aligned}
F^h(y_i;M_Z^2) &= -2c_W^2\left[M_Z^2(\overline{C}_1+\overline{C}_2+\overline{C}_{12})+6\overline{C}_{00}-1\right]-(1-2s_W^2)\frac{1}{y_i}\overline{C}_{00}-2s_W^2\frac{1}{y_i}M_W^2\overline{C}_0\\
&\quad-\frac{1}{2}(1-2s_W^2)\left[(2+\frac{1}{y_i})\overline{B}_1+1\right],\\
G^h(y_i,y_j;M_Z^2) &= -M_Z^2(C_0+C_1+C_2+C_{12})+2C_{00}-1-\frac{1}{2}\frac{1}{y_i y_j}M_W^2C_0,\\
H^h(y_i,y_j;M_Z^2) &= M_W^2C_0+\frac{1}{2}M_Z^2C_{12}-C_{00}+\frac{1}{4},
\end{aligned} \tag{452}$$

with $y_{i,j} = M_W^2/M_{i,j}^2$, $M_{i,j}$ are the heavy neutrino masses. Analytic expressions for the functions F^h, G^h, and H^h at order of M_Z^2 are written as

$$\begin{aligned}
F^h(y_i;M_Z^2) &= -\left(\frac{5}{2}-2s_W^2\right)\Delta_\epsilon-\frac{5\,\ln y_i}{2(1-y_i)^2}-\frac{5}{2(1-y_i)}+\frac{1}{4}\\
&\quad+\frac{M_Z^2}{72M_W^2}\frac{1}{(1-y_i)^4}\left(6[24y_i^2(s_W^2-1)-4y_i(5s_W^2-8)-(2s_W^2-1)]\,\ln y_i\right.\\
&\quad\left.-(1-y_i)[88y_i^3(s_W^2-1)-2y_i^2(164s_W^2-171)-y_i(297-230s_W^2)-(2s_W^2+11)]\right),\\
G^h(y_i,y_j;M_Z^2) &= \frac{1}{2}\left(\Delta_\epsilon-\frac{1}{2}\right)-\frac{1}{2(y_i-y_j)}\left(-\frac{(1-y_j)\,\ln y_i}{(1-y_i)}+\frac{(1-y_i)\,\ln y_j}{(1-y_j)}\right)+\frac{M_Z^2}{M_j^2}\times(\text{terms}),\\
H^h(y_i,y_j;M_Z^2) &= -\frac{1}{4}\left(\Delta_\epsilon+\frac{1}{2}\right)-\frac{1}{4(y_i-y_j)}\left(-\frac{(1-4y_i)y_j\,\ln y_i}{(1-y_i)}+\frac{(1-4y_j)y_i\,\ln y_j}{(1-y_j)}\right)+\frac{M_Z^2}{M_i^2}\times(\text{terms}).
\end{aligned} \tag{453}$$

These functions are parameterized under the consideration of heavy neutrino masses ($M_i \gg M_W$), where we have defined the variable $y_i = M_W^2/M_i^2$. We observe that the variable y_i is the inverse of x_i, which is the one defined by light neutrino masses $x_i = m_i^2/M_W^2$ ($m_i \ll M_W$). Then, if we rewrite the F^h, G^h and H^h functions with the $x_{i,j}$ variables instead of $y_{i,j}$ we recover the results reported for $M_Z^2 \to 0$ in [44, 48, 54].

We can see from G^h and H^h that the term of order M_Z^2 is suppressed by $\frac{M_Z^2}{M_{i,j}^2}$, being $M_{i,j}$ the heavy neutrino masses. For heavy neutrinos we know that $M_i \gg M_W$, therefore, it satisfies $M_i \gg M_Z$ as well. So, we just consider terms at the lowest order in G^h and H^h functions. Otherwise, from the F^h function the term of order M_Z^2 is not suppressed by heavy neutrino masses, hence we need

to do a more detailed analysis. We do a series expansion of F^h function to higher orders of M_Z to study its behavior. In this expansion there appear terms like $\frac{1}{M_i^n}\ln\left(M_i^2/M_W^2\right)$ with $n \geq 2$ which are suppressed due to $M_i \gg 1$. Besides, the terms whose behavior is $(M_Z/M_W)^n$ with $n \geq 4$ vanish because of unitarity of the mixing matrices. Finally, the F^h is given by

$$F^h(y_i; M_Z^2) \approx \frac{5}{2}\ln\left(\frac{M_i^2}{M_W^2}\right) - \frac{M_Z^2}{M_W^2}\left(\frac{1}{12}(1-2s_W^2)\ln\left(\frac{M_i^2}{M_W^2}\right)\right), \tag{454}$$

where $\frac{M_Z^2}{M_W^2} = \frac{1}{c_W^2} = 1.286$ and $s_W^2 = 0.23153$ [6], it yields

$$F^h(y_i; M_Z^2) \approx \frac{5}{2}\ln\left(\frac{M_i^2}{M_W^2}\right) - (0.09567)\ln\left(\frac{M_i^2}{M_W^2}\right), \tag{455}$$

we see the second term is 26.13 times smaller than the first one. To finish, we write the equation above in terms of y_i

$$F^h(y_i; M_Z^2) \approx -\frac{5}{2}\ln(y_i) + (0.09567)\ln(y_i). \tag{456}$$

7.3 The $\mu - e$ conversion in nuclei

The $\mu - e$ conversion in nuclei has penguin and box contributions as $\ell \to \ell'\ell''\bar{\ell}'''$ decay, replacing the last two leptons by a quark q = u or d. It has no crossed penguin diagrams because the lower fermionic line where the gauge boson is attached is now a coherent sum of quarks composing the probed nucleus. There is also no crossed box contributions due to the exchange of leptons.
We can write the interaction with a quark q = u or d

$$\mathcal{M}^{\mu q\to eq} = \mathcal{M}_\gamma^{\mu q\to eq} + \mathcal{M}_Z^{\mu q\to eq} + \mathcal{M}_{box}^{\mu q\to eq}, \tag{457}$$

with the amplitudes defined as [37]

$$\begin{aligned}
\mathcal{M}_\gamma^{\mu q\to eq} =& \overline{u}(p_1)e\left[iF_M^\gamma(0)2P_R\sigma^{\mu\nu}(p_1-p_\ell)_\nu + F_L^\gamma((p_1-p_\ell)^2)\gamma^\mu P_L\right]u(p_\ell) \\
&\times\frac{1}{(p_1-p_\ell)^2}\overline{u}(p_3)\gamma_\mu(g_{Lq}^\gamma P_L + g_{Rq}^\gamma P_R)v(p_2), \\
\mathcal{M}_Z^{\mu q\to eq} =& \overline{u}(p_1)\left(-eF_L^Z(0)\right)\gamma^\mu P_L u(p_\ell)\frac{1}{M_Z^2}\overline{u}(p_3)\gamma_\mu\left(g_{Lq}^Z P_L + g_{Rq}^Z P_R\right)v(p_2), \\
\mathcal{M}_{box}^{\ell\to\ell_1'\ell_2'\bar{\ell}_3'} =& e^2 B_L^q(0)\overline{u}(p_1)\gamma^\mu P_L u(p_\ell)\overline{u}(p_3)\gamma_\mu P_L v(p_2).
\end{aligned} \tag{458}$$

The form factors $F_M^\gamma(0)$, F_L^γ and $F_L^Z(0)$ are given by (405), (406), and (414), respectively while the couplings $g^Z_{L(R)q}$ read [48]

$$\begin{aligned} g^Z_{Lu} &= \frac{1-\frac{4}{3}s_W^2}{2s_W c_W}, \qquad g^Z_{Ru} = -\frac{2s_W}{3c_W}, \\ g^Z_{Ld} &= \frac{-1+\frac{2}{3}s_W^2}{2s_W c_W}, \qquad g^Z_{Rd} = \frac{s_W}{3c_W}. \end{aligned} \tag{459}$$

We have a couple of new box diagrams shown in Figure 40 We have been working under the approxi-

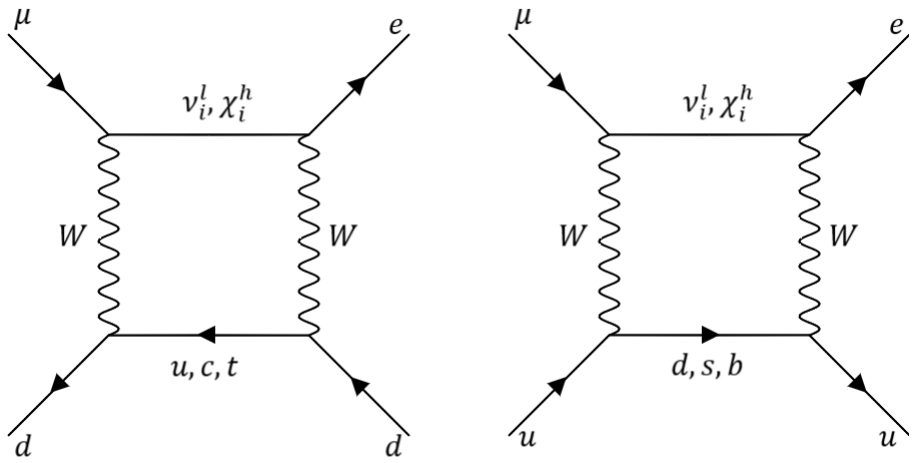

Figure 40: Box diagrams contributing to $\mu - e$ conversion in nuclei considering light-heavy Majorana neutrinos.

mation where light Majorana neutrinos are massless. Then, we just consider the contribution which is coming from heavy Majorana neutrinos χ^h. The form factors corresponding to diagrams in Figure 40 are written as

$$B_L^d = \frac{\alpha_W}{16\pi M_W^2 s_W^2} \sum_{i,j=1}^{3} \theta^\dagger_{\mu i}\theta_{ei}|V_{jd}|^2 f_{B_d}\left(y_i, x_j^u\right), \tag{460}$$

$$B_L^u = \frac{\alpha_W}{16\pi M_W^2 s_W^2} \sum_{i,j=1}^{3} \theta^\dagger_{\mu i}\theta_{ei}|V_{uj}|^2 f_{B_u}\left(y_i, x_j^d\right), \tag{461}$$

where $y_i = M_W^2/M_i^2$ with M_i the mass of heavy neutrinos, $x_i^q = m_{q_i}^2/M_W^2$ with m_{q_i} the mass of the i-th quark, V_{ij} is the CKM matrix. In agreement with [48] and recalling the eqs. (727), (728), and (729) in Appendix G

$$f_{B_d}(y_i, x_j^u) = \left(1 + \frac{1}{4}\frac{x_j^u}{y_i}\right)\bar{d}_0^{lh}(y_i, x_j^u) - 2\frac{x_j^u}{y_i}d_0^{lh}(y_i, x_j^u), \tag{462}$$

where (making the necessary adjustments)

$$d_0^{lh}(y_i,x_j^u)=\frac{y_i^2\ \ln y_i}{(1-y_i)^2(1-y_ix_j^u)}+\frac{x_j^u y_i\ \ln x_j^u}{(1-x_j^u)^2(1-y_ix_j^u)}+\frac{y_i}{(1-y_i)(1-x_j^u)}, \tag{463}$$

$$\bar{d}_0^{lh}(y_i,x_j^u)=\frac{y_i\ \ln y_i}{(1-y_i)^2(1-y_ix_j^u)}+\frac{y_i(x_j^u)^2\ \ln x_j^u}{(1-x_j^u)^2(1-y_ix_j^u)}+\frac{y_i}{(1-y_i)(1-x_j^u)}, \tag{464}$$

with $y_i=M_W^2/M_i^2$ $(i=1,2,3)$ and $x_j^u=m_{q_j}^2/M_W^2$ $(j=1,2,3)$. The function f_{B_u} is written

$$f_{B_u}(y_i,x_j^d)=-\left(4+\frac{x_j^d}{4y_i}\right)\bar{d}_0^{lh}(y_i,x_j^u)+2\frac{x_j^u}{y_i}d_0^{lh}(y_i,x_j^u). \tag{465}$$

We can neglect all the quark masses, except that of the top quark, and defining $x_t=m_t^2/M_W^2$, we may reduce the f_{B_q} functions

$$\sum_{i=j}^{3}|V_{jd}|^2 f_{B_d}\left(y_i,x_j^u\right)=|V_{td}|^2\left[f_{B_d}(y_i,x_t)-f_{B_d}(y_i,0)\right]-f_{B_d}(y_i,0), \tag{466}$$

$$\sum_{i=j}^{3}|V_{uj}|^2 f_{B_u}(y_i,x_j^d)=f_{B_u}(y_i,0), \tag{467}$$

as we observe in [48]. Afterwards, the $\mu-e$ conversion rate in a nucleus with Z protons and $N=A-Z$ neutrons yields [37, 48]

$$\mathcal{R}=\frac{\alpha^5 Z_{\text{eff}}^4}{\Gamma_{\text{Capt}}Z}F_P^2 m_\mu^5\left|2Z(A_{1L}+A_{2R})-(2Z+N)(F_{LL}^u+F_{LR}^u+B_L^u)-(Z+2N)(F_{LL}^d+F_{LR}^d+B_L^d)\right|^2, \tag{468}$$

where Z_{eff} is the nucleus effective charge for the muon and F_P the associated for factor. In Table 14 we gather the input parameters for Al and for Ti and Au [37, 48, 55, 56].

Nucleus	N	Z	Z_{eff}	F_P	$\Gamma_{Capt}[GeV]$
$^{27}_{13}$Al	14	13	11.5	0.64	4.6×10^{-19}
$^{48}_{22}$Ti	26	22	17.6	0.54	1.7×10^{-18}
$^{197}_{79}$Au	118	79	33.5	0.16	8.6×10^{-18}

Table 14: Input parameters for different nuclei.

8 Limits on LFV processes driven by $\mathcal{O}$(TeV) Majorana neutrinos

In this section we show the numerical results for each LFV processes through Monte Carlo simulations. We are going to consider the light neutrinos massless approximation. Therefore, only diagrams that involve heavy Majorana neutrinos contribute to the processes. We begin the discussion with LFV Z decays, LFV Type I and II and $\mu - e$ conversion in nuclei as they share the same free parameters: three heavy neutrinos masses M_i with $i = 1, 2, 3$ and neutral couplings given by $(\theta S \theta^\dagger)$. Afterwards, we focus in wrong sign processes to bind the corresponding LNV couplings, and we finish with $\mu - e$ conversions in nuclei. In the following subsections we are using the limits of $(\theta\theta^\dagger)_{\ell'\ell}$ previously obtained by $\ell \to \ell'\gamma$ decays. These limits are written in eqs. (397), (400), and (402).

8.1 LFV Z decays

We start with LFV Z decays ($Z \to \bar{\ell}\ell'$) whose branching ratios are given by

$$Br(Z \to \bar{\ell}\ell') = \frac{\Gamma(Z \to \bar{\ell}\ell')}{\Gamma_Z}, \tag{469}$$

with $\Gamma_Z = 2.4952 \pm 0.0023$ GeV [6]. Because we are considering the light neutrinos massless approximation the Z width is written as follows

$$\begin{aligned} 7\Gamma(Z \to \bar{\ell}\ell') = \frac{\alpha_W^3}{192\pi^2 c_W^2} M_Z \Bigg| \sum_{i,j=1}^{3} \Big[& \theta_{\ell' i}\theta^\dagger_{\ell i} F^h(y_i; M_Z^2) \\ & + \theta_{\ell' j} S_{ji} \theta^\dagger_{\ell i} \left(G^h(y_i, y_j; M_Z^2) + \frac{1}{\sqrt{y_i y_j}} H^h(y_i, y_j; M_Z^2) \right) \Big] \Bigg|^2, \end{aligned} \tag{470}$$

where the F^h, G^h and H^h functions are given by the eq.(453).

8.1.1 $Z \to \bar{\mu}e$

In this process we know that

$$\left| \theta_{ej}\theta^\dagger_{\mu j} \right| < 0.14 \times 10^{-4}, \tag{471}$$

and from PDG [6] $\text{Br}(Z \to \bar{\mu}e) < 7.5 \times 10^{-7}$ (C.L. = 95%), it yields

$$\begin{aligned} \text{Br}(Z \to \bar{\mu}e) = & \frac{\alpha_W^3}{192\pi^2 c_W^2 \Gamma_Z} M_Z \Bigg| \Big[(0.14 \times 10^{-4}) F^h(y_i; M_Z^2) \\ & + \theta_{ej} S_{ji} \theta^\dagger_{\mu i} \left(G^h(y_i, y_j; M_Z^2) + \frac{1}{\sqrt{y_i y_j}} H^h(y_i, y_j; M_Z^2) \right) \Big] \Bigg|^2 < 7.5 \times 10^{-7}. \end{aligned} \tag{472}$$

8.1.2 $Z \to \bar{\tau} e$

For this process the limit on the mixing coupling $\theta_{ej}\theta^{\dagger}_{\tau j}$ is

$$\left|\theta_{ej}\theta^{\dagger}_{\tau j}\right| < 0.95 \times 10^{-2}, \tag{473}$$

and from PDG [6] $\mathrm{Br}(Z \to \bar{\tau} e) < 9.8 \times 10^{-6}$ (C.L. = 95%), it yields

$$\begin{aligned}\mathrm{Br}(Z \to \bar{\tau} e) =& \frac{\alpha_W^3}{192\pi^2 c_W^2 \Gamma_Z} M_Z \left|\left[(0.95 \times 10^{-2}) F^h(y_i; M_Z^2)\right.\right. \\ &\left.\left. + \theta_{ej} S_{ji} \theta^{\dagger}_{\tau i} \left(G^h(y_i, y_j; M_Z^2) + \frac{1}{\sqrt{y_i y_j}} H^h(y_i, y_j; M_Z^2) \right) \right]\right|^2 < 9.8 \times 10^{-6}.\end{aligned} \tag{474}$$

8.1.3 $Z \to \bar{\tau} \mu$

The mixing coupling is given by

$$\left|\theta_{\mu j}\theta^{\dagger}_{\tau j}\right| < 0.011, \tag{475}$$

and from PDG [6] $\mathrm{Br}(Z \to \bar{\tau} \mu) < 1.2 \times 10^{-5}$ (C.L. = 95%), it yields

$$\begin{aligned}\mathrm{Br}(Z \to \bar{\tau} \mu) =& \frac{\alpha_W^3}{192\pi^2 c_W^2 \Gamma_Z} M_Z \left|\left[(0.011) F^h(y_i; M_Z^2)\right.\right. \\ &\left.\left. + \theta_{\mu j} S_{ji} \theta^{\dagger}_{\tau i} \left(G^h(y_i, y_j; M_Z^2) + \frac{1}{\sqrt{y_i y_j}} H^h(y_i, y_j; M_Z^2) \right) \right]\right|^2 < 1.2 \times 10^{-5}.\end{aligned} \tag{476}$$

8.2 Type I: $\ell \to \ell'\ell''\bar{\ell}'''$ with $\ell \neq \ell' = \ell'' = \ell'''$

In this section we write explicitly the form factors and the limits on the mixing couplings for $\mu \to ee\bar{e}$, $\tau \to ee\bar{e}$ and $\tau \to \mu\mu\bar{\mu}$ decays.

8.2.1 $\mu \to ee\overline{e}$

The form factors involved in this decay are given as follows

$$
\begin{aligned}
A_L &= \frac{F_L^{\sigma}}{Q^2} = \frac{\alpha_W}{8\pi M_W^2}\sum_{i=1}^{3}\theta_{ei}\theta_{\mu i}^{\dagger}\left(-\frac{(12y_i^2-10y_i+1)\,\ln y_i}{6(1-y_i)^4}+\frac{20y_i^3-96y_i^2+57y_i+1}{36(1-y_i)^3}\right),\\
A_R &= \frac{2F_M^{\gamma}(0)}{m_\mu} = \frac{\alpha_W}{8\pi M_W^2}\sum_{i=1}^{3}\theta_{ei}\theta_{\mu i}^{\dagger}\left(-\frac{2y_i^3-7y_i^2+11y_i}{4(1-y_i)^3}+\frac{3y_i\,\ln y_i}{2(1-y_i)^4}\right),\\
F_{LL} &= -\frac{g_L F_L^Z(0)}{eM_Z^2} = -\frac{\alpha_W}{16\pi s_W^2 M_W^2}(-1+2s_W^2)\sum_{i,j=1}^{3}\left[\theta_{ei}\theta_{\mu i}^{\dagger}\left(-\frac{5\,\ln y_i}{2(1-y_i)^2}-\frac{5}{2(1-y_i)}\right)\right.\\
&\quad +\theta_{ej}S_{ji}\theta_{\mu i}^{\dagger}\left(-\frac{1}{2(y_i-y_j)}\left(-\frac{(1-y_j)\,\ln y_i}{(1-y_i)}+\frac{(1-y_i)\,\ln y_j}{(1-y_j)}\right)\right.\\
&\quad \left.\left.-\frac{1}{\sqrt{y_iy_j}}\frac{1}{4(y_i-y_j)}\left(-\frac{y_j(1-4y_i)\,\ln y_i}{1-y_i}+\frac{y_i(1-4y_j)\,\ln y_j}{1-y_j}\right)\right)\right],\\
F_{LR} &= -\frac{g_R F_L^Z(0)}{eM_Z^2} = -\frac{\alpha_W}{8\pi M_W^2}\sum_{i,j=1}^{3}\left[\theta_{ei}\theta_{\mu i}^{\dagger}\left(-\frac{5\,\ln y_i}{2(1-y_i)^2}-\frac{5}{2(1-y_i)}\right)\right.\\
&\quad +\theta_{ej}S_{ji}\theta_{\mu i}^{\dagger}\left(-\frac{1}{2(y_i-y_j)}\left(-\frac{(1-y_j)\,\ln y_i}{(1-y_i)}+\frac{(1-y_i)\,\ln y_j}{(1-y_j)}\right)\right.\\
&\quad \left.\left.-\frac{1}{\sqrt{y_iy_j}}\frac{1}{4(y_i-y_j)}\left(-\frac{y_j(1-4y_i)\,\ln y_i}{1-y_i}+\frac{y_i(1-4y_j)\,\ln y_j}{1-y_j}\right)\right)\right],\\
B_L &= B_L(0) = \frac{\alpha_W}{8\pi M_W^2 s_W^2}\sum_{i,j=1}^{3}\theta_{\mu i}^{\dagger}\theta_{ei}\theta_{ej}^{\dagger}\theta_{ej}\left[\left(\frac{1}{2y_j}-3\right)\frac{y_i}{2y_j}\,\ln\left(\frac{y_i}{y_j}\right)+\frac{1}{4y_j}\ln\left(\frac{y_i}{y_j}\right)+\frac{1}{4}\,(6\,\ln y_j+7)\right],
\end{aligned}
\tag{477}
$$

with $x_{i,j} = M_{i,j}^2/M_W^2$, $y_{i,j} = M_W^2/M_{i,j}^2$, where $M_{i,j}$ are the masses of heavy neutrinos. We can bind the form factor above with the following limits [57]

$$
|\theta_{\mu i}\theta_{ei}^{\dagger}| < 0.14\times 10^{-4}, \quad \text{and} \quad \theta_{ei}\theta_{ei}^{\dagger} = |\theta_e|^2 < 2.5\times 10^{-3}, \tag{478}
$$

and we take the value from the PDG [6] for $\mathrm{Br}(\mu \to ee\bar{e}) < 1\times 10^{-12}$ (C.L = 90%).

8.2.2 $\tau \to ee\overline{e}$

The form factors involved in this decay are given by the eq. (477), we only need to change $\mu \to \tau$ in the mixing matrices.

We can bind the couplings terms as follows [57]

$$|\theta_{\tau i}\theta^{\dagger}_{ei}| < 0.95 \times 10^{-2}, \quad \text{and} \quad \theta_{ei}\theta^{\dagger}_{ei} = |\theta_e|^2 < 2.5 \times 10^{-3}, \tag{479}$$

ant we take the value from the PDG [6] for $\text{Br}(\tau \to ee\bar{e}) < 2.7 \times 10^{-8}$ (C.L = 90%).

8.2.3 $\tau \to \mu\mu\overline{\mu}$

The form factors in this decay are given by the eq. (477) considering τ instead of μ, and μ instead of e in the θ matrices.
We can limit the couplings terms as follows [57]

$$|\theta_{\tau i}\theta^{\dagger}_{\mu i}| < 0.011, \quad \text{and} \quad \theta_{\mu i}\theta^{\dagger}_{\mu i} = |\theta_\mu|^2 < 0.021, \tag{480}$$

ant we take the value from the PDG [6] for $\text{Br}(\tau \to \mu\mu\bar{\mu}) < 2.1 \times 10^{-8}$ (C.L = 90%).

8.3 Type II: $\ell \to \ell'\ell''\bar{\ell}'''$ with $\ell \neq \ell' \neq \ell'' = \ell'''$

8.3.1 $\tau \to e\mu\bar{\mu}$

The form factors involved in this decay are given as follows

$$
\begin{aligned}
A_L &= \frac{F_L^\sigma}{Q^2} = \frac{\alpha_W}{8\pi M_W^2}\sum_{i=1}^{3}\theta_{ei}\theta_{\tau i}^\dagger\left(-\frac{(12y_i^2-10y_i+1)\,\ln y_i}{6(1-y_i)^4}+\frac{20y_i^3-96y_i^2+57y_i+1}{36(1-y_i)^3}\right),\\
A_R &= \frac{2F_M^\gamma(0)}{m_\mu} = \frac{\alpha_W}{8\pi M_W^2}\sum_{i=1}^{3}\theta_{ei}\theta_{\tau i}^\dagger\left(-\frac{2y_i^3-7y_i^2+11y_i}{4(1-y_i)^3}+\frac{3y_i\,\ln y_i}{2(1-y_i)^4}\right),\\
F_{LL} &= -\frac{g_L F_L^Z(0)}{eM_Z^2} = -\frac{\alpha_W}{16\pi s_W^2 M_W^2}(-1+2s_W^2)\sum_{i,j=1}^{3}\left[\theta_{ei}\theta_{\tau i}^\dagger\left(-\frac{5\,\ln y_i}{2(1-y_i)^2}-\frac{5}{2(1-y_i)}\right)\right.\\
&\quad+\theta_{ej}S_{ji}\theta_{\tau i}^\dagger\left(-\frac{1}{2(y_i-y_j)}\left(-\frac{(1-y_j)\,\ln y_i}{(1-y_i)}+\frac{(1-y_i)\,\ln y_j}{(1-y_j)}\right)\right.\\
&\quad\left.\left.-\frac{1}{\sqrt{y_iy_j}}\frac{1}{4(y_i-y_j)}\left(-\frac{y_j(1-4y_i)\,\ln y_i}{1-y_i}+\frac{y_i(1-4y_j)\,\ln y_j}{1-y_j}\right)\right)\right],\\
F_{LR} &= -\frac{g_R F_L^Z(0)}{eM_Z^2} = -\frac{\alpha_W}{8\pi M_W^2}\sum_{i,j=1}^{3}\left[\theta_{ei}\theta_{\tau i}^\dagger\left(-\frac{5\,\ln y_i}{2(1-y_i)^2}-\frac{5}{2(1-y_i)}\right)\right.\\
&\quad+\theta_{ej}S_{ji}\theta_{\tau i}^\dagger\left(-\frac{1}{2(y_i-y_j)}\left(-\frac{(1-y_j)\,\ln y_i}{(1-y_i)}+\frac{(1-y_i)\,\ln y_j}{(1-y_j)}\right)\right.\\
&\quad\left.\left.-\frac{1}{\sqrt{y_iy_j}}\frac{1}{4(y_i-y_j)}\left(-\frac{y_j(1-4y_i)\,\ln y_i}{1-y_i}+\frac{y_i(1-4y_j)\,\ln y_j}{1-y_j}\right)\right)\right],\\
B_L &= B_L(0) = \frac{\alpha_W}{8\pi M_W^2 s_W^2}\sum_{i,j=1}^{3}\{\theta_{\tau i}^\dagger\theta_{ei}\theta_{\mu j}^\dagger\theta_{\mu j}+\theta_{\tau i}^\dagger\theta_{\mu i}\theta_{\mu j}^\dagger\theta_{ej}\}\left[\left(\frac{1}{2y_j}-3\right)\frac{y_i}{2y_j}\,\ln\left(\frac{y_i}{y_j}\right)\right.\\
&\quad\left.+\frac{1}{4y_j}\ln\left(\frac{y_i}{y_j}\right)+\frac{1}{4}\,(6\,\ln y_j+7)\right],
\end{aligned}
\tag{481}
$$

with $x_{i,j} = M_{i,j}^2/M_W^2$, $y_{i,j} = M_W^2/M_{i,j}^2$, where $M_{i,j}$ are the masses of heavy neutrinos. We can bind this processes from the PDG [6] $\mathrm{Br}(\tau \to e\mu\bar{\mu}) < 2.7\times10^{-8}$ (C.L. = 90%) and the mixing couplings [57]

$$
|\theta_{ei}\theta_{\mu i}^\dagger| < 0.14\times10^{-4},\quad |\theta_{ei}\theta_{\tau i}^\dagger| < 0.95\times10^{-2},\quad |\theta_{\mu i}\theta_{\tau i}^\dagger| < 0.011,\quad |\theta_\mu|^2 < 0.021. \tag{482}
$$

8.3.2 $\tau \to \mu e\bar{e}$

The form factors in these processes are very similar to the $\tau \to e\mu\bar{\mu}$ decay, we need to replace μ by e. From the PDG [6] $\mathrm{Br}(\tau \to e\mu\bar{\mu}) < 1.8\times10^{-8}$ (C.L. = 90%) and we add the mixing coupling [57]

$$
|\theta_e|^2 < 2.5\times10^{-8}. \tag{483}
$$

8.4 The $\mu - e$ conversion rate

In this section we are going to study the $\mu - e$ conversion in nuclei taking into account Majorana neutrinos. The form factors involved in these processes are

$$
\begin{aligned}
A_{1L} &= \frac{F_L^\gamma(Q^2)}{Q^2} = \frac{\alpha_W}{8\pi M_W^2}\sum_{i=1}^{3}\theta_{ei}\theta_{\mu i}^\dagger\left(-\frac{(12y_i^2-10y_i+1)\ \mathrm{ln}y_i}{6(1-y_i)^4}+\frac{20y_i^3-96y_i^2+57y_i+1}{36(1-y_i)^3}\right),\\
A_{2R} &= \frac{2F_M^\gamma(0)}{m_\mu} = \frac{\alpha_W}{8\pi M_W^2}\sum_{i=1}^{3}\theta_{ei}\theta_{\mu i}^\dagger\left(-\frac{2y_i^3-7y_i^2+11y_i}{4(1-y_i)^3}+\frac{3y_i\ \mathrm{ln}y_i}{2(1-y_i)^4}\right),\\
F_{LL}^u &= -\frac{F_L^Z(0)g_{Lu}^Z}{M_Z^2} = -\frac{\alpha_W}{16\pi M_W^2 s_W^2}\left(1-\frac{4}{3}s_W^2\right)\sum_{i,j=1}^{3}\left[\theta_{ei}\theta_{\mu i}^\dagger\left(-\frac{5\ \mathrm{ln}y_i}{2(1-y_i)^2}-\frac{5}{2(1-y_i)}\right)\right.\\
&\quad +\theta_{ej}S_{ji}\theta_{\mu i}^\dagger\left(-\frac{1}{2(y_i-y_j)}\left(-\frac{(1-y_j)\ \mathrm{ln}y_i}{(1-y_i)}+\frac{(1-y_i)\ \mathrm{ln}y_j}{(1-y_j)}\right)\right.\\
&\quad \left.\left.-\frac{1}{\sqrt{y_iy_j}}\frac{1}{4(y_i-y_j)}\left(-\frac{y_j(1-4y_i)\ \mathrm{ln}y_i}{1-y_i}+\frac{y_i(1-4y_j)\ \mathrm{ln}y_j}{1-y_j}\right)\right)\right],\\
F_{LR}^u &= -\frac{F_L^Z(0)g_{Ru}^Z}{M_Z^2} = \frac{\alpha_W}{12\pi M_W^2}\sum_{i,j=1}^{3}\left[\theta_{ei}\theta_{\mu i}^\dagger\left(-\frac{5\ \mathrm{ln}y_i}{2(1-y_i)^2}-\frac{5}{2(1-y_i)}\right)\right.\\
&\quad +\theta_{ej}S_{ji}\theta_{\mu i}^\dagger\left(-\frac{1}{2(y_i-y_j)}\left(-\frac{(1-y_j)\ \mathrm{ln}y_i}{(1-y_i)}+\frac{(1-y_i)\ \mathrm{ln}y_j}{(1-y_j)}\right)\right.\\
&\quad \left.\left.-\frac{1}{\sqrt{y_iy_j}}\frac{1}{4(y_i-y_j)}\left(-\frac{y_j(1-4y_i)\ \mathrm{ln}y_i}{1-y_i}+\frac{y_i(1-4y_j)\ \mathrm{ln}y_j}{1-y_j}\right)\right)\right],\\
F_{LL}^d &= -\frac{F_L^Z(0)g_{Lu}^Z}{M_Z^2} = -\frac{\alpha_W}{16\pi M_W^2 s_W^2}\left(-1+\frac{2}{3}s_W^2\right)\sum_{i,j=1}^{3}\left[\theta_{ei}\theta_{\mu i}^\dagger\left(-\frac{5\ \mathrm{ln}y_i}{2(1-y_i)^2}-\frac{5}{2(1-y_i)}\right)\right.\\
&\quad +\theta_{ej}S_{ji}\theta_{\mu i}^\dagger\left(-\frac{1}{2(y_i-y_j)}\left(-\frac{(1-y_j)\ \mathrm{ln}y_i}{(1-y_i)}+\frac{(1-y_i)\ \mathrm{ln}y_j}{(1-y_j)}\right)\right.\\
&\quad \left.\left.-\frac{1}{\sqrt{y_iy_j}}\frac{1}{4(y_i-y_j)}\left(-\frac{y_j(1-4y_i)\ \mathrm{ln}y_i}{1-y_i}+\frac{y_i(1-4y_j)\ \mathrm{ln}y_j}{1-y_j}\right)\right)\right],\\
F_{LR}^d &= -\frac{F_L^Z(0)g_{Ru}^Z}{M_Z^2} = -\frac{\alpha_W}{24\pi M_W^2}\sum_{i,j=1}^{3}\left[\theta_{ei}\theta_{\mu i}^\dagger\left(-\frac{5\ \mathrm{ln}y_i}{2(1-y_i)^2}-\frac{5}{2(1-y_i)}\right)\right.\\
&\quad +\theta_{ej}S_{ji}\theta_{\mu i}^\dagger\left(-\frac{1}{2(y_i-y_j)}\left(-\frac{(1-y_j)\ \mathrm{ln}y_i}{(1-y_i)}+\frac{(1-y_i)\ \mathrm{ln}y_j}{(1-y_j)}\right)\right.\\
&\quad \left.\left.-\frac{1}{\sqrt{y_iy_j}}\frac{1}{4(y_i-y_j)}\left(-\frac{y_j(1-4y_i)\ \mathrm{ln}y_i}{1-y_i}+\frac{y_i(1-4y_j)\ \mathrm{ln}y_j}{1-y_j}\right)\right)\right],\\
B_L^d &= \frac{\alpha_W}{16\pi M_W^2 s_W^2}\sum_{i=1}^{3}\theta_{\mu i}^\dagger\theta_{ei}\left(|V_{td}|^2\left[f_{B_d}(y_i,x_t)-f_{B_d}(y_i,0)\right]-f_{B_d}(y_i,0)\right),\\
B_L^u &= \frac{\alpha_W}{16\pi M_W^2 s_W^2}\sum_{i=1}^{3}\theta_{\mu i}^\dagger\theta_{ei}f_{B_u}(y_i,0),
\end{aligned}
\tag{484}
$$

where

$$
\begin{aligned}
f_{B_d}(y_i,x_t) &= \left(1+\frac{1}{4}\frac{x_t}{y_i}\right)\left[\frac{y_i\,\ln y_i}{(1-y_i)^2(1-y_ix_t)}+\frac{y_ix_t^2\,\ln x_t}{(1-x_t)^2(1-y_ix_t)}+\frac{y_i}{(1-y_i)(1-x_t)}\right]\\
&\quad -2\frac{x_t}{y_i}\left[\frac{y_i^2\,\ln y_i}{(1-y_i)^2(1-y_ix_t)}+\frac{x_ty_i\,\ln x_t}{(1-x_t)^2(1-y_ix_t)}+\frac{y_i}{(1-y_i)(1-x_t)}\right],\\
f_{B_d}(y_i,0) &= \vec{d}_0^{lh}(y_i,0)=\frac{y_i\,\ln y_i}{(1-y_i)^2}+\frac{y_i}{(1-y_i)},\\
f_{B_u}(y_i,0) &= -4\vec{d}_0^{lh}(y_i,0)=-4\left(\frac{y_i\,\ln y_i}{(1-y_i)^2}+\frac{y_i}{(1-y_i)}\right),
\end{aligned}
\tag{485}
$$

with $y_i = M_W^2/M_i^2$ and $x_t = m_t^2/M_W^2$, being M_i and m_t the masses of heavy neutrinos and quark top respectively. From the eq. (397) we can bind the form factors above by

$$
|\theta_{ei}\theta^{\dagger}_{\mu i}| < 0.14\times 10^{-4}, \tag{486}
$$

and taking the following values from PDG [6]: $m_t = 172.76 \pm 0.30$ GeV and $|V_{td}| = (8.0 \pm 0.3)\times 10^{-3}$. We are able to measure these processes via two nuclei: $^{48}_{22}$Ti and $^{197}_{79}$Au, which share the same form factors, they differ by constants in the conversion rate. Such constants are given in Table 14, therefore

$$
\mathcal{R}_{Ti} = \frac{\alpha^5 Z^4_{\mathrm{eff}_{\mathrm{Ti}}}}{22\Gamma_{\mathrm{Capt}_{\mathrm{Ti}}}} F^2_{P_{Ti}} m_\mu^5 \left|44(A_{1L}+A_{2R}) - 70(F^u_{LL}+F^u_{LR}+B^u_L) - 74(F^d_{LL}+F^d_{LR}+B^d_L)\right|^2, \tag{487}
$$

$$
\mathcal{R}_{Au} = \frac{\alpha^5 Z^4_{\mathrm{eff}_{\mathrm{Au}}}}{79\Gamma_{\mathrm{Capt}_{\mathrm{Au}}}} F^2_{P_{Au}} m_\mu^5 \left|158(A_{1L}+A_{2R}) - 276(F^u_{LL}+F^u_{LR}+B^u_L) - 315(F^d_{LL}+F^d_{LR}+B^d_L)\right|^2, \tag{488}
$$

from PDG [6]: $\mathcal{R}(\mathrm{Ti}) < 4.3\times 10^{-12}$ (C.L. = 90%) and $\mathcal{R}(Au) < 7\times 10^{-13}$ (C.L. = 90%).

8.5 Global Analysis

In this subsection we do a global analysis of the 10 processes above: LFV Z decays $Z\to\bar{\mu}e$, $Z\to\bar{\tau}e$, and $Z\to\bar{\tau}\mu$; LFV Type I $\mu\to ee\bar{e}$, $\tau\to ee\bar{e}$ and $\tau\to\mu\mu\bar{\mu}$; LFV Type II $\tau\to e\mu\bar{\mu}$ and $\tau\to\mu e\bar{e}$; $\mu-e$ conversion in nuclei $^{48}_{22}$Ti and $^{197}_{79}$Au.

We do the analysis through a single Monte Carlo simulation where the 10 processes are run simultaneously. The peculiarity of all these LFV processes is that they share the same free parameters: three heavy neutrino masses $\mathrm{M_i}$ with $i=1,2,3$ and the neutral couplings given by $(\theta S\theta^{\dagger})$ matrices.

Every process is submitted under its own limit reported by PDG [6], though the conditions on the heavy neutrinos masses and neutral couplings of heavy Majorana neutrinos are the same for all, hence after several attempts we decided to take the heavy neutrino masses interval from 15 to 20 TeV, since

in this interval is where there are the greatest number of results that satisfy the limit of the branching ratios and conversion rates.

From the form factors of all those LFV decays we can see that they receive two contributions: one is coming from charged couplings ($\theta\theta^\dagger$) and the second one comes from neutral couplings ($\theta S\theta^\dagger$). It implies that there is an interference between them. Therefore, we are able to determine the sign of each entry of the ($\theta\theta^\dagger$) matrices, i.e., we can know whether the interference is constructive or destructive. We will set ($\theta\theta^\dagger$) elements positive in order to determine the (relative) sign of the ($\theta S\theta^\dagger$) elements.

What the Monte Carlo simulation does is finding combinations of the free parameters values that return a value for each branching ratio and conversion rate that is less than the experimentally measured upper limit [6]. In the following Table we show the predicted values for the branching ratios, conversion rates and heavy neutrino masses. The modulus of the $(\theta S\theta^\dagger)_{e\mu}$ elements are all

LFV Z decays	Our mean values	Present limits [6]
Br($Z \to \bar{\mu}e$)	1.20×10^{-14}	3.7×10^{-7}
Br($Z \to \bar{\tau}e$)	1.46×10^{-8}	4.9×10^{-6}
Br($Z \to \bar{\tau}\mu$)	1.09×10^{-8}	0.6×10^{-5}
LFV Type I		
Br($\mu \to ee\bar{e}$)	1.85×10^{-14}	1.0×10^{-12}
Br($\tau \to ee\bar{e}$)	4.16×10^{-9}	2.7×10^{-8}
Br($\tau \to \mu\mu\bar{\mu}$)	4.24×10^{-9}	2.1×10^{-8}
LFV Type II		
Br($\tau \to e\mu\bar{\mu}$)	3.60×10^{-9}	2.7×10^{-8}
Br($\tau \to \mu e\bar{e}$)	2.48×10^{-9}	1.8×10^{-8}
$\mu - e$ conversion rate		
$\mathcal{R}$(Ti)	6.21×10^{-14}	4.3×10^{-13}
$\mathcal{R}$(Au)	7.82×10^{-14}	7.0×10^{-12}
Heavy neutrino masses		
M_1 (TeV)	17.186	
M_2 (TeV)	17.185	
M_3 (TeV)	17.187	

Table 15: Mean values for branching ratios, conversion rates and three heavy neutrino masses compared to current upper limits (at 95% confidence level for the Z decays and at 90% for all other processes). Statistical errors are at the 1% level and order permille for the heavy neutrino masses.

smaller than 7.5×10^{-10}, while for the other flavor combinations we get $|(\theta S\theta^\dagger)_{e\tau}| < 5.13 \times 10^{-7}$ and $|(\theta S\theta^\dagger)_{\mu\tau}| < 6.2 \times 10^{-7}$.

In order to find relations among the above processes we group them into 3 categories because of

their neutral couplings: $(\theta S\theta^\dagger)_{e\mu}$, $(\theta S\theta^\dagger)_{e\tau}$, and $(\theta S\theta^\dagger)_{\mu\tau}$.

- $(\theta S\theta^\dagger)_{e\mu}-$processes: $Z \to \bar{\mu}e$, $\mu \to ee\bar{e}$, and $\mu - e$ conversion in nuclei $^{48}_{22}$Ti and $^{197}_{79}$Au.
- $(\theta S\theta^\dagger)_{e\tau}-$processes: $Z \to \bar{\tau}e$, $\tau \to ee\bar{e}$, and $\tau \to e\mu\bar{\mu}$.
- $(\theta S\theta^\dagger)_{\mu\tau}-$processes: $Z \to \bar{\tau}\mu$, $\tau \to \mu\mu\bar{\mu}$, and $\tau \to \mu e\bar{e}$.

In next Figures 41, 42 and 43 we present the distribution of values for LFV Type I processes (similarly for all other processes analyzed in this thesis) in histograms where we can see their main values indicated.

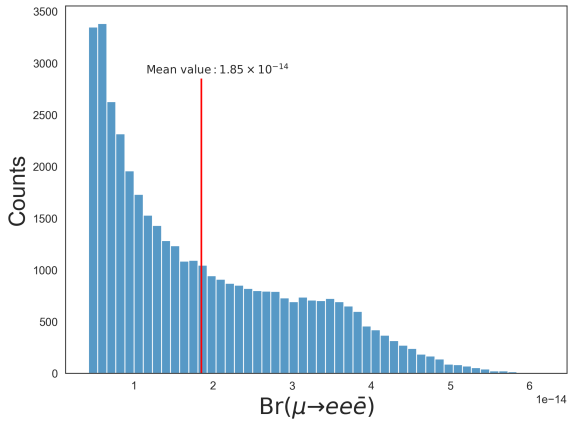

Figure 41: Histogram for Br($\mu \to ee\bar{e}$) where the main value is shown.

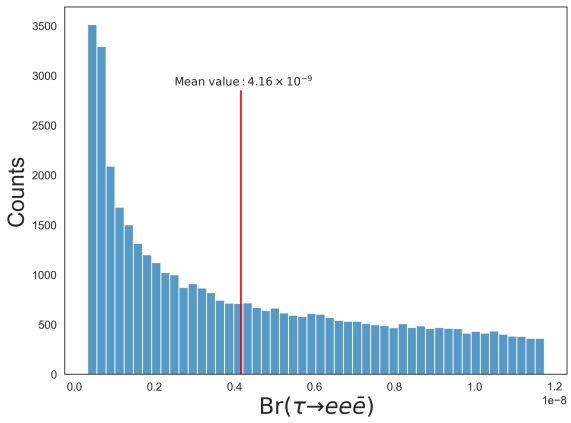

Figure 42: Histogram for Br($\tau \to ee\bar{e}$) where the main value is shown.

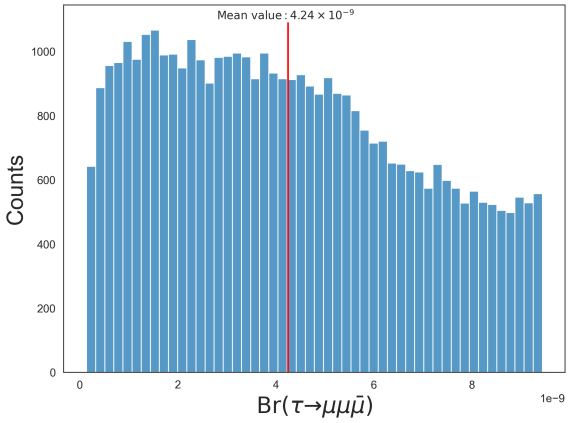

Figure 43: Histogram for Br($\tau \to \mu\mu\bar{\mu}$) where the main value is shown.

In Figure 44 a heat map is shown that stands for the correlation matrix among $(\theta S\theta^\dagger)_{e\mu}-$processes and their free parameters. First of all, we see that there is no sizeable correlation among any process with its free parameters. Second, the small correlation among every entry of $(\theta S\theta^\dagger)_{e\mu}$ matrix is negative, it indicates that while one of them increases the other decreases. Furthermore, $Z \to \bar{\mu}e$

decay is strongly correlated with $\mu \to ee\bar{e}$ as well as conversion rate in $^{48}_{22}$Ti with $^{197}_{79}$Au. In Figures 45 and 46 the behavior of their correlations are shown in scatter plots.

In Figure 47 we can see the correlations among $(\theta S\theta^\dagger)_{e\tau}-$processes and their free parameters. The interpretation of this plot is very similar to Figure 44. The branching ratios of these decays have a sizeable correlation to each other, but the predominant one is between $\mathrm{Br}(Z \to \bar{\tau}e)$ and $\mathrm{Br}(\tau \to ee\bar{e})$. We show all these behaviors in Figures 48, 49 and 50.

For $(\theta S\theta^\dagger)_{\mu\tau}-$processes their branching ratios are not correlated with any free parameter as we can observe in Figure 51. Nevertheless, we can see sizeable correlations among branching ratios, where the largest one is between $\mathrm{Br}(Z \to \bar{\tau}\mu)$ and $\mathrm{Br}(\tau \to \mu e\bar{e})$. The correlations of every decay to all others are displayed in Figures 52, 53 and 54.

If we observe the three heat maps for the processes whose behavior involves neutral couplings given by $(\theta S\theta^\dagger)_{\ell'\ell}$ matrix, we realize that the three heavy masses are strongly correlated with each other (recall that the values for heavy neutrinos are the same for all processes).

Finally, we add a heat map in Figure 55 where only branching ratios and conversion rates are involved. This heat map that stands for a correlation matrix seems a block matrix where each block represents a category of $(\theta S\theta^\dagger)_{\ell'\ell}-$processes, with aid of this plot we can conclude that processes with different neutral coupling have a very small correlation.

The scatter plots among two pairs of heavy neutrino masses in Figures 56 and 57 show neatly that solutions do not restrict to the nearly degenerate case.

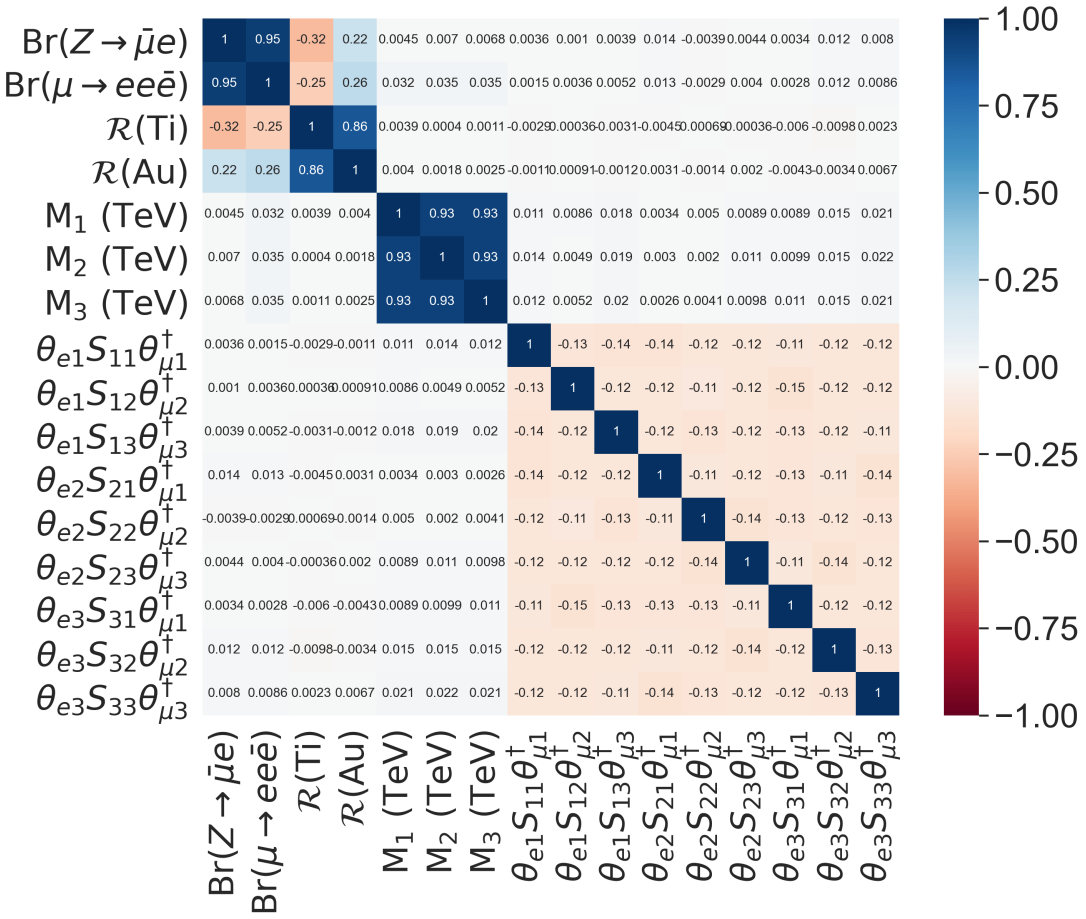

Figure 44: Heat map that stands for the correlation matrix among $(\theta S\theta^\dagger)_{e\mu}-$processes: $Z \to \bar{\mu}e$, $\mu \to ee\bar{e}$, $\mu - e$ conversion in nuclei $^{48}_{22}$Ti and $^{197}_{79}$Au, and their free parameters.

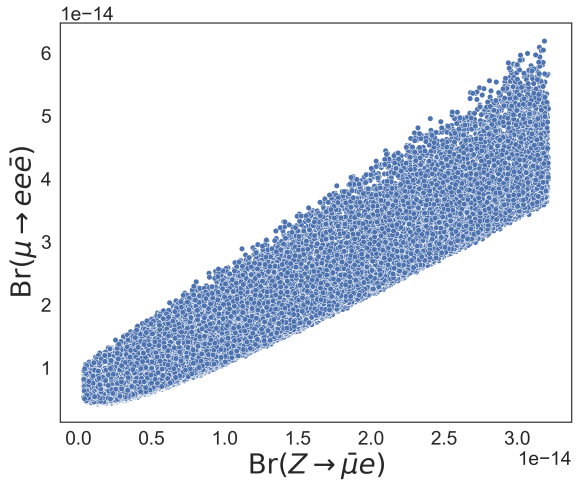

Figure 45: Scatter plot $\mathrm{Br}(Z \to \bar{\mu}e)$ vs. $\mathrm{Br}(\mu \to ee\bar{e})$.

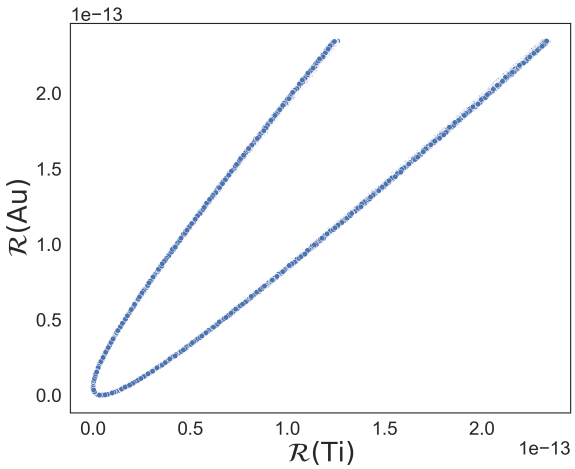

Figure 46: Scatter plot $\mathcal{R}(\mathrm{Ti})$ vs. $\mathcal{R}(\mathrm{Au})$.

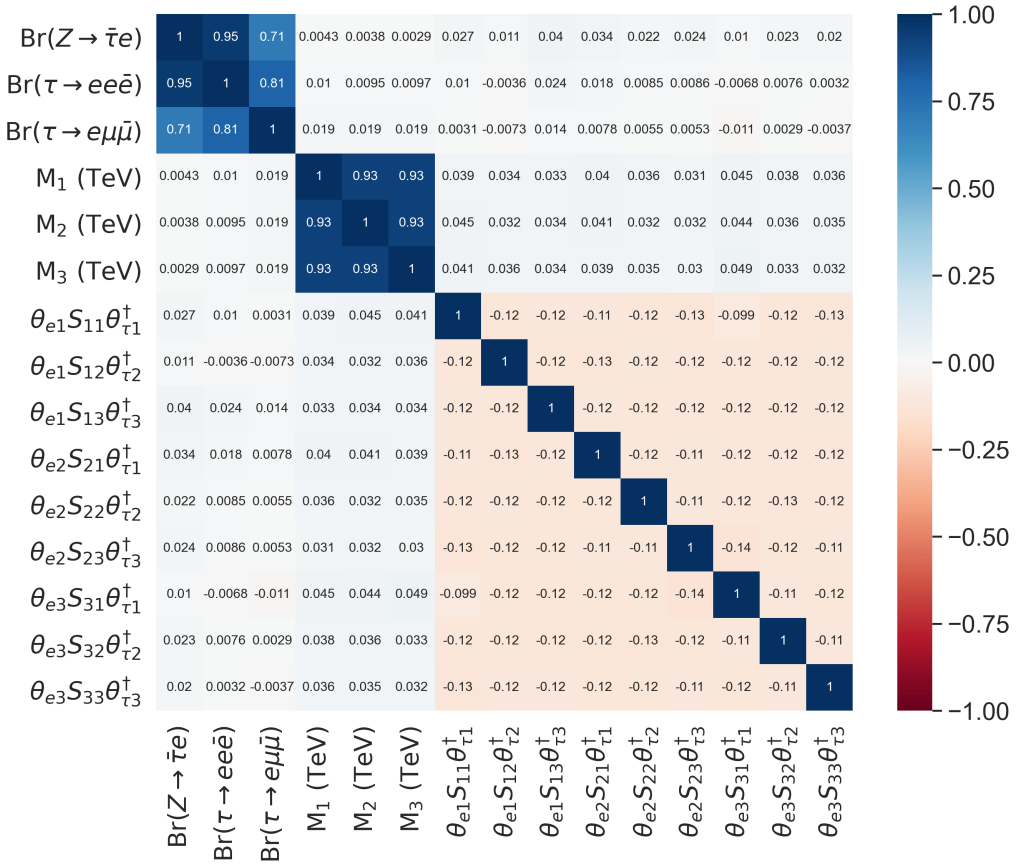

Figure 47: Heat map that stands for the correlation matrix among $(\theta S\theta^{\dagger})_{e\tau}-$processes: $Z \to \bar{\tau}e$, $\tau \to ee\bar{e}$, $\tau \to e\mu\bar{\mu}$, and their free parameters.

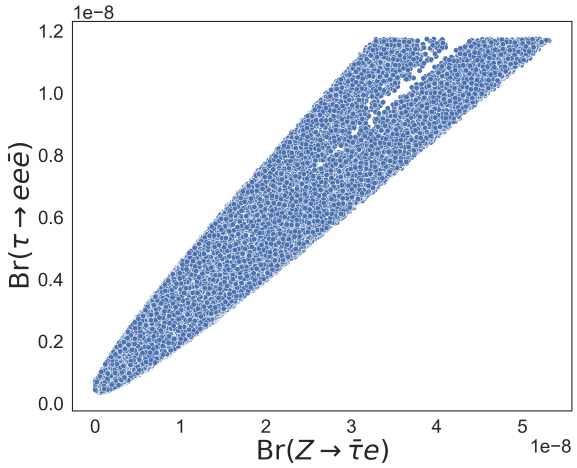

Figure 48: Scatter plot $\text{Br}(Z \to \bar{\tau}e)$ vs. $\text{Br}(\tau \to ee\bar{e})$.

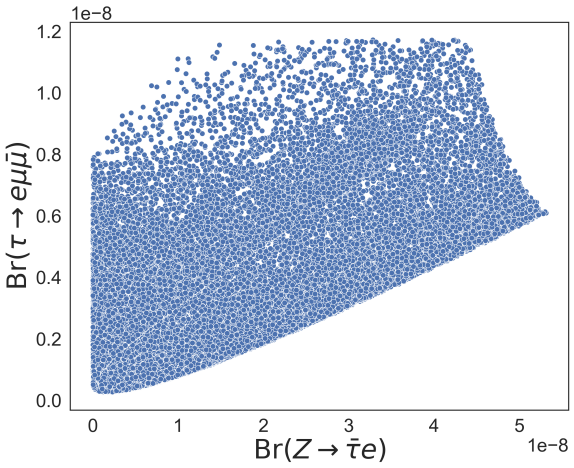

Figure 49: Scatter plot $\text{Br}(Z \to \bar{\tau}e)$ vs. $\text{Br}(\tau \to e\mu\bar{\mu})$.

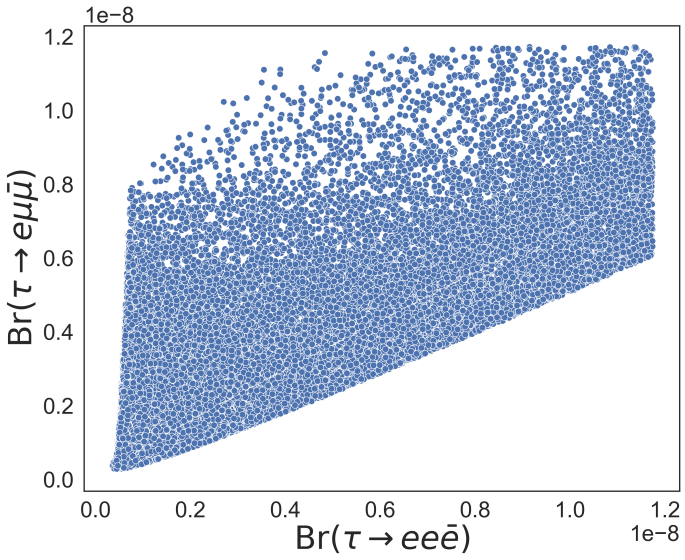

Figure 50: Scatter plot Br($Z \to ee\bar{e}$) vs. Br($\tau \to e\mu\bar{\mu}$).

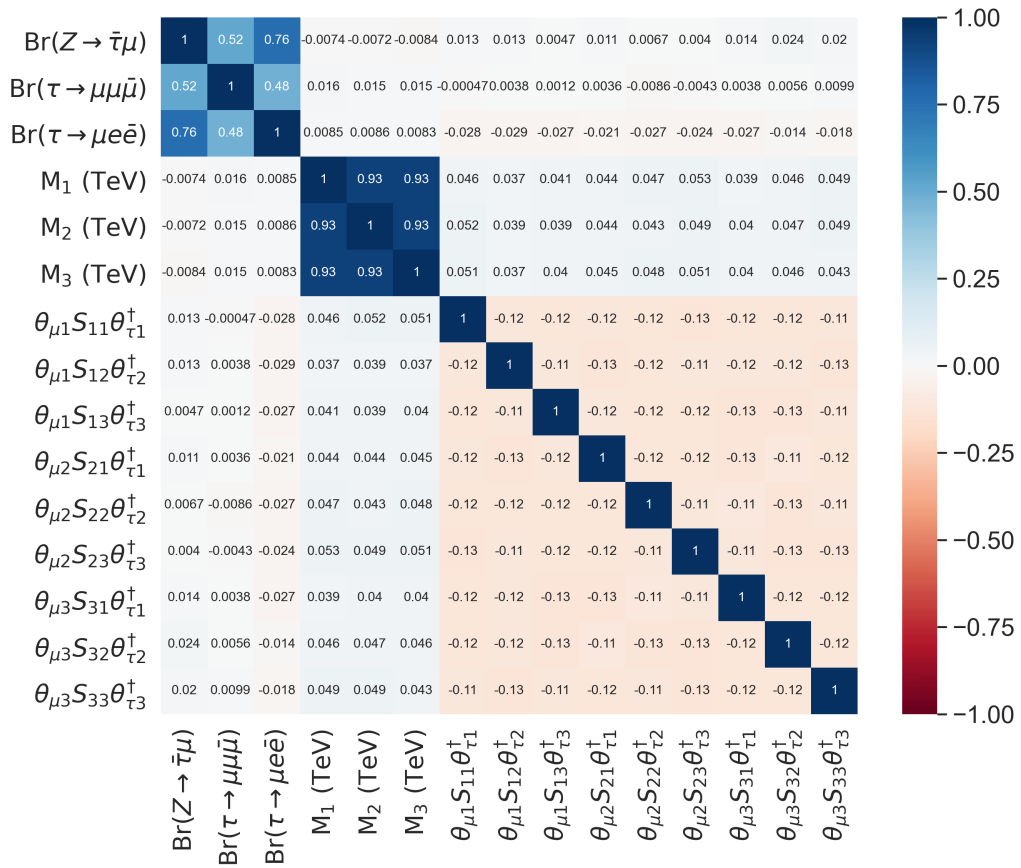

Figure 51: Heat map that stands for the correlation matrix among $(\theta S \theta^{\dagger})_{\mu\tau}-$processes: $Z \to \bar{\tau}\mu$, $\tau \to \mu\mu\bar{\mu}$, $\tau \to \mu e\bar{e}$, and their free parameters.

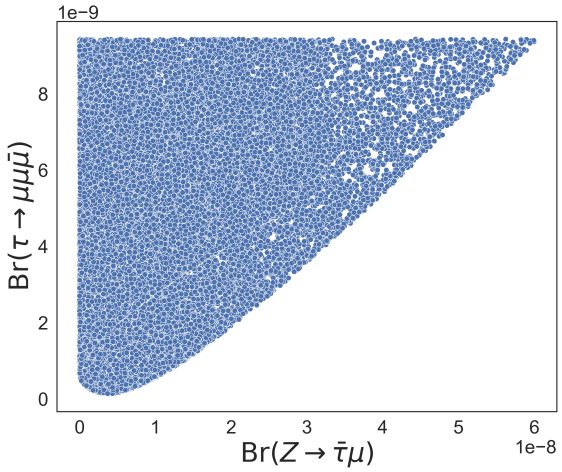

Figure 52: Scatter plot $\mathrm{Br}(Z \to \bar{\tau}\mu)$ vs. $\mathrm{Br}(\tau \to \mu\mu\bar{\mu})$.

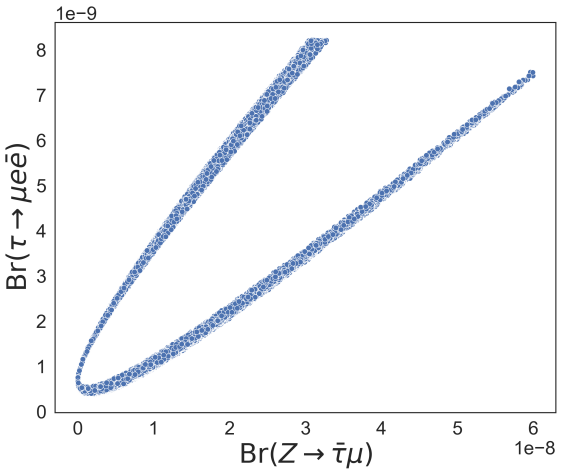

Figure 53: $\mathrm{Br}(Z \to \bar{\tau}\mu)$ vs. $\mathrm{Br}(\tau \to \mu e\bar{e})$.

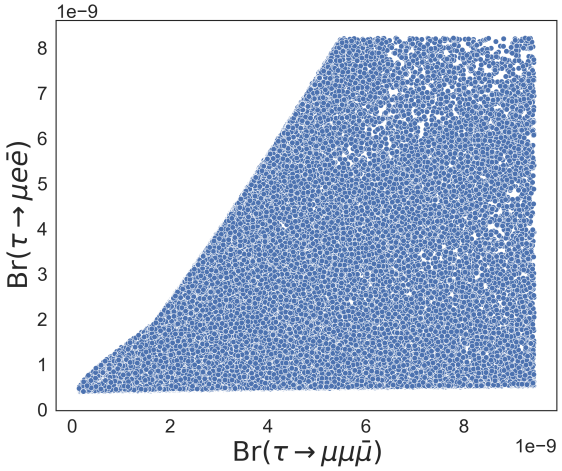

Figure 54: $\mathrm{Br}(\tau \to \mu\mu\bar{\mu})$ vs. $\mathrm{Br}(\tau \to \mu e\bar{e})$.

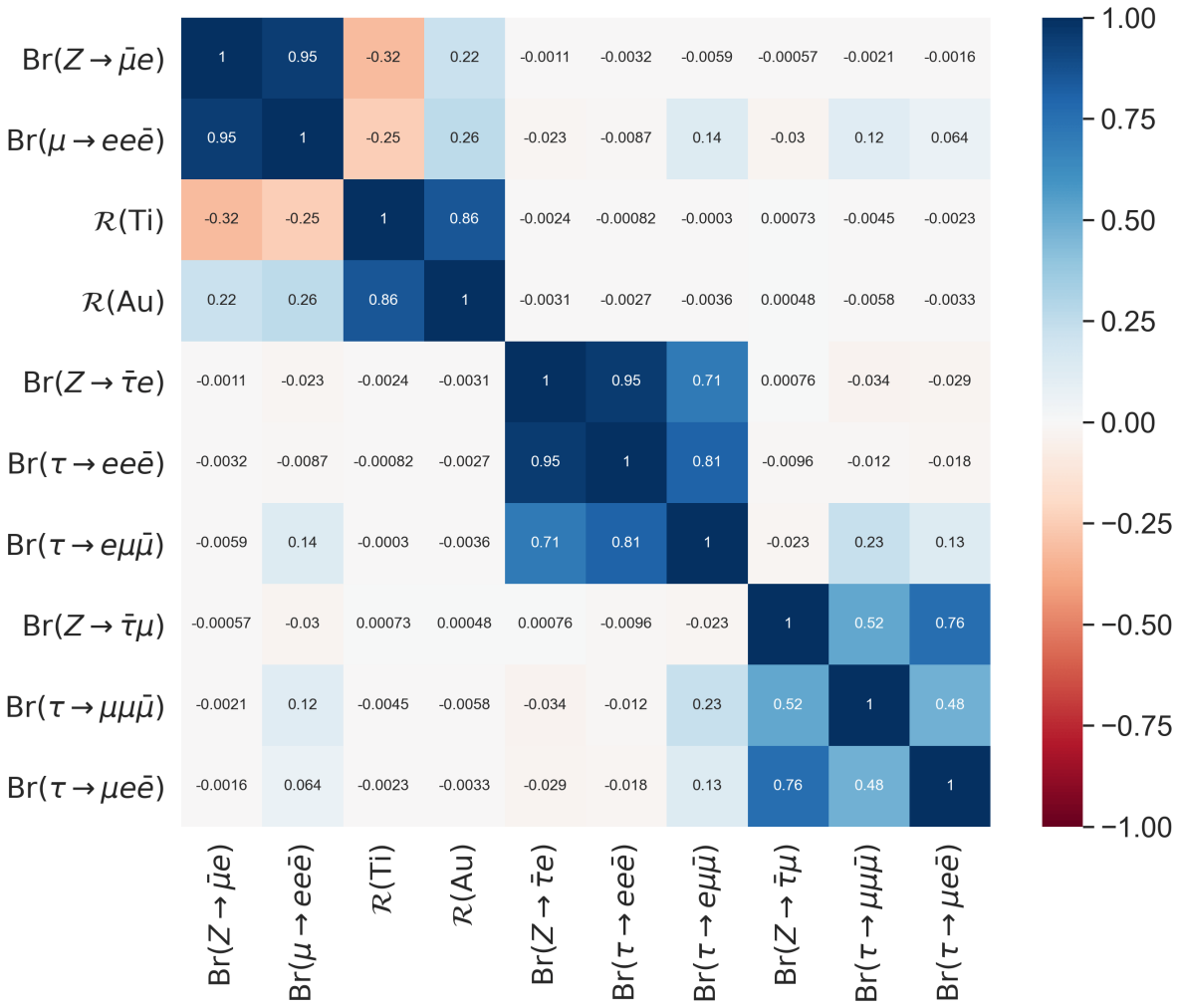

Figure 55: Heat map that stands for the correlation matrix exclusively among the 10 processes analysed in this section. We can distinguish that this matrix seems a block matrix representation where each block corresponds to each neutral coupling category.

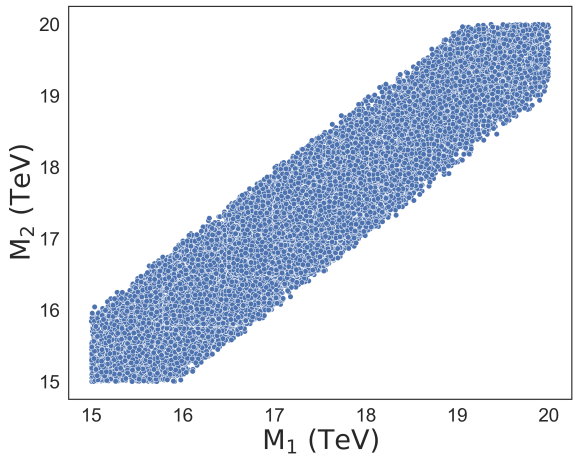

Figure 56: Scatter plot M_1 vs. M_2.

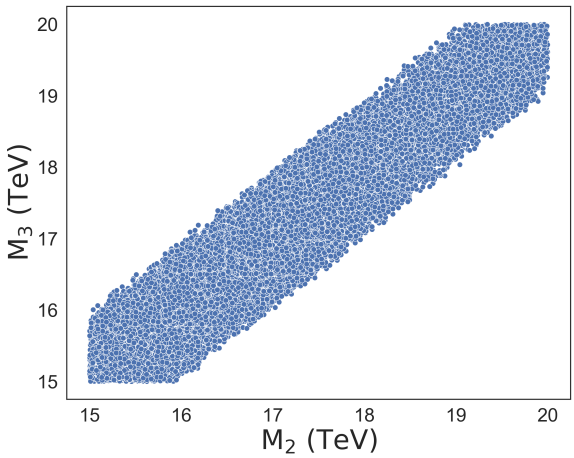

Figure 57: Scatter plot M_2 vs. M_3.

8.6 Bounds for wrong sign processes, Type III: $\ell \to \ell' \ell'' \bar{\ell}'''$ with $\ell \neq \ell' = \ell'' \neq \ell'''$

In this subsection we are going to study two tau decays which are known as wrong processes: $\tau \to ee\bar{\mu}$ and $\tau \to \mu\mu\bar{e}$. We analyze them assuming that the terms associated with LNV vertices are free parameters, thus we are able to bind these couplings.

8.6.1 $\tau \to ee\bar{\mu}$

This case is a realistic method to find a possible branching ratio limit as we do not assume the $(\theta_{\mu i}\theta_{\tau i})^\dagger(\theta_{ej}\theta_{ej})$ term as a global factor. We work in the light neutrinos massless approximation, therefore we get rid of the first term of in eq. (439)

$$\begin{aligned}\mathrm{Br}(\tau \to ee\bar{\mu}) = (0.17)\frac{\alpha_W^2}{128\pi^2}\Bigg| 2.66\times 10^{-7}\sum_{i,j=1}^{3}\Bigg[\left(\frac{1}{2y_j}-3\right)\frac{y_i}{2y_j}\,\ln\left(\frac{y_i}{y_j}\right)+\frac{1}{4y_j}\ln\left(\frac{y_i}{y_j}\right)\\ +\frac{1}{4}\left(6\,\ln y_j+7\right)\Bigg]+\sum_{i,j=1}^{3}(\theta_{\mu i}\theta_{\tau i})^\dagger(\theta_{ej}\theta_{ej})\Bigg[\sqrt{\frac{y_i}{y_j^3}}\ln\left(\frac{y_j}{y_i}\right)+\sqrt{\frac{y_i}{y_j}}(2\,\ln y_i+1)\\ +\frac{1}{\sqrt{y_i y_j}}(\ln y_j+1)+\sqrt{\frac{y_j}{y_i}}(2\,\ln y_j+1)\Bigg]\Bigg|^2 < 1.5\times 10^{-8}(\mathrm{C.L}=90\%),\end{aligned} \tag{489}$$

with $y_{i,j} = M_W^2/M_{i,j}^2$, being $M_{i,j}$ the masses of heavy neutrinos. We have 9 free parameters: M_i, $(\theta_{\mu i}\theta_{\tau i})^\dagger$, and $\theta_{ei}\theta_{ei}$ with $i = 1, 2, 3$.
We bind the coupling terms as follows [57]

$$\begin{aligned}&|\theta_{\mu 1}\theta_{\tau 1}| + |\theta_{\mu 2}\theta_{\tau 2}| + |\theta_{\mu 3}\theta_{\tau 3}| < 0.32\times 10^{-3},\\ &|\theta_{e1}\theta_{e1}| + |\theta_{e2}\theta_{e2}| + |\theta_{e3}\theta_{e3}| < 0.01,\end{aligned} \tag{490}$$

from the equations above we limit each term

$$\begin{aligned}&-0.32\times 10^{-3} \leq (\theta_{\mu 1}\theta_{\tau 1})^\dagger, (\theta_{\mu 2}\theta_{\tau 2})^\dagger, (\theta_{\mu 3}\theta_{\tau 3})^\dagger \leq 0.32\times 10^{-3},\\ &-0.01 \leq (\theta_{e1}\theta_{e1}), (\theta_{e2}\theta_{e2}), (\theta_{e3}\theta_{e3}) \leq 0.01,\end{aligned} \tag{491}$$

and the product of them must satisfy that

$$|\theta_{\mu i}\theta_{\tau i}||\theta_{ej}\theta_{ej}| < 0.32\times 10^{-5}. \tag{492}$$

8.6.2 $\tau \to \mu\mu\bar{e}$

We will work with the branching ratio for $\tau \to \mu\mu\bar{e}$ decay assuming that the $(\theta_{ei}\theta_{\tau i})^{\dagger}(\theta_{\mu j}\theta_{\mu j})$ term is not a global factor, it is written as follows

$$\begin{aligned}\mathrm{Br}(\tau \to \mu\mu\bar{e}) < (0.17)\frac{\alpha_W^2}{128\pi^2}\Bigg|3.08\times10^{-7}\sum_{i,j=1}^{3}\Bigg[\left(\frac{1}{2y_j}-3\right)\frac{y_i}{2y_j}\,\ln\left(\frac{y_i}{y_j}\right)+\frac{1}{4y_j}\ln\left(\frac{y_i}{y_j}\right)\\ +\frac{1}{4}\left(6\,\ln y_j+7\right)\Bigg]+\sum_{i,j=1}^{3}(\theta_{ei}\theta_{\tau i})^{\dagger}(\theta_{\mu j}\theta_{\mu j})\Bigg[\sqrt{\frac{y_i}{y_j^3}}\ln\left(\frac{y_j}{y_i}\right)+\sqrt{\frac{y_i}{y_j}}(2\,\ln y_i+1)\\ +\frac{1}{\sqrt{y_i y_j}}(\ln y_j+1)+\sqrt{\frac{y_j}{y_i}}(2\,\ln y_j+1)\Bigg]\Bigg|^2<1.7\times10^{-8}(\mathrm{C.L}=90\%),\end{aligned} \tag{493}$$

with $y_{i,j} = M_W^2/M_{i,j}^2$, being $M_{i,j}$ the masses of heavy neutrinos. Therefore, now we have 9 free parameters: M_i, $(\theta_{ei}\theta_{\tau i})^{\dagger}$, and $(\theta_{\mu i}\theta_{\mu i})$ with $i = 1, 2, 3$.
We bind the coupling terms as follows

$$\begin{aligned}&|\theta_{e1}\theta_{\tau 1}|+|\theta_{e2}\theta_{\tau 2}|+|\theta_{e3}\theta_{\tau 3}|<0.9\times10^{-3},\\ &|\theta_{\mu 1}\theta_{\mu 1}|+|\theta_{\mu 2}\theta_{\mu 2}|+|\theta_{\mu 3}\theta_{\mu 3}|<0.0075,\end{aligned} \tag{494}$$

from the equations above we limit each term

$$\begin{aligned}&-0.9\times10^{-3}\times10^{-3}\leq(\theta_{\mu 1}\theta_{\tau 1})^{\dagger},(\theta_{\mu 2}\theta_{\tau 2})^{\dagger},(\theta_{\mu 3}\theta_{\tau 3})^{\dagger}\leq0.9\times10^{-3},\\ &-0.0075\leq(\theta_{e1}\theta_{e1}),(\theta_{e2}\theta_{e2}),(\theta_{e3}\theta_{e3})\leq0.0075,\end{aligned} \tag{495}$$

and the product of them must satisfy that

$$|\theta_{ei}\theta_{\tau i}||\theta_{\mu j}\theta_{\mu j}|<0.68\times10^{-5}. \tag{496}$$

8.7 Joint Analysis

We are analysing the wrong sign processes which were computed simultaneously through a single Monte Carlo simulation[5]. As we have seen from eqs. (489) and (493) the free parameters are the heavy neutrino masses ($M_{i=1,2,3}$) and the LNV couplings. The heavy neutrino masses $\mathrm{M_i}$ ($i = 1, 2, 3$) run from 15 to 20 TeV, we decided to take this interval based on the experience gained in the previous processes as in this one data are more concentrated. The conditions on LNV couplings are given by (491) and (495).
In the following Table 16 we show the final results for branching ratios of wrong sign processes, heavy

[5]Before doing the simultaneous Monte Carlo simulation we did a simplified analysis for each process aiming to examine the results for quasi-degenerated cases.

neutrino masses and LNV couplings.

Branching Ratios	Our mean values
$\mathrm{Br}(\tau \to ee\bar{\mu})$	1.8×10^{-9}
$\mathrm{Br}(\tau \to \mu\mu\bar{e})$	1.9×10^{-9}
Heavy neutrino masses	
M_1 (TeV)	17.170
M_2 (TeV)	17.166
M_3 (TeV)	17.166
LNV couplings	
$(\theta_{e1}\theta_{\tau 1})^\dagger$	$(2.24 \pm 9.59) \times 10^{-7}$
$(\theta_{e2}\theta_{\tau 2})^\dagger$	$(14.82 \pm 9.69) \times 10^{-7}$
$(\theta_{e3}\theta_{\tau 3})^\dagger$	$(1.84 \pm 9.79) \times 10^{-7}$
$\lvert\theta_{ei}\theta_{\tau i}\rvert$	2.76×10^{-4}
$(\theta_{\mu 1}\theta_{\mu 1})$	$(0.75 \pm 2.98) \times 10^{-5}$
$(\theta_{\mu 2}\theta_{\mu 2})$	$-(8.78 \pm 2.99) \times 10^{-5}$
$(\theta_{\mu 3}\theta_{\mu 3})$	$(1.02 \pm 2.98) \times 10^{-5}$
$\lvert\theta_{\mu i}\theta_{\mu i}\rvert$	8.5×10^{-3}
$(\theta_{\mu 1}\theta_{\tau 1})^\dagger$	$(2.08 \pm 2.26) \times 10^{-6}$
$(\theta_{\mu 2}\theta_{\tau 2})^\dagger$	$-(0.39 \pm 2.27) \times 10^{-6}$
$(\theta_{\mu 3}\theta_{\tau 3})^\dagger$	$(0.55 \pm 2.25) \times 10^{-6}$
$\lvert\theta_{\mu i}\theta_{\tau i}\rvert$	6.52×10^{-4}
$(\theta_{e1}\theta_{e1})$	$(3.88 \pm 1.95) \times 10^{-5}$
$(\theta_{e2}\theta_{e2})$	$(4.59 \pm 1.96) \times 10^{-5}$
$(\theta_{e3}\theta_{e3})$	$-(5.04 \pm 1.95) \times 10^{-5}$
$\lvert\theta_{ei}\theta_{ei}\rvert$	5.65×10^{-3}

Table 16: Mean values for the free parameters and branching ratios in the wrong sign processes considering Majorana neutrinos in the LHT. Statistical errors which are not shown are smaller than the last significant figure. We recall the 90% C.L. limits [6]: 1.5×10^{-8} (on $\mathrm{Br}(\tau \to ee\bar{\mu})$) and 1.7×10^{-8} (on $\mathrm{Br}(\tau \to \mu\mu\bar{e})$).

The heavy neutrino masses (M_i) present a sizeable correlation among them as in the previous analysis. Also, LNV couplings: $|\theta_{ei}\theta_{\tau i}|$ and $|\theta_{\mu i}\theta_{\mu i}|$ are moderately correlated with the heavy neutrino masses, while $|\theta_{\mu i}\theta_{\tau i}|$ and $|\theta_{ei}\theta_{ei}|$ have a minimum correlation with them.
LHT is not to able to bind LFV processes known as "wrong sign" throught T-odd leptons [37]. However, when we extend the LHT model involving Majorana neutrinos with aid of ISS, the branching ratios get a finite value of order $\sim 10^{-9}$. LHT extended with Majorana neutrinos also allows us to

propose values for LNV couplings shown in Table 16, which have not reported before in papers as [57]. The mean values for the heavy neutrino masses from the studies in the previous section differ only slightly from the 'Wrong Sign' analysis, $\sim 0.12\%$ in all cases.

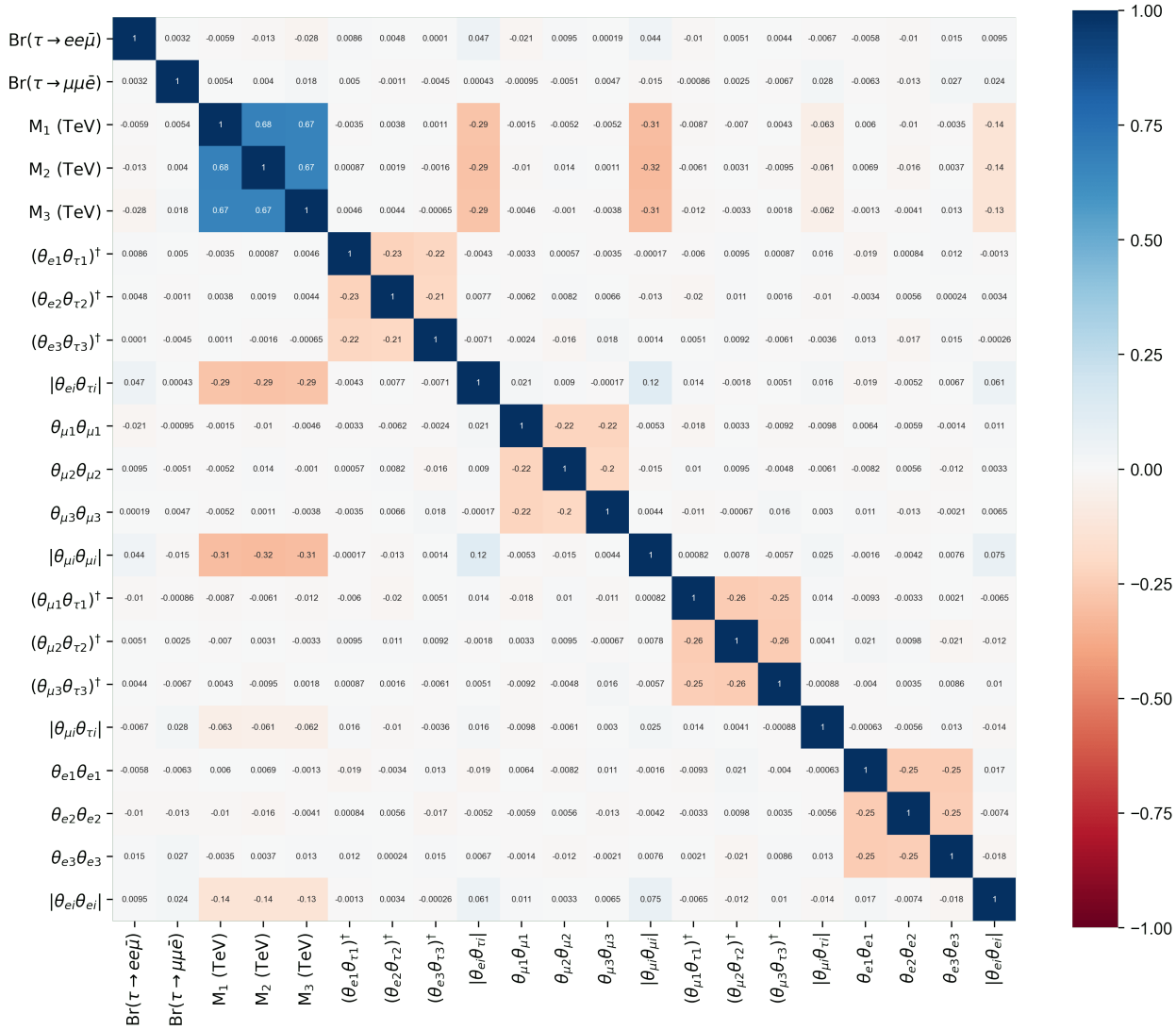

Figure 58: Heat map that stands for a correlation matrix among wrong sign branching ratios and free parameters.

9 Neutrinoless Double Beta Decay $0\nu\beta\beta$ and its analogous tau decay

Total lepton number $L = L_e + L_\mu + L_\tau$ is an absolutely conserved quantum number in the Standard Model (SM). Some extensions of the SM include interactions that can induce L non-conservation [58]. The hypothesis of the neutrino mixing was confirmed by the observation of the neutrino oscillations in experiments with the atmospheric, solar, reactor and accelerator neutrinos.
The electric charges of neutrinos are equal to zero. For neutrinos there are two fundamentally different possibilities:

- if the total lepton number $L = L_e + L_\mu + L_\tau$ is conserved, neutrino fields $\nu_i(x)$ are complex four component Dirac fields. In this case neutrinos ν_i and antineutrinos $\bar{\nu}_i$ have the same mass and different lepton numbers ($L(\nu_i) = -L(\bar{\nu}_i) = 1$).

- If there are no conserved lepton numbers, neutrino fields $\nu_i(x)$ are two component Majorana fields. In this case $\nu_i \equiv \bar{\nu}_i$.

Investigation of the neutrino oscillations does not allow to distinguish these two possibilities. In order to reveal the Majorana nature of ν_i it seems necessary to observe processes in which the total lepton number is violated. Neutrinoless double β-decay of some nuclei is the only such process whose study allows to reach the necessary sensitivity [59].
The usual double beta decay is the process in which a nucleus A(Z, N) decays into an isobar with the electric charge differing by two units

$$A(Z, N) \to A(Z \pm 2, N \mp 2) + 2e^{\mp} + 2\bar{\nu}_e(2\nu_e),$$

double beta decay is the process of the second order in weak interaction (G_F), and the corresponding decay rates are very low: typical lifetimes of the nuclei with respect to the 2β decay are $T \gtrsim 10^{19}$ years.
If neutrinos are Majorana particles, the lepton number is not conserved, and the neutrino emitted in one of the elementary beta decay processes forming the 2β decay can be absorbed in another, leading to the neutrinoless double beta ($0\nu\beta\beta$) decay

$$A(Z, N) \to A(Z \pm 2, N \mp 2) + 2e^{\mp}.$$

Such processes would have a very clear experimental signature: since the recoil energy of a daughter nucleus is negligibly small, the sum of the energies of the two electrons or positrons in the final state should be equal to the total energy release, i.e. should be represented by a discrete energy line [60]. There are many experiments whose aim is searching for new limits of neutrinoless double beta decays [61].

9.1 Limits from Neutrinoless Double Beta Decay $0\nu\beta\beta$

In the neutrino sector, lepton number violation by two units (ΔL = 2), as implied by a Majorana mass term, plays a crucial role. If the neutrino has a Majorana mass, then it will contribute to (ΔL = 2) LNV processes. The basic process with (ΔL = 2) can be generically expressed by [62]

$$W^-W^- \to \ell_1^-\ell_2^-, \tag{497}$$

where W^- is a virtual SM weak boson and $\ell_{1,2} = e, \mu, \tau$. The best known example is neutrinoless double-beta decay ($0\nu\beta\beta$), which proceeds via the parton-level subprocess $dd \to uu\, W^*W \to uu\, e^-e^-$. The key subprocess in ($0\nu\beta\beta$) is $W^-W^- \to e^-e^-$, mediated by a Majorana ν_e.
One possible future collider which is being vigorously investigated at the moment is a high-energy linear e^+e^- collider, known generically as the Next Linear Collider (NLC). With such a collider, it is possible to replace the positron by another electron and look at e^-e^- collisions. If the electron neutrino has a Majorana mass, it may be possible to observe the process $e^-e^- \to W^-W^-$. This is essentially the inverse of neutrinoless double beta decay [63].
Suppose that the ν_e mixes with other neutrinos. So, once the mass matrix is diagonalized, ν_e can be expressed in terms of the mass eigenstates N_i

$$\nu_e = \sum_i U_{ei} N_i, \tag{498}$$

where we have left the number of new neutrinos unspecified and the mixing matrix U is unitary [63]. Assuming that the N_i are Majorana neutrinos, they will contribute to the process $e^-e^- \to W^-W^-$ through the diagrams of Figure 59.

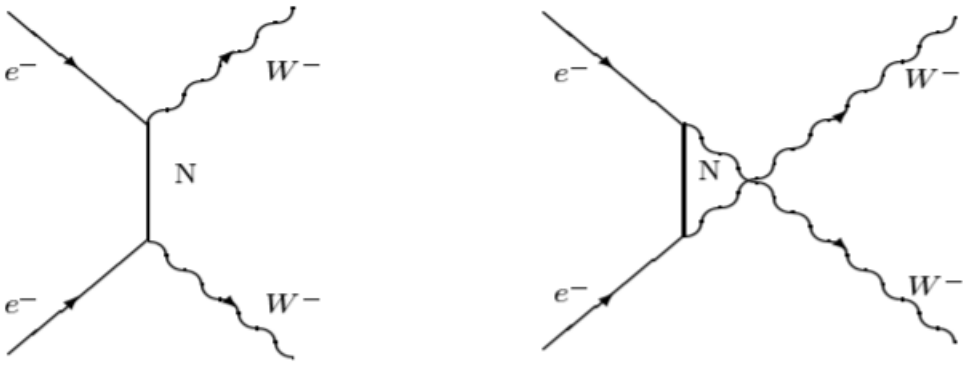

Figure 59: Diagrams contributing to $e^-e^- \to W^-W^-$.

We begin by studying constraints on light and heavy neutrino. The most commonly assumed mechanism of $0\nu\beta\beta$ is light neutrino exchange, for which the “effective mass” or "Majorana mass"

$|m_{ee}|$ is constrained as follows [63, 64], with the most recent one [65]

$$|m_{ee}| \equiv \sum_i (U_{ei})^2 (m_\nu)_i \leq (36 - 156) \text{ meV}, \tag{499}$$

where the sum is over the light neutrinos and their masses are called $(m_\nu)_i$. In this case we are considering that $(m_\nu)_i \ll 1$ GeV.
In case heavy neutrinos ($M_i \gg 1$ GeV) are exchanged in neutrinoless double beta decay, the following quantity is constrained in [62–64], with an updated limit in [66]

$$\frac{1}{|M_{ee}|} \equiv \sum_{m'} \frac{|V_{em'}|^2}{m_{N_{m'}}} \leq (2.33 \ - \ 4.12) \times 10^{-6} \text{ TeV}^{-1}, \tag{500}$$

where the sum is over the heavy neutrinos and the matrix describing their mixing with leptons is called V.
Now, focusing in our model, we have three heavy neutrinos and the mixing matrix is called θ. From Tables 15 and 16 we approximate the values for each heavy neutrino mass ~ 17.2 TeV (assuming a degenerate case), then we may bind the eq. (500)

$$\begin{aligned} &\left(\frac{1}{17.2 \text{ TeV}}\right) \left(|\theta_{e1}|^2 + |\theta_{e2}|^2 + |\theta_{e3}|^2\right) < \sum_{i=1}^{3} \frac{|\theta_{ei}|^2}{m_i} \\ &\left(\frac{1}{17.2 \text{ TeV}}\right) \left(|\theta_{e1}|^2 + |\theta_{e2}|^2 + |\theta_{e3}|^2\right) < (2.33 \ - \ 4.12) \times 10^{-6} \text{ TeV}^{-1}. \end{aligned} \tag{501}$$

So, we can limit the mixing of ν_e with the three heavy neutrinos as follows

$$\sum_{i=1}^{3} |\theta_{ei}|^2 < (4.0 \ - 7.1) \times 10^{-5}. \tag{502}$$

It is important to recall that we have approached this value by assuming degenerate heavy neutrino masses $M \approx 17.2$ TeV. Tau decays that we study in the next section and neutrinoless double beta decay ($0\nu\beta\beta$) are examples of LNV processes. The result from the eq. (502) agrees with the value of $|\theta_{ei}\theta_{ei}|$ from Table 16 due to it being one order of magnitude smaller than the limit of LNV coupling predicted for the model. One possibility to find LNV processes is the Majorana neutrinos existence. It is shown to be observable for masses up to 10^6 GeV, which has to be compared with an LHC reach not exceeding 400 GeV [64].

9.2 Lepton Number Violating Tau Decays

In this section we are studying tau decays into an anti-lepton and two mesons

$$\tau^-(p_\tau) \to \ell^+(p_{\ell^+}) M_1^-(q_1) M_2^-(q_2), \tag{503}$$

where $M_1^-, M_2^- = \pi, K$. Lepton number violation in three-body decays of τ leptons has been widely investigated previously [62, 67–71]. Typical neutrino-exchange diagrams contributing in this type of τ decay are shown in Figure 60.

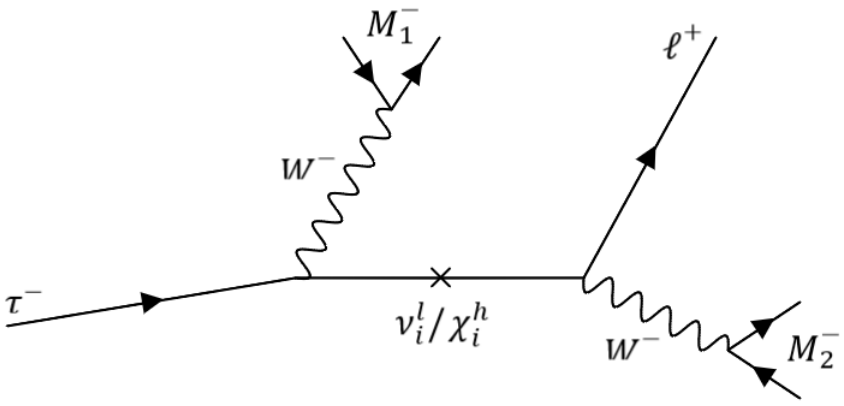

Figure 60: Neutrino-exchange tree level diagram induced by crossing of the $W^-W^- \to \ell^-\ell^-$ to LNV in $\tau \to \ell^+ M_1^- M_2^-$.

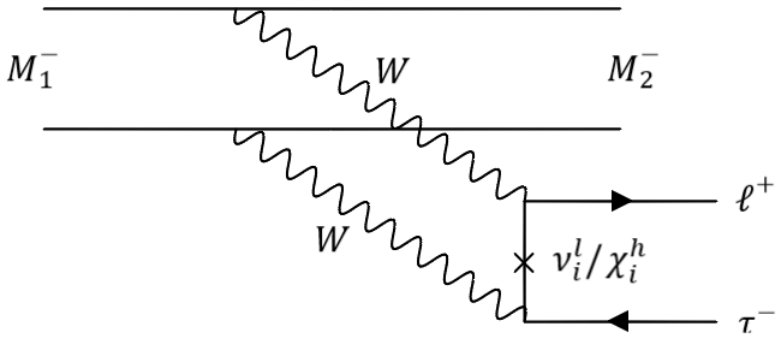

Figure 61: Box level diagram to LNV in $\tau \to \ell^+ M_1^- M_2^-$.

This mode is cleaner in principle than $0\nu\beta\beta$ since the hadronic part does not involve complicated nuclear structure. For the tree level amplitude, the hadronic part can be expressed in terms of the decay constants of the mesons in a model independent way. The box diagram includes hadronic matrix elements which cannot be simplified in terms of decay constants and needs to be evaluated in a model dependent way. We expect the tree level amplitude to dominate and do not include the box diagram. The decay amplitude for lepton number violating tau decays can be separated into leptonic and hadronic parts [62, 71]

$$i\mathcal{M} = (\mathcal{M}_{lep})_{\mu\nu}(\mathcal{M}^{had})^{\mu\nu}. \tag{504}$$

The leptonic part of the subprocess $\tau^- \to \ell^+ W^{-*} W^{-*}$ is obtained by crossing the $W^-W^- \to \ell^-\ell^-$

amplitude, therefore, we will develop that amplitude first.
As the decay is mediated solely by the exchange of Majorana neutrinos, we recall how these ones interact with W bosons and leptons from the eq. (350)

$$\mathcal{L}_W^l = \frac{g}{\sqrt{2}} W_\mu^+ \sum_{j=1}^{3}\sum_{i=1}^{3} \overline{\nu_i^l} W_{ij} \gamma^\mu P_L \ell_j + h.c., \quad \text{with} \quad W_{ij} = \sum_{k=1}^{3} (U_{PMNS}^\dagger)_{ik} [\mathbf{1}_{3\times 3} - \frac{1}{2}(\theta\theta^\dagger)]_{kj},$$
$$\mathcal{L}_W^{lh} = \frac{g}{\sqrt{2}} W_\mu^+ \sum_{j=1}^{3}\sum_{i=7}^{9} \overline{\chi_i^h} \theta_{ij}^\dagger \gamma^\mu P_L \ell_j + h.c..$$

where $W_{ij}(\theta_{ij})$ is the light(heavy) neutrino mixing matrix. We see in Figure 60 that both light and heavy neutrinos contribute to the process, so the amplitude contains a lepton part of the form [72]

$$(\mathcal{M}_{lep})_{\mu\nu} = \frac{g^2}{2}\sum_{i=1}^{3} (\bar{\ell}_1 \gamma_\mu P_L W_{\ell_1 i}^\dagger \underbrace{\nu_i^l)(\bar{\ell}_2 \gamma_\nu P_L W_{\ell_2 i}^\dagger \nu_i^l)}_{} + \frac{g^2}{2}\sum_{i=1}^{3} (\bar{\ell}_1 \gamma_\mu P_L \theta_{\ell_1 i} \chi_i^h)\underbrace{(\bar{\ell}_2 \gamma_\nu P_L \theta_{\ell_2 i} \chi_i^h)}_{}, \quad (505)$$

where the underbrackets indicate contraction. Following the useful relations from eqs. (361)-(364), it is straightforward to see that the second fermion chain in the above equation transforms as follows

$$\begin{aligned} \bar{\ell}_2 \gamma_\nu P_L \nu_i^l + \bar{\ell}_2 \gamma_\nu P_L \chi_i^h &= \overline{\nu_i^l}(\gamma_\nu P_L)^c \ell_2^c + \overline{\chi_i^h}(\gamma_\nu P_L)^c \ell_2^c \\ &= -(\overline{\nu_i^l}\gamma_\nu P_R \ell_2^c + \overline{\chi_i^h}\gamma_\nu P_R \ell_2^c), \end{aligned} \quad (506)$$

since ν_i^l and χ_i^h are Majorana neutrinos $(\nu_i^l)^c = \nu_i^l$, $(\chi_i^h)^c = \chi_i^h$ and $(\gamma_\nu P_L)^c = -\gamma_\nu P_R$, therefore,

$$(\mathcal{M}_{lep})_{\mu\nu} = -\frac{g^2}{2}\sum_{i=1}^{3} W_{\ell_1 i}^\dagger W_{\ell_2 i}^\dagger (\bar{\ell}_1 \gamma_\mu P_L \nu \underbrace{\nu_i^l}\gamma_\nu P_R \ell_2^c) - \frac{g^2}{2}\sum_{i=1}^{3} \theta_{\ell_1 i}\theta_{\ell_2 i} (\bar{\ell}_1 \gamma_\mu P_L \chi \underbrace{\chi_i^h}\gamma_\nu P_R \ell_2^c), \quad (507)$$

the contraction of Majorana neutrino fields turns out to be the usual fermion propagator. Then, $\bar{\ell}_1 = \overline{u}(p_{\ell_1})$ and $\ell_2^c = v(p_{\ell_2})$ the $(\mathcal{M}_{lep})_{\mu\nu}$ takes the form

$$(\mathcal{M}_{lep})_{\mu\nu} = -\frac{g^2}{2}\sum_{i=1}^{3} \overline{u}(p_{\ell_1})\gamma_\mu P_L \left(W_{\ell_1 i}^\dagger W_{\ell_2 i}^\dagger \frac{\not{k} + m_i}{k^2 - m_i^2} + \theta_{\ell_1 i}\theta_{\ell_2 i} \frac{\not{q} + M_i}{q^2 - M_i^2} \right) \gamma_\nu P_R v(p_{\ell_2}), \quad (508)$$

where $k(q)$ and $m_i(M_i)$ are the momentum exchanged and mass by the light(heavy) neutrinos of Majorana, respectively. The $\not{k}$ and $\not{q}$ terms vanish

$$\begin{aligned} \overline{u}(p_{\ell_1})\gamma_\mu P_L \not{k} \gamma_\nu P_R v(p_{\ell_2}) &= k^\alpha \overline{u}(p_{\ell_1})\gamma_\mu P_L \gamma_\alpha \gamma_\nu P_R v(p_{\ell_2}) \\ &= k^\alpha \overline{u}(p_{\ell_1})\gamma_\mu \gamma_\alpha \gamma_\nu P_L P_R v(p_{\ell_2}) \\ &= 0, \end{aligned} \quad (509)$$

hence,

$$(\mathcal{M}_{lep})_{\mu\nu} = -\frac{g^2}{2}\sum_{i=1}^{3}\overline{u}(p_{\ell_1})\left(\frac{W^{\dagger}_{\ell_1 i}W^{\dagger}_{\ell_2 i}m_i}{k^2-m_i^2}+\frac{\theta_{\ell_1 i}\theta_{\ell_2 i}M_i}{q^2-M_i^2}\right)\gamma_\mu\gamma_\nu P_R v(p_{\ell_2}). \tag{510}$$

Finally, we obtain the leptonic amplitude for $\tau^- \to \ell^+W^-W^-$ by crossing the above expression ($\overline{u}(p_{\ell_1}) \to \overline{v}(p_\tau)$ and $v(p_{\ell_2}) = v(p_{\ell^+})$)

$$(\mathcal{M}_{lep})_{\mu\nu} = -\frac{g^2}{2}\sum_{i=1}^{3}\overline{v}(p_{\tau})\left(\frac{W^{\dagger}_{\tau i}W^{\dagger}_{\ell^+ i}m_i}{k^2-m_i^2}+\frac{\theta_{\tau i}\theta_{\ell^+ i}M_i}{q^2-M_i^2}\right)\gamma_\mu\gamma_\nu P_R v(p_{\ell^+}). \tag{511}$$

Now, we analyze the hadronic part

$$(\mathcal{M}^{had})^{\mu\nu} = \mathcal{M}^{\mu}_{M_1}\mathcal{M}^{\nu}_{M_2} + (M_1 \leftrightarrow M_2), \tag{512}$$

where $\mathcal{M}^{\mu}_{M_1}$ and $\mathcal{M}^{\nu}_{M_2}$ are the amplitudes for the M_1 and M_2 meson, respectively.

$$\begin{aligned}\mathcal{M}^{\mu}_{M_1} &= \frac{g}{\sqrt{2}}V^{CKM}_{M_1}\left[\overline{q}\gamma^\mu P_L q\right],\\ \mathcal{M}^{\nu}_{M_2} &= \frac{g}{\sqrt{2}}V^{CKM}_{M_2}\left[\overline{q}\gamma^\nu P_L q\right],\end{aligned} \tag{513}$$

where $V^{CKM}_{M_i}$ are the quark flavor-mixing matrix elements for the mesons. In the hadronic case we consider the initial state to be the vacuum state. This is because the initial state contains no quarks. Let us denote the hadronic current appearing in the square bracket $j^{\mu,\nu}(x)$, where the co-ordinate dependence comes from the field operators. This dependence can be factored out in the form of an exponential. This exponential does not enter the Feynman amplitude, but rather contributes to an energy-momentum conserving delta function. Once this factor is taken out, we are left with the matrix element of $j^{\mu,\nu}(0)$. Thus we can write [2]

$$\begin{aligned}\langle M_1^-(q_1)|j^\mu(0)|0\rangle &= \sqrt{2}if_{M_1}q_1^\mu,\\ \langle M_2^-(q_2)|j^\nu(0)|0\rangle &= \sqrt{2}if_{M_2}q_2^\nu,\end{aligned} \tag{514}$$

where f_{M_i} are constants. They are called meson decay constants. Therefore, the eq. (512) is written as

$$(\mathcal{M}^{had})^{\mu\nu} = -g^2V^{CKM}_{M_1}V^{CKM}_{M_2}f_{M_1}f_{M_2}q_1^\mu q_2^\nu + (M_1 \leftrightarrow M_2). \tag{515}$$

From the eqs. (511) and (515) we obtain the whole amplitude of $\tau^-(p_\tau) \to \ell^+(p_{\ell^+})M_1^-(q_1)M_2^-(q_2)$

by substituting them in the eq. (504), it reads

$$\begin{aligned} i\mathcal{M} =& \frac{g^4}{2} V_{M_1}^{CKM} V_{M_2}^{CKM} f_{M_1} f_{M_2} \sum_{i=1}^{3} W_{\tau i}^{\dagger} W_{\ell^+ i}^{\dagger} m_i \left(\frac{\overline{v}(p_\tau) \not{q}_1 \not{q}_2 P_R v(p_{\ell^+})}{(p_\tau - q_1)^2 - m_i^2} + \frac{\overline{v}(p_\tau) \not{q}_2 \not{q}_1 P_R v(p_{\ell^+})}{(p_\tau - q_2)^2 - m_i^2} \right) \\ &+ \frac{g^4}{2} V_{M_1}^{CKM} V_{M_2}^{CKM} f_{M_1} f_{M_2} \sum_{i=1}^{3} \theta_{\tau i} \theta_{\ell^+ i} M_i \left(\frac{\overline{v}(p_\tau) \not{q}_1 \not{q}_2 P_R v(p_{\ell^+})}{(p_\tau - q_1)^2 - M_i^2} + \frac{\overline{v}(p_\tau) \not{q}_2 \not{q}_1 P_R v(p_{\ell^+})}{(p_\tau - q_2)^2 - M_i^2} \right) \\ =& \mathcal{M}_{light} + \mathcal{M}_{heavy}. \end{aligned} \tag{516}$$

The total amplitude receives two contributions: one of them comes from light neutrinos ($W_{\tau i}^{\dagger} W_{\ell^+ i}^{\dagger}$) and the other one comes from heavy neutrinos ($\theta_{\tau i} \theta_{\ell^+ i}$).

Now, we can compare the energy scale of the process to the square of the masses of the Majorana neutrinos and see what impact this comparison has on the amplitude. For light neutrinos compared to the energy scale in the processes ($m_i^2 \ll (p_\tau - q_1)^2, (p_\tau - q_2)^2$), we can neglect the mass in the denominator, so the light neutrino amplitude becomes as follows

$$\mathcal{M}_{light} = \frac{g^4}{2} V_{M_1}^{CKM} V_{M_2}^{CKM} f_{M_1} f_{M_2} \langle m_{\tau \ell^+} \rangle \left(\frac{\overline{v}(p_\tau) \not{q}_1 \not{q}_2 P_R v(p_{\ell^+})}{(p_\tau - q_1)^2} + \frac{\overline{v}(p_\tau) \not{q}_2 \not{q}_1 P_R v(p_{\ell^+})}{(p_\tau - q_2)^2} \right), \tag{517}$$

where we have defined $\langle m_{\tau \ell^+} \rangle \equiv \sum_{i=1}^{3} W_{\tau i}^{\dagger} W_{\ell^+ i}^{\dagger} m_i$, similarly to the eq. (499). $\langle m_{\tau \ell^+} \rangle$ is an effective mass of a light Majorana neutrino [73].

If the heavy neutrinos satisfy that ($M_i^2 \gg (p_\tau - q_1)^2, (p_\tau - q_2)^2$), the contribution of the second term in eq. (516) is dominated by a similar factor to the eq. (500)

$$\mathcal{M}_{heavy} = -\frac{g^4}{2} V_{M_1}^{CKM} V_{M_2}^{CKM} f_{M_1} f_{M_2} \frac{1}{\langle M_{\tau \ell^+} \rangle} \left(\overline{v}(p_\tau) \not{q}_1 \not{q}_2 P_R v(p_{\ell^+}) + \overline{v}(p_\tau) \not{q}_2 \not{q}_1 P_R v(p_{\ell^+}) \right), \tag{518}$$

where $\frac{1}{\langle M_{\tau \ell^+} \rangle} = \sum_{i=1}^{3} \frac{\theta_{\tau i} \theta_{\ell^+ i}}{M_i}$. Then, with the latter assumptions the total amplitude is written as follows

$$\begin{aligned} i\mathcal{M} =& \frac{g^4}{2} V_{M_1}^{CKM} V_{M_2}^{CKM} f_{M_1} f_{M_2} \langle m_{\tau \ell^+} \rangle \left(\frac{\overline{v}(p_\tau) \not{q}_1 \not{q}_2 P_R v(p_{\ell^+})}{(p_\tau - q_1)^2} + \frac{\overline{v}(p_\tau) \not{q}_2 \not{q}_1 P_R v(p_{\ell^+})}{(p_\tau - q_2)^2} \right) \\ &- \frac{g^4}{2} V_{M_1}^{CKM} V_{M_2}^{CKM} f_{M_1} f_{M_2} \frac{1}{\langle M_{\tau \ell^+} \rangle} \left(\overline{v}(p_\tau) \not{q}_1 \not{q}_2 P_R v(p_{\ell^+}) + \overline{v}(p_\tau) \not{q}_2 \not{q}_1 P_R v(p_{\ell^+}) \right). \end{aligned} \tag{519}$$

This expression has a suppression issue in the Majorana light neutrinos sector: the $\mathcal{M}_{light}$ is neglected since the Majorana light neutrinos are identified as SM ones and it is well known their masses are very small.

When the heavy neutrino mass is kinematically accessible ($M_i^2 \simeq (p_\tau - q_1)^2, (p_\tau - q_2)^2$), the process may undergo a resonant production of the heavy neutrino which substantially enhances the transition rate. Therefore, the decay amplitude for the process can be enhanced through the resonant production of a heavy Majorana neutrino. This enhancement of the amplitude is known as the resonant mechanism

[62]. For tau decays the resonant contribution is from heavy Majorana neutrinos with masses of order MeV to GeV, but in the Subsection 8.7 we estimated masses for heavy Majorana neutrinos in this model (LHT) of the order TeV, so we can not contemplate the resonant contribution.
The other contibution $\mathcal{M}_{heavy}$ is suppressed by a $\sim \frac{1}{M_i}$ factor with $M_i \sim \mathcal{O}(\text{TeV})$. Nevertheless, we expect that $\mathcal{M}_{heavy}$ will be less suppressed than $\mathcal{M}_{light}$, it being the dominant contribution of $\tau^- \to \ell^+ M_1^- M_2^-$. Then, from the eq.(519) we are focusing only in $\mathcal{M}_{heavy}$

$$\begin{aligned} i\mathcal{M} &= -\frac{g^4}{2} V_{M_1}^{CKM} V_{M_2}^{CKM} f_{M_1} f_{M_2} \frac{1}{\langle M_{\tau\ell^+} \rangle} \left(\overline{v}(p_\tau) \not{q}_1 \not{q}_2 P_R v(p_{\ell^+}) + \overline{v}(p_\tau) \not{q}_2 \not{q}_1 P_R v(p_{\ell^+}) \right) \\ &= -\frac{g^4}{2} V_{M_1}^{CKM} V_{M_2}^{CKM} f_{M_1} f_{M_2} \frac{1}{\langle M_{\tau\ell^+} \rangle} (\mathcal{M}_1 + \mathcal{M}_2). \end{aligned} \tag{520}$$

Considering $G_F/\sqrt{2} = g^2/8$, then

$$\Gamma(\tau^- \to \ell^+ M_1^- M_2^-) = 16 G_F^4 f_{M_1}^2 f_{M_2}^2 \left| V_{M_1}^{CKM} V_{M_2}^{CKM} \right|^2 \left| \frac{1}{\langle M_{\tau\ell^+} \rangle} \right|^2 |\mathcal{M}_1 + \mathcal{M}_2|^2 , \tag{521}$$

where

$$\begin{aligned} |\mathcal{M}_1 + \mathcal{M}_2|^2 = \frac{1}{2m_\tau} \int \frac{d^3\vec{p_\ell}}{(2\pi)^3 2E_\ell} \int \frac{d^3\vec{q_1}}{(2\pi)^3 2E_{M_1}} \int \frac{d^3\vec{q_2}}{(2\pi)^3 2E_{M_2}} \\ \times (2\pi)^4 \delta^{(4)}(p_\tau - p_\ell - q_1 - q_2) 8 (p_\tau \cdot p_\ell)(q_1 \cdot q_2)^2. \end{aligned} \tag{522}$$

Working at the tau rest frame and taking $m_{\ell^+} \approx 0$

$$p_\tau = (m_\tau, \vec{0}), \quad p_\ell = (|\vec{p_\ell}|, \vec{p_\ell}), \quad q_1 = (E_{M_1}, \vec{q_1}), \quad q_2 = (E_{M_2}, \vec{q_2}) \tag{523}$$

yields

$$8(p_\tau \cdot p_\ell)(q_1 \cdot q_2) = 2 m_\tau E_\ell \left(m_\tau^2 - m_{M_1}^2 - m_{M_2}^2 - 2 m_\tau E_\ell \right)^2 . \tag{524}$$

In the case $M_1 = M_2 (m_{M_1} = m_{M_2} = m)$, the eq. (522) becomes

$$|\mathcal{M}_1 + \mathcal{M}_2|^2 = \frac{1}{4(2\pi)^3} \int_m^{m_\tau/2} dE_M \int_{|\vec{p_\ell}|_-}^{|\vec{p_\ell}|_+} d|\vec{p_\ell}| |\vec{p_\ell}| (m_\tau^2 - 2m^2 - 2m_\tau |\vec{p_\ell}|)^2, \tag{525}$$

where

$$\frac{m_\tau^2 - 2 m_\tau E_M}{2\left(m_\tau - E_M + \sqrt{E_M^2 - m^2} \right)} < |\vec{p_\ell}| < \frac{m_\tau^2 - 2 m_\tau E_M}{2\left(m_\tau - E_M - \sqrt{E_M^2 - m^2} \right)}. \tag{526}$$

The $|\mathcal{M}_1 + \mathcal{M}_2|^2$ is a function which depends of $m = m_\pi, m_K$, and we computed it in FeynCalc [36].

9.2.1 $\tau \to e^+(\mu^+)\pi^-\pi^-$

Because we are considering $m_{\ell^+} \approx 0$, the $|\mathcal{M}_1 + \mathcal{M}_2|^2$ term does not depend of m_{ℓ^+}, hence, both processes end up sharing the same value of $|\mathcal{M}_1 + \mathcal{M}_2|^2$.

$$\Gamma(\tau^- \to e^+\pi^-\pi^-) = 16 G_F^4 f_{\pi^-}^4 \, |V_{ud}|^4 \left| \frac{1}{\langle M_{\tau e^+} \rangle} \right|^2 |\mathcal{M}_1 + \mathcal{M}_2|^2 \,, \tag{527}$$

$$\Gamma(\tau^- \to \mu^+\pi^-\pi^-) = 16 G_F^4 f_{\pi^-}^4 \, |V_{ud}|^4 \left| \frac{1}{\langle M_{\tau \mu^+} \rangle} \right|^2 |\mathcal{M}_1 + \mathcal{M}_2|^2 \,. \tag{528}$$

We know that

$$\frac{1}{\langle M_{\tau e^+} \rangle} = \sum_{i=1}^{3} \frac{\theta_{\tau i}\theta_{ei}}{M_i}, \quad \text{and} \quad \frac{1}{\langle M_{\tau \mu^+} \rangle} = \sum_{i=1}^{3} \frac{\theta_{\tau i}\theta_{\mu i}}{M_i}. \tag{529}$$

We may bind the above equations as we did in eq. (501) considering the neutrino mass (4 TeV) and taking from the Table 16 the values of $|\theta_{ei}\theta_{\tau i}| = 8.763 \times 10^{-4}$ and $|\theta_{\mu i}\theta_{\tau i}| = 1.937 \times 10^{-3}$, therefore,

$$\begin{aligned} \left| \frac{1}{\langle M_{\tau e^+} \rangle} \right| &< \frac{|\theta_{\tau i}\theta_{ei}|}{17.2 \text{ TeV}} = \frac{2.76 \times 10^{-4}}{17.2 \text{ TeV}} = 1.604 \times 10^{-8} \text{GeV}^{-1}, \\ \left| \frac{1}{\langle M_{\tau \mu^+} \rangle} \right| &< \frac{|\theta_{\tau i}\theta_{\mu i}|}{17.2 \text{ TeV}} = \frac{6.52 \times 10^{-4}}{17.2 \text{ TeV}} = 3.79 \times 10^{-8} \text{GeV}^{-1}. \end{aligned} \tag{530}$$

Taking $m_\tau = 1.77686$ GeV and $m_\pi = 0.13957039$ GeV, the value of $|\mathcal{M}_1 + \mathcal{M}_2|^2$ is given by

$$|\mathcal{M}_1 + \mathcal{M}_2|^2 = 2.13957 \times 10^{-4} (\text{GeV})^7. \tag{531}$$

Using the following constant values [6]

$$\begin{aligned} G_F &= 1.166378 \times 10^{-5} (\text{GeV})^{-2}, \\ |V_{ud}| &= 0.9737, \\ f_\pi &= 0.093 \text{GeV}. \end{aligned} \tag{532}$$

This is a cautionary note to point out that there are different conventions of defining f_π which differ by a factor of $\sqrt{2}$. Some people do not put the factor of $\sqrt{2}$ on the right hand side of eq. (514), so for them f_π turns out to be about 130 MeV [2].
So, $\Gamma(\tau^- \to e^+\pi^-\pi^-)$ and $\Gamma(\tau^- \to \mu^+\pi^-\pi^-)$ are given as follows

$$\Gamma(\tau^- \to e^+\pi^-\pi^-) < 1.096 \times 10^{-42} \text{ GeV}, \tag{533}$$

$$\Gamma(\tau^- \to \mu^+\pi^-\pi^-) < 6.11 \times 10^{-42} \text{ GeV}. \tag{534}$$

The branching ratios for both processes are obtained dividing by the SM tau decay width, hence

$$\mathrm{Br}(\tau^- \to e^+\pi^-\pi^-) = \frac{\Gamma(\tau^- \to e^+\pi^-\pi^-)}{\Gamma_\tau} < 1.59 \times 10^{-29}, \tag{535}$$

$$\mathrm{Br}(\tau^- \to \mu^+\pi^-\pi^-) = \frac{\Gamma(\tau^- \to \mu^+\pi^-\pi^-)}{\Gamma_\tau} < 8.89 \times 10^{-29}. \tag{536}$$

9.2.2 $\tau \to e^+(\mu^+)K^-K^-$

In this case the decay widths are given by

$$\Gamma(\tau^- \to e^+K^-K^-) = 16G_F^4 f_{K^-}^4 \left|V_{us}\right|^4 \left|\frac{1}{\langle M_{\tau e^+}\rangle}\right|^2 \left|\mathcal{M}_1 + \mathcal{M}_2\right|^2, \tag{537}$$

$$\Gamma(\tau^- \to \mu^+K^-K^-) = 16G_F^4 f_{K^-}^4 \left|V_{us}\right|^4 \left|\frac{1}{\langle M_{\tau \mu^+}\rangle}\right|^2 \left|\mathcal{M}_1 + \mathcal{M}_2\right|^2, \tag{538}$$

where the value of kaon decay constant (similar comment with respect to its normalization applies as in the pion case above) is [2]

$$f_K = 0.110 \text{ GeV}, \tag{539}$$

the m_K and the CKM matrix elements are taken from [6]

$$m_K = 0.493677 \text{ GeV}, \quad |V_{us}| = 0.2221. \tag{540}$$

In this case

$$|\mathcal{M}_1 + \mathcal{M}_2|^2 = 6.30908 \times 10^{-5} \text{ (GeV)}^7. \tag{541}$$

Then, the eqs. (537) and (538) yield

$$\Gamma(\tau^- \to e^+K^-K^-) < 1.71 \times 10^{-45} \text{ GeV}, \tag{542}$$

$$\Gamma(\tau^- \to \mu^+K^-K^-) < 9.56 \times 10^{-45} \text{ GeV}. \tag{543}$$

Finally, the branching ratios for these processes read

$$\mathrm{Br}(\tau^- \to e^+K^-K^-) = \frac{\Gamma(\tau^- \to e^+K^-K^-)}{\Gamma_\tau} < 2.48 \times 10^{-32}, \tag{544}$$

$$\mathrm{Br}(\tau^- \to \mu^+K^-K^-) = \frac{\Gamma(\tau^- \to \mu^+K^-K^-)}{\Gamma_\tau} < 1.38 \times 10^{-31}. \tag{545}$$

We see that theses processes are more suppressed when the mesons are K^- than π^- due to K^- being heavier.

9.2.3 $\tau \to e^+(\mu^+)\pi^- K^-$

In this case both π^- and K^- take place in the tau decay

$$\tau^-(p_\tau) \to \ell^+(p_{\ell^+})\pi^-(q_1)K^-(q_2), \tag{546}$$

where, the four-momentum of each particle is

$$p_\tau = (m_\tau, \vec{0}), \quad p_\ell = (|\vec{p_\ell}|, \vec{p_\ell}), \quad q_1 = (E_\pi, \vec{q_\pi}), \quad q_2 = (E_K, \vec{q_K}), \tag{547}$$

so, the eq.(524) becomes

$$8(p_\tau \cdot p_\ell)(q_1 \cdot q_2) = 2m_\tau|\vec{p_\ell}|\left(m_\tau^2 - m_\pi^2 - m_K^2 - 2m_\tau|\vec{p_\ell}|\right)^2. \tag{548}$$

In this case the eq. (522) is written as follows

$$|\mathcal{M}_1 + \mathcal{M}_2|^2 = \frac{1}{4(2\pi)^3}\int_{m_\pi}^{\frac{m_\tau^2+m_\pi^2-m_K^2}{2m_\tau}} dE_\pi \int_{|\vec{p_\ell}|_-}^{|\vec{p_\ell}|_+} d|\vec{p_\ell}||\vec{p_\ell}|\left(m_\tau^2 - m_\pi^2 - m_K^2 - 2m_\tau|\vec{p_\ell}|\right)^2, \tag{549}$$

with

$$\frac{m_\tau^2 - 2m_\tau E_\pi + m_\pi^2 - m_K^2}{2\left(m_\tau - E_\pi + \sqrt{E_\pi^2 - m_\pi^2}\right)} < |\vec{p_\ell}| < \frac{m_\tau^2 - 2m_\tau E_\pi + m_\pi^2 - m_K^2}{2\left(m_\tau - E_\pi - \sqrt{E_\pi^2 - m_\pi^2}\right)}. \tag{550}$$

The decay width of these processes is expressed as

$$\Gamma(\tau^- \to \ell^+\pi^- K^-) = 16G_F^4 f_\pi^2 f_k^2 \left|V_\pi^{CKM} V_K^{CKM}\right|^2 \left|\frac{1}{\langle M_{\tau\ell^+}\rangle}\right|^2 |\mathcal{M}_1 + \mathcal{M}_2|^2, \tag{551}$$

thus, writing explicitly the decay width for each process

$$\Gamma(\tau^- \to e^+\pi^- K^-) = 16G_F^4 f_\pi^2 f_k^2 \left|V_{ud}V_{us}\right|^2 \left|\frac{1}{\langle M_{\tau e^+}\rangle}\right|^2 |\mathcal{M}_1 + \mathcal{M}_2|^2, \tag{552}$$

$$\Gamma(\tau^- \to \mu^+\pi^- K^-) = 16G_F^4 f_\pi^2 f_k^2 \left|V_{ud}V_{us}\right|^2 \left|\frac{1}{\langle M_{\tau\mu^+}\rangle}\right|^2 |\mathcal{M}_1 + \mathcal{M}_2|^2. \tag{553}$$

The integral from eq. (549) was computed with aid of FeynCalc [36], so that the above equations yield

$$\Gamma(\tau^- \to e^+\pi^- K^-) < 4.63 \times 10^{-44}\ \text{GeV}, \tag{554}$$

$$\Gamma(\tau^- \to \mu^+\pi^-K^-) < 2.58 \times 10^{-43}\ \text{GeV}. \tag{555}$$

Therefore, $\text{Br}(\tau^- \to e^+\pi^-K^-)$ and $\text{Br}(\tau^- \to \mu^+\pi^-K^-)$ are given by

$$\text{Br}(\tau^- \to e^+\pi^-K^-) < 6.73 \times 10^{-31}, \tag{556}$$

$$\text{Br}(\tau^- \to \mu^+\pi^-K^-) < 3.75 \times 10^{-30}. \tag{557}$$

Taking the current values from Particle Data Group [6]

$$\begin{aligned}
\text{Br}(\tau^- \to e^+\pi^-\pi^-) &< 2.0 \times 10^{-8}\ (\text{C.L} = 90\%),\\
\text{Br}(\tau^- \to \mu^+\pi^-\pi^-) &< 3.9 \times 10^{-8}\ (\text{C.L} = 90\%),\\
\text{Br}(\tau^- \to e^+K^-K^-) &< 3.3 \times 10^{-8}\ (\text{C.L} = 90\%),\\
\text{Br}(\tau^- \to \mu^+K^-K^-) &< 4.7 \times 10^{-8}\ (\text{C.L} = 90\%),\\
\text{Br}(\tau^- \to e^+\pi^-K^-) &< 3.2 \times 10^{-8}\ (\text{C.L} = 90\%),\\
\text{Br}(\tau^- \to \mu^+\pi^-K^-) &< 4.8 \times 10^{-8}\ (\text{C.L} = 90\%),
\end{aligned} \tag{558}$$

we can see that our results obtained by LHT are more constrained than the current limits. It was expected because we started from the fact that $\mathcal{M}_{heavy}$ is small due to the masses of the heavy neutrinos as we explained before in the eqs. (519) and (520). Another possible process may be $\tau^- \to \ell^+\rho^-\rho^-$, but this is also suppressed by space phase as $m_\rho = 775.26$ MeV, so it is not considered in our discussion.

10 Lepton Flavour Violation in Hadron Decays of the Tau Lepton in LHT

Throughout this work [74] LFV processes have been studied considering, firstly, the effects of T-odd particles, which are specific to the traditional LHT, in $\mu \to e\gamma$ and $\mu \to ee\bar{e}$ decays. Such contributions can be extended to general processes $\ell \to \ell'\gamma$ and $\ell \to \ell'\ell''\bar{\ell}'''$ or $\mu \to e$ conversion in nuclei. In addition, we have introduced Majorana neutrinos through an Inverse Seesaw (ISS) mechanism and examined the scenario where just heavy Majorana neutrinos have a sizeable contribution to LFV processes.
Now, in this section we apply our model for the study of LFV tau decays into hadrons: $\tau \to \mu P$, $\tau \to \mu V$ and $\tau \to \mu PP$ where P (V) is short for a pseudoscalar (vector) meson.
We are going to consider the effects of T-odd particles as well as heavy Majorana neutrinos since terms at order of $\mathcal{O}(v^2/f^2)$ are taken into account, where v is the vev of the SM Higgs and f is the energy scale of NP ($\sim$ TeV), it yields $v^2/f^2 \ll 1$. We begin our analysis determining the amplitudes of the $\tau \to \mu q\bar{q}$ with q = u, d, s quarks and, afterwards, proceed to hadronize the corresponding quarks bilinears. For this latter step we will employ the tools given by chiral symmetry and dispersion relations, enforcing the right short-distance behaviour to the form factors.
As we said before, we are taking into account T-odd fermions, thus partner leptons $\bar{\ell}^c = (\bar{\nu}^c, \bar{\ell}^c)$ also will appear. We recall the content of particles given by eqs. (318) and (321), and the Lagrangian (322) that gives masses to heavy leptons. To give mass to partner leptons we need to introduce two incomplete $SO(5)$ multiplets [23, 27, 51]

$$\Psi_L = \begin{pmatrix} \tilde{\psi}^c_L \\ 0 \\ 0 \end{pmatrix}, \quad \Psi^\chi_L = \begin{pmatrix} 0 \\ \chi_L \\ 0 \end{pmatrix}, \quad \text{with } \Psi_L \xrightarrow{T} \Omega\Psi_L, \text{ and } \Psi^\chi_L \xrightarrow{T} \Omega\Psi^\chi_L. \tag{559}$$

This multiplet introduces Dirac mass terms for the $\tilde{\psi}^c_R$ (the superscript (^{c}) denotes partner lepton fields, not to be confused with charge conjugation) and χ_R fields as follows

$$\mathcal{L}_{Y_H} = -\kappa f \left(\overline{\Psi}_2\xi + \overline{\Psi}_1\Sigma_0\xi^\dagger\right)\Psi_R - \kappa_2\overline{\Psi_L}\Psi_R - M\overline{\Psi^\chi_L}\Psi_R + \text{h.c.}, \tag{560}$$

Then, partner and singlet leptons receive a κ_2 and M masses.

10.1 $\tau \to \ell q\bar{q}$ ($\ell = e, \mu$)

Two generic topologies are involved in this amplitude: i) penguin-like diagrams, namely $\tau \to \ell\{\gamma, Z\}$, followed by $\{\gamma, Z\} \to q\bar{q}$ and ii) box diagrams. We will assume, for simplicity, that light quarks and leptons (ℓ) are massless in our calculation. Corrections induced by their finite masses can be safely neglected.
The full amplitude is given by two contributions: one of them comes from T-odd particles and the

other from heavy Majorana neutrinos, then

$$\mathcal{M} = \mathcal{M}^{\mathrm{T-odd}} + \mathcal{M}^{\mathrm{Maj}}, \tag{561}$$

where each one is written

$$\begin{aligned} \mathcal{M}^{\mathrm{T-odd}} &= \mathcal{M}_{\gamma}^{\mathrm{T-odd}} + \mathcal{M}_{Z}^{\mathrm{T-odd}} + \mathcal{M}_{\mathrm{box}}^{\mathrm{T-odd}}, \\ \mathcal{M}^{\mathrm{Maj}} &= \mathcal{M}_{\gamma}^{\mathrm{Maj}} + \mathcal{M}_{Z}^{\mathrm{Maj}} + \mathcal{M}_{\mathrm{box}}^{\mathrm{Maj}}, \end{aligned} \tag{562}$$

we will use the 't Hooft-Feynman gauge along the calculation and will write $\ell = \mu$ for definiteness.

10.1.1 T-odd contribution

The Feynman diagrams that contribute to the $\mathcal{M}_{\gamma}^{\mathrm{T-odd}}$ amplitude are shown in Figure 6 (it is important to recall the contribution from partner leptons $\bar{\ell}^c = (\bar{\nu}^c, \bar{\ell}^c)$), whose structure is similar to eq. (142) doing the corresponding adjustments

$$\begin{aligned} \mathcal{M}_{\gamma}^{\mathrm{T-odd}} = \frac{e^2}{Q^2}\overline{\mu}(p')[Q^2\gamma^{\mu}(A_L^1 P_L + A_R^1 P_R) + im_{\tau}\sigma^{\mu\nu}Q_{\nu}(A_L^2 P_L + A_R^2 P_R)]\tau(p) \\ \times\, \overline{q}(p_q)Q_q\gamma_{\mu}q(p_{\bar{q}}), \end{aligned} \tag{563}$$

where Q_q is the electric charge matrix:

$$Q_q = \frac{1}{3}\begin{pmatrix} 2 & & \\ & -1 & \\ & & -1 \end{pmatrix}, \tag{564}$$

in units of $|e|$, $q = (u, d, s)^T$, and $Q^2 = (p_q + p_{\bar{q}})^2$ is the squared momentum transfer.
The form factors have been defined as [25]

$$A_L^1 = F_L^{\gamma}/Q^2, \quad A_R^1 = F_R^{\gamma}/Q^2, \quad A_L^2 = \left(F_M^{\gamma} + iF_E^{\gamma}\right)/m_{\tau}, \quad A_R^2 = \left(F_M^{\gamma} - iF_E^{\gamma}\right)/m_{\tau}. \tag{565}$$

We have that $F_M^{\gamma} = -iF_E^{\gamma}$, so that $A_L^2 = 0$, and A_R^1 vanishes with m_{μ} [37]. Therefore, only A_L^1 and A_R^2 contribute to the amplitude, and it becomes

$$\mathcal{M}_{\gamma}^{\mathrm{T-odd}} = \frac{e^2}{Q^2}\overline{\mu}(p')[2iF_M^{\gamma}(Q^2)P_R\sigma^{\mu\nu}Q_{\nu} + F_L^{\gamma}(Q^2)\gamma^{\mu}P_L]\tau(p)\overline{q}(p_q)Q_q\gamma_{\mu}q(p_{\bar{q}}), \tag{566}$$

where F_M^{γ} is given by

$$F_M^{\gamma} = F_M^{\gamma}|_{W_H} + F_M^{\gamma}|_{Z_H} + F_M^{\gamma}|_{A_H} + F_M^{\gamma}|_{\bar{\nu}^c} + F_M^{\gamma}|_{\bar{\ell}^c}, \tag{567}$$

whose $F_M^\gamma|_{Z_H,A_H,W_H,\bar{\nu^c},\bar{\ell^c}}$ functions were already computed in eqs. (246), (249), (258), (263), and (265), respectively, but in this case we consider terms at order of $\mathcal{O}(Q^2)$. All those functions agree with [37]. We write explicitly the form factor above

$$\begin{aligned}F_M^\gamma =&\frac{\alpha_W}{16\pi}\frac{m_\tau}{M_W^2}\frac{v^2}{4f^2}\sum_i V_{H\ell}^{i\mu\dagger}V_{H\ell}^{i\tau}\left[F_{W_H}(y_i,Q^2)+F_{Z_H}(y_i,Q^2)+\frac{1}{5}F_{Z_H}(ay_i,Q^2)\right]\\&+\frac{\alpha_W}{16\pi}\frac{m_\tau}{M_\Phi^2}\frac{v^2}{4f^2}\sum_{i,j,k}V_{H\ell}^{i\mu\dagger}\frac{m_{\ell_{Hi}}}{M_W}W_{ij}^\dagger W_{jk}\frac{m_{\ell_{Hk}}}{M_W}V_{H\ell}^{k\tau}\left[F_{\bar{\nu^c}}\left(\frac{m_{\nu_j^c}^2}{M_\Phi^2},Q^2\right)+F_{\bar{\ell^c}}\left(\frac{m_{\nu_j^c}^2}{M_\Phi^2},Q^2\right)\right],\end{aligned}\tag{568}$$

where

$$\begin{aligned}F_{Z_H}(y)=&-\frac{1}{3}+\frac{2y+5y^2-y^3}{8(1-y)^3}+\frac{3y^2}{4(1-y)^4}\ln y\\&+\frac{1}{48}\frac{Q^2}{M_{Z_H}^2}\left(\frac{24+546y-2479y^2+561y^3-339y^4+67y^5}{60(1-y)^5}+\frac{y(6-17y-16y^2)\ln y}{(1-y)^6}\right),\\F_{W_H}(y)=&\frac{5}{6}-\frac{3y-15y^2-6y^3}{12(1-y)^3}+\frac{3y^3}{2(1-y)^4}\ln y\\&+\frac{y}{24}\frac{Q^2}{M_{W_H}^2}\left(\frac{134-759y+1941y^2-2879y^3-69y^4+12x^5}{60(1-y)^5}+\frac{y^3(4-34y+3y^3)\ln y}{(1-y)^6}\right),\\F_{\bar{\nu^c}}(x)=&\frac{-1+5x+2x^2}{12(1-x)^3}+\frac{x^2}{2(1-x)^4}\ln x\\&+\frac{x^2}{24}\frac{Q^2}{M_\Phi^2}\left(\frac{13-87x+333x^2+293x^3-12x^4}{60(1-x)^5}+\frac{x^3(8+x)\ln x}{(1-x)^6}\right),\\F_{\bar{\ell^c}}(x)=&\frac{-4+5x+5x^2}{6(1-x)^3}-\frac{x(1-2x)}{(1-x)^4}\ln x\\&+\frac{1}{8}\frac{Q^2}{M_\Phi^2}\left(\frac{4+129x-231x^2-91x^3+9x^4}{60(1-x)^5}+\frac{x(1-4x^2)\ln x}{(1-x)^6}\right),\end{aligned}\tag{569}$$

with $y_i=\frac{m_{H_i}^2}{M_{W_H}^2}$ being $m_{H_i}\equiv m_{\ell_H^i}\simeq m_{\nu_H^i}$, $a=\frac{M_{W_H}^2}{M_{A_H}^2}=\frac{5c_W^2}{s_W^2}\sim 15$, $M_{W_H}=M_{Z_H}$, and $x=\frac{m_{\nu_j^c}^2}{M_\Phi^2}$. We have used $M_W^2/M_{W_H}^2=v^2/(4f^2)$. Here $V_{H\ell}^i$ are the matrix elements of the 3×3 unitary mixing matrix parametrizing the misalignment between the SM left-handed charged leptons ℓ with the heavy mirror ones ℓ_H. The W_{jk} are the matrix elements of the 3×3 unitary mixing matrix parametrizing the misalignment between the mirror leptons and their partners ℓ^c in the $SO(5)$ (right-handed) multiplets [37].

We list the masses of particles which are involved in the form factors [24, 25, 29]

$$\begin{aligned}
&M_W = \frac{\upsilon}{2s_W}\left(1-\frac{\upsilon^2}{12f^2}\right), \quad M_Z = M_W/c_W, \quad \upsilon \simeq 246 \text{ GeV}, \quad (\rho \text{ factor is conserved}),\\
&M_{W_H} = M_{Z_H} = \frac{f}{s_W}\left(1-\frac{\upsilon^2}{8f^2}\right), \quad M_{A_H} = \frac{f}{\sqrt{5}c_W}\left(1-\frac{5\upsilon^2}{8f^2}\right), \quad M_\Phi = \sqrt{2}M_h\frac{f}{\upsilon},\\
&m_{\ell_H^i} = \sqrt{2}\kappa_{ii}f \equiv m_{Hi}, \quad m_{\nu_H^i} = m_{Hi}\left(1-\frac{\upsilon^2}{8f^2}\right), \quad m_{\ell^c,\nu^c} = \kappa_2,
\end{aligned} \tag{570}$$

with M_h being the mass of the SM Higgs scalar and κ_{ii} the diagonal entries of the κ matrix (see eq. (323)). We observe from eq. (568) that the contributions from partner leptons seem to behave as $\sim \frac{v^2}{4f^2}\frac{1}{M_\Phi^2} \sim \frac{v^4}{4f^4}$, but m_{Hi}/M_W is of order of $\mathcal{O}(f^2/v^2)$, then the partner lepton term is like $\sim \upsilon^2/f^2$. The F_L^γ form factor is given by the eqs. (270), (273), (274), and (277). Therefore, F_L^γ can be expressed as follows [25, 37]

$$\begin{aligned}
F_L^\gamma|_{Z_H} =& \frac{\alpha_W}{4\pi}\frac{Q^2}{M_{W_H}^2}\sum_i V_{H\ell}^{i\mu *}V_{H\ell}^{i\tau}\left(G_Z^{(1)}(y_i)+\frac{1}{5}G_Z^{(1)}(ay_i)+G_W^{(1)}(y_i)\right)\\
&+\frac{\alpha_W}{4\pi}\frac{Q^2}{2M_h^2}\frac{\upsilon^4}{4f^4}\sum_{ijk}V_{H\ell}^{i\mu\dagger}\frac{m_{\ell_{Hi}}}{M_W}W_{ij}^\dagger W_{jk}\frac{m_{\ell_{Hk}}}{M_W}V_{H\ell}^{k\tau}\left(G_{\overline{\nu^c}}^{(1)}(x)+G_{\overline{\ell}^c}^{(1)}(x)\right),
\end{aligned} \tag{571}$$

where

$$\begin{aligned}
G_Z^{(1)}(y) &= \frac{1}{36}+\frac{y(18-11y-y^2)}{48(1-y)^3}-\frac{4-16y+9y^2}{24(1-y)^4}\ln y,\\
G_W^{(1)}(y) &= -\frac{5}{18}+\frac{y(12+y-7y^2)}{24(1-y)^3}+\frac{y^2(12-10y+y^2)}{12(1-y)^4}\ln y,\\
G_{\overline{\nu^c}}^{(1)}(x) &= \frac{2-7x+11x^2}{72(1-x)^3}+\frac{x^3}{12(1-x)^4}\ln x,\\
G_{\overline{\ell}^c}^{(1)}(x) &= \frac{20-43x+29x^2}{36(1-x)^3}+\frac{2-3x+2x^3}{6(1-x)^4}\ln x.
\end{aligned} \tag{572}$$

with $y_i = \frac{m_{H_i}^2}{M_{W_H}^2}$, $x_i = \frac{m_{\nu_i^c}^2}{M_{W_H}^2}$ and $a = \frac{5c_W^2}{s_W^2}$.
The penguin-like diagrams with Z are given in Figure 6. They are expressed in eq. (143)

$$\mathcal{M}_Z^{\text{T-odd}} = \frac{e^2}{M_Z^2}\overline{\mu}(p')[\gamma^\mu(F_L^Z P_L + F_R^Z P_R)]\tau(p)\overline{q}(p_q)[\gamma_\mu(Z_L P_L + Z_R P_R)]q(p_{\bar{q}}), \tag{573}$$

where

$$\begin{aligned}
Z_L &= \frac{g}{c_W}(T_3^q - s_W^2 Q_q),\\
Z_R &= -\frac{g}{c_W}s_W^2 Q_q,
\end{aligned} \tag{574}$$

being

$$T_3^q = \frac{1}{2}\begin{pmatrix} 1 & & \\ & -1 & \\ & & -1 \end{pmatrix}. \tag{575}$$

The corresponding right-handed vector form factor F_R^Z is $\mathcal{O}\left(m_\tau^2/f^2\right)$ in the LHT and thus negligible as $f \sim \mathcal{O}(\text{TeV})$. The left-handed form factor F_L^Z, at order of $\mathcal{O}(\text{Q}^2)$ according to [37], is given by

$$\begin{aligned} F_L^Z &= F_L^Z|_{W_H} + F_L^Z|_{A_H} + F_L^Z|_{Z_H} + F_L^Z|_{\overline{\nu}^c} + F_L^Z|_{\overline{\ell}^c} \\ &= \frac{\alpha_W}{8\pi c_W s_W}\sum_i V_{H\ell}^{i\mu\dagger}V_{H\ell}^{i\tau}\left\{\frac{v^2}{8f^2}H_L^{W(0)}(y_i) + \frac{Q^2}{M_{W_H}^2}\left[H_L^W(y_i) + (1-2c_W^2)\left(\frac{1}{5}H_L^{A/Z}(ay_i) + H_L^{A/Z}(y_i)\right)\right]\right\} \\ &+ \frac{\alpha_W}{8\pi c_W s_W}\frac{Q^2}{M_h^2}\frac{v^2}{2f^2}\sum_{ijk} V_{H\ell}^{i\mu\dagger}\frac{m_{\ell_{Hi}}}{M_{W_H}}W_{ij}^\dagger W_{jk}\frac{m_{\ell_{Hk}}}{M_{W_H}}V_{H\ell}^{k\tau}\left[H_L^{\bar{\nu}}(x) + (1-2c_w^2)H_L^{\bar{\ell}}(x)\right], \end{aligned} \tag{576}$$

with

$$\begin{aligned} H_L^{W(0)}(y) &= \frac{6-y}{1-y} + \frac{2+3y}{(1-y)^2}\ln y, \\ H_L^W(y) &= 2G_Z^{(1)}(y) - 2c_W^2 G_W^{(1)}(y), \\ H_L^{A/Z}(y) &= G_Z^{(1)}(y), \\ H_L^{\bar{\nu}}(x) &= \frac{1}{2}G_{\overline{\ell}^c}^{(1)}(x) - 2c_W^2 G_{\overline{\nu}^c}^{(1)}(x), \\ H_L^{\bar{\ell}}(x) &= G_{\overline{\ell}^c}^{(1)}(x), \end{aligned} \tag{577}$$

being $y_i = m_{Hi}^2/M_{W_H}^2$ and $y_i = m_{\tilde{\nu}_i^c}^2/M_\Phi^2$. The expression for $G_Z^{(1)}$, $G_W^{(1)}$, $G_{\overline{\nu}^c}^{(1)}$ and $G_{\overline{\ell}^c}^{(1)}$ can be consulted in eqs. (272), (276), (278) and (279), respectively.

To add the contributions from box diagrams we need to introduce the quark sector in the LHT, we will see that this part is very similar to the lepton sector. As in the eq. (318) we embed two $SU(5)$ incomplete quintuplets and introduce a right-handed $SO(5)$ multiplet Ψ_R [24]

$$\Psi_1 = \begin{pmatrix} i\psi_1 \\ 0 \\ 0 \end{pmatrix}, \quad \Psi_2 = \begin{pmatrix} 0 \\ 0 \\ i\psi_2 \end{pmatrix}, \quad \Psi_R = \begin{pmatrix} \psi_R^c \\ \chi_R \\ \psi_R \end{pmatrix}, \tag{578}$$

with (σ^2 is the second Pauli matrix)

$$\psi_i = -\sigma^2 q_i = -\sigma^2\begin{pmatrix} u_i \\ d_i \end{pmatrix} \qquad (i=1,2), \qquad \psi_R = -\sigma^2\begin{pmatrix} u_{HR} \\ d_{HR} \end{pmatrix}. \tag{579}$$

Ψ_i and Ψ_R satisfy the eqs. (319) and (321), respectively. We also have T-parity eigenstates which are T-even and T-odd, they are given by

$$q_{\rm SM} = \frac{q_1 - q_2}{\sqrt{2}}, \qquad q_H = \frac{q_1 + q_2}{\sqrt{2}}, \tag{580}$$

$q_{\rm SM}$ are the left-handed SM quark doublets (T-even), and q_H are the left-handed mirror quark doublets (T-odd).The right-handed mirror quark doublet is given by Ψ_R. The mirror quarks can be given $\mathcal{O}(f)$ masses via eq. (322)

$$\mathcal{L}_{Y_H} = -\kappa^q f \left(\overline{\Psi}_2 \xi + \overline{\Psi}_1 \Sigma_0 \xi^\dagger\right) \Psi_R + h.c. \tag{581}$$

The mirror fermions thus acquire masses after EWSB, given by (similarly to the lepton sector) [24,28]

$$m^d_{Hi} = \sqrt{2}\kappa^q_i f \equiv m_{Hi}, \quad m^u_{Hi} = m_{Hi}\left(1 - \frac{\upsilon^2}{8f^2}\right), \tag{582}$$

where κ^q_i are the eigenvalues of the mass matrix κ^q. As in the lepton sector, we have partner quarks $\bar{q}^c = (\bar{u}^c, \bar{d}^c)$ as well. Due to the symmetries on field content, there are analogies between both sectors. We show the Feynman rules in Tables 17, 18 and 19 [24,37].

$$\begin{aligned} [\mathrm{V}_\mu \mathrm{FF}] &= i\gamma^\mu (g_L P_L + g_R P_R) \qquad (g_{L,R} \leftrightarrow g^*_{L,R}), \\ [\mathrm{SFF}] &= i(c_L P_L + c_R P_R) \qquad (c_{L,R} \leftrightarrow c^*_{R,L}). \end{aligned} \tag{583}$$

$\mathrm{V}_\mu\mathrm{FF}$	g_L
$\overline{u}_{Hi} A_H u_j$	$\left(\frac{1}{10c_W} + \frac{1}{2s_W} x_H \frac{\upsilon^2}{f^2}\right) V^{ij}_{Hu}$
$\overline{u}_{Hi} Z_H u_j$	$\left(\frac{1}{2s_W} - \frac{1}{10c_W} x_H \frac{\upsilon^2}{f^2}\right) V^{ij}_{Hu}$
$\overline{d}_{Hi} A_H d_j$	$\left(\frac{1}{10c_W} - \frac{1}{2s_W} x_H \frac{\upsilon^2}{f^2}\right) V^{ij}_{Hd}$
$\overline{d}_{Hi} Z_H d_j$	$-\left(\frac{1}{2s_W} + \frac{1}{10c_W} x_H \frac{\upsilon^2}{f^2}\right) V^{ij}_{Hd}$
$\overline{u}_{Hi} W^+_H d_j$	$\frac{1}{\sqrt{2}s_W} V^{ij}_{Hd}$
$\overline{d}_{Hi} W^-_H u_j$	$\frac{1}{\sqrt{2}s_W} V^{ij}_{Hu}$

Table 17: Fermion couplings to SM and heavy gauge bosons. The mixing angle between heavy neutral bosons is given by $x_H = 5gg'/(4(5g^2 - g'^2))$ with $e = gs_W = g'c_W$. We neglect the g_R component because light quarks are massless in our approximation and the corresponding contribution vanishes in this limit.

Partner quarks $\bar{q}^c = (\bar{u}^c, \bar{d}^c)$ do not couple to one T-odd gauge boson and SM charged lepton [37]. They just couple to the scalar Φ, thus ϕ^+, ϕ^0 and ϕ^P are propagated. We will discuss the Feynman rules of these fields next.

The Feynman rule for $\phi^0 \bar{u}_{Hi} u_j$ ($\phi^0 \bar{d}_{Hi} d_j$) only has the P_R component which behaves as $\sim m_u$ (m_d) [43], but we are considering that light quarks are massless, hence box diagrams that involve these

SFF	c_L
$\overline{u}_{Hi}\omega^+ d_j$	$-i\frac{m^d_{Hi}}{\sqrt{2}f}V^{ij}_{Hd}$
$\overline{u}_{Hi}\omega^0 u_j$	$-i\frac{m^d_{Hi}}{2f}\left(1+\frac{v^2}{f^2}\left(\frac{1}{8}-\frac{x_H}{tg_W}\right)\right)V^{ij}_{Hu}$
$\overline{u}_{Hi}\eta u_j$	$i\frac{m^d_{Hi}}{2\sqrt{5}f}\left(1+\frac{v^2}{f^2}\left(\frac{9}{8}+x_H tg_W\right)\right)V^{ij}_{Hu}$
$\overline{d}_{Hi}\omega^- u_j$	$-i\frac{m^d_{Hi}}{\sqrt{2}f}V^{ij}_{Hu}$
$\overline{d}_{Hi}\omega^0 d_j$	$i\frac{m^d_{Hi}}{2f}\left(1+\frac{v^2}{f^2}\left(-\frac{1}{8}+\frac{x_H}{tg_W}\right)\right)V^{ij}_{Hd}$
$\overline{d}_{Hi}\eta d_j$	$i\frac{m^d_{Hi}}{2\sqrt{5}f}\left(1-\frac{v^2}{f^2}\left(\frac{5}{8}+x_H tg_W\right)\right)V^{ij}_{Hd}$
$\overline{u^c_i}\eta u_j$	$-iW^q_{ik}\frac{m_{d_{HK}}}{2\sqrt{5}f}V^{kj}_{Hu}\frac{3v^2}{4f^2}$

Table 18: Fermion couplings to heavy Goldstone bosons. We have assumed that light quarks are massless, this is why we neglect the c_R factor, which does not contribute in this limit. In this process we do not take into account $\overline{u^c_i}\eta u_j$ interaction as it behaves as $\sim \mathcal{O}(v^2/f^2)$. As there are two vertices like that in box diagrams their total contribution is suppressed by $\mathcal{O}(v^4/f^4)$ and thus negligible.

interactions do not contribute. The $\phi^0\overline{u^c_i}u_j$ vertex is connected to the $\phi^0\overline{\ell_{Hi}}\ell_j$ one through ϕ^0. The second vertex behaves as $\sim m_{\ell_j}$ [37], where in one case ℓ will be τ but in the other ℓ' will be μ and we are taking $m_\mu = 0$, therefore box diagrams with these couplings vanish. So, box diagrams with ϕ^0 Goldstone boson do not contribute to the $\tau \to \mu q\bar{q}$ decay.

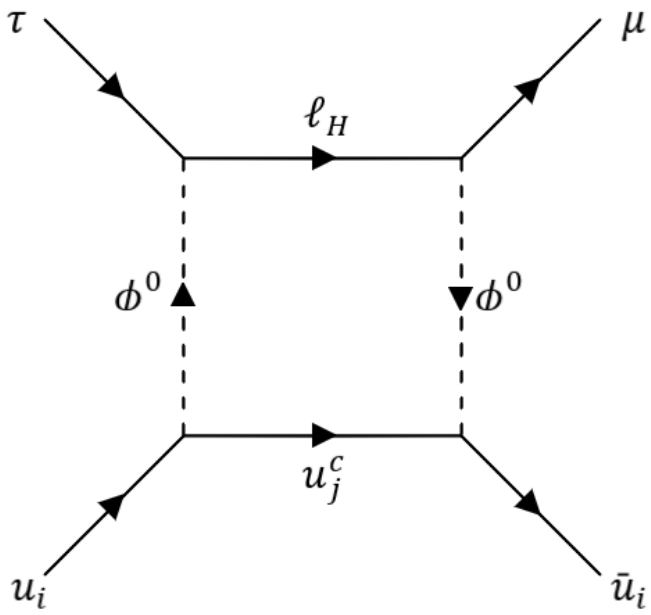

Figure 62: Box diagram that contains $\phi^0\overline{u^c_i}u_j$ and $\phi^0\overline{\ell_{Hi}}\ell_j$ vertices connected by ϕ^0. We see $\phi^0\overline{\ell_{Hi}}\mu$ vertex is proportional to m_μ. Hence it vanishes for massless daughter lepton.

There are three couplings of the ϕ^P Goldstone boson: $\phi^P\overline{u_{Hi}}u_j$, $\phi^P\overline{d_{Hi}}d_j$, and $\phi^P\overline{u^c_i}u_j$ which can

be related to $\phi^P\overline{\ell_{Hi}}\ell_j$. The latter vertex is given by $iV_{ij}\frac{m_{\ell_j}}{\sqrt{2}f}\left(1+\frac{v^2}{4f^2}\right)P_R$ [29], when $\ell_j=\mu$ this contribution vanishes as $m_\mu=0$. Therefore, ϕ^P Goldstone does not contribute to the process.

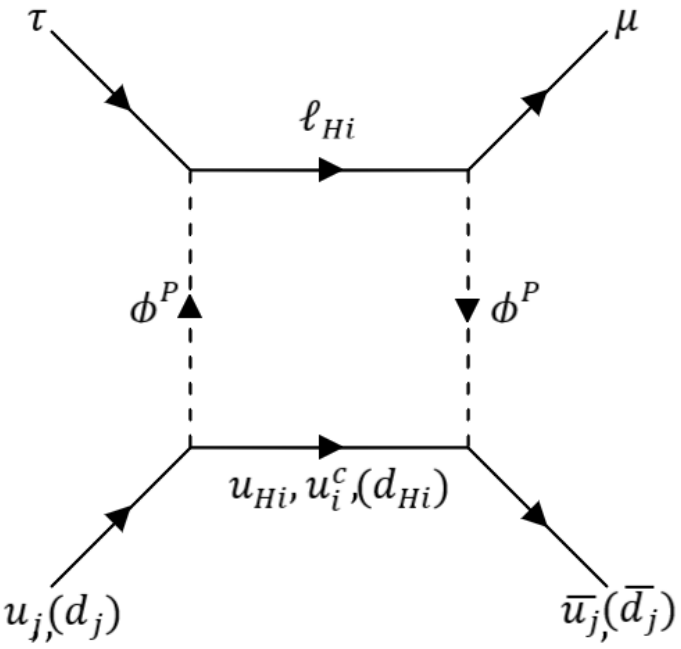

Figure 63: Box diagrams with ϕ^P contribution. It is cancelled by $\phi^P\overline{\ell_{Hi}}\ell_j$ vertex due to $m_\mu=0$.

SFF	c_L
$\Phi^+\overline{\nu_{Hi}}\ell_j$	$\frac{m_{\ell_{Hi}}}{\sqrt{2}f}V^{ij}_{H\ell}\frac{v^2}{8f^2}$
$\Phi^+\overline{\nu_i^c}\ell_j$	$W_{ik}\frac{m_{\ell_{Hk}}}{\sqrt{2}f}V^{kj}_{H\ell}$
$\Phi^+\overline{u_{Hi}}d_j$	$\frac{m_{d_{Hi}}}{\sqrt{2}f}V^{ij}_{Hd}\frac{v^2}{8f^2}$
$\Phi^-\overline{d_{Hi}}u_j$	$-\frac{m_{d_{Hi}}}{\sqrt{2}f}V^{ij}_{Hu}\frac{v^2}{8f^2}$
$\Phi^+\overline{u_i^c}d_j$	$W^q_{ik}\frac{m_{d_{Hk}}}{\sqrt{2}f}V^{kj}_{Hd}$
$\Phi^-\overline{d_i^c}u_j$	$-W^q_{ik}\frac{m_{d_{Hk}}}{\sqrt{2}f}V^{kj}_{Hu}$

Table 19: ϕ^+ couplings to partner leptons and quarks [29, 37].

We see in Table 19 that the Feynman rules for the some vertices containing ϕ^+, neglecting the masses of the SM fermions, involve couplings of $\mathcal{O}(v^2/f^2)$. As each diagram contains at least two such vertices, if any, they are suppressed by a factor of $\mathcal{O}(v^4/f^4)$. So we do not take into account those contributions. Only the box diagram which involves interaction between $\Phi^+\overline{\nu_i^c}\ell_j$ with $\Phi^+\overline{u_i^c}d_j$ (and its h.c.) contributes. Finally we show in Figure 64 all box diagrams that appear when T-odd and partner fermions are considered.

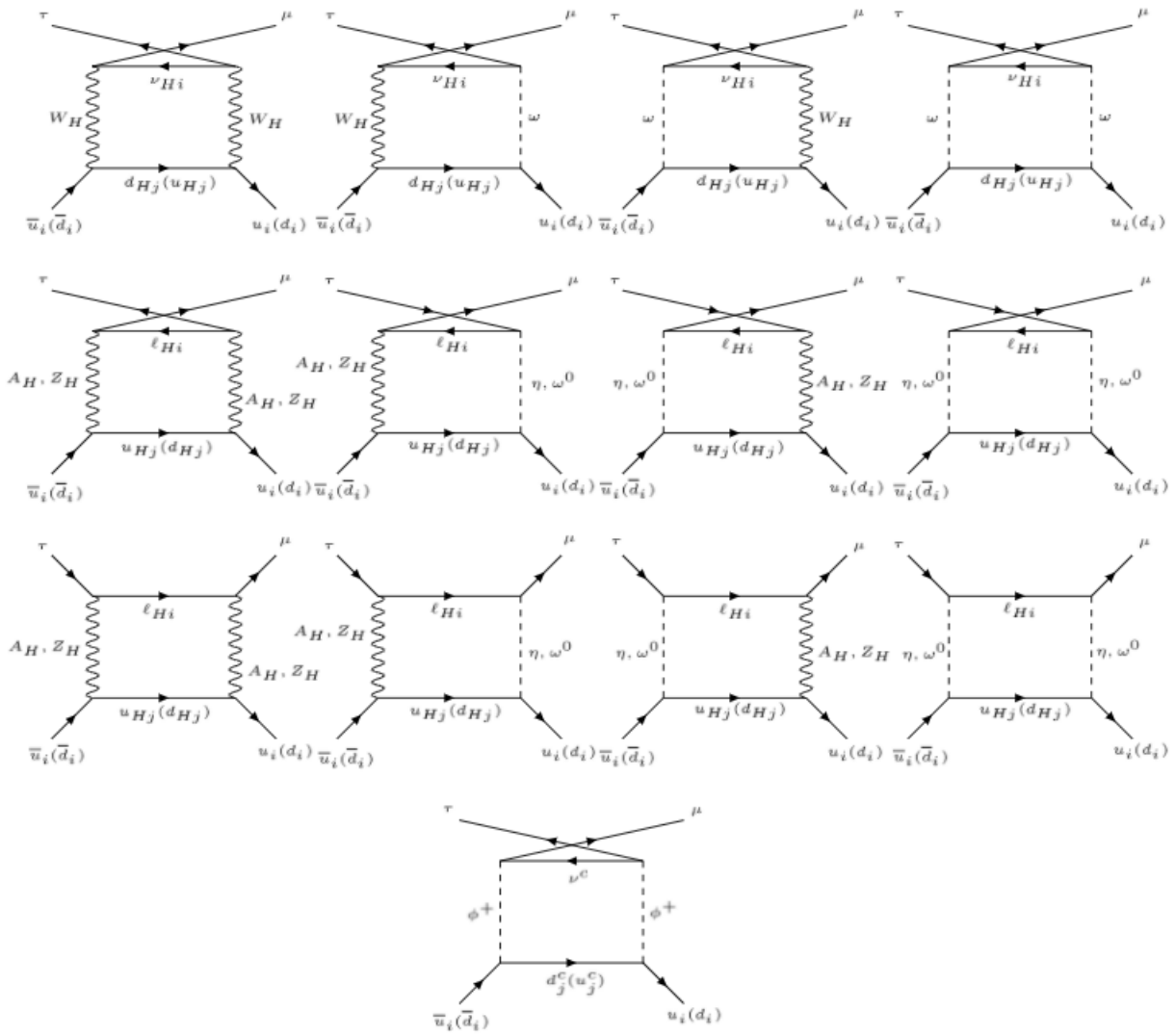

Figure 64: Box diagrams where T-odd particles, partner leptons and quarks, are involved.

The box amplitude is defined as

$$\mathcal{M}_{\text{box}}^{\text{T-odd}} = e^2 B_L^q(0)\overline{\mu}(p')\gamma^\mu P_L \tau(p)\overline{q}(p_q)\gamma_\mu P_L q(p_{\overline{q}}), \tag{584}$$

where $q = \{u, d, s\}$.

Therefore, in accordance to [37], the form factors from box diagrams are given by

$$
\begin{aligned}
B_L^u =& \frac{\alpha_W}{32\pi s_W^2}\left\{\frac{1}{M_W^2}\frac{v^2}{4f^2}\sum_{i,j}\chi_{ij}^u\left[-\left(8+\frac{1}{2}x_i^{\ell_H}y_j^{d_H}\right)\bar{d}_0(x_i^{\ell_H},y_j^{d_H})+4x_i^{\ell_H}y_j^{d_H}d_0(x_i^{\ell_H},y_j^{d_H})\right.\right.\\
&\left.\left.-\frac{3}{2}\bar{d}_0(x_i^{\nu_H}y_j^{d_H})-\frac{3}{50a}\bar{d}_0(ax_i^{\nu_H},ay_j^{d_H})+\frac{3}{5}\bar{d}_0(ax_i^{\nu_H},ay_j^{d_H},a)\right]+\frac{1}{f^2}\sum_{i,j}\bar{\chi}_{ij}^u\bar{d}_0\left(\frac{2m_{\nu_i^c}^2}{f^2},\frac{2m_{d_j^c}^2}{f^2}\right)\right\},\\
B_L^d =& \frac{\alpha_W}{32\pi s_W^2}\left\{\frac{1}{M_W^2}\frac{v^2}{4f^2}\sum_{i,j}\chi_{ij}^d\left[\left(2+\frac{1}{2}x_i^{\ell_H}y_j^{u_H}\right)\bar{d}_0(x_i^{\ell_H},y_j^{u_H})-4x_i^{\ell_H}y_j^{u_H}d_0(x_i^{\ell_H},y_j^{u_H})\right.\right.\\
&\left.\left.-\frac{3}{2}\bar{d}_0(x_i^{\nu_H}y_j^{u_H})-\frac{3}{50a}\bar{d}_0(ax_i^{\nu_H},ay_j^{u_H})-\frac{3}{5}\bar{d}_0(ax_i^{\nu_H},ay_j^{u_H},a)\right]+\frac{5}{f^2}\sum_{i,j}\bar{\chi}_{ij}^d\bar{d}_0\left(\frac{2m_{\nu_i^c}^2}{f^2},\frac{2m_{u_j^c}^2}{f^2}\right)\right\},
\end{aligned}
\tag{585}
$$

with $x_i^{(\nu,\ell)_H}=m_{(\nu,\ell)_H^i}^2/M_{W_H}^2$, $y_j^{(u,d)_H}=(m_{Hj}^{u,d})^2/M_{W_H}^2$, $a=M_{W_H}^2/M_{A_H}^2=5c_W^2/s_W^2$. The mixing coefficients involve mirror lepton mixing matrices as well as mirror quark ones

$$
\chi_{ij}^u=V_{H\ell}^{i\mu\dagger}V_{H\ell}^{i\tau}V_{Hq}^{ju\dagger}V_{Hq}^{ju},\quad \chi_{ij}^d=V_{H\ell}^{i\mu\dagger}V_{H\ell}^{i\tau}V_{Hq}^{jd\dagger}V_{Hq}^{jd},
\tag{586}
$$

and

$$
\begin{aligned}
\bar{\chi}_{ij}^u&=\sum_{k,n,r,s}V_{H\ell}^{k\mu\dagger}\frac{m_{\ell_{Hk}}}{M_{W_H}}W_{ki}^{\dagger}W_{in}\frac{m_{\ell_{Hn}}}{M_{W_H}}V_{H\ell}^{n\tau}V_{Hq}^{ru\dagger}\frac{m_{d_{Hr}}}{M_{W_H}}W_{rj}^{q\dagger}W_{js}^{q}\frac{m_{d_{Hs}}}{M_{W_H}}V_{Hq}^{su},\\
\bar{\chi}_{ij}^d&=\sum_{k,n,r,s}V_{H\ell}^{k\mu\dagger}\frac{m_{\ell_{Hk}}}{M_{W_H}}W_{ki}^{\dagger}W_{in}\frac{m_{\ell_{Hn}}}{M_{W_H}}V_{H\ell}^{n\tau}V_{Hq}^{rd\dagger}\frac{m_{u_{Hr}}}{M_{W_H}}W_{rj}^{q\dagger}W_{js}^{q}\frac{m_{u_{Hs}}}{M_{W_H}}V_{Hq}^{sd}.
\end{aligned}
\tag{587}
$$

In analogy to the lepton sector, the misalignment between the partner quark mass eigenstates and the mirror quarks as well as those between the mirror and SM quarks are parametrized by the corresponding 3×3 unitary matrices, V_{Hq}^i and W_{ij}^q, respectively.

10.1.2 Majorana contribution

Now, we are going to compute the $\mathcal{M}^{\rm Maj}$ contribution. As we showed in eq.(562), it is composed by three parts

$$
\mathcal{M}^{\rm Maj}=\mathcal{M}_{\gamma}^{\rm Maj}+\mathcal{M}_{Z}^{\rm Maj}+\mathcal{M}_{\rm box}^{\rm Maj},
\tag{588}
$$

γ and Z penguin diagrams and box diagrams which involve Majorana neutrinos. In this case we will work with the assumption that light Majorana neutrinos are massless, therefore just heavy Majorana neutrinos are taken into account.

The contributions from $\gamma-$ and $Z-$penguin diagrams and box diagrams are very similar to the ones

for $\mu \to e$ conversion in nuclei (see eq. (458)):

$$\mathcal{M}_{\gamma}^{\text{Maj}} = \frac{e^2}{Q^2}\overline{\mu}(p')[i2F_M^{\gamma}(Q^2)P_R\sigma^{\mu\nu}Q_\nu + F_L^{\gamma}(Q^2)\gamma^\mu P_L]\tau(p)\overline{q}(p_q)\gamma_\mu Q_q q(p_{\bar{q}}),$$
$$\mathcal{M}_{Z}^{\text{Maj}} = \frac{e^2}{M_Z^2}\overline{\mu}(p')[\gamma^\mu(F_L^Z P_L + F_R^Z P_R)]\tau(p)\overline{q}(p_q)[\gamma_\mu\left(g_{Lq}^Z P_L + g_{Rq}^Z P_R\right)]q(p_{\bar{q}}),$$
$$\mathcal{M}_{\text{box}}^{\text{Maj}} = e^2 B_L^q(0)\overline{\mu}(p')\gamma^\mu P_L\tau(p)\overline{q}(p_q)\gamma_\mu P_L q(p_{\bar{q}}), \tag{589}$$

with Q_q given by eq. (564) and the couplings $g_{L(R)q}^Z$ indicated in eq. (459).
The form factors F_M^{γ} (from Feynman diagrams II, IV, V and VI shown in the Figure 6), F_L^{γ} (from diagrams in Figure 38) and F_L^Z (see Figure 39) are given by (405), (406), and (414) respectively (omitting the light Majorana neutrinos contribution) are:

$$F_M^{\gamma} = F_M^{\chi^h} = \frac{\alpha_W}{16\pi}\frac{m_\tau}{M_W^2}\sum_{j=1}^{3}\theta_{\mu j}\theta_{\tau j}^{\dagger}F_M^{\chi^h}(y_j, Q^2), \tag{590}$$

$$F_L^{\gamma} = F_L^{\chi^h} = \frac{\alpha_W}{8\pi}\sum_{i}^{3}\theta_{\mu j}\theta_{\tau j}^{\dagger}F_L^{\chi^h}(y_j, Q^2),$$

$$F_L^{Z-\chi^h}(Q^2) = \frac{\alpha_W}{8\pi c_W s_W}\sum_{i,j=1}^{3}\left[\theta_{\mu i}\theta_{\tau i}^{\dagger}F^h(y_i;Q^2) + \theta_{\mu j}S_{ji}\theta_{\tau i}^{\dagger}\left(G^h(y_i,y_j;Q^2) + \frac{1}{\sqrt{y_i y_j}}H^h(y_i,y_j;Q^2)\right)\right], \tag{591}$$

where

$$F_M^{\chi^h}(y,Q^2) = \frac{1}{3} - \frac{2y^3-7y^2+11y}{4(1-y)^3} + \frac{3y}{2(1-y)^4}\ln y \tag{592}$$
$$- \frac{1}{24}\frac{Q^2}{M_j^2}\left(\frac{134y_j^5 - 759y_j^4 + 1941y_j^3 - 2879y_j^2 - 69y_j + 12}{60y_j(1-y_j)^5} + \frac{(4y_j^2 - 34y_j + 3)\ln y_j}{(1-y_j)^6}\right),$$

$$F_L^{\chi^h}(y,Q^2) = 2\Delta_\epsilon + \frac{Q^2}{M_j^2}\left(-\frac{(12y^2-10y+1)\ln y}{6y(1-y)^4} + \frac{20y^3-96y^2+57y+1}{36y(1-y)^3}\right), \tag{593}$$

with $y = \frac{M_W^2}{M_j^2}$, $\Delta_\epsilon = \frac{1}{\epsilon} - \gamma_E + \ln(4\pi) + \ln\left(\frac{\mu^2}{M_W^2}\right)$ which regulates the ultraviolet divergence in $4-2\epsilon$ dimensions, and is canceled by unitarity of mixing matrices (eq. (417)). The explicit functions F^h, G^h, and H^h are written in eq. (452), and their analytic expressions are in eq. (453) where it is

necessary to change M_Z^2 by Q^2 and the $(terms)$ expressions are as follows

$$
\begin{aligned}
F^h(y_i;Q^2) &\approx -\frac{5}{2}\,\ln y_i + \frac{Q^2}{M_j^2}\left(\frac{1}{12y_i}(1-2s_W^2)\,\ln y_i\right),\\
G^h(y_i,y_j;Q^2):\ (\text{terms}) &= -\frac{1}{12(1-y_i)^2}\frac{Q^2}{M_j^2}\left(\frac{(1-y_i)(3(1+y_j)-2y_i(2+6y_j-y_j^2)+y_i^2(1+y_j))}{(y_i-y_j)(1-y_j)^2}\right.\\
&\quad+\frac{(-6+y_i(3+15y_j-4y_j^2)+y_i^2(6-20y_j-4y_j^2)+y_i^2(6-20y_j+6y_j^2))\ln y_j}{(1-y_j)^3}\\
&\quad\left.+\frac{y_i(3-4y_j+6y_i(1+y_j)-12y_i^2)\ln\left(\frac{y_j}{y_i}\right)}{(y_i-y_j)^2}\right),\\
H^h(y_i,y_j;Q^2):\ (\text{terms}) &= -\frac{Q^2}{M_i^2}\frac{y_j}{6(1-y_i)^2}\left(-\frac{y_j(y_i(1+3y_j)-(3+y_j))\ln y_j}{(1-y_j)^3}\right.\\
&\quad\left.+\frac{(1-y_i)((1-3y_j-2y_j^2)-y_i+5y_iy_j)}{(y_i-y_j)(1-y_j)^2}+\frac{y_j(1-3y_i)\ln\left(\frac{y_j}{y_i}\right)}{(y_i-y_j)^2}\right).
\end{aligned}
\tag{594}
$$

For box diagrams we just consider the contribution coming from heavy Majorana neutrinos χ^h in Figure 40, they read

$$
B_L^d = \frac{\alpha_W}{16\pi M_W^2 s_W^2}\sum_{i,j=1}^{3}\theta_{\mu i}\theta_{\tau i}^{\dagger}|V_{jd}|^2 f_{B_d}\left(y_i,x_j^u\right), \tag{595}
$$

$$
B_L^u = \frac{\alpha_W}{16\pi M_W^2 s_W^2}\sum_{i,j=1}^{3}\theta_{\mu i}\theta_{\tau i}^{\dagger}|V_{uj}|^2 f_{B_u}(y_i,x_j^d), \tag{596}
$$

where $y_i = M_W^2/M_i^2$ with M_i the mass of heavy neutrinos, $x_i^q = m_{q_i}^2/M_W^2$ with m_{q_i} the mass of the i-th quark, V_{ij} is the CKM matrix. The f_{B_d} and f_{B_u} functions yield (eqs. (462) and (465) respectively)

$$
f_{B_d}(y_i,x_j^u) = \left(1+\frac{1}{4}\frac{x_j^u}{y_i}\right)\bar{d}_0^{lh}(y_i,x_j^u) - 2\frac{x_j^u}{y_i}d_0^{lh}(y_i,x_j^u), \tag{597}
$$

$$
f_{B_u}(y_i,x_j^d) = -\left(4+\frac{x_j^d}{4y_i}\right)\bar{d}_0^{lh}(y_i,x_j^u) + 2\frac{x_j^u}{y_i}d_0^{lh}(y_i,x_j^u). \tag{598}
$$

where $d_0^{lh}(y_i,x_j^u)$ and $\bar{d}_0^{lh}(y_i,x_j^u)$ are taken from eqs. (463) and (464).
Under the same assumption as in the calculation of $\mu \to e$ conversion in nuclei, the f_{B_q} functions become [48]

$$
\sum_{i=j}^{3}|V_{jd}|^2 f_{B_d}\left(y_i,x_j^u\right) = |V_{td}|^2\left[f_{B_d}(y_i,x_t) - f_{B_d}(y_i,0)\right] - f_{B_d}(y_i,0), \tag{599}
$$

$$\sum_{i=j}^{3} |V_{uj}|^2 f_{B_u}(y_i, x_j^d) = f_{B_u}(y_i, 0), \tag{600}$$

with $x_t = m_t^2/M_W^2$.

10.2 Hadronization

Tau decays we are considering have as final states pseudoscalar mesons and vector resonances. Hadronization of quark bilinears gives rise to the final-state hadrons.

Resonance Chiral Theory (RχT), that naturally includes Chiral Perturbation Theory (χPT), considers the resonances as active degrees of freedom into the Lagrangian since they participate in the dynamics of the processes. We are working under RχT scheme in order to hadronize the relevant currents involved in our analysis. For more details on the procedure followed in this part, see [75, 76] where the definitions of all expressions are fully given.

In Appendix H we write all the useful tools for the development which is shown next.

We remind that the complete amplitude has two contributions:

$$\mathcal{M} = \mathcal{M}^{\text{T-odd}} + \mathcal{M}^{\text{Maj}}, \tag{601}$$

where each one receives contributions coming from $\gamma-$, $Z-$penguins and box diagrams.

The F_M^γ form factor, considering both contributions of T-odd leptons (eq. (568)) and Majorana neutrinos (eq. (591)), is written as follows

$$\begin{aligned} F_M^\gamma =& \frac{\alpha_W}{16\pi}\frac{m_\tau}{M_W^2}\left\{\sum_{i=1}^{3}\left(\theta_{\mu i}\theta_{\tau i}^\dagger F_M^{\chi^h}(z_i,Q^2) + \frac{v^2}{4f^2}V_{H\ell}^{i\mu *}V_{H\ell}^{i\tau}\left[F_{W_H}(x_i^{\ell_H},Q^2) + F_{Z_H}(x_i^{\nu_H},Q^2) + \frac{1}{5}F_{Z_H}(ax_i^{\nu_H},Q^2)\right]\right)\right. \\ &\left. + \frac{1}{M_h^2}\frac{v^4}{4f^2}\sum_{i,j,k=1}^{3} V_{H\ell}^{i\mu\dagger}\kappa_{ii}W_{ij}^\dagger W_{jk}\kappa_{kk}V_{H\ell}^{k\tau}\left[F_{\bar{\nu^c}}\left(\frac{2m_{\nu_j^c}^2}{f^2},Q^2\right) + F_{\bar{\ell}^c}\left(\frac{2m_{\ell_j^c}^2}{f^2},Q^2\right)\right]\right\}, \end{aligned} \tag{602}$$

Similarly, F_L^γ can be written from eqs. (571) and (591) as

$$\begin{aligned} F_L^\gamma =& \frac{\alpha_W}{4\pi M_W^2}\left\{\sum_{i=1}^{3}\left(\frac{1}{2}\theta_{\mu i}\theta_{\tau i}^\dagger F_L^{\chi^h}(z_i,Q^2) + M_W^2\frac{Q^2}{M_{W_H}^2}V_{H\ell}^{i\mu *}V_{H\ell}^{i\tau}\left[G_W^{(1)}(x_i^{\ell_H}) + G_Z^{(1)}(x_i^{\nu_H}) + \frac{1}{5}G_Z^{(1)}(ax_i^{\nu_H})\right]\right)\right. \\ &\left. + v^2\frac{M_W^2}{M_h^2}\frac{Q^2}{M_{W_H}^2}\sum_{i,j,k=1}^{3} V_{H\ell}^{i\mu\dagger}\kappa_{ii}W_{ij}^\dagger W_{jk}\kappa_{kk}V_{H\ell}^{k\tau}\left[G_{\bar{\nu^c}}^{(1)}\left(\frac{2m_{\nu_i^c}^2}{f^2}\right) + G_{\bar{\ell}^c}^{(1)}\left(\frac{2m_{\nu_j^c}^2}{f^2}\right)\right]\right\}. \end{aligned} \tag{603}$$

The form factor coming from $Z-$penguin diagrams, taking into account T-odd particles (eq. (576)) as well as Majorana neutrinos (eq. (591)) reads

$$\begin{aligned}F_L^Z =&\frac{\alpha_W}{8\pi c_W s_W}\sum_{i,j=1}^{3}\left[\theta_{\mu i}\theta^\dagger_{\tau i}F^h(z_i;Q^2)+\theta_{\mu j}S_{ji}\theta^\dagger_{\tau i}\left(G^h(z_i,z_j;Q^2)+\frac{1}{\sqrt{z_i,z_j}}H^h(z_i,z_j;Q^2)\right)\right.\\&+\sum_i V^{i\mu\dagger}_{H\ell}V^{i\tau}_{H\ell}\left\{\frac{\upsilon^2}{8f^2}H_L^{W(0)}(x_i^{\ell_H})+\frac{Q^2}{M_{W_H}^2}\left[H_L^W(x_i^{\ell_H})+(1-2c_W^2)\left(\frac{1}{5}H_L^{A/Z}(ax_i^{\nu_H})+H_L^{A/Z}(x_i^{\nu_H})\right)\right]\right\}\\&\left.+\frac{Q^2}{M_\Phi^2}\frac{\upsilon^2}{2M_W^2}\sum_{ijk}V^{i\mu\dagger}_{H\ell}\kappa_{ii}W^\dagger_{ij}W_{jk}\kappa_{kk}V^{k\tau}_{H\ell}\left[H_L^{\bar\nu}\left(\frac{2m^2_{\nu_j^c}}{f^2}\right)+(1-2c_w^2)H_L^{\bar\ell}\left(\frac{2m^2_{\nu_j^c}}{f^2}\right)\right]\right].\end{aligned}\tag{604}$$

For box diagrams the B_L^q form factors are given by eqs. (585), (595) and (596)

$$\begin{aligned}B_L^u =& \frac{\alpha_W}{16\pi M_W^2 s_W^2}\left\{\sum_{i,j=1}^{3}\theta_{\mu i}\theta^\dagger_{\tau i}f_{B_u}(z_i,0)\right.\\&-\frac{\upsilon^2}{8f^2}\sum_{i,j}\chi^u_{ij}\left[\left(8+\frac{1}{2}x_i^{\ell_H}y_j^{d_H}\right)\bar d_0(x_i^{\ell_H},y_j^{d_H})-4x_i^{\ell_H}y_j^{d_H}d_0(x_i^{\ell_H},y_j^{d_H})\right.\\&\left.\left.+\frac{3}{2}\bar d_0(x_i^{\nu_H}y_j^{d_H})+\frac{3}{50a}\bar d_0(ax_i^{\nu_H},ay_j^{d_H})-\frac{3}{5}\bar d_0(ax_i^{\nu_H},ay_j^{d_H},a)\right]+\frac{M_W^2}{2f^2}\sum_{i,j}\bar\chi^u_{ij}\bar d_0\left(\frac{2m^2_{\nu_i^c}}{f^2},\frac{2m^2_{d_j^c}}{f^2}\right)\right\},\end{aligned}\tag{605}$$

$$\begin{aligned}B_L^d =& \frac{\alpha_W}{16\pi M_W^2 s_W^2}\left\{\sum_{i,j=1}^{3}\theta_{\mu i}\theta^\dagger_{\tau i}\left(|V_{td}|^2\left[f_{B_d}(z_i,x_t)-f_{B_d}(z_i,0)\right]-f_{B_d}(z_i,0)\right)\right.\\&+\frac{\upsilon^2}{8f^2}\sum_{i,j}\chi^d_{ij}\left[\left(2+\frac{1}{2}x_i^{\ell_H}y_j^{u_H}\right)\bar d_0(x_i^{\ell_H},y_j^{u_H})-4x_i^{\ell_H}y_j^{u_H}d_0(x_i^{\ell_H},y_j^{u_H})\right.\\&\left.\left.-\frac{3}{2}\bar d_0(x_i^{\nu_H}y_j^{u_H})-\frac{3}{50a}\bar d_0(ax_i^{\nu_H},ay_j^{u_H})-\frac{3}{5}\bar d_0(ax_i^{\nu_H},ay_j^{u_H},a)\right]+\frac{5}{2}\frac{M_W^2}{f^2}\sum_{i,j}\bar\chi^d_{ij}\bar d_0\left(\frac{2m^2_{\nu_i^c}}{f^2},\frac{2m^2_{u_j^c}}{f^2}\right)\right\},\end{aligned}\tag{606}$$

with $x_i^{(\nu,\ell)_H}=m^2_{(\nu,\ell)^i_H}/M^2_{W_H}$, $y_j^{(u,d)_H}=(m^{u,d}_{Hj})^2/M^2_{W_H}$, $a=M^2_{W_H}/M^2_{A_H}=5c_W^2/s_W^2$ and $z_i=M_W^2/M_i^2$ being M_i the heavy Majorana neutrino mass.

10.3 $\tau \to \mu P$

These decays where $P = \{\pi^0, \eta, \eta'\}$ are mediated only by axial-vector current (Z gauge boson) and box diagrams. Thus, the amplitude is given by

$$\mathcal{M}_{\tau\to\mu P} = \mathcal{M}_Z^P + \mathcal{M}_{\text{Box}}^P. \tag{607}$$

From Appendix H each contribution reads

$$\begin{aligned}\mathcal{M}_Z^P &= -i\frac{g^2}{2c_W}\frac{F}{M_Z^2}C(P)\sum_i \overline{\mu}(p')\left[\not{q}F_L^Z P_L\right]\tau(p),\\ \mathcal{M}_{\text{Box}}^P &= -ig^2F\sum_i B_i(P)\overline{\mu}(p')\left[\not{q}P_L\right]\tau(p),\end{aligned} \tag{608}$$

where $C(P)$ and $B_j(P)$ functions are shown in Appendix H, $F \simeq 0.0922$ GeV is the decay constant of the pion, F_L^Z is given by eq. (604) and, as we know, F_R^Z is negligible.
So we can write explicitly the amplitude for each decay considering $P = \{\pi^0, \eta, \eta'\}$. Mixing effects among these particles, which are isospin-suppressed [77], are negligible.

10.3.1 $\tau \to \mu\pi^0$

In this case where we are considering that $P = \pi^0$ with $\pi^0 = \frac{u\bar{u}-d\bar{d}}{\sqrt{2}}$, taking into account the $C(P)$ and $B_j(P)$ functions from Appendix H, the contributions to the amplitude become

$$\begin{aligned}\mathcal{M}_Z^{\pi^0} &= -i\frac{g^2}{2c_W}\frac{F}{M_Z^2}C(\pi^0)\overline{\mu}(p')\left[\not{q}F_L^Z P_L\right]\tau(p) = -i\frac{g^2}{2c_W}\frac{F}{M_Z^2}\overline{\mu}(p')\left[\not{q}F_L^Z P_L\right]\tau(p),\\ \mathcal{M}_{\text{Box}}^{\pi^0} &= -ig^2FB(\pi^0)\overline{\mu}(p')\left[\not{q}P_L\right]\tau(p) = -ig^2F\frac{1}{2}(B_L^d - B_L^u)\overline{\mu}(p')\left[\not{q}P_L\right]\tau(p).\end{aligned} \tag{609}$$

Unlike the expressions from Appendix H, in the equation above the sum over the mixing matrices does not appear because it is included within the form factors F_L^Z and B_L^q, which are defined in eqs. (604), (605) and (606).
We can write the branching ratio of this decay as follows

$$\text{Br}(\tau \to \mu\pi^0) = \frac{1}{4\pi}\frac{\lambda^{1/2}(m_\tau^2, m_\mu^2, m_{\pi^0}^2)}{m_\tau^2\Gamma_\tau}\frac{1}{2}\sum_{i,f}|\mathcal{M}_{\tau\to\mu\pi^0}|^2, \tag{610}$$

where $\mathcal{M}_{\tau\to\mu P}$ is defined in eq. (739). Hence, it yields

$$\sum_{i,f}|\mathcal{M}_{\tau\to\mu\pi^0}|^2 = \frac{1}{2m_\tau}\sum_{k,l}\left[(m_\tau^2 + m_\mu^2 - m_{\pi^0}^2)(a_{\pi^0}^k a_{\pi^0}^{l*} + b_{\pi^0}^k b_{\pi^0}^{l*}) + 2m_\mu m_\tau(a_{\pi^0}^k a_{\pi^0}^{l*} - b_{\pi^0}^k b_{\pi^0}^{l*})\right]. \tag{611}$$

Considering from [6] $m_{\pi^0} = 134.9768$ MeV, $m_\mu = 105.6583$ MeV, and $m_\tau = 1776.86$ MeV

$$\sum_{i,f} |\mathcal{M}_{\tau\to\mu\pi^0}|^2 = \frac{1}{2m_\tau}\sum_{k,l}\left[(m_\tau^2 + m_\mu^2 - m_{\pi^0}^2)(a^k_{\pi^0}a^{l*}_{\pi^0} + b^k_{\pi^0}b^{l*}_{\pi^0}) + 2m_\mu m_\tau(a^k_{\pi^0}a^{l*}_{\pi^0} - b^k_{\pi^0}b^{l*}_{\pi^0})\right],$$
$$\approx (886.44\text{ MeV})\sum_{k,l}\left[1.12a^k_{\pi^0}a^{l*}_{\pi^0} + 0.88b^k_{\pi^0}b^{l*}_{\pi^0}\right]. \tag{612}$$

The generic expressions for a_P^k and b_P^k are indicated in eq. (746), for $P = \pi^0$ they become

$$\begin{aligned} a^Z_{\pi^0} &= -\frac{1}{2M_Z^2 s_W^2 c_W}\frac{F}{2}\Delta_{\tau\mu}F_L^Z, \\ b^Z_{\pi^0} &= -\frac{1}{2M_Z^2 s_W^2 c_W}\frac{F}{2}\Sigma_{\tau\mu}F_L^Z, \\ a^B_{\pi^0} &= -\frac{F}{2s_W^2}\Delta_{\tau\mu}\frac{1}{2}(B_L^d - B_L^u), \\ b^B_{\pi^0} &= -\frac{F}{2s_W^2}\Sigma_{\tau\mu}\frac{1}{2}(B_L^d - B_L^u). \end{aligned} \tag{613}$$

10.3.2 $\tau \to \mu\eta$

Considering $P = \eta$ with $\eta \approx \frac{1}{\sqrt{6}}(u\bar{u} + d\bar{d} - 2s\bar{s})$ [6], and $C(P)$ and $B_j(P)$ functions from Appendix H, the contributions to the amplitude are given by

$$\begin{aligned} \mathcal{M}_Z^\eta &= -i\frac{g^2}{2c_W}\frac{F}{M_Z^2}\frac{1}{\sqrt{6}}\left(\sin\theta_\eta + \sqrt{2}\cos\theta_\eta\right)\overline{\mu}(p')\left[\not{q}F_L^Z P_L\right]\tau(p), \\ \mathcal{M}_{\text{Box}}^\eta &= -ig^2F\frac{1}{2\sqrt{3}}\left[(\sqrt{2}\sin\theta_\eta - \cos\theta_\eta)B_L^u + (2\sqrt{2}\sin\theta_\eta + \cos\theta_\eta)B_L^d\right]\overline{\mu}(p')\left[\not{q}P_L\right]\tau(p). \end{aligned} \tag{614}$$

The branching ratio reads

$$\text{Br}(\tau\to\mu\eta) = \frac{1}{4\pi}\frac{\lambda^{1/2}(m_\tau^2, m_\mu^2, m_\eta^2)}{m_\tau^2\Gamma_\tau}\frac{1}{2}\sum_{i,f}|\mathcal{M}_{\tau\to\mu\eta}|^2, \tag{615}$$

where $\mathcal{M}_{\tau\to\mu\eta}$ yields

$$\sum_{i,f}|\mathcal{M}_{\tau\to\mu\eta}|^2 = \frac{1}{2m_\tau}\sum_{k,l}\left[(m_\tau^2 + m_\mu^2 - m_\eta^2)(a^k_\eta a^{l*}_\eta + b^k_\eta b^{l*}_\eta) + 2m_\mu m_\tau(a^k_\eta a^{l*}_\eta - b^k_\eta b^{l*}_\eta)\right]. \tag{616}$$

[6] A more refined hadronization requires using the double-angle mixing scheme for the $\eta - \eta'$ mesons [78]. See, for instance, Refs. [79, 80].

From [6] $m_\eta = 547.862$ MeV and $m_{\mu,\tau}$ given previously, we get

$$\begin{aligned}\sum_{i,f}|\mathcal{M}_{\tau\to\mu\eta}|^2 &= \frac{1}{2m_\tau}\sum_{k,l}\left[(m_\tau^2+m_\mu^2-m_\eta^2)(a_\eta^k a_\eta^{l*}+b_\eta^k b_\eta^{l*})+2m_\mu m_\tau(a_\eta^k a_\eta^{l*}-b_\eta^k b_\eta^{l*})\right],\\ &\approx (807.10\text{ MeV})\sum_{k,l}\left[1.13a_\eta^k a_\eta^{l*}+0.87b_\eta^k b_\eta^{l*}\right].\end{aligned} \tag{617}$$

For $P=\eta$ from eq. (742) and (743) the a_P^k and b_P^k factors turn out to be

$$\begin{aligned}a_\eta^Z &= -\frac{g^2}{2M_Z^2 c_W}\frac{F}{2}\frac{1}{\sqrt{6}}\left(\sin\theta_\eta+\sqrt{2}\cos\theta_\eta\right)\Delta_{\tau\mu}F_L^Z,\\ b_\eta^Z &= -\frac{g^2}{2M_Z^2 c_W}\frac{F}{2}\frac{1}{\sqrt{6}}\left(\sin\theta_\eta+\sqrt{2}\cos\theta_\eta\right)\Sigma_{\tau\mu}F_L^Z,\\ a_\eta^B &= -\frac{g^2F}{2}\Delta_{\tau\mu}\frac{1}{2\sqrt{3}}\left[(\sqrt{2}\sin\theta_\eta-\cos\theta_\eta)B_L^u+(2\sqrt{2}\sin\theta_\eta+\cos\theta_\eta)B_L^d\right],\\ b_\eta^B &= -\frac{g^2F}{2}\Sigma_{\tau\mu}\frac{1}{2\sqrt{3}}\left[(\sqrt{2}\sin\theta_\eta-\cos\theta_\eta)B_L^u+(2\sqrt{2}\sin\theta_\eta+\cos\theta_\eta)B_L^d\right].\end{aligned} \tag{618}$$

10.3.3 $\tau\to\mu\eta'$

For the case $P=\eta'$ with $\eta'\approx\frac{1}{\sqrt{3}}(u\bar{u}+d\bar{d}+s\bar{s})$ taking the $C(P)$ and $B_j(P)$ functions from Appendix H, the amplitude contributions are written as follows

$$\begin{aligned}\mathcal{M}_Z^\eta &= -i\frac{g^2}{2c_W}\frac{F}{M_Z^2}\frac{1}{\sqrt{6}}\left(\sqrt{2}\sin\theta_\eta-\cos\theta_\eta\right)\overline{\mu}(p')\left[\not{q}F_L^Z P_L\right]\tau(p),\\ \mathcal{M}_{\text{Box}}^\eta &= -ig^2F\frac{1}{2\sqrt{3}}\left[(\sin\theta_\eta-2\sqrt{2}\cos\theta_\eta)B_L^d-(\sin\theta_\eta+\sqrt{2}\cos\theta_\eta)B_L^u\right]\overline{\mu}(p')\left[\not{q}P_L\right]\tau(p).\end{aligned} \tag{619}$$

The branching fraction is given by

$$\text{Br}(\tau\to\mu\eta') = \frac{1}{4\pi}\frac{\lambda^{1/2}(m_\tau^2,m_\mu^2,m_{\eta'}^2)}{m_\tau^2\Gamma_\tau}\frac{1}{2}\sum_{i,f}|\mathcal{M}_{\tau\to\mu\eta'}|^2, \tag{620}$$

where $\mathcal{M}_{\tau\to\mu\eta'}$ yields

$$\sum_{i,f}|\mathcal{M}_{\tau\to\mu\eta'}|^2 = \frac{1}{2m_\tau}\sum_{k,l}\left[(m_\tau^2+m_\mu^2-m_{\eta'}^2)(a_{\eta'}^k a_{\eta'}^{l*}+b_{\eta'}^k b_{\eta'}^{l*})+2m_\mu m_\tau(a_{\eta'}^k a_{\eta'}^{l*}-b_{\eta'}^k b_{\eta'}^{l*})\right]. \tag{621}$$

From [6] $m_{\eta'} = 957.78$ MeV and $m_{\mu,\tau}$ given previously, we obtain

$$\begin{aligned}\sum_{i,f}|\mathcal{M}_{\tau\to\mu\eta'}|^2 &= \frac{1}{2m_\tau}\sum_{k,l}\left[(m_\tau^2+m_\mu^2-m_{\eta'}^2)(a^k_{\eta'}a^{l*}_{\eta'}+b^k_{\eta'}b^{l*}_{\eta'})+2m_\mu m_\tau(a^k_{\eta'}a^{l*}_{\eta'}-b^k_{\eta'}b^{l*}_{\eta'})\right],\\ &\approx (633.43\text{ MeV})\sum_{k,l}\left[1.17a^k_{\eta'}a^{l*}_{\eta'}+0.83b^k_{\eta'}b^{l*}_{\eta'}\right].\end{aligned} \tag{622}$$

For $P=\eta'$ from eq. (742) and (743) in Appendix H the a_P^k and b_P^k factors become

$$\begin{aligned}a^Z_{\eta'} &= -\frac{g^2}{2M_Z^2c_W}\frac{F}{2}\frac{1}{\sqrt{6}}\left(\sqrt{2}\sin\theta_\eta-\cos\theta_\eta\right)\Delta_{\tau\mu}F_L^Z,\\ b^Z_{\eta'} &= -\frac{g^2}{2M_Z^2c_W}\frac{F}{2}\frac{1}{\sqrt{6}}\left(\sqrt{2}\sin\theta_\eta-\cos\theta_\eta\right)\Sigma_{\tau\mu}F_L^Z,\\ a^B_{\eta'} &= -\frac{g^2F}{2}\Delta_{\tau\mu}\frac{1}{2\sqrt{3}}\left[(\sin\theta_\eta-2\sqrt{2}\cos\theta_\eta)B_L^d-(\sin\theta_\eta+\sqrt{2}\cos\theta_\eta)B_L^u\right],\\ b^B_{\eta'} &= -\frac{g^2F}{2}\Sigma_{\tau\mu}\frac{1}{2\sqrt{3}}\left[(\sin\theta_\eta-2\sqrt{2}\cos\theta_\eta)B_L^d-(\sin\theta_\eta+\sqrt{2}\cos\theta_\eta)B_L^u\right].\end{aligned} \tag{623}$$

10.4 $\tau\to\mu PP$

In this part we will consider the decays into the pairs $P\overline{P}=\{\pi^+\pi^-,K^+K^-,K^0\overline{K^0}\}$ (others are CKM- or isospin-suppressed). The contributions to this kind of decays come from $\gamma-$, $Z-$ penguins and box diagrams. Thus, the total amplitude can be written as follows

$$\mathcal{M}_{\tau\to\mu PP}=\mathcal{M}_\gamma^{P\overline{P}}+\mathcal{M}_Z^{P\overline{P}}+\mathcal{M}_{\text{Box}}^{P\overline{P}}. \tag{624}$$

Using the expressions shown in Appendix H we hadronize the quark bilinears and get the contributions for each decay that are presented next.

10.4.1 $\tau\to\mu\pi^+\pi^-$

As mentioned earlier, the total amplitude receives three contributions coming from $\gamma-$, $Z-$ penguins and box diagrams, hence the amplitude for this decay is

$$\mathcal{M}_{\tau\to\mu\pi^+\pi^-}=\mathcal{M}_\gamma^{\pi^+\pi^-}+\mathcal{M}_Z^{\pi^+\pi^-}+\mathcal{M}_{\text{Box}}^{\pi^+\pi^-}, \tag{625}$$

where each amplitude is given by eq. (749) (see Appendix H)

$$\begin{aligned}
\mathcal{M}_{\gamma}^{\pi^+\pi^-} =& \frac{e^2}{Q^2} F_V^{\pi\pi}(s)\overline{\mu}(p')[Q^2(\not{p}_q - \not{p}_{\overline{q}})F_L^{\gamma}(Q^2)P_L + 2im_\tau p_q^\mu \sigma_{\mu\nu} p_{\overline{q}}^\nu F_M^{\gamma}(Q^2)P_R]\tau(p), \\
\mathcal{M}_{Z}^{\pi^+\pi^-} =& g^2 \frac{2s_W^2 - 1}{2c_W M_Z^2} F_V^{\pi\pi}(s)\overline{\mu}(p')(\not{p}_q - \not{p}_{\overline{q}})[F_L^{Z}P_L]\tau(p), \\
\mathcal{M}_{\text{Box}}^{\pi^+\pi^-} =& \frac{g^2}{2} F_V^{\pi\pi}(s)(B_L^u - B_L^d)\overline{\mu}(p')(\not{p}_q - \not{p}_{\overline{q}})P_L\tau(p),
\end{aligned} \tag{626}$$

(recalling that the sum over the mixing matrices does not appear because it is included within the form factors). The vector form factor $F_V^{\pi\pi}$ is given by eq. (757) in Appendix I.
From Appendix H the branching ratio for this decay yields

$$\text{Br}(\tau \to \mu\pi^+\pi^-) = \frac{1}{64\pi^3 m_\tau^2 \Gamma_\tau} \int_{s_-}^{s_+} ds \int_{t_-}^{t_+} dt \frac{1}{2} \sum_{i,f} |\mathcal{M}_{\tau\to\mu\pi^+\pi^-}|^2, \tag{627}$$

where $s = (p_q + p_{\overline{q}})^2$ and $t = (p - p_{\overline{q}})^2$, so the limits of the integrals are

$$\begin{aligned}
t_-^+ &= \frac{1}{4s}\left[\left(m_\tau^2 - m_\mu^2\right)^2 - \left(\lambda^{1/2}(s, m_{\pi^+}^2, m_{\pi^-}^2) \mp \lambda^{1/2}(m_\tau^2, s, m_\mu^2)\right)^2\right], \\
s_- &= 4m_{\pi^+}^2, \\
s_+ &= (m_\tau - m_\mu)^2.
\end{aligned} \tag{628}$$

10.4.2 $\tau \to \mu K^+ K^-$

The total amplitude for this decays reads as

$$\mathcal{M}_{\tau\to\mu K^+K^-} = \mathcal{M}_{\gamma}^{K^+K^-} + \mathcal{M}_{Z}^{K^+K^-} + \mathcal{M}_{\text{Box}}^{K^+K^-}, \tag{629}$$

where from Appendix H each amplitude can be written

$$\begin{aligned}
\mathcal{M}_{\gamma}^{K^+K^-} =& \frac{e^2}{Q^2} F_V^{K^+K^-}(s)\overline{\mu}(p')[Q^2(\not{p}_q - \not{p}_{\overline{q}})F_L^{\gamma}(Q^2)P_L + 2im_\tau p_q^\mu \sigma_{\mu\nu} p_{\overline{q}}^\nu F_M^{\gamma}(Q^2)P_R]\tau(p), \\
\mathcal{M}_{Z}^{K^+K^-} =& g^2 \frac{2s_W^2 - 1}{2c_W M_Z^2} F_V^{K^+K^-}(s)\overline{\mu}(p')(\not{p}_q - \not{p}_{\overline{q}})[F_L^{Z}P_L]\tau(p), \\
\mathcal{M}_{\text{Box}}^{K^+K^-} =& \frac{g^2}{2} F_V^{K^+K^-}(s)(B_L^u - B_L^d)\overline{\mu}(p')(\not{p}_q - \not{p}_{\overline{q}})P_L\tau(p),
\end{aligned} \tag{630}$$

the vector form factor $F_V^{K^+K^-}$ is shown in Appendix I. The branching ratio expression is very similar to $\tau \to \mu\pi^+\pi^+$, we just need to replace m_π by m_K in the integral limits.

10.4.3 $\tau \to \mu K^0 \overline{K^0}$

The total amplitude is given by

$$\mathcal{M}_{\tau\to\mu K^0\overline{K^0}} = \mathcal{M}_{\gamma}^{K^0\overline{K^0}} + \mathcal{M}_{Z}^{K^0\overline{K^0}} + \mathcal{M}_{\text{Box}}^{K^0\overline{K^0}}. \tag{631}$$

From Appendix H each amplitude is expressed as follows

$$\begin{aligned}
\mathcal{M}_{\gamma}^{K^0\overline{K^0}} =& \frac{e^2}{Q^2} F_V^{K^0\overline{K^0}}(s)\overline{\mu}(p')[Q^2(\not{p}_q - \not{p}_{\overline{q}})F_L^{\gamma}(Q^2)P_L + 2im_\tau p_q^\mu \sigma_{\mu\nu} p_{\overline{q}}^\nu F_M^{\gamma}(Q^2)P_R]\tau(p),\\
\mathcal{M}_{Z}^{K^0\overline{K^0}} =& g^2 \frac{2s_W^2 - 1}{2c_W M_Z^2} F_V^{K^0\overline{K^0}}(s)\overline{\mu}(p')(\not{p}_q - \not{p}_{\overline{q}})[F_L^{Z}P_L]\tau(p),\\
\mathcal{M}_{\text{Box}}^{K^0\overline{K^0}} =& \frac{g^2}{2} F_V^{K^0\overline{K^0}}(s)(B_L^u - B_L^d)\overline{\mu}(p')(\not{p}_q - \not{p}_{\overline{q}})P_L\tau(p),
\end{aligned} \tag{632}$$

with $F_V^{K^0\overline{K^0}}$ given in Appendix I. The branching ratio can be obtained from eq. (750) with $m_{P_1} = m_{P_2} = m_{K^0}$ in the limits of the integral.

10.5 $\tau \to \mu V$

The calculation of observables involving hadron resonances as external states is not properly defined within quantum field theory because hadron resonances decay strongly and are not proper asymptotic states, as is required in that framework. When an experiment measures a final state with a vector resonance, the experiment reconstructs its structure from the pair of pseudoscalar mesons with a squared total mass approaching m_V^2, where $V = \rho, \phi$. For instance, from the chiral point of view, two pions in a $J = I = 1$ state are indistinguishable from a ρ. Then, following the expressions from Appendix H the branching ratios can be obtained. The procedure is very similar to $\tau \to \mu PP$ decays, we need to computed the same integral (eq. 750) where now the limits on s are different. They are given by eq. (753).

10.6 Numerical Analysis

First of all, we recall the masses of particles which come from LHT that are involved in the processes under study [24, 25, 29]:

$$\begin{aligned}
&M_W = \frac{\upsilon}{2s_W}\left(1 - \frac{\upsilon^2}{12f^2}\right), \quad M_Z = M_W/c_W, \quad \upsilon \simeq 246 \text{ GeV}, \quad (\rho \text{ factor is conserved}),\\
&M_{W_H} = M_{Z_H} = \frac{f}{s_W}\left(1 - \frac{\upsilon^2}{8f^2}\right), \quad M_{A_H} = \frac{f}{\sqrt{5}c_W}\left(1 - \frac{5\upsilon^2}{8f^2}\right), \quad M_\Phi = \sqrt{2}M_h\frac{f}{\upsilon},\\
&m_{\ell_H^i} = \sqrt{2}\kappa_{ii} f \equiv m_{Hi}, \quad m_{\nu_H^i} = m_{Hi}\left(1 - \frac{\upsilon^2}{8f^2}\right), \quad m_{\ell^c,\nu^c} = \kappa_2,
\end{aligned} \tag{633}$$

with M_h being the mass of the SM Higgs scalar, κ_{ii} the diagonal entries of the κ matrix (see eq. (323)) (similarly for the masses of T-odd quarks with κ^q_{ii} instead of κ_{ii} and replacing d_H-quark by ℓ_H and u_H-quark by ν_H) and κ_2 the mass matrix of partner leptons from eq. (560) (κ^q_2 similarly for partner quarks of u and d types). Due to $M_h = 125.25 \pm 0.17$ GeV [6] and $\upsilon \simeq 246$ GeV, we can approximate

$$M_\Phi = \sqrt{2} M_h \frac{f}{\upsilon} \approx \frac{\sqrt{2}}{2} f, \tag{634}$$

and assuming universality [39],

$$|\kappa_{ii}| < 0.17 \left(\frac{M_i}{\text{TeV}}\right) \leq 2.136 \left(\frac{f}{\text{TeV}}\right), \tag{635}$$

for f larger than a TeV. This effective description requires $M_i \lesssim 4\pi f$ with M_i the heavy Majorana neutrino masses.

So far, the free parameters are: f (scale of new physics); κ_{ii} and κ^q_{ii} (Yukawa couplings for T-odd leptons and quarks); κ_2 and κ^q_2, mass matrices for partner leptons.

The expressions χ^u_{ij}, χ^d_{ij}, $\bar{\chi}^u_{ij}$ and $\bar{\chi}^d_{ij}$ (see eq. (587)) describe the interaction vertices from box diagrams, those can be re-written in terms of free parameters as follows

$$\begin{aligned}
\bar{\chi}^u_{ij} &= \frac{\upsilon^4}{4M_W^4} \sum_{k,n,r,s} V^{k\mu\dagger}_{H\ell} \kappa_{kk} W^\dagger_{ki} W_{in} \kappa_{nn} V^{n\tau}_{H\ell} V^{ru\dagger}_{Hq} \kappa^d_{rr} W^{q\dagger}_{rj} W^q_{js} \kappa^d_{ss} V^{su}_{Hq}, \\
\bar{\chi}^d_{ij} &= \frac{\upsilon^4}{4M_W^4} \left(1 - \frac{\upsilon^2}{8f^2}\right)^2 \sum_{k,n,r,s} V^{k\mu\dagger}_{H\ell} \kappa_{kk} W^\dagger_{ki} W_{in} \kappa_{nn} V^{n\tau}_{H\ell} V^{rd\dagger}_{Hq} \kappa^u_{rr} W^{q\dagger}_{rj} W^q_{js} \kappa^u_{ss} V^{sd}_{Hq},
\end{aligned} \tag{636}$$

where we see a small shift between interaction vertices of order $\mathcal{O}(\upsilon^2/8f^2)$. The mixing matrix of heavy Majorana neutrinos is bounded by eq. (402)

$$|\theta_{\mu j} \theta^\dagger_{\tau j}| < 0.011. \tag{637}$$

Considering just mixing between two lepton families the mixing matrix of T-odd leptons ($V^{i\mu *}_{H\ell} V^{i\tau}_{H\ell}$) and the mixing matrix among partner leptons ($W^\dagger_{ij} W_{jk}$) can be parameterized as follows [37]

$$V = \begin{pmatrix} 1 & 0 & 0 \\ 0 & \cos\theta_V & \sin\theta_V \\ 0 & -\sin\theta_V & \cos\theta_V \end{pmatrix}, \quad W = \begin{pmatrix} 1 & 0 & 0 \\ 0 & \cos\theta_W & \sin\theta_W \\ 0 & -\sin\theta_W & \cos\theta_W \end{pmatrix}, \tag{638}$$

where $\theta_V, \theta_W \in [0, \pi/2)$ is the physical range for the mixing angles and θ_W must not be confused with the weak-mixing ('Weinberg') angle. We have assumed $\mu - \tau$ mixing, similarly for the evaluation of processes with $\tau - e$ but the 2×2 rotation matrices now involve the first and third T–odd lepton families (analogous mixings, in the top left 2×2 submatrix, can be used for quark contributions to

$\mu \to e$ conversion in nuclei).

We will assume no extra quark mixing and degenerate heavy quarks, then $V^q_{H\ell}$ and W^q will be equal to the identity. Therefore, the other free parameter are: θ_V, θ_W and neutral couplings of heavy Majorana neutrinos: $(\theta S \theta^\dagger)_{\mu\tau}$.

For the form factors we do a consistent expansion on the squared transfer momenta over both the squared masses of heavy particles Q^2/λ^2 being $\lambda = \{M_{W_H}, M_{Z_H}, M_{A_H}, M_\Phi, M_i\}$. This amounts to an expansion, at the largest, in the m_τ^2/f^2 ratio.

For completeness, we include two analyses: first we do not assume heavy Majorana neutrinos contributions and the second case involves the presence of heavy Majorana neutrinos raising from the Inverse See Saw mechanism seen in previous sections. We have decided to include the first case because there is not a previous analysis without contributions coming from Majorana neutrinos for those processes.

10.6.1 $\tau \to \ell P$ $(\ell = e, \mu)$

We begin the discussion of results with the case where the processes have no Majorana neutrinos. These processes are computed in a single Monte Carlo simulation which runs them simultaneously. The resulting values obtained from our analysis are shown in Table 20.

$\tau \to \ell P$ $(\ell = e, \mu)$ (C.L. = 90%) without Majorana neutrinos contribution.			
New physics (NP) scale (TeV)		Mixing angles	
f	1.49	θ_V	42.78°
Branching ratio		θ_W	42.69°
$\mathrm{Br}(\tau \to e\pi^0)$	5.24×10^{-9}	Masses of partner leptons ($m_{\nu^c} = m_{\ell^c}$)(TeV)	
$\mathrm{Br}(\tau \to \mu\pi^0)$	3.42×10^{-9}	$m_{\nu_1^c}$	3.12
$\mathrm{Br}(\tau \to e\eta)$	2.32×10^{-9}	$m_{\nu_2^c}$	3.15
$\mathrm{Br}(\tau \to \mu\eta)$	1.91×10^{-9}	$m_{\nu_3^c}$	3.37
$\mathrm{Br}(\tau \to e\eta')$	2.20×10^{-8}	Masses of partner quarks ($m_{u^c} = m_{d^c}$) (TeV)	
$\mathrm{Br}(\tau \to \mu\eta')$	1.79×10^{-8}	$m_{u_i^c}$	3.55
Masses of T-odd leptons (TeV)			
$m_{\ell_H^1}$	2.11		
$m_{\ell_H^2}$	2.11		
$m_{\ell_H^3}$	2.12		
$m_{\nu_H^1}$	2.10		
$m_{\nu_H^2}$	2.11		
$m_{\nu_H^3}$	2.11		
Masses of T-odd quarks (TeV)			
$m_{d_H^i}$	2.71		
$m_{u_H^i}$	2.70		

Table 20: Mean values for branching ratios, masses of LHT heavy particles, and mixing angles obtained by Monte Carlo simulation of $\tau \to \ell P$ $(\ell = e, \mu)$ processes where Majorana neutrinos contribution is not considered.

During all Monte Carlo simulations of our analysis each branching ratio has been delimited considering their C.L. with aid of SpaceMath package [81].

We observe that T-odd leptons are lighter than T-odd quarks by 0.6 TeV which means that $|\kappa_{ii}| < |\kappa^q_{ii}|$, that is, the Yukawa couplings of T-odd quarks are more intense ($|\kappa_{ii}| < 1.002$ and $|\kappa^q_{ii}| < 1.282$). We recall that in our model we are considering degenerate T-odd quarks for simplicity.

Regarding partner leptons ($m_{\nu^c_i}$) and partner quarks ($m_{u^c_i}$) their masses are above 3 TeV, being the latter the heaviest particles coming from LHT.

The mean values for mixing angles θ_V and θ_W are 42.78° and 42.69°, respectively. If these values are transformed to rad (perhaps it is a more comfortable way to read this information), they become $\theta_V \approx \theta_W \approx \pi/4.2$. This result is close to maximize the LFV effects, since this happens when $\theta_V = \theta_W = \pi/4$.

In Figures 65 and 66 the correlations among branching ratios and their free parameters are shown for both decay modes, $\ell = e$ and $\ell = \mu$. We want to highlight the free parameters that have sizeable correlations among them. The magnitude of Yukawa couplings for T-odd leptons is anticorrelated with the T-odd quark ones. This could explain why the T-odd leptons are lighter than T-odd quarks. On the other hand, the correlations among the Yukawa couplings of T-odd leptons are high, which implies their masses are very similar.

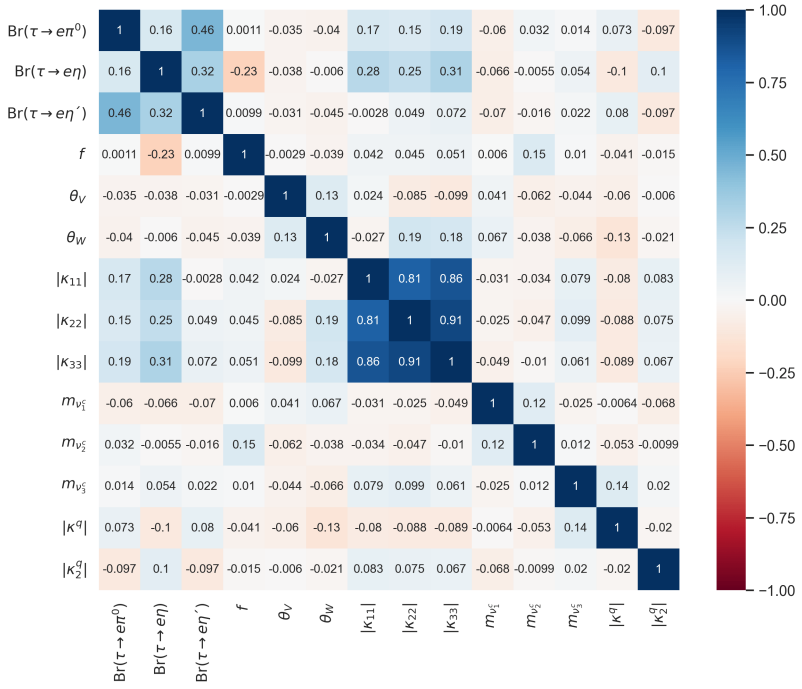

Figure 65: Heat map where we can see that there is no correlation among $\tau \to eP$ decays and their free parameters (case without Majorana neutrinos).

In the following scatter plots in Figures 67 and 68 we observe that the data accumulates in the lower left corner, which means that we have more points with small branching ratios. In Figures 69

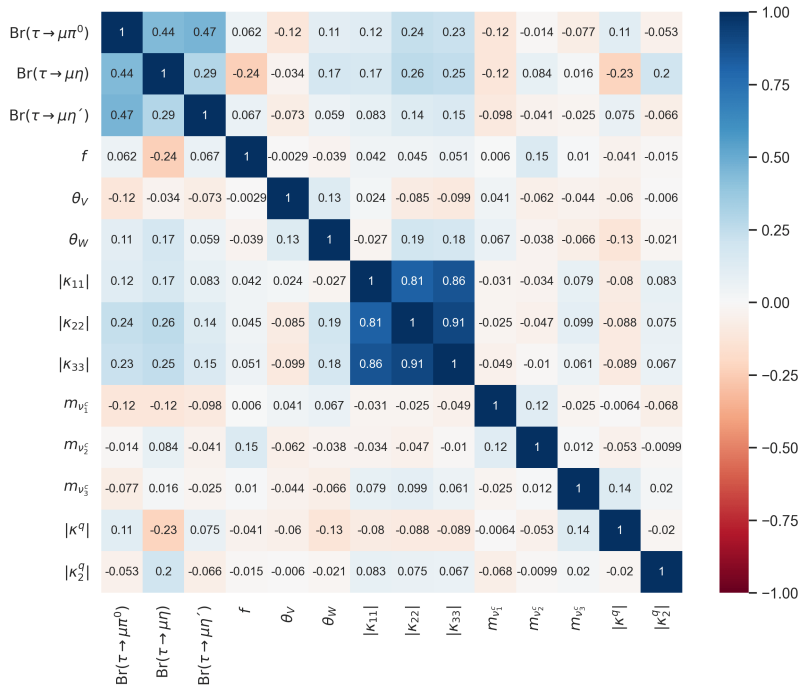

Figure 66: Heat map for $\tau \to \mu P$ decays and their free parameters, where we see a similar behavior to $\tau \to eP$ decays (case without Majorana neutrinos).

and 70 we see how the branching ratios for both decay modes behave versus f. In both scatter plots the decay mode with $P = \eta'$ reaches the highest values, meanwhile the $P = \eta$ channel is the most restricted one.

The mean values of branching ratios from our numerical analysis are at most just by 2 orders of magnitude smaller than the current ones [6], recalling that we considered only particles from LHT.

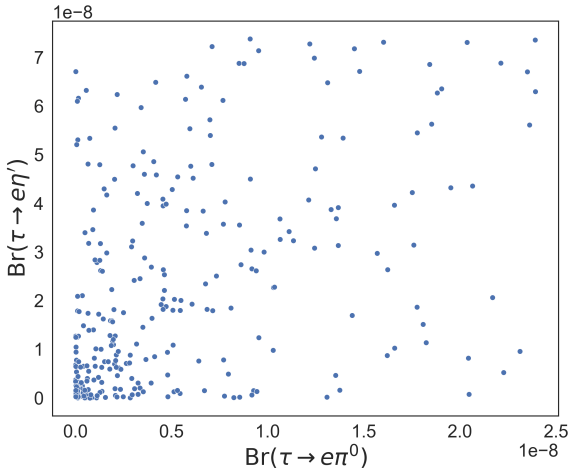

Figure 67: Scatter plot $\mathrm{Br}(\tau \to e\pi^0)$ vs. $\mathrm{Br}(\tau \to e\eta')$ without Majorana neutrinos.

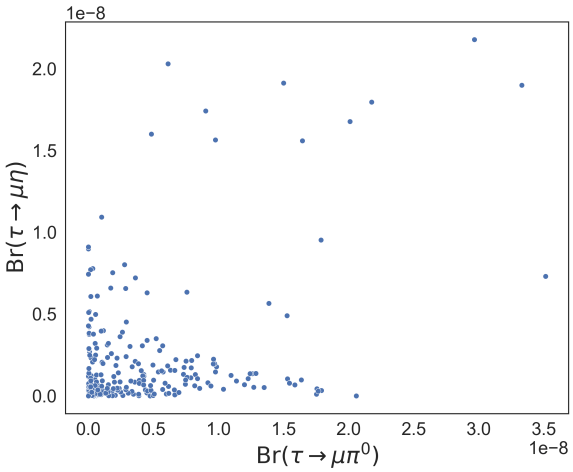

Figure 68: Scatter plot $\mathrm{Br}(\tau \to \mu\pi^0)$ vs. $\mathrm{Br}(\tau \to \mu\eta)$ without Majorana neutrinos.

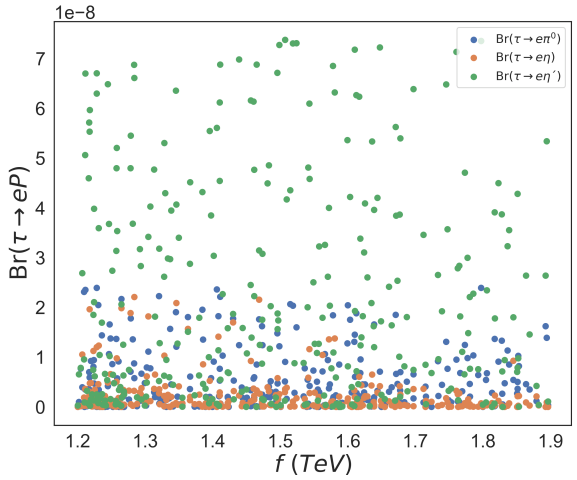

Figure 69: Scatter plot f vs. $\text{Br}(\tau \to eP)$ without Majorana neutrinos.

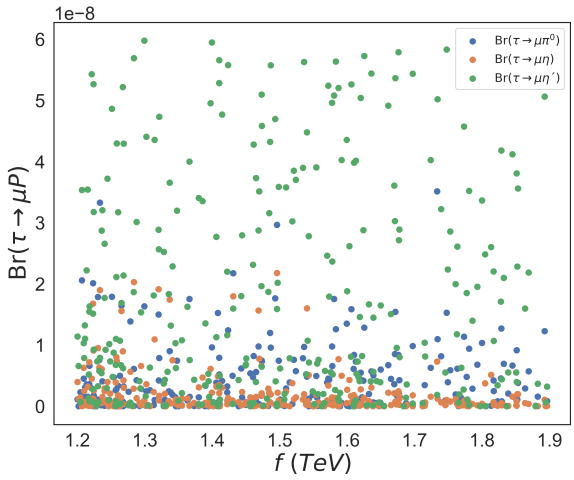

Figure 70: Scatter plot f vs. $\text{Br}(\tau \to \mu P)$ without Majorana neutrinos.

Now we include the contribution from Majorana neutrinos. Then, as in Section 8, the decays can be distinguished by their neutral couplings: $(\theta S \theta^\dagger)_{e\tau}-$processes and $(\theta S \theta^\dagger)_{\mu\tau}-$processes. Both types of decays share almost the same free parameters just differing by the neutral couplings of heavy Majorana neutrinos. Therefore, the phenomenological analysis for $\tau \to \ell P$ $(\ell = e, \mu)$ decays is done through a single Monte Carlo simulation in which the six decays are run simultaneously. In Table 21 the corresponding analysis results are shown.

In this case, with heavy Majorana neutrinos contribution, the new physics (NP) scale is greater than the case without them, the difference is not really sizeable, just ~ 0.02 TeV. In this case we realize that the T-odd leptons are heavier that the previous case by ~ 0.09 TeV, but the T-odd quarks keep basically the same values. Actually, here the mass ordering between T-odd leptons and quarks $(m_{(\ell,\nu)^i_H} > m_{(d,u)^i_H})$ is reversed with respect to the analysis without Majorana neutrinos.

The partner particles behavior is different that the T-odd ones. In partner particles the quarks are heavier than leptons. The presence of Majorana neutrinos causes the partner leptons have very similar masses to partner quarks.

Now, the new values that appear in this analysis are the masses of heavy Majorana neutrinos and their neutral couplings. We observe that the masses of Majorana neutrinos are above 19 TeV, being the maximum difference among them ~ 0.18 TeV. Their neutral couplings for both processes have the same order of magnitude, $\sim \mathcal{O}(10^{-7})$.

In the following two heatmaps in Figures 71 and 72 we realize that branching ratios are almost uncorrelated with their free parameters.

The relation among Yukawa couplings of T-odd leptons and quarks is kept from the previous case, without Majorana neutrinos. Likewise, the high correlation among Yukawa couplings of T-odd leptons continues when Majorana neutrinos are added.

The way the branching ratios are correlated in this analysis looks different than the case without

$\tau \to \ell P$ ($\ell = e, \mu$) (C.L. = 90%) with Majorana neutrinos contribution.			
New physics (NP) scale (TeV)		Mixing angles	
f	1.51	θ_V	43.07°
Branching ratio		θ_W	42.82°
$\mathrm{Br}(\tau \to e\pi^0)$	8.69×10^{-9}	Masses of partner leptons ($m_{\nu^c} = m_{\ell^c}$)(TeV)	
$\mathrm{Br}(\tau \to \mu\pi^0)$	6.96×10^{-9}	$m_{\nu_1^c}$	3.26
$\mathrm{Br}(\tau \to e\eta)$	6.19×10^{-9}	$m_{\nu_2^c}$	3.26
$\mathrm{Br}(\tau \to \mu\eta)$	5.19×10^{-9}	$m_{\nu_3^c}$	3.30
$\mathrm{Br}(\tau \to e\eta')$	2.19×10^{-8}	Masses of partner quarks ($m_{u^c} = m_{d^c}$) (TeV)	
$\mathrm{Br}(\tau \to \mu\eta')$	1.94×10^{-8}	$m_{u_i^c}$	3.31
Masses of T-odd leptons (TeV)		Masses of heavy Majorana neutrinos (TeV)	
$m_{\ell_H^1}$	3.06	M_1	19.18
$m_{\ell_H^2}$	3.03	M_2	19.07
$m_{\ell_H^3}$	3.03	M_3	19.25
$m_{\nu_H^1}$	3.05	Neutral couplings of heavy Majorana neutrinos	
$m_{\nu_H^2}$	3.02	$\lvert(\theta S \theta^\dagger)_{e\tau}\rvert$	3.32×10^{-7}
$m_{\nu_H^3}$	3.02	$\lvert(\theta S \theta^\dagger)_{\mu\tau}\rvert$	3.90×10^{-7}
Masses of T-odd quarks (TeV)			
$m_{d_H^i}$	2.78		
$m_{u_H^i}$	2.78		

Table 21: Mean values for branching ratios, masses of LHT heavy particles, mixing angles and neutral couplings obtained by Monte Carlo simulation of $\tau \to \ell P$ ($\ell = e, \mu$) processes.

Majorana neutrinos. For both processes with $\ell = e$ and $\ell = \mu$ considering Majorana neutrinos contribution, the decay modes with $P = \eta$ and $P = \eta'$ have the highest correlations. To explain that, we need to get back to eqs. (618) and (623) and see that their a_P^k and b_P^k factors look similar in these cases.

In contrast to the analysis done in Subsections 8.5 and 8.7, here the heavy Majorana neutrinos are barely correlated among them. Recalling the results obtained in Subsections 8.5 and 8.7 the mean value for heavy Majorana masses is around 17.2 TeV, differing slightly ($\sim 0.12\%$) in all cases. In this analysis the mean value for heavy Majorana neutrinos is ~ 19.16 TeV. Thus, the difference between these new results and the previous ones is just $\sim 10.23\%$.

The mean values for mixing angles θ_V and θ_W are 43.07° and 42.82°, respectively. They become in rad $\theta_V \approx \theta_W \approx \pi/4.18$, this result is close to maximize the LFV effects, since this happens when $\theta_V = \theta_W = \pi/4$.

The two neutral couplings $|(\theta S \theta^\dagger)_{\ell\tau}|$ ($\ell = e, \mu$) have the same order of magnitude, $\mathcal{O}(10^{-7})$, which matches the values obtained in Subsections 8.5.

The interpretation of the following Figures 73, 74, 75, 76, 77 and 78 is analogous to the case without Majorana neutrinos contributions, but now we include the correlation between branching ratio versus masses of Majorana neutrinos, that looks similar to the branching ratios with respect to

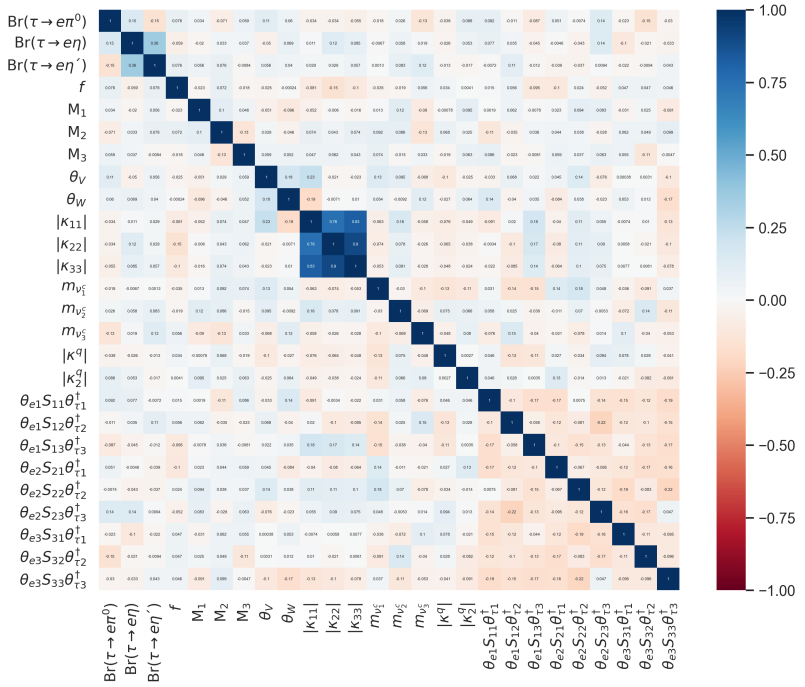

Figure 71: Heat map where we can see that there is no correlation among $\tau \to eP$ decays and their free parameters.

f plots.

We realize that the mean values of branching ratios from this numerical analysis, considering Majorana neutrinos contribution are smaller just by 2 orders of magnitude with respect to the current ones [6], similarly as the previous case, with only particles from LHT.

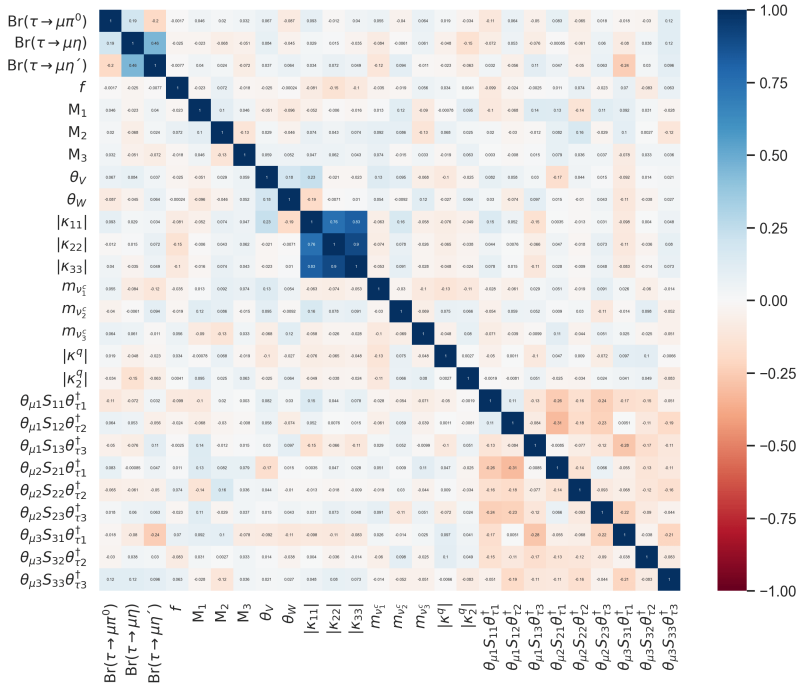

Figure 72: Heat map for $\tau \to \mu P$ decays and their free parameters, where we see a similar behavior to $\tau \to eP$ decays.

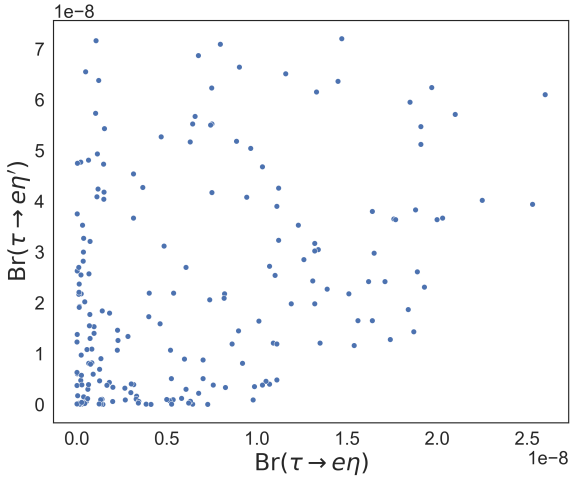

Figure 73: Scatter plot $\mathrm{Br}(\tau \to e\eta)$ vs. $\mathrm{Br}(\tau \to e\eta')$.

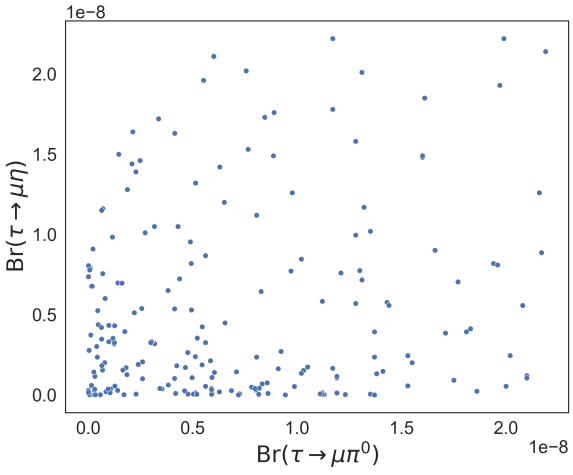

Figure 74: Scatter plot $\mathrm{Br}(\tau \to \mu\pi^0)$ vs. $\mathrm{Br}(\tau \to \mu\eta)$.

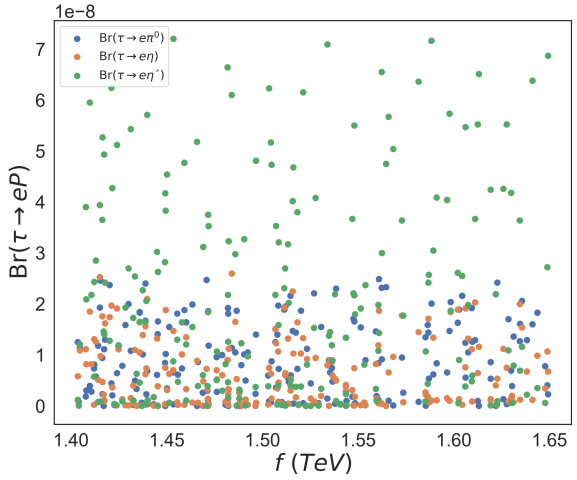

Figure 75: Scatter plot f vs. $\mathrm{Br}(\tau \to eP)$.

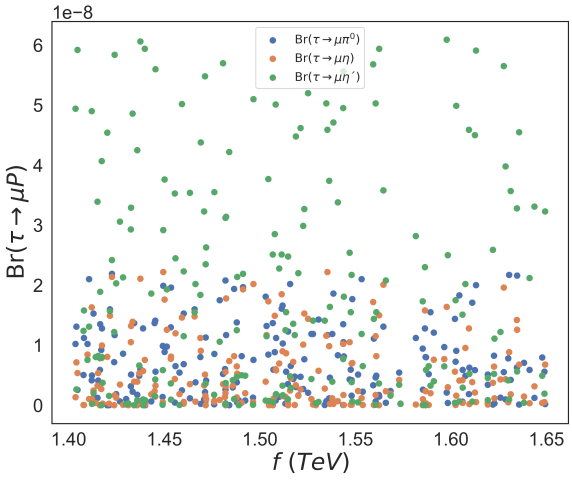

Figure 76: Scatter plot f vs. $\mathrm{Br}(\tau \to \mu P)$.

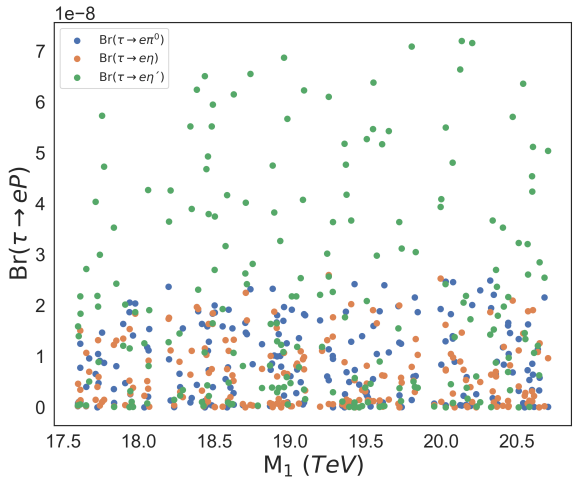

Figure 77: Scatter plot $\mathrm{M_1}$ vs. $\mathrm{Br}(\tau \to eP)$.

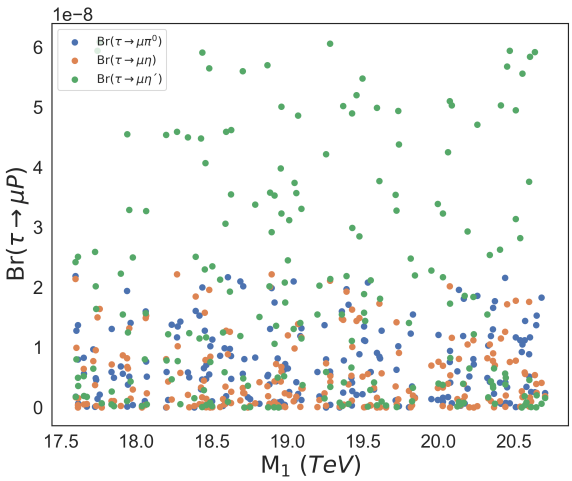

Figure 78: Scatter plot $\mathrm{M_1}$ vs. $\mathrm{Br}(\tau \to \mu P)$.

10.6.2 $\tau \to \ell PP,\ \ell V\ (\ell = e, \mu)$

Because the structure of the branching ratios for the processes $\tau \to \ell PP$ and $\tau \to \ell V\ (\ell = e, \mu)$ is very similar they have been computed simultaneously by a single Monte Carlo simulation. We can see the obtained results for this analysis in Tables 22 and 23, where two cases have been handled: firstly when particles coming from LHT are involved in the processes. Second, adding the effects of Majorana neutrinos.

$\tau \to \ell PP,\ \ell V\ (\ell = e, \mu)$ (C.L. = 90%) without Majorana neutrinos contribution			
New physics (NP) scale (TeV)		Mixing angles	
f	1.50	θ_V	43.36°
Branching ratio		θ_W	41.50°
$\mathrm{Br}(\tau \to e\pi^+\pi^-)$	3.92×10^{-9}	Masses of partner leptons ($m_{\nu^c} = m_{\ell^c}$)(TeV)	
$\mathrm{Br}(\tau \to \mu\pi^+\pi^-)$	3.96×10^{-9}	$m_{\nu_1^c}$	3.20
$\mathrm{Br}(\tau \to eK^+K^-)$	2.38×10^{-9}	$m_{\nu_2^c}$	3.15
$\mathrm{Br}(\tau \to \mu K^+K^-)$	2.85×10^{-9}	$m_{\nu_3^c}$	3.31
$\mathrm{Br}(\tau \to eK^0\overline{K^0})$	1.15×10^{-9}	Masses of partner quarks ($m_{u^c} = m_{d^c}$) (TeV)	
$\mathrm{Br}(\tau \to \mu K^0\overline{K^0})$	1.33×10^{-9}	$m_{u_i^c}$	3.32
$\mathrm{Br}(\tau \to e\rho)$	1.10×10^{-9}		
$\mathrm{Br}(\tau \to \mu\rho)$	1.12×10^{-9}		
$\mathrm{Br}(\tau \to e\phi)$	1.77×10^{-9}		
$\mathrm{Br}(\tau \to \mu\phi)$	1.87×10^{-9}		
Masses of T-odd leptons (TeV)			
$m_{\ell_H^1}$	3.13		
$m_{\ell_H^2}$	2.99		
$m_{\ell_H^3}$	3.10		
$m_{\nu_H^1}$	3.12		
$m_{\nu_H^2}$	2.98		
$m_{\nu_H^3}$	3.09		
Masses of T-odd quarks (TeV)			
$m_{d_H^i}$	2.92		
$m_{u_H^i}$	2.91		

Table 22: Mean values for branching ratios, masses of LHT heavy particles, mixing angles and neutral couplings obtained by Monte Carlo simulation of $\tau \to \ell PP,\ \ell V\ (\ell = e, \mu)$ processes without Majorana neutrinos.

We see that the Majorana neutrinos effects on the new physics scale (NP) and T-odd particles is that they are both larger than when those contributions are not considered. The new physics (NP) scale and T-odd leptons increase by ~ 0.05 TeV whereas the T-odd quarks grow by ~ 0.8 TeV. The mass ordering in T-odd particles seen in $\tau \to \ell P$ without Majorana neutrinos case is conserved when Majorana neutrinos contribution is added in $\tau \to \ell PP,\ \ell V$, i.e., T-odd quarks are heavier. This hierarchy of masses is reversed if Majorana neutrinos are taken into account in $\tau \to \ell P$ and they are

excluded in $\tau \to \ell PP,\ \ell V$, though.

While in Tables 20, 21 and 22, the masses of T-odd quarks do not exceed 3 TeV, in Table 23 are around 3.7 TeV, which is above ~ 1 TeV from the values obtained by $\tau \to \ell P$ analysis.

Unlike $\tau \to \ell PP,\ \ell V$ processes with Majorana neutrinos, in all other cases the masses of partner leptons are above 3 TeV. For partner quarks, in all cases they are heavier than lepton partners. Only in $\tau \to \ell PP,\ \ell V$ processes with Majorana neutrinos the T-odd particles are heavier than the partners ones.

The values for mixing angles θ_V and θ_W do not have a sizeable difference between this section and the previous one $\sim \pi/4.20$. We see that the values tend to maximize the LFV effects.

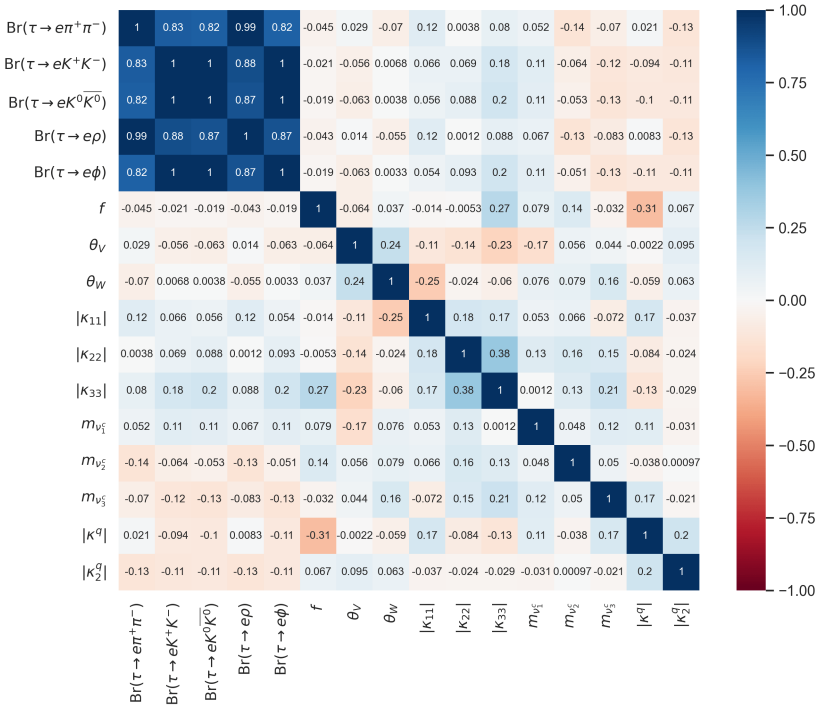

Figure 79: Heat map for $\tau \to ePP,\ eV$ decays and their free parameters not considering Majorana neutrinos.

The Figures 79, 80, 93 and 94 stand for a correlation matrix where we can see how branching ratios and free parameters are correlated.

It does not matter whether there are Majorana neutrinos or not, the correlation among branching ratios for $\tau \to \ell PP,\ \ell V$ processes look very similar in both cases. This can be understood as a result of the largest contribution for every processes coming from the pions loop in the $F_V^{PP}(s)$ function. Then, as this dominant contribution is proportional for all decays modes, this causes the correlations among them to be maximal.

In the cases from this section the high correlation among Yukawa couplings, which appears in the $\tau \to \ell P$ decays, vanishes. It can bee seen from the mass values of T-odd particles in Tables 20 and

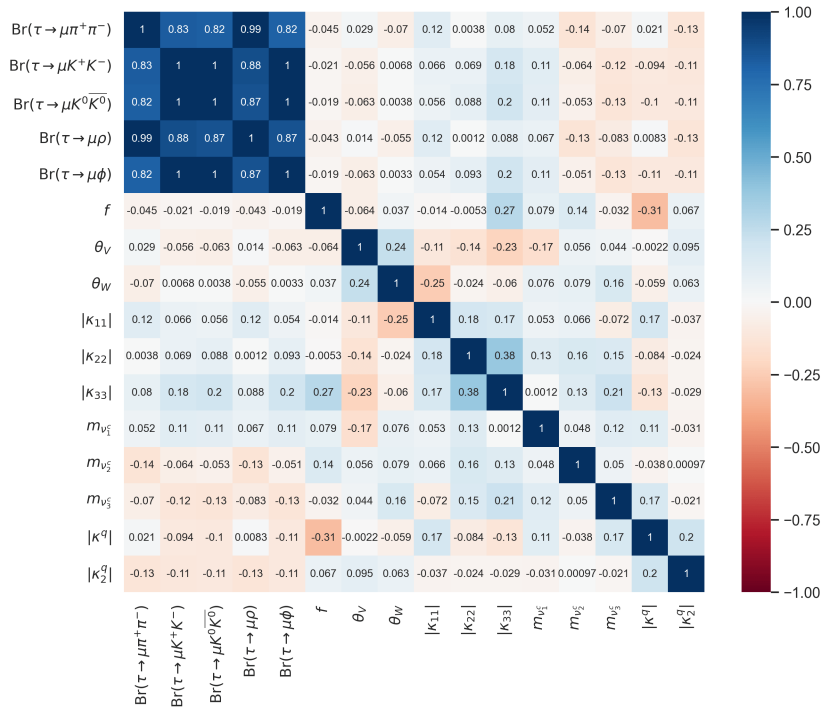

Figure 80: Heat map for $\tau \to \mu PP,\ \mu V$ decays and their free parameters, where we see a similar behavior to $\tau \to ePP,\ eV$ decays not considering Majorana neutrinos.

21 where they are practically the same. On the other hand, in Tables 22 and 23 the masses of T-odd particles can be distinguished from each other easily.

If the magnitudes of neutral couplings in Table 23 are compared with the ones in Table 21, we will realize that they conserve the order of magnitude.

If a comparison is done among Majorana neutrino masses obtained by the analysis of $\tau \to \ell P$ and $\tau \to \ell PP,\ \ell V$, two masses in the latter case are lighter since their values are below 19 TeV. Yet, this case has the heaviest Majorana neutrino $\mathrm{M}_2 < 19.33$ TeV.

The branching ratios for all processes, when Majorana neutrinos contribution is considered, are greater than when this contribution is excluded. All our results for $\tau \to \ell P, PP, V$ $(\ell = e, \mu)$ are very promising, as they are only, at most, 2 orders of magnitude smaller than current bounds [6].

In the scatter plots in Figures 81, 82, 83, 84, 85, 86, 87 and 88 we see how the branching ratios are related. For scatter plots with $\ell\pi^+\pi^-$ vs. ℓK^+K^-, $(\ell = e, \mu)$ the points are more spread out as the BR of $\pi\pi$ increases. The scatter plots in Figures 86 and 88 show a similar behavior, they have a gap when $\mathrm{Br}(\tau \to \mu K^+K^-) \sim 3 - 4 \times 10^{-9}$, If we had more points, the gap would reduce and eventually vanish.

We observe that the branching ratios are arranged in triplets in Figures 89 and 90 where sometimes the two points representing the KK modes are closer and sometimes not that much, but the triplet pattern is maintained. Figures 91 and 92 show how the branching ratios for $\tau \to \ell V$ processes behave

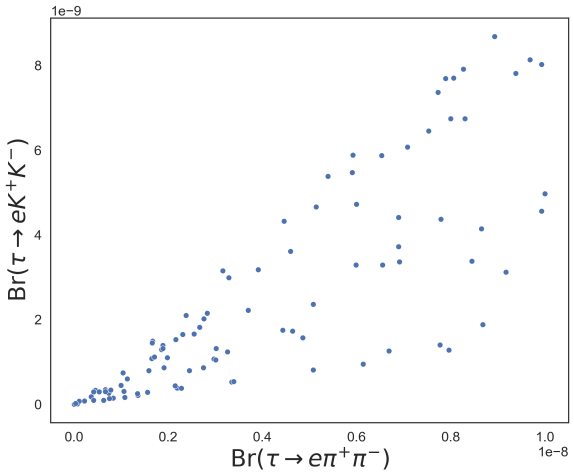

Figure 81: Scatter plot $\mathrm{Br}(\tau \to e\pi^+\pi^-)$ vs. $\mathrm{Br}(\tau \to eK^+K^-)$ without Majorana neutrinos contribution.

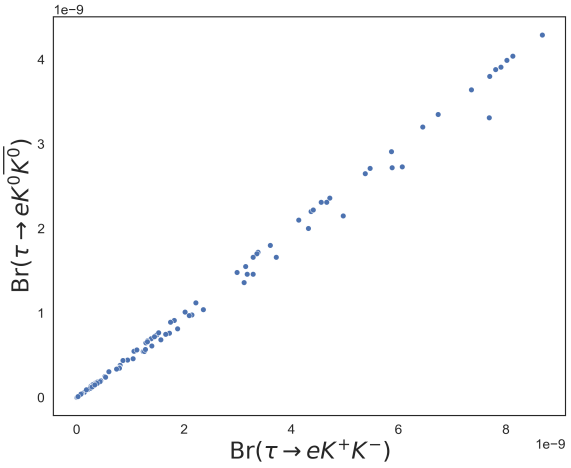

Figure 82: Scatter plot $\mathrm{Br}(\tau \to eK^+K^-)$ vs. $\mathrm{Br}(\tau \to eK^0\overline{K^0})$ without Majorana neutrinos contribution.

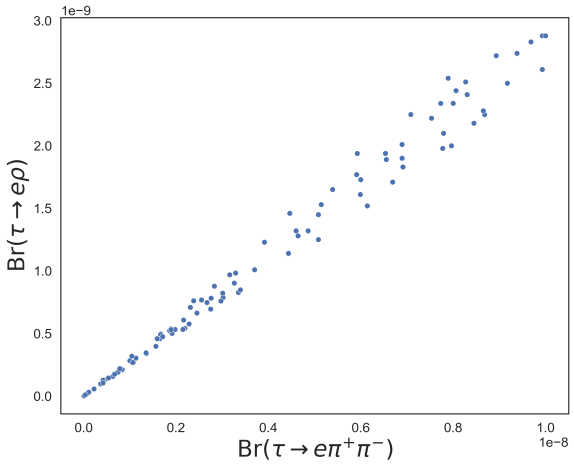

Figure 83: Scatter plot $\mathrm{Br}(\tau \to e\pi^+\pi^-)$ vs. $\mathrm{Br}(\tau \to e\rho)$ without Majorana neutrinos contribution.

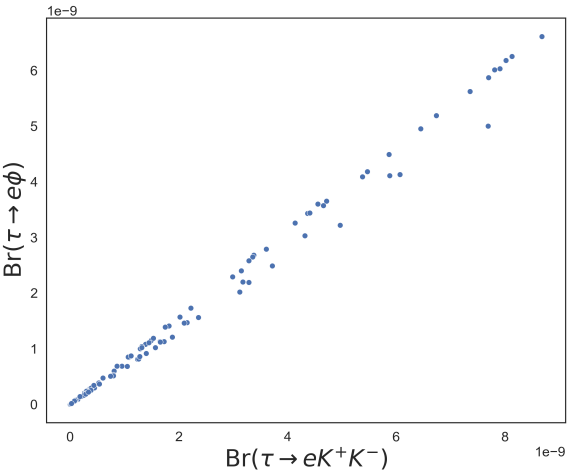

Figure 84: Scatter plot $\mathrm{Br}(\tau \to eK^+K^-)$ vs. $\mathrm{Br}(\tau \to e\phi)$ without Majorana neutrinos contribution.

with respect to f, where the decay modes with $V = \phi$ as final state reach the highest values.

The interpretation of scatter plots in Figures 95, 96, 97, 98, 99, 100, 101, 102, 103, 104, 105 and 106 is analogous to the scatter plots in which Majorana neutrinos are not involved, since the behavior that scatter plots describe when effects of Majorana neutrinos are considered does not change. Additionally, in the case with Majorana neutrinos we can see how branching ratios behave faced to Majorana neutrino masses M_i in Figures 107, 108, 109 and 110. They look like the scatter plots with $\mathrm{Br}(\tau \to \ell PP(V))$ vs. f, which makes sense because the masses of Majorana neutrinos are related to f as $\leq 4\pi f$

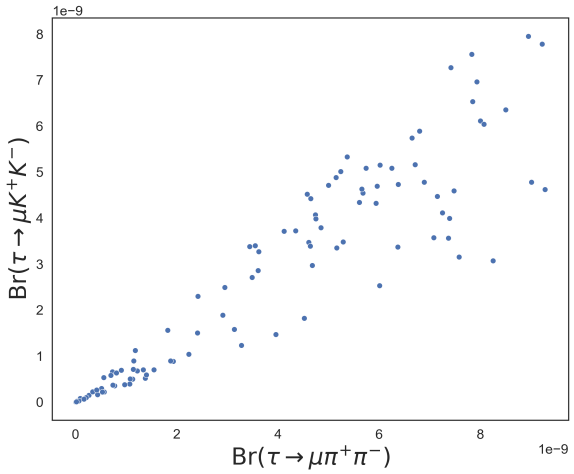

Figure 85: Scatter plot $\mathrm{Br}(\tau \to \mu\pi^+\pi^-)$ vs. $\mathrm{Br}(\tau \to \mu K^+K^-)$ without Majorana neutrinos contribution.

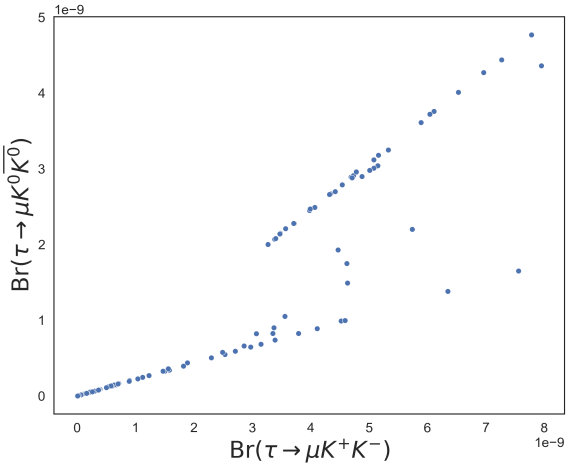

Figure 86: Scatter plot $\mathrm{Br}(\tau \to \mu K^+K^-)$ vs. $\mathrm{Br}(\tau \to \mu K^0\overline{K^0})$ without Majorana neutrinos contribution.

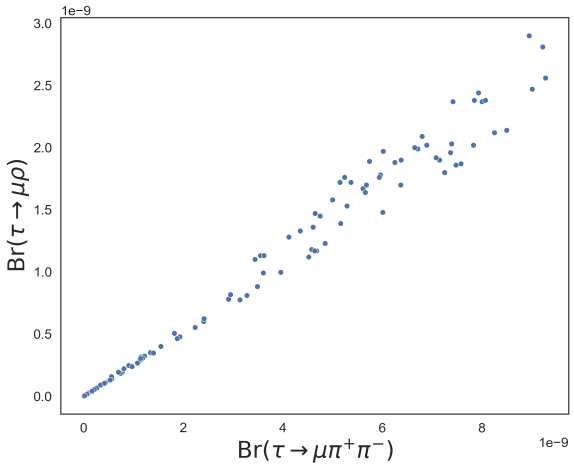

Figure 87: Scatter plot $\mathrm{Br}(\tau \to \mu\pi^+\pi^-)$ vs. $\mathrm{Br}(\tau \to \mu\rho)$ without Majorana neutrinos contribution.

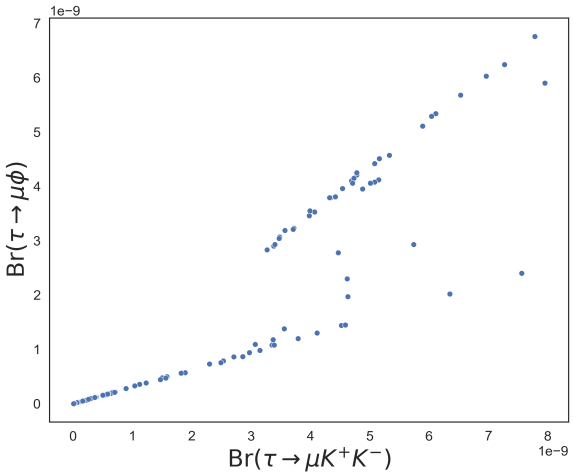

Figure 88: Scatter plot $\mathrm{Br}(\tau \to \mu K^+K^-)$ vs. $\mathrm{Br}(\tau \to \mu\phi)$ without Majorana neutrinos contribution.

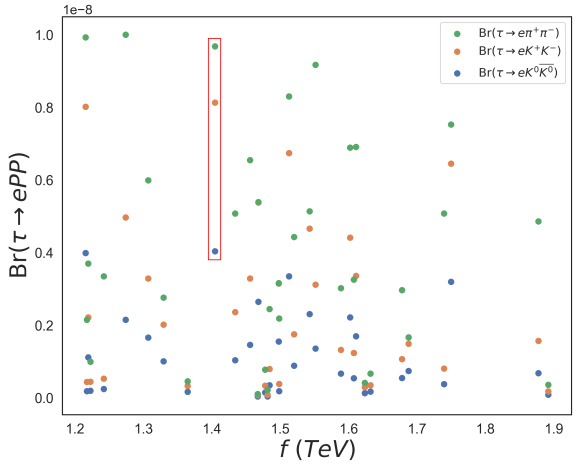

Figure 89: Scatter plot f vs. $\mathrm{Br}(\tau \to ePP)$ without Majorana neutrinos contribution.

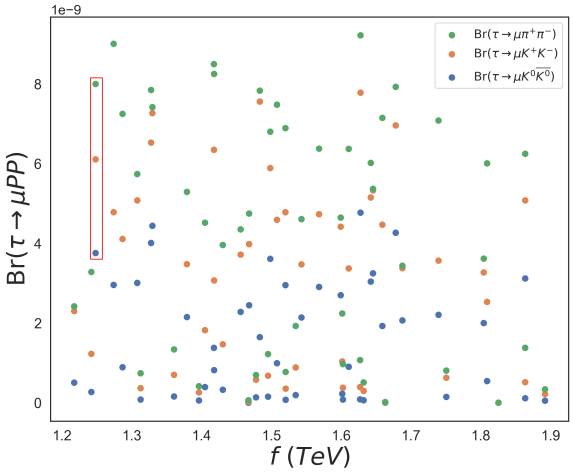

Figure 90: Scatter plot f vs. $\mathrm{Br}(\tau \to \mu PP)$ without Majorana neutrinos contribution.

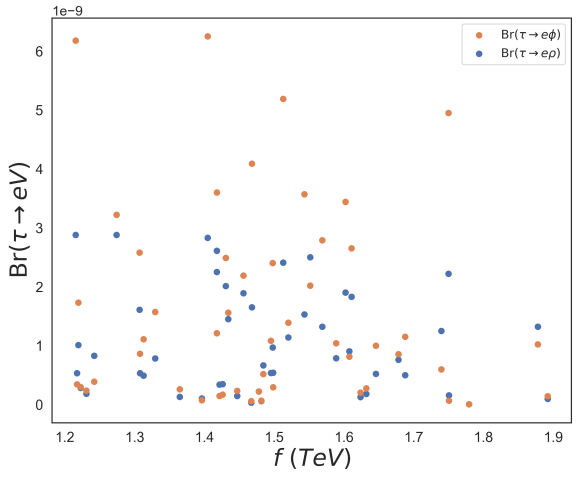

Figure 91: Scatter plot f vs. $\mathrm{Br}(\tau \to eV)$ without Majorana neutrinos contribution.

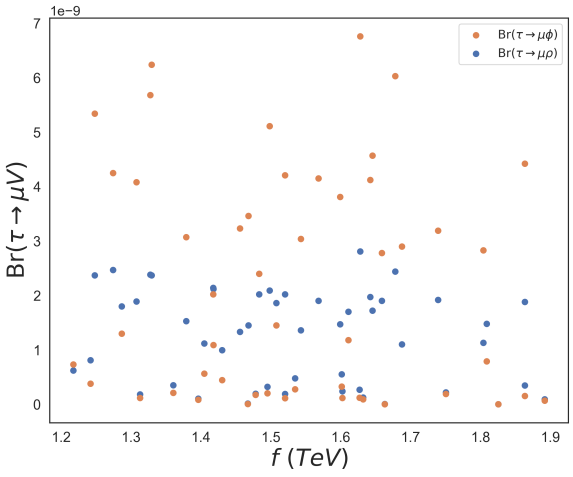

Figure 92: Scatter plot f vs. $\mathrm{Br}(\tau \to \mu V)$ without Majorana neutrinos contribution.

$\tau \to \ell PP,\ \ell V\ (\ell = e, \mu)$ (C.L. = 90%) with Majorana neutrinos contribution			
New physics (NP) scale (TeV)		Mixing angles	
f	1.54	θ_V	43.61°
Branching ratio		θ_W	42.21°
$\mathrm{Br}(\tau \to e\pi^+\pi^-)$	4.75×10^{-9}	Masses of partner leptons ($m_{\nu^c} = m_{\ell^c}$)(TeV)	
$\mathrm{Br}(\tau \to \mu\pi^+\pi^-)$	4.90×10^{-9}	$m_{\nu_1^c}$	2.91
$\mathrm{Br}(\tau \to eK^+K^-)$	2.53×10^{-9}	$m_{\nu_2^c}$	2.99
$\mathrm{Br}(\tau \to \mu K^+K^-)$	3.38×10^{-9}	$m_{\nu_3^c}$	2.95
$\mathrm{Br}(\tau \to eK^0\overline{K^0})$	1.16×10^{-9}	Masses of partner quarks ($m_{u^c} = m_{d^c}$) (TeV)	
$\mathrm{Br}(\tau \to \mu K^0\overline{K^0})$	1.50×10^{-9}	$m_{u_i^c}$	3.08
$\mathrm{Br}(\tau \to e\rho)$	1.33×10^{-9}	Masses of heavy Majorana neutrinos (TeV)	
$\mathrm{Br}(\tau \to \mu\rho)$	1.39×10^{-9}	M_1	18.82
$\mathrm{Br}(\tau \to e\phi)$	1.78×10^{-9}	M_2	19.33
$\mathrm{Br}(\tau \to \mu\phi)$	2.08×10^{-9}	M_3	18.92
Masses of T-odd leptons (TeV)		Neutral couplings of heavy Majorana neutrinos	
$m_{\ell_H^1}$	3.49	$\lvert(\theta S \theta^\dagger)_{e\tau}\rvert$	2.20×10^{-7}
$m_{\ell_H^2}$	3.47	$\lvert(\theta S \theta^\dagger)_{\mu\tau}\rvert$	3.14×10^{-7}
$m_{\ell_H^3}$	3.21		
$m_{\nu_H^1}$	3.48		
$m_{\nu_H^2}$	3.46		
$m_{\nu_H^3}$	3.20		
Masses of T-odd quarks (TeV)			
$m_{d_H^i}$	3.73		
$m_{u_H^i}$	3.71		

Table 23: Mean values for branching ratios, masses of LHT heavy particles, mixing angles and neutral couplings obtained by Monte Carlo simulation of $\tau \to \ell PP,\ \ell V\ (\ell = e, \mu)$ processes.

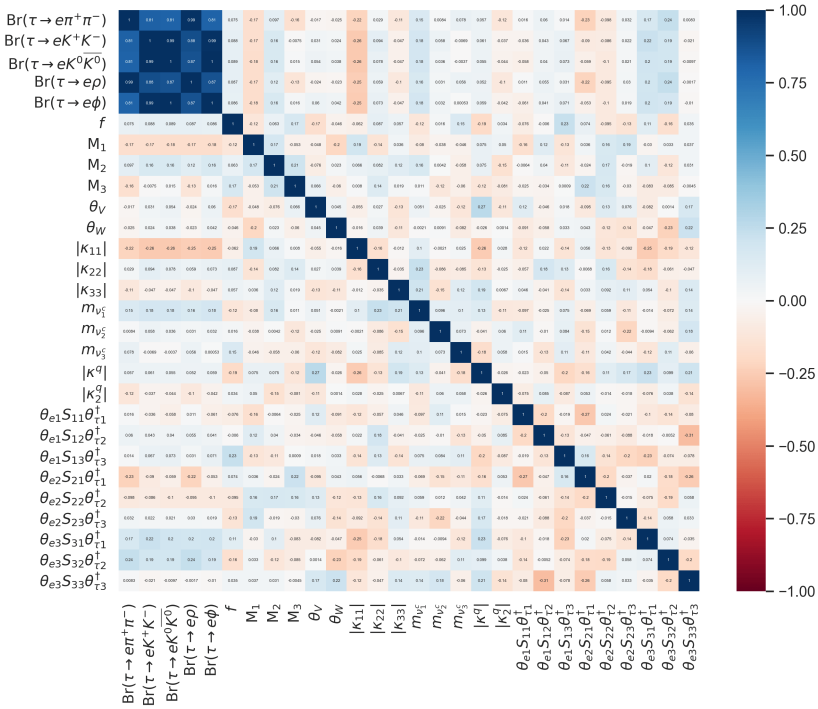

Figure 93: Heat map for $\tau \to ePP,\ eV$ decays and their free parameters.

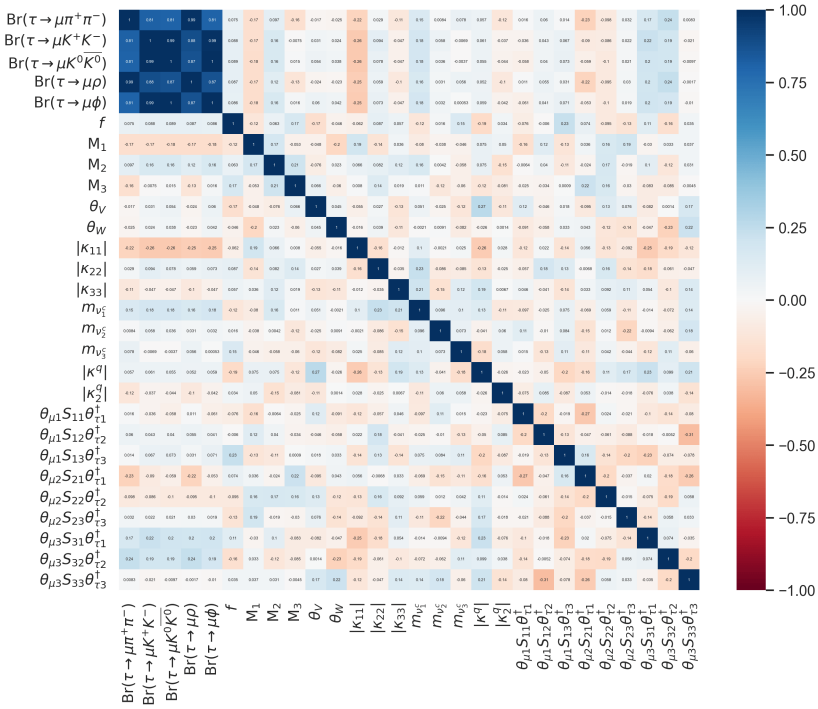

Figure 94: Heat map for $\tau \to \mu PP,\ \mu V$ decays and their free parameters, where we see a similar behavior to $\tau \to ePP,\ eV$ decays.

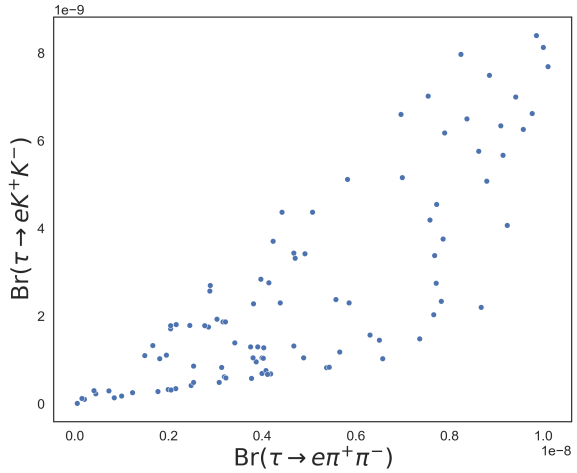

Figure 95: Scatter plot $\mathrm{Br}(\tau \to e\pi^+\pi^-)$ vs. $\mathrm{Br}(\tau \to eK^+K^-)$.

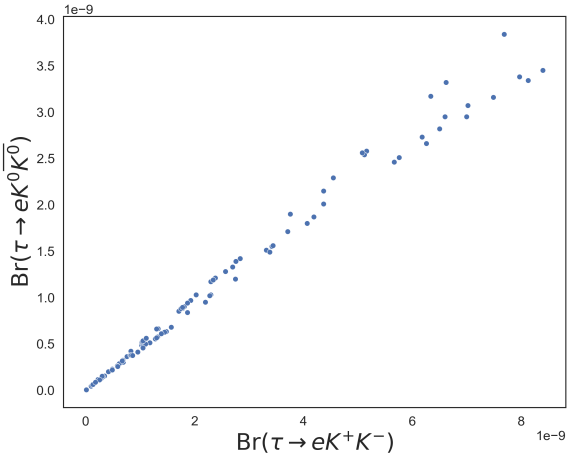

Figure 96: Scatter plot $\mathrm{Br}(\tau \to eK^+K^-)$ vs. $\mathrm{Br}(\tau \to eK^0\overline{K^0})$.

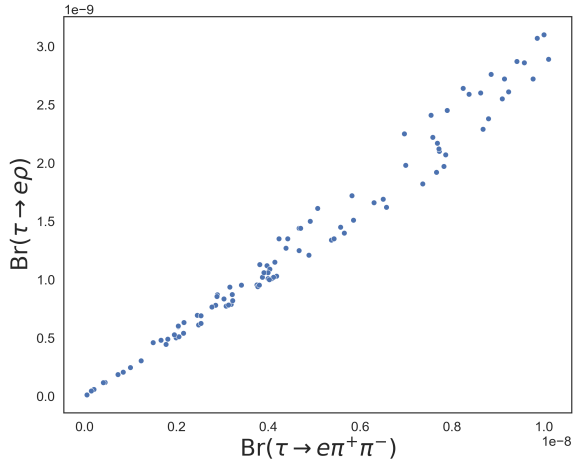

Figure 97: Scatter plot $\mathrm{Br}(\tau \to e\pi^+\pi^-)$ vs. $\mathrm{Br}(\tau \to e\rho)$.

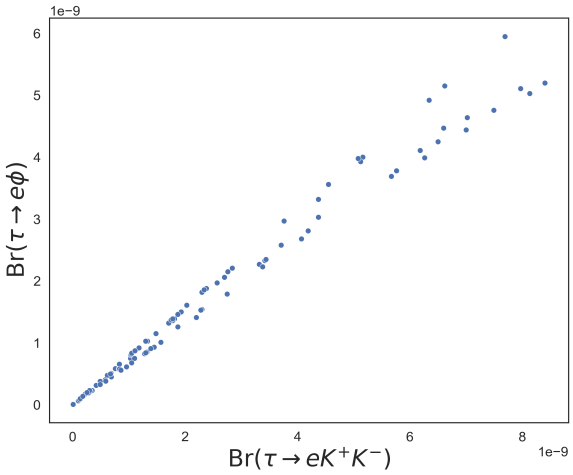

Figure 98: Scatter plot $\mathrm{Br}(\tau \to eK^+K^-)$ vs. $\mathrm{Br}(\tau \to e\phi)$.

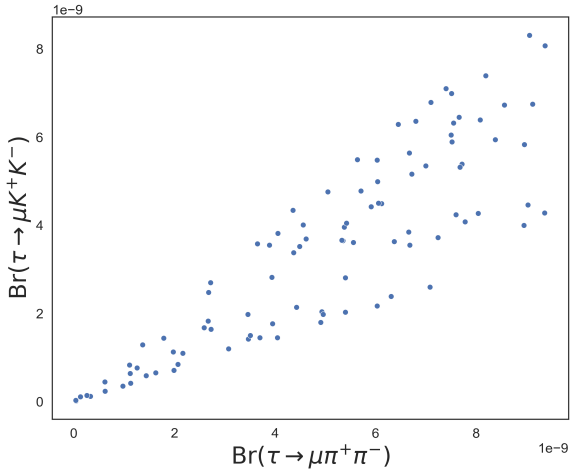

Figure 99: Scatter plot $\mathrm{Br}(\tau \to \mu\pi^+\pi^-)$ vs. $\mathrm{Br}(\tau \to \mu K^+K^-)$.

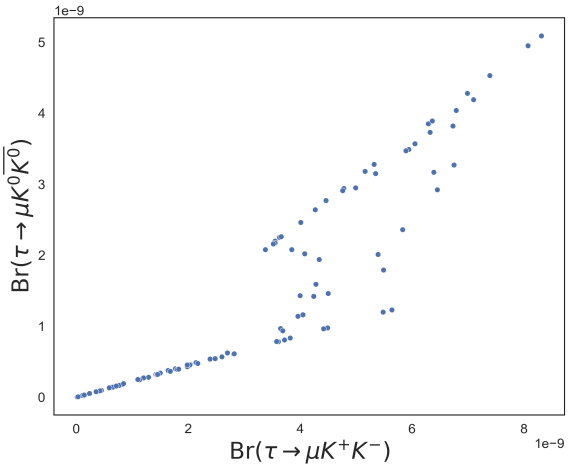

Figure 100: Scatter plot $\mathrm{Br}(\tau \to \mu K^+K^-)$ vs. $\mathrm{Br}(\tau \to \mu K^0\overline{K^0})$.

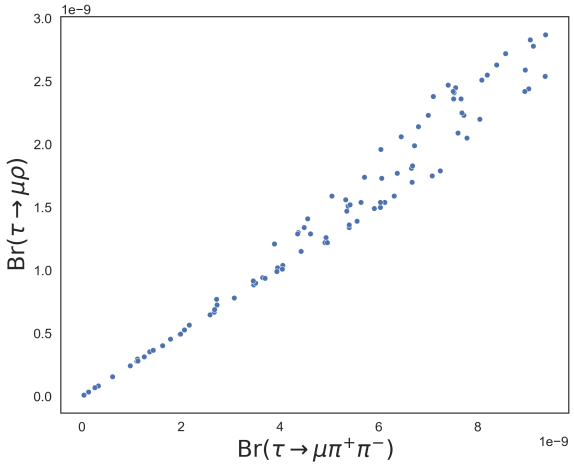

Figure 101: Scatter plot $\mathrm{Br}(\tau \to \mu\pi^+\pi^-)$ vs. $\mathrm{Br}(\tau \to \mu\rho)$.

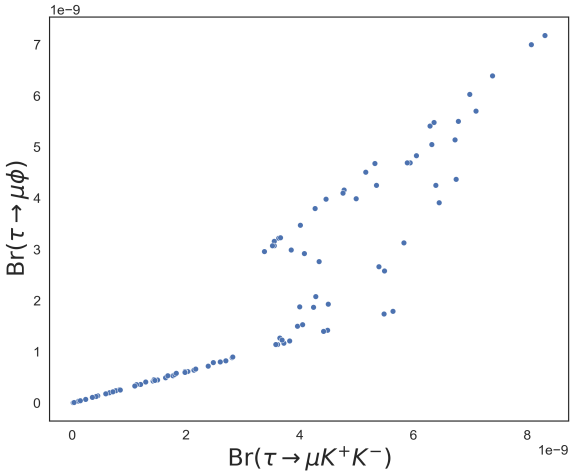

Figure 102: Scatter plot $\mathrm{Br}(\tau \to \mu K^+K^-)$ vs. $\mathrm{Br}(\tau \to \mu\phi)$.

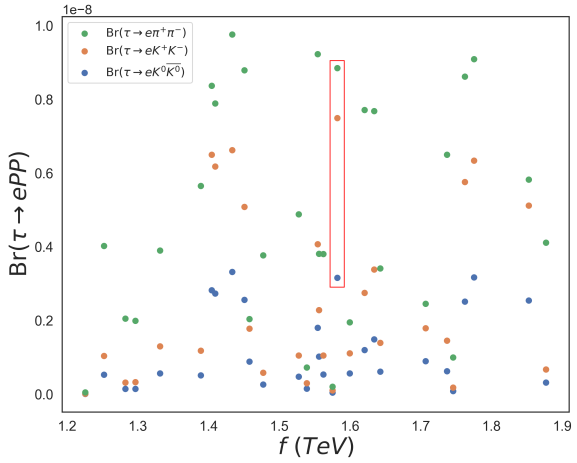

Figure 103: Scatter plot f vs. $\mathrm{Br}(\tau \to ePP)$.

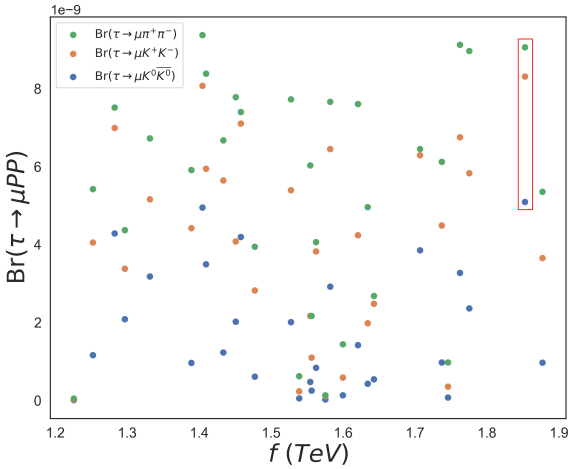

Figure 104: Scatter plot f vs. $\mathrm{Br}(\tau \to \mu PP)$.

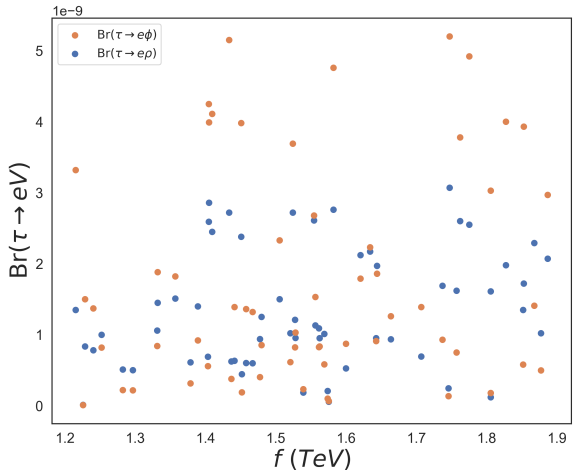

Figure 105: Scatter plot f vs. $\mathrm{Br}(\tau \to eV)$.

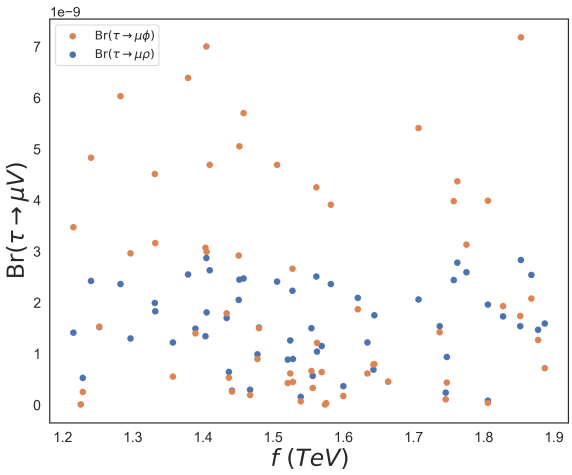

Figure 106: Scatter plot f vs. $\mathrm{Br}(\tau \to \mu V)$.

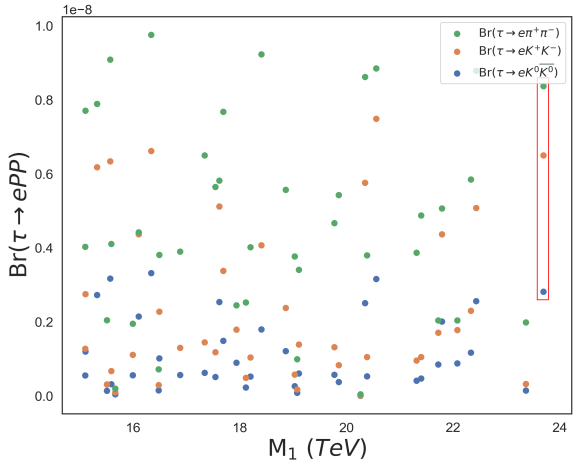

Figure 107: Scatter plot M_1 vs. $\mathrm{Br}(\tau \to ePP)$.

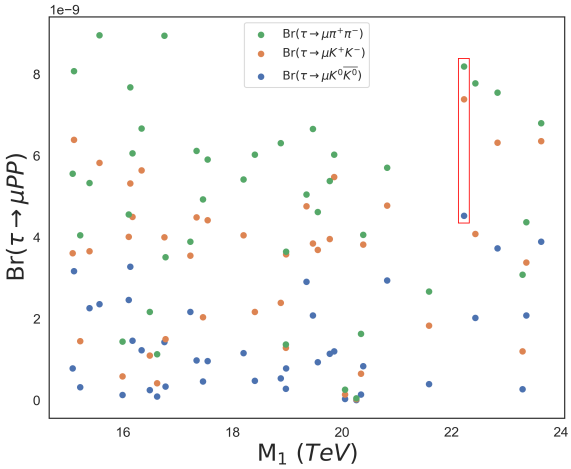

Figure 108: Scatter plot M_1 vs. $\mathrm{Br}(\tau \to \mu PP)$.

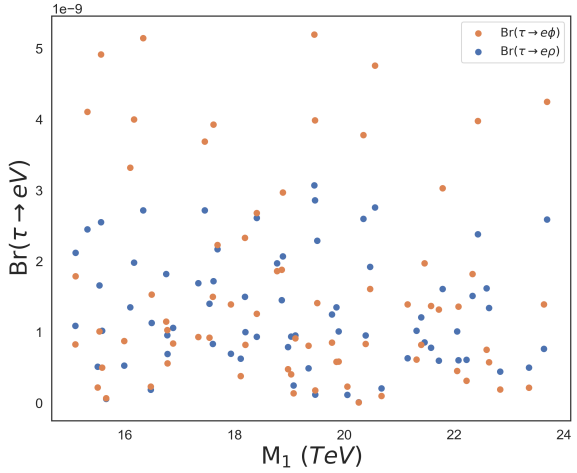

Figure 109: Scatter plot M_1 vs. $\mathrm{Br}(\tau \to eV)$.

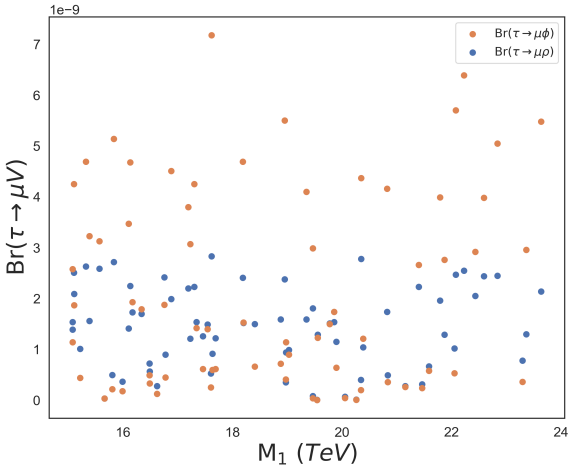

Figure 110: Scatter plot M_1 vs. $\mathrm{Br}(\tau \to \mu V)$.

11 Conclusions and Prospects

Littlest Higgs Model with T-parity, LHT, is such an exciting framework trying to better understand processes beyond SM as (observable) LFV and LNV ones, while at the same time attempting to alleviate the hierarchy problem affecting, generically, the Higgs mass. Simultaneously, within our setting, it could shed light on the smallness of neutrino masses (and possibly on baryogenesis through leptogenesis). For that purpose, LHT, through a spontaneous collective breaking of a global symmetry, gives us a large number of new particles whose masses are of order $\mathcal{O}(f)$, the new physics (NP) scale of energy, $f \sim \mathcal{O}$ (TeV). Our results for the studied LFV decays are quite promising as they lie approximately one order of magnitude below current bounds, so probing the theory at current and forthcoming colliders is possible. Nevertheless, the story does not end here, thanks to LHT symmetry that enables adding neutrinos realizing an ISS mechanism, i.e., LHT can be extended to a model with neutrinos of Majorana nature, which is really marvelous because we can tackle LNV processes as well (this has not been fully explored yet and it appears as a bright avenue for future research).

In this work we developed all the needed tools in order to get the numerical predictions of branching ratios, particle masses, couplings, etc., coming from our model.

Our effort was focused firstly on studying purely leptonic decays involved in Section 7. Afterwards, the analysis was extended to LFV hadronic decays of the tau lepton, in Section 10. The most important results can be summarized as follows:

- From the numerical analysis done in Section 8 the new physics (NP) energy scale is around $f \sim 1.36$ TeV, whereas in Section 10 $f \sim 1.50$ TeV. The difference between these two figures is $\sim 9.34\%$, which is reasonable at this stage (a global analysis of all LFV processes is needed and will be presented elsewhere).

- LHT with Majorana neutrinos extension enables to bind the LNV couplings shown in Table 16. This is a novel result since they were not restricted in ref. [57].

- Regarding new couplings that we first encounter, there arise the neutral couplings of heavy Majorana neutrinos, denoted as $(\theta S \theta^\dagger)_{\ell\ell'}$. The magnitude of these couplings agree in both sets of analyses, as reported in Sections 8 and 10.

- Masses of particles coming from LHT, T-odd and partner fermions, are below 4 TeV, almost 5 times lighter than heavy Majorana neutrinos. This is consistent with the first item.

- The masses of heavy Majorana neutrinos in Section 10 are $\mathrm{M}_i \sim 19$ TeV (we recall that $\mathrm{M}_i \sim 4\pi f$). Compared to previous analyses in Section 8, these masses of heavy Majorana neutrinos are heavier by ~ 2 TeV ($\sim 10\%$ of difference) and f is fully consistent.

- In all $\tau \to \ell\ell'\bar{\ell}''$ (including wrong-sign) decays and in $\mu \to e$ conversion in Ti, the mean values of our simulated events satisfying all present bounds are only one order of magnitude smaller

than current limits. In $\mu \to ee\bar{e}$, $Z \to \bar{\tau}\ell$ and conversion in Au, our mean values are around two orders of magnitude smaller than current limits (only $Z \to \bar{\mu}e$ does not have the potential for probing our results in the near future).

- The pattern of correlations among processes is completely different to the 'traditional' LHT (without heavy Majorana neutrinos), where for instance wrong-sign decays are negligible. It should also be noted that the correlation between $L \to \ell\gamma$ and $L \to \ell\ell'\bar{\ell}''$ decays, which is a celebrated signature distinguishing underlying models producing the LFV, here is broken, as the former decays depend only on the charged current mixings $\theta\theta^\dagger$ and the neutral current ones also on the neutral current admixtures, $\theta S\theta^\dagger$, which reduces sizeably the correlation among both decay modes. Only within the LHT, upon eventual discovery of LFV in charged leptons in several processes, correlations among them would immediately distinguish the usual scenario [37] from the one studied here.

All these results have been published in [33] and [74] and they offer us rosy prospects in a near future:

- Due to mean values of new physics (NP) energy scale f, masses of heavy Majorana neutrinos M_i and neutral couplings $(\theta S\theta^\dagger)_{\ell\ell'}$ matching in all our studies, we plan to undertake a global analysis (including purely leptonic processes and conversions in nuclei, see e.g. refs. [76, 89, 90]), which is required and will be presented elsewhere.

- All our results are very promising and will be probed in current and near future measurements, as they lie approximately only one order of magnitude below currents bounds [6].

A Appendix: SU(5) generators

We begin by enumerating the generalized generators of the $SU(5)$ symmetry group [82].

$SU(3)$ Generators

The $SU(3)$ generators are embedded in $SU(5)$

$$\lambda_1 = \begin{pmatrix} 0 & 1 & 0 & 0 & 0 \\ 1 & 0 & 0 & 0 & 0 \\ 0 & 0 & 0 & 0 & 0 \\ 0 & 0 & 0 & 0 & 0 \\ 0 & 0 & 0 & 0 & 0 \end{pmatrix}, \quad \lambda_2 = \begin{pmatrix} 0 & -i & 0 & 0 & 0 \\ i & 0 & 0 & 0 & 0 \\ 0 & 0 & 0 & 0 & 0 \\ 0 & 0 & 0 & 0 & 0 \\ 0 & 0 & 0 & 0 & 0 \end{pmatrix}, \quad \lambda_3 = \begin{pmatrix} 1 & 0 & 0 & 0 & 0 \\ 0 & -1 & 0 & 0 & 0 \\ 0 & 0 & 0 & 0 & 0 \\ 0 & 0 & 0 & 0 & 0 \\ 0 & 0 & 0 & 0 & 0 \end{pmatrix},$$

$$\lambda_4 = \begin{pmatrix} 0 & 0 & 1 & 0 & 0 \\ 0 & 0 & 0 & 0 & 0 \\ 1 & 0 & 0 & 0 & 0 \\ 0 & 0 & 0 & 0 & 0 \\ 0 & 0 & 0 & 0 & 0 \end{pmatrix}, \quad \lambda_5 = \begin{pmatrix} 0 & 0 & -i & 0 & 0 \\ 0 & 0 & 0 & 0 & 0 \\ i & 0 & 0 & 0 & 0 \\ 0 & 0 & 0 & 0 & 0 \\ 0 & 0 & 0 & 0 & 0 \end{pmatrix}, \quad \lambda_6 = \begin{pmatrix} 0 & 0 & 0 & 0 & 0 \\ 0 & 0 & 1 & 0 & 0 \\ 0 & 1 & 0 & 0 & 0 \\ 0 & 0 & 0 & 0 & 0 \\ 0 & 0 & 0 & 0 & 0 \end{pmatrix},$$

$$\lambda_7 = \begin{pmatrix} 0 & 0 & 0 & 0 & 0 \\ 0 & 0 & -i & 0 & 0 \\ 0 & i & 0 & 0 & 0 \\ 0 & 0 & 0 & 0 & 0 \\ 0 & 0 & 0 & 0 & 0 \end{pmatrix}, \qquad \lambda_8 = \frac{1}{\sqrt{3}} \begin{pmatrix} 1 & 0 & 0 & 0 & 0 \\ 0 & 1 & 0 & 0 & 0 \\ 0 & 0 & -2 & 0 & 0 \\ 0 & 0 & 0 & 0 & 0 \\ 0 & 0 & 0 & 0 & 0 \end{pmatrix}.$$

Mixed Quantum Numbers Generators

The generators with non vanishing SU(3) and SU(2) quantum numbers are not present in the SM. They can be computed through the commutator relations between the generators of SU(3) and the

generators of SU(2)

$$\lambda_9 = \begin{pmatrix} 0 & 0 & 0 & 1 & 0 \\ 0 & 0 & 0 & 0 & 0 \\ 0 & 0 & 0 & 0 & 0 \\ 1 & 0 & 0 & 0 & 0 \\ 0 & 0 & 0 & 0 & 0 \end{pmatrix}, \quad \lambda_{10} = \begin{pmatrix} 0 & 0 & 0 & i & 0 \\ 0 & 0 & 0 & 0 & 0 \\ 0 & 0 & 0 & 0 & 0 \\ i & 0 & 0 & 0 & 0 \\ 0 & 0 & 0 & 0 & 0 \end{pmatrix}, \quad \lambda_{11} = \begin{pmatrix} 0 & 0 & 0 & 0 & 0 \\ 0 & 0 & 0 & 1 & 0 \\ 0 & 0 & 0 & 0 & 0 \\ 0 & 1 & 0 & 0 & 0 \\ 0 & 0 & 0 & 0 & 0 \end{pmatrix},$$

$$\lambda_{12} = \begin{pmatrix} 0 & 0 & 0 & 0 & 0 \\ 0 & 0 & 0 & -i & 0 \\ 0 & 0 & 0 & 0 & 0 \\ 0 & i & 0 & 0 & 0 \\ 0 & 0 & 0 & 0 & 0 \end{pmatrix}, \quad \lambda_{13} = \begin{pmatrix} 0 & 0 & 0 & 0 & 0 \\ 0 & 0 & 0 & 0 & 0 \\ 0 & 0 & 0 & 1 & 0 \\ 0 & 0 & 1 & 0 & 0 \\ 0 & 0 & 0 & 0 & 0 \end{pmatrix}, \quad \lambda_{14} = \begin{pmatrix} 0 & 0 & 0 & 0 & 0 \\ 0 & 0 & 0 & 0 & 0 \\ 0 & 0 & 0 & -i & 0 \\ 0 & 0 & i & 0 & 0 \\ 0 & 0 & 0 & 0 & 0 \end{pmatrix},$$

$$\lambda_{15} = \begin{pmatrix} 0 & 0 & 0 & 0 & 1 \\ 0 & 0 & 0 & 0 & 0 \\ 0 & 0 & 0 & 0 & 0 \\ 0 & 0 & 0 & 0 & 0 \\ 1 & 0 & 0 & 0 & 0 \end{pmatrix}, \quad \lambda_{16} = \begin{pmatrix} 0 & 0 & 0 & 0 & -i \\ 0 & 0 & 0 & 0 & 0 \\ 0 & 0 & 0 & 0 & 0 \\ 0 & 0 & 0 & 0 & 0 \\ i & 0 & 0 & 0 & 0 \end{pmatrix}, \quad \lambda_{17} = \begin{pmatrix} 0 & 0 & 0 & 0 & 0 \\ 0 & 0 & 0 & 0 & 1 \\ 0 & 0 & 0 & 0 & 0 \\ 0 & 0 & 0 & 0 & 0 \\ 0 & 1 & 0 & 0 & 0 \end{pmatrix},$$

$$\lambda_{18} = \begin{pmatrix} 0 & 0 & 0 & 0 & 0 \\ 0 & 0 & 0 & 0 & -i \\ 0 & 0 & 0 & 0 & 0 \\ 0 & 0 & 0 & 0 & 0 \\ 0 & i & 0 & 0 & 0 \end{pmatrix}, \quad \lambda_{19} = \begin{pmatrix} 0 & 0 & 0 & 0 & 0 \\ 0 & 0 & 0 & 0 & 0 \\ 0 & 0 & 0 & 0 & 1 \\ 0 & 0 & 0 & 0 & 0 \\ 0 & 0 & 1 & 0 & 0 \end{pmatrix}, \quad \lambda_{20} = \begin{pmatrix} 0 & 0 & 0 & 0 & 0 \\ 0 & 0 & 0 & 0 & 0 \\ 0 & 0 & 0 & 0 & -i \\ 0 & 0 & 0 & 0 & 0 \\ 0 & 0 & i & 0 & 0 \end{pmatrix}.$$

SU(2) Generators

The SU(2) generators are embedded in SU(5)

$$\lambda_{21} = \begin{pmatrix} 0 & 0 & 0 & 0 & 0 \\ 0 & 0 & 0 & 0 & 0 \\ 0 & 0 & 0 & 0 & 0 \\ 0 & 0 & 0 & 0 & 1 \\ 0 & 0 & 0 & 1 & 0 \end{pmatrix}, \quad \lambda_{22} = \begin{pmatrix} 0 & 0 & 0 & 0 & 0 \\ 0 & 0 & 0 & 0 & 0 \\ 0 & 0 & 0 & 0 & 0 \\ 0 & 0 & 0 & 0 & -i \\ 0 & 0 & 0 & i & 0 \end{pmatrix}, \quad \lambda_{23} = \begin{pmatrix} 0 & 0 & 0 & 0 & 0 \\ 0 & 0 & 0 & 0 & 0 \\ 0 & 0 & 0 & 0 & 0 \\ 0 & 0 & 0 & 1 & 0 \\ 0 & 0 & 0 & 0 & -1 \end{pmatrix}.$$

Diagonal Generator

We have another diagonal generator that we will identify eventually with the SM hypercharge

$$\lambda_{24} = \frac{1}{\sqrt{15}} \begin{pmatrix} -2 & 0 & 0 & 0 & 0 \\ 0 & -2 & 0 & 0 & 0 \\ 0 & 0 & -2 & 0 & 0 \\ 0 & 0 & 0 & 3 & 0 \\ 0 & 0 & 0 & 0 & 3 \end{pmatrix},$$

where, under the unitary transformation.

$$\hat{\lambda}_a = A\lambda_a A^{-1}.$$

The unbroken generators are $\hat{\lambda}_2, \hat{\lambda}_5, \hat{\lambda}_7, \hat{\lambda}_{10}, \hat{\lambda}_{12}, \hat{\lambda}_{14}, \hat{\lambda}_{16}, \hat{\lambda}_{18}, \hat{\lambda}_{20}, \hat{\lambda}_{22}$ and the broken generators are $\hat{\lambda}_1, \hat{\lambda}_3, \hat{\lambda}_4, \hat{\lambda}_6, \hat{\lambda}_8, \hat{\lambda}_9, \hat{\lambda}_{11}, \hat{\lambda}_{13}, \hat{\lambda}_{15}, \hat{\lambda}_{17}, \hat{\lambda}_{19}, \hat{\lambda}_{21}, \hat{\lambda}_{23}, \hat{\lambda}_{24}$.

B Appendix: T-even and T-odd combinations

We choose the $[SU(2) \times U(1)]_1 \times [SU(2) \times U(1)]_2$ generators as

$$Q_1^a = \begin{pmatrix} \sigma^a/2 & 0 \\ 0 & 0_{3\times 3} \end{pmatrix}, \qquad Y_1 = diag(3, 3, -2, -2, -2)/10, \tag{639}$$

$$Q_2^a = \begin{pmatrix} 0_{3\times 3} & 0 \\ 0 & -\sigma^{a*}/2 \end{pmatrix}, \qquad Y_2 = diag(2, 2, 2, -3, -3)/10 \tag{640}$$

with $\{\sigma^a\}$ are the Pauli matrices. As $\{Q_1^a + Q_2^a, Y_1 + Y_2\}$ is unbroken then

$$W = W_1^a Q_1^a + W_2^a Q_2^a = W_1^1 Q_1^1 + W_1^2 Q_1^2 + W_1^3 Q_1^3 + W_2^1 Q_2^1 + W_2^2 Q_2^2 + W_2^3 Q_2^3 =$$
$$\begin{pmatrix} \frac{W_1^3}{2} & \frac{W_1^1}{2} - \frac{iW_1^2}{2} & & & \\ \frac{W_1^1}{2} + \frac{iW_1^2}{2} & -\frac{W_1^3}{2} & & & \\ & & 0 & & \\ & & & -\frac{W_2^3}{2} & -\left(\frac{W_2^1}{2} + \frac{iW_2^2}{2}\right) \\ & & & -\left(\frac{W_2^1}{2} - \frac{iW_2^2}{2}\right) & \frac{W_2^3}{2} \end{pmatrix},$$

and

$$B = B_1 Y_1 + B_2 Y_2 = \frac{1}{5}\begin{pmatrix} \frac{3B_1}{2}+B_2 & & & & \\ & \frac{3B_1}{2}+B_2 & & & \\ & & B_2-B_1 & & \\ & & & -B_1-\frac{3B_2}{2} & \\ & & & & -B_1-\frac{3B_2}{2} \end{pmatrix}. \tag{641}$$

Since SM gauge bosons are T-even, it satisfies

$$W\Sigma_0 - \Sigma_0 W^T = \tag{642}$$

$$\begin{pmatrix} & & & \frac{W_1^3+W_2^3}{2} & \frac{(W_1^1+W_2^1)-i(W_1^2+W_2^2)}{2} \\ & & & \frac{(W_1^1+W_2^1)+i(W_1^2+W_2^2)}{2} & -\frac{W_1^3+W_2^3}{2} \\ & & 0 & & \\ -\frac{W_1^3+W_2^3}{2} & -\frac{(W_1^1+W_2^1)+i(W_1^2+W_2^2)}{2} & & & \\ -\frac{(W_1^1+W_2^1)-i(W_1^2+W_2^2)}{2} & \frac{W_1^3+W_2^3}{2} & & & \end{pmatrix}, \tag{643}$$

and

$$B\Sigma_0 - \Sigma_0 B^T = \begin{pmatrix} & & \frac{B_1+B_2}{2} & & \\ & & & \frac{B_1+B_2}{2} & \\ 0 & & & & \\ -\frac{B_1+B_2}{2} & & & & \\ & -\frac{B_1+B_2}{2} & & & \end{pmatrix}. \tag{644}$$

Thus, we have respectively

$$W^{\pm} = \frac{1}{2}[(W_1^1+W_2^1) \mp i(W_1^2+W_2^2)], \qquad W^3 = \frac{W_1^3+W_2^3}{\sqrt{2}}, \qquad B = \frac{B_1+B_2}{\sqrt{2}}. \tag{645}$$

And now, as $\{Q_1^a - Q_2^a, Y_1 - Y_2\}$ is broken, then

$$W_H = W_1^a Q_1^a - W_2^a Q_2^a = W_1^1 Q_1^1 + W_1^2 Q_1^2 + W_1^3 Q_1^3 - W_2^1 Q_2^1 - W_2^2 Q_2^2 - W_2^3 Q_2^3 = \tag{646}$$

$$\begin{pmatrix} \frac{W_1^3}{2} & \frac{W_1^1-iW_1^2}{2} & & & \\ \frac{W_1^1+iW_1^2}{2} & -\frac{W_1^3}{2} & & & \\ & & 0 & & \\ & & & \frac{W_2^3}{2} & \frac{W_2^1+iW_2^2}{2} \\ & & & \frac{W_2^1-iW_2^2}{2} & -\frac{W_2^3}{2} \end{pmatrix}, \tag{647}$$

and

$$B_H = B_1 Y_1 - B_2 Y_2 = \frac{1}{5}\begin{pmatrix} \frac{3B_1}{2} - B_2 & & & & & \\ & \frac{3B_1}{2} - B_2 & & & & \\ & & -(B_1+B_2) & & & \\ & & & \frac{3B_2}{2} - B_1 & & \\ & & & & \frac{3B_2}{2} - B_1 \end{pmatrix}. \quad (648)$$

So

$$W_H\Sigma_0 - \Sigma_0 W_H^T = \quad (649)$$

$$\begin{pmatrix} & & & \frac{W_1^3-W_2^3}{2} & \frac{(W_1^1-W_2^1)-i(W_1^2-W_2^2)}{2} \\ & & & \frac{(W_1^1-W_2^1)+i(W_1^2-W_2^2)}{2} & -\frac{W_1^3-W_2^3}{2} \\ & & 0 & & \\ -\frac{W_1^3-W_2^3}{2} & -\frac{(W_1^1-W_2^1)+i(W_1^2-W_2^2)}{2} & & & \\ -\frac{(W_1^1-W_2^1)-i(W_1^2-W_2^2)}{2} & \frac{W_1^3-W_2^3}{2} & & & \end{pmatrix}, \quad (650)$$

and

$$B_H\Sigma_0 - \Sigma_0 B_H^T = \begin{pmatrix} & & \frac{B_1-B_2}{2} & & \\ & & & \frac{B_1-B_2}{2} & \\ & 0 & & & \\ -\frac{B_1-B_2}{2} & & & & \\ & -\frac{B_1-B_2}{2} & & & \end{pmatrix}. \quad (651)$$

Finally the T-odd combinations expand the heavy gauge sector

$$W_H^{\pm} = \frac{1}{2}[(W_1^1 - W_2^1) \mp i(W_1^2 - W_2^2)], \qquad W_H^3 = \frac{W_1^3 - W_2^3}{\sqrt{2}}, \qquad B_H = \frac{B_1 - B_2}{\sqrt{2}}. \quad (652)$$

C Appendix: Scalar Sector

We know that the Scalar Lagrangian in Littlest Higgs is

$$\mathcal{L}_S = \frac{f^2}{8} Tr[(\mathcal{D}_\mu\Sigma)(\mathcal{D}^\mu\Sigma)^\dagger], \quad (653)$$

where

$$\mathcal{D}_\mu\Sigma = \partial_\mu\Sigma - i\sum_{j=1}^{2}\left[g_j W_j^a\left(Q_j^a\Sigma + \Sigma Q_j^{aT}\right) + g_j' B_j\left(Y_j\Sigma + \Sigma Y_j^T\right)\right], \quad (654)$$

when we introduce the T-parity, the Scalar Lagrangian must be T-even, thus, we have that $g_1 = g_2 = \sqrt{2}g_W$ and $g_1' = g_2' = \sqrt{2}g'$, so the eq. (654) is written as

$$\mathcal{D}_\mu\Sigma = \partial_\mu\Sigma - i\sqrt{2}\sum_{j=1}^{2}\left[g_W W_j^a\left(Q_j^a\Sigma + \Sigma Q_j^{aT}\right) + g'B_j\left(Y_j\Sigma + \Sigma Y_j^T\right)\right]. \tag{655}$$

Recall that the action of T-parity in the scalar sector is defined as

$$\Pi \to -\Omega\Pi\Omega, \quad and \quad \Sigma \to \widetilde{\Sigma} = \Sigma_0\Omega\Sigma^\dagger\Omega\Sigma_0, \tag{656}$$

with $\Omega = diag\,(-1,-1,1,-1,-1)$. The term relevant for computing the mass of gauge bosons, under the T-parity, is

$$\left|-i\sqrt{2}\sum_{j=1}^{2}\left[g_W W_j^a\left(Q_j^a\widetilde{\Sigma} + \widetilde{\Sigma}Q_j^{aT}\right) + g'B_j\left(Y_j\widetilde{\Sigma} + \widetilde{\Sigma}Y_j^T\right)\right]\right|^2. \tag{657}$$

Calculating before introducing EWSM effects and taking at first order $\Sigma = \Sigma_0$, then

$$\widetilde{\Sigma} = \Sigma_0\Omega\Sigma^\dagger\Omega\Sigma_0 = \Sigma_0\Omega\Sigma_0\Omega\Sigma_0 = \Sigma_0. \tag{658}$$

Developing the eq.(657) by parts

$$g_W W_1^a\left(Q_1^a\Sigma_0 + \Sigma_0 Q_1^{aT}\right) = \begin{pmatrix} 0 & 0 & g_W W_1^a/2 \\ 0 & 0 & 0 \\ g_W W_1^a/2 & 0 & 0 \end{pmatrix}, \tag{659}$$

where $W_1^a = W_1^a\sigma^a$,

$$g'B_1\left(Y_1\Sigma_0 + \Sigma_0 Y_1^T\right) = \begin{pmatrix} 0 & 0 & g'B_1/10 \\ 0 & -2g\prime B_1/5 & 0 \\ g'B_1/10 & 0 & 0 \end{pmatrix}, \tag{660}$$

$$g_W W_2^a\left(Q_2^a\Sigma_0 + \Sigma_0 Q_2^{aT}\right) = \begin{pmatrix} 0 & 0 & -g_W W_2^a/2 \\ 0 & 0 & 0 \\ -g_W W_2^a/2 & 0 & 0 \end{pmatrix}, \tag{661}$$

where $W_2^a = W_2^a\sigma^{a*}$,

$$g'B_2\left(Y_2\Sigma_0 + \Sigma_0 Y_2^T\right) = \begin{pmatrix} 0 & 0 & -g'B_2/10 \\ 0 & 2g\prime B_2/5 & 0 \\ -g'B_2/10 & 0 & 0 \end{pmatrix}. \tag{662}$$

Therefore

$$\begin{pmatrix} 0 & 0 & \frac{g_W}{2}\left(W_1^a - W_2^a\right) + \frac{g'}{10}\left(B_1 - B_2\right) \\ 0 & \frac{2g'}{5}\left(B_2 - B_1\right) & 0 \\ \frac{g_W}{2}\left(W_1^a - W_2^a\right) + \frac{g'}{10}\left(B_1 - B_2\right) & 0 & 0 \end{pmatrix}, \tag{663}$$

then

$$2\left|\begin{pmatrix} 0 & 0 & \left(\frac{g_W}{2}\left(W_1^a - W_2^a\right) + \frac{g'}{10}\left(B_1 - B_2\right)\right)\mathbb{I}_{2\times 2} \\ 0 & \frac{2g'}{5}\left(B_2 - B_1\right) & 0 \\ \left(\frac{g_W}{2}\left(W_1^a - W_2^a\right) + \frac{g'}{10}\left(B_1 - B_2\right)\right)\mathbb{I}_{2\times 2} & 0 & 0 \end{pmatrix}\right|^2, \tag{664}$$

where $\mathbb{I}_{2\times 2}$ is a identity matrix 2×2, and omitting all crossed terms of W_j^a and B_j, we have

$$\begin{pmatrix} \left(\frac{g_W^2}{2}\left(W_1^a - W_2^a\right)^2 + \frac{g'^2}{50}\left(B_1 - B_2\right)^2\right)_{2\times 2} & 0 & 0 \\ 0 & \frac{8g'^2}{25}\left(B_1 - B_2\right)^2 & 0 \\ 0 & 0 & \left(\frac{g_W^2}{2}\left(W_1^a - W_2^a\right)^2 + \frac{g'^2}{50}\left(B_1 - B_2\right)^2\right)_{2\times 2} \end{pmatrix}, \tag{665}$$

since $\mathcal{L}_S = \frac{f^2}{8} Tr[(\mathcal{D}_\mu \Sigma)(\mathcal{D}^\mu \Sigma)^\dagger]$, we have that

$$\begin{aligned} \mathcal{L}_S &= \frac{f^2}{8}\left(2g_W^2\left(W_1^a - W_2^2\right)^2 + \frac{2}{5}\left(B_1 - B_2\right)^2\right) \\ &= \frac{f^2}{8}\left(2g_W^2\left(W_1^{a2} + W_2^{a2} - 2W_1^a W_2^a\right) + \frac{2}{5}\left(B_1^2 + B_2^2 - 2B_1 B_2\right)\right) \\ &= \frac{f^2}{4} g_W^2 \begin{pmatrix} W_1^a & W_2^a \end{pmatrix} \begin{pmatrix} 1 & -1 \\ -1 & 1 \end{pmatrix} \begin{pmatrix} W_1^a \\ W_2^a \end{pmatrix} \\ &+ \frac{f^2}{20} g'^2 \begin{pmatrix} B_1 & B_2 \end{pmatrix} \begin{pmatrix} 1 & -1 \\ -1 & 1 \end{pmatrix} \begin{pmatrix} B_1 \\ B_2 \end{pmatrix}. \end{aligned} \tag{666}$$

We defined gauge bosons mass eigenstates

$$\begin{aligned} \begin{pmatrix} W_L^a \\ W_H^a \end{pmatrix} &= \frac{1}{\sqrt{2}} \begin{pmatrix} 1 & 1 \\ 1 & -1 \end{pmatrix} \begin{pmatrix} W_1^a \\ W_2^a \end{pmatrix}, \\ \begin{pmatrix} B_L \\ B_H \end{pmatrix} &= \frac{1}{\sqrt{2}} \begin{pmatrix} 1 & 1 \\ 1 & -1 \end{pmatrix} \begin{pmatrix} B_1 \\ B_2 \end{pmatrix}. \end{aligned} \tag{667}$$

We can see that W_L^a and B_L are T-even, while W_H^a and B_H are T-odd. Also we can write this as

$$W_L^a = \cos\psi W_1^a + \sin\psi W_2^a, \qquad W_H^a = \sin\psi W_1^a - \cos\psi W_2^a, \tag{668}$$

where the mixing angle is given by $\sin\psi = \cos\psi = 1/\sqrt{2}$. Thus, diagonalizing the matrices, we have

$$\begin{aligned}
\mathcal{L}_S &= \frac{f^2}{4} g_W^2 \begin{pmatrix} W_1^a & W_2^a \end{pmatrix} \begin{pmatrix} 1 & -1 \\ -1 & 1 \end{pmatrix} \begin{pmatrix} W_1^a \\ W_2^a \end{pmatrix} \\
&\quad + \frac{f^2}{20} g'^2 \begin{pmatrix} B_1 & B_2 \end{pmatrix} \begin{pmatrix} 1 & -1 \\ -1 & 1 \end{pmatrix} \begin{pmatrix} B_1 \\ B_2 \end{pmatrix} \\
&= \frac{f^2}{4} g_W^2 \begin{pmatrix} W_L^a & W_H^a \end{pmatrix} \begin{pmatrix} 0 & 0 \\ 0 & 2 \end{pmatrix} \begin{pmatrix} W_L^a \\ W_H^a \end{pmatrix} \\
&\quad + \frac{f^2}{20} g'^2 \begin{pmatrix} B_L & B_H \end{pmatrix} \begin{pmatrix} 0 & 0 \\ 0 & 2 \end{pmatrix} \begin{pmatrix} B_L \\ B_H \end{pmatrix} + \cdots , \\
&= \frac{f^2}{2} g_W^2 W_H^{a\,2} + \frac{f^2}{10} g'^2 B_H^2, \\
&= \frac{1}{2} \left(f^2 g_W^2 W_H^{a2} + \frac{f^2 g'^2}{5} B_H^2 \right).
\end{aligned} \tag{669}$$

Thus, the masses of gauge bosons are

$$M_{W_H^a} = g_W f, \qquad M_{B_H} = \frac{g' f}{\sqrt{5}}. \tag{670}$$

If we consider EWSB effects of order $(v_h/f)^2$, the Σ field is

$$\Sigma = \begin{pmatrix} 0 & 0 & 0 & 1 & 0 \\ 0 & \epsilon^4/12 - \epsilon^2/2 & i\left(\epsilon - \epsilon^3/3\right) & 0 & 1 - \epsilon^2/2 + \epsilon^4/12 \\ 0 & i\left(\epsilon - \epsilon^3/3\right) & 1 - \epsilon^2 + \epsilon^4/6 & 0 & i\left(\epsilon - \epsilon^3/3\right) \\ 1 & 0 & 0 & 0 & 0 \\ 0 & 1 - \epsilon^2/2 + \epsilon^4/12 & i\left(\epsilon - \epsilon^3/3\right) & 0 & \epsilon^4/12 - \epsilon^2/2 \end{pmatrix}, \tag{671}$$

with $\epsilon = v_h/f$.

We can recalculate the masses of gauge bosons as above, now we do not omit the crossed terms of W_j^a and B_j, where $a = 1, 2$. We have that

$$\begin{aligned}
\mathcal{L}_S &= \frac{f^2 g_W^2}{4} \left[-\frac{\epsilon^4}{6} W_1 W_2 + \epsilon^2 W_1 W_2 + (W_1 - W_2)^2 \right] \\
&\quad + \frac{f^2 g_W^2}{4} \left[\frac{\epsilon^4}{8} \left(\left(W_1^3 - W_2^3\right)^2 - \frac{1}{4} W_1^3 W_2^3 \right) + \epsilon^2 W_1^3 W_2^3 + \left(W_1^3 - W_2^3\right)^2 \right] \\
&\quad + \frac{f^2 g'^2}{4} \left[\epsilon^4 \left(\frac{1}{8} \left(B_1^2 + B_2^2\right) - \frac{5}{12} B_1 B_2 \right) + \epsilon^2 B_1 B_2 + \frac{1}{5} \left(B_1 - B_2\right)^2 \right] \\
&\quad + \frac{f^2 g_W g'}{4} \left[\frac{\epsilon^4}{4} \left(- \left(W_1^3 - W_2^3\right) \left(B_1 - B_2\right) + \frac{2}{3} \left(B_1 W_2^3 + B_2 W_1^3\right) \right) - \epsilon^2 \left(B_1 W_2^3 + B_2 W_1^3\right) \right].
\end{aligned} \tag{672}$$

Analyzing the Scalar Lagrangian by parts, taking the eigenstates defined above and diagonalizing the matrices from eq.(672)

$$-\frac{\epsilon^4}{6}W_1^aW_2^a+\epsilon^2W_1^aW_2^a+(W_1^a-W_2^a)^2=\begin{pmatrix} W_L^a & W_H^a \end{pmatrix}\begin{pmatrix} \frac{\epsilon^2}{2}\left(1-\epsilon^2/6\right) & 0 \\ 0 & 2\left(1-\epsilon^2/4\right)\end{pmatrix}\begin{pmatrix} W_L^a \\ W_H^a\end{pmatrix}$$
$$=\frac{\epsilon^2}{2}\left(1-\frac{\epsilon^2}{6}\right)W_L^{a2}+2\left(1-\frac{\epsilon^2}{4}\right)W_H^{a2}. \tag{673}$$

If we defined as [25]

$$W_H^{\pm}=\frac{1}{\sqrt{2}}\left(W_H^1\mp iW_H^2\right),\qquad W_L^{\pm}=\frac{1}{\sqrt{2}}\left(W_L^1\mp iW_L^2\right), \tag{674}$$

then

$$-\frac{\epsilon^4}{6}W_1^aW_2^a+\epsilon^2W_1^aW_2^a+(W_1^a-W_2^a)^2=\frac{\epsilon^2}{2}\left(1-\frac{\epsilon^2}{6}\right)W_L^+W_L^-+2\left(1-\frac{\epsilon^2}{4}\right)W_H^+W_H^-. \tag{675}$$

Now, the second line of Lagrangian

$$\frac{\epsilon^4}{8}\left(\left(W_1^3-W_2^3\right)^2-\frac{1}{4}W_1^3W_2^3\right)+\epsilon^2W_1^3W_2^3+\left(W_1^3-W_2^3\right)^2=\frac{\epsilon^4}{8}\left((W_1^3)^2+(W_2^3)^2-\frac{10}{3}W_1^3W_2^3\right)$$
$$+\epsilon^2W_1^3W_2^3+(W_1^3-W_2^3)^2, \tag{676}$$

$$\begin{pmatrix} W_L^3 & W_H^3 \end{pmatrix}\begin{pmatrix} \frac{\epsilon^2}{2}\left(1-\frac{\epsilon^2}{6}\right) & 0 \\ 0 & 2\left(1-\frac{\epsilon^2}{4}\right)\end{pmatrix}\begin{pmatrix} W_L^3 \\ W_H^3\end{pmatrix}=\frac{\epsilon^2}{2}\left(1-\frac{\epsilon^2}{6}\right)\left(W_L^3\right)^2+2\left(1-\frac{\epsilon^2}{4}\right)\left(W_H^3\right)^2. \tag{677}$$

For the third line of the Lagrangian

$$\epsilon^4\left(\frac{1}{8}\left(B_1^2+B_2^2\right)-\frac{5}{12}B_1B_2\right)+\epsilon^2B_1B_2+\frac{1}{5}\left(B_1-B_2\right)^2$$
$$=\begin{pmatrix} B_L & B_H \end{pmatrix}\begin{pmatrix} \frac{\epsilon^2}{2}\left(1-\frac{\epsilon^2}{6}\right) & 0 \\ 0 & \frac{2}{5}\left(1-\frac{5\epsilon^2}{4}\right)\end{pmatrix}\begin{pmatrix} B_L \\ B_H\end{pmatrix}=\frac{\epsilon^2}{2}\left(1-\frac{\epsilon^2}{6}\right)\left(B_L\right)^2+\frac{2}{5}\left(1-\frac{5\epsilon^2}{4}\right)\left(B_H\right)^2. \tag{678}$$

Finally

$$\frac{\epsilon^4}{4}\left(-\left(W_1^3-W_2^3\right)\left(B_1-B_2\right)+\frac{2}{3}\left(B_1W_2^3+B_2W_1^3\right)\right)-\epsilon^2\left(B_1W_2^3+B_2W_1^3\right), \tag{679}$$

with the aid of

$$\begin{aligned} B_1W_2^3 + B_2W_1^3 &= \frac{1}{2}\left[\left(W_1^3 + W_2^3\right)(B_1 + B_2) - \left(W_1^3 - W_2^3\right)(B_1 - B_2)\right] \\ &= W_L^3 B_L - W_H^3 B_H, \end{aligned} \tag{680}$$

we will obtain

$$\frac{\epsilon^4}{4}\left(-\frac{8}{3}W_H^3 B_H + \frac{2}{3}W_L^3 B_L\right) - \epsilon^2\left(W_L^3 B_L - W_H^3 B_H\right) = -\epsilon^2\left(1 - \frac{\epsilon^2}{6}\right)W_L^3 B_L + \epsilon^2\left(1 - \frac{2\epsilon^2}{3}\right)W_H^3 B_H. \tag{681}$$

Finally the Lagrangian looks

$$\begin{aligned} \mathcal{L}_S = &\frac{1}{2}\left[\frac{g_W^2 \upsilon_h^2}{4}\left(1 - \frac{\upsilon_h^2}{6f^2}\right)\right] W_L^+ W_L^- \\ &+ \frac{1}{2}\left[f^2 g_W^2\left(1 - \frac{\upsilon_h^2}{4f^2}\right)\right] W_H^+ W_H^- \\ &+ \frac{1}{2}\left[\frac{g_W^2 \upsilon_h^2}{4}\left(1 - \frac{\upsilon_h^2}{6f^2}\right)\right] \left(W_L^3\right)^2 \\ &+ \frac{1}{2}\left[f^2 g_W^2\left(1 - \frac{\upsilon_h^2}{4f^2}\right)\right] \left(W_H^3\right)^2 \\ &+ \frac{1}{2}\left[\frac{g'^2 \upsilon_h^2}{4}\left(1 - \frac{\upsilon_h^2}{6f^2}\right)\right] \left(B_L\right)^2 \\ &+ \frac{1}{2}\left[\frac{f^2 g'^2}{5}\left(1 - \frac{5\upsilon_h^2}{4f^2}\right)\right] \left(B_H\right)^2 \\ &+ \frac{1}{2}\left[-\frac{g_W g' \upsilon_h^2}{2}\left(1 - \frac{\upsilon_h^2}{6f^2}\right)\right] W_L^3 B_L \\ &+ \frac{1}{2}\left[\frac{g_W g' \upsilon_h^2}{2}\left(1 - \frac{2\upsilon_h^2}{3f^2}\right)\right] W_H^3 B_H. \end{aligned} \tag{682}$$

As we can see in the Lagrangian above the neutral light sector is given by W_L^3, B_L, and $W_L^3 B_L$

$$\frac{\upsilon_h^2}{4}\left(1 - \frac{\upsilon_h^2}{6f^2}\right)\left(g_W^2\left(W_L^3\right)^2 - 2g_W g' W_L^3 B_L + g'^2\left(B_L\right)^2\right). \tag{683}$$

The eq. (683) has the same form that the off-diagonal terms of the standard model for electroweak interactions, so from this sector we will get the SM neutral gauge bosons Z_L and A_L. We need to diagonalize the matrix

$$\begin{pmatrix} W_L^3 & B_L \end{pmatrix}\begin{pmatrix} g_W^2 & -g_w g' \\ -g_w g' & g'^2 \end{pmatrix}\begin{pmatrix} W_L^3 \\ B_L \end{pmatrix}, \tag{684}$$

the physical fields Z_L and A_L are [7]

$$\begin{pmatrix} Z_L \\ A_L \end{pmatrix} = \frac{1}{\sqrt{g_W^2 + g'^2}} \begin{pmatrix} g_W & -g' \\ g' & g_W \end{pmatrix} \begin{pmatrix} W_L^3 \\ B_L \end{pmatrix}, \tag{685}$$

For the light sector the mixing angle is just the SM Weinberg angle

$$\frac{g'}{g_W} = \tan\theta_W, \tag{686}$$

in terms of θ_W

$$A_L = \cos\theta_W B_L + \sin\theta_W W_L^3, \qquad Z_L = -\sin\theta_W B_L + \cos\theta_W W_L^3. \tag{687}$$

Thus,

$$\begin{pmatrix} W_L^3 & B_L \end{pmatrix} \begin{pmatrix} g_W^2 & -g_w g' \\ -g_w g' & g'^2 \end{pmatrix} \begin{pmatrix} W_L^3 \\ B_L \end{pmatrix} = \begin{pmatrix} Z_L & A_L \end{pmatrix} \begin{pmatrix} g_W^2 + g'^2 & 0 \\ 0 & 0 \end{pmatrix} \begin{pmatrix} Z_L \\ A_L \end{pmatrix}, \tag{688}$$

so the eq.(683) looks like

$$\frac{\upsilon_h^2}{4}\left(1 - \frac{\upsilon_h^2}{6f^2}\right)\left(g_W^2 \left(W_L^3\right)^2 - 2g_W g' W_L^3 B_L + g'^2 \left(B_L\right)^2\right) = \frac{\upsilon_h^2}{4}\left(1 - \frac{\upsilon_h^2}{6f^2}\right)\left(g_W^2 + g'^2\right) Z_L^2. \tag{689}$$

then

$$\frac{\upsilon_h^2}{4}\left(1 - \frac{\upsilon_h^2}{6f^2}\right)\left(g_W^2 + g'^2\right) Z_L^2 = \frac{g_W^2 \upsilon_h^2}{4\cos^2\theta_W}\left(1 - \frac{\upsilon_h^2}{6f^2}\right) Z_L^2. \tag{690}$$

Replacing this in the Lagrangian

$$\begin{aligned}
\mathcal{L}_S = & \frac{1}{2}\left[\frac{g_W^2 \upsilon_h^2}{4}\left(1 - \frac{\upsilon_h^2}{6f^2}\right)\right] W_L^+ W_L^- \\
& + \frac{1}{2}\left[f^2 g_W^2 \left(1 - \frac{\upsilon_h^2}{4f^2}\right)\right] W_H^+ W_H^- \\
& + \frac{1}{2}\left[f^2 g_W^2 \left(1 - \frac{\upsilon_h^2}{4f^2}\right)\right] \left(W_H^3\right)^2 \\
& + \frac{1}{2}\left[\frac{f^2 g'^2}{5}\left(1 - \frac{5\upsilon_h^2}{4f^2}\right)\right] \left(B_H\right)^2 \\
& + \frac{1}{2}\left[\frac{g_W g' \upsilon_h^2}{2}\left(1 - \frac{2\upsilon_h^2}{3f^2}\right)\right] W_H^3 B_H \\
& + \frac{1}{2}\left[\frac{g_W^2 \upsilon_h^2}{4\cos^2\theta_W}\left(1 - \frac{\upsilon_h^2}{6f^2}\right) Z_L^2\right].
\end{aligned} \tag{691}$$

Now, the heavy gauge sector is

$$f^2 g_W^2 \left(1 - \frac{v_h^2}{4f^2}\right) \left(W_H^3\right)^2 + \frac{g_W g' v_h^2}{2} \left(1 - \frac{2v_h^2}{3f^2}\right) W_H^3 B_H + \frac{f^2 g'^2}{5} \left(1 - \frac{5v_h^2}{4f^2}\right) \left(B_H\right)^2 . \tag{692}$$

The new mass eigenstates in the neutral heavy sector will be a linear combination of the W_H^3 and the B_H gauge bosons, producing an A_H and a Z_H. The mixing angle introduced into the neutral heavy sector by EWSB will be of order $\left(v_h^2/f^2\right)$ [23]

$$\sin\theta_H \approx x_H \frac{v_h^2}{f^2}, \qquad x_H = \frac{5 g_W g'}{4\left(5g_W^2 - g'^2\right)}. \tag{693}$$

The new heavy neutral mass eigenstates are given by

$$Z_H = \sin\theta_H B_H + \cos\theta_H W_H^3, \qquad\qquad A_H = \cos\theta_H B_H - \sin\theta_H W_H^3. \tag{694}$$

So we have

$$\begin{pmatrix} Z_H \\ A_H \end{pmatrix} = \begin{pmatrix} 1 & x_H \frac{v_h^2}{f^2} \\ -x_H \frac{v_h^2}{f^2} & 1 \end{pmatrix} \begin{pmatrix} W_H^3 \\ B_H \end{pmatrix}, \tag{695}$$

and their masses are [23]

$$M_{Z_H}^2 = g_W^2 f^2 \left(1 - \frac{v_h^2}{4f^2}\right), \qquad M_{A_H}^2 = \frac{g'^2 f^2}{5} \left(1 - \frac{5v_h^2}{4f^2}\right). \tag{696}$$

Finally, the Scalar Lagrangian is

$$\begin{aligned} \mathcal{L}_S = & \frac{1}{2}\left[\frac{g_W^2 v_h^2}{4}\left(1 - \frac{v_h^2}{6f^2}\right)\right] W_L^+ W_L^- \\ & + \frac{1}{2}\left[f^2 g_W^2 \left(1 - \frac{v_h^2}{4f^2}\right)\right] W_H^+ W_H^- \\ & + \frac{1}{2}\left[f^2 g_W^2 \left(1 - \frac{v_h^2}{4f^2}\right)\right] \left(Z_H\right)^2 \\ & + \frac{1}{2}\left[\frac{f^2 g'^2}{5}\left(1 - \frac{5v_h^2}{4f^2}\right)\right] \left(A_H\right)^2 \\ & + \frac{1}{2}\left[\frac{g_W^2 v_h^2}{4\cos^2\theta_W}\left(1 - \frac{v_h^2}{6f^2}\right)\right] Z_L^2. \end{aligned} \tag{697}$$

The light gauge sector includes $W_L^\pm$, Z_L, and A_L bosons, that we identify as the SM gauge bosons

with masses

$$\begin{aligned} M_{W_L^\pm} &= \frac{g_W v_h}{2}\left(1-\frac{v_h^2}{6f^2}\right)^{1/2} \approx \frac{g_W v_h}{2}\left(1-\frac{v_h^2}{12f^2}\right), \\ M_{Z_L} &= \frac{g_W v_h}{2\cos\theta_H}\left(1-\frac{v_h^2}{6f^2}\right)^{1/2} = \frac{M_{W_L^\pm}}{\cos\theta_W}, \\ M_{A_L} &= 0, \end{aligned} \tag{698}$$

and the mass of the heavy bosons are

$$\begin{aligned} M_{W_H^\pm} = M_{Z_H} &= f g_W\left(1-\frac{v_h^2}{4f^2}\right)^{1/2} \approx f g_W\left(1-\frac{v_h^2}{8f^2}\right), \\ M_{A_H} &= \frac{f g'}{\sqrt{5}}\left(1-\frac{5v_h^2}{4f^2}\right)^{1/2} \approx \frac{f g'}{\sqrt{5}}\left(1-\frac{5v_h^2}{8f^2}\right). \end{aligned} \tag{699}$$

D Appendix: Two-point Functions

Considering a diagram with two legs, the general form to write the corresponding loop amplitude is

$$\frac{i}{16\pi^2}\{B_0, B^\mu\} = \mu^{4-D}\int \frac{d^Dq}{(2\pi)^D}\frac{\{1, q^\mu\}}{(q^2-m_0^2)[(q+p)^2-m_1^2]}, \tag{700}$$

where m_0 and m_1 are the internal masses in the loop. The corresponding tensor coefficients are functions of the invariant quantities $(args) = (p^2, m_0^2, m_1^2)$, where p is the momentum of the particle. The functions $B \equiv B(0; M_1^2, M_2^2)$ and $\overline{B} \equiv B(0; M_2^2, M_1^2)$ read

$$B_0 = \overline{B}_0 = \Delta_\epsilon + 1 - \frac{M_1^2 \ln\frac{M_1^2}{\mu^2} - M_2^2 \ln\frac{M_2^2}{\mu^2}}{M_1^2 - M_2^2}, \tag{701}$$

$$\begin{aligned} B_1 &= -\frac{\Delta_\epsilon}{2} + \frac{4M_1^2M_2^2 - 3M_1^4 - M_2^4 + 2M_1^4\ln\frac{M_1^2}{\mu^2} + 2M_2^2(M_2^2-2M_1^2)\ln\frac{M_2^2}{\mu^2}}{4(M_1^2-M_2^2)^2} \\ &= -\overline{B}_0 - \overline{B}_1, \end{aligned} \tag{702}$$

with $\Delta_\epsilon \equiv \frac{2}{\epsilon} - \gamma + \ln 4\pi$. These functions are ultraviolet divergent in $D = 4$ dimensions.

E Appendix: Three-point Functions

In the Appendix C of [25] are shown the three-point functions that we used in the amplitude development. The function's arguments are $(args) = (p_1^2, Q^2, p_2^2; m_0^2, m_1^2, m_2^2)$, with p_1 and p_2 the external momenta, m_0 the mass propagator, M_1 and M_2 the masses of particles within the loop and $Q \equiv p_2 - p_1$.

$$\frac{i}{16\pi^2} = \{C_0, C^\mu, C^{\mu\nu}\}(args) = \mu^{4-D} \int \frac{d^D q}{(2\pi)^D} \frac{\{1, q^\mu, q^\mu q^\nu\}}{(q^2 - m_0^2)[(q+p_1)^2 - m_1^2][(q+p_2)^2 - m_2^2]}. \tag{703}$$

The functions $C \equiv C(0, Q^2, 0; M_1^2, M_2^2, M_2^2)$ with $x \equiv M_2^2/M_1^2$ are given by

$$C_0 = \frac{1}{M_2^2}\left[\frac{1 - x + \ln x}{(1-x)^2} + \frac{Q^2}{M_1^2}\frac{-2 - 3x + 6x^2 - x^3 - 6x\ln x}{12x(1-x)^4}\right], \tag{704}$$

$$C_1 = C_2 = \frac{1}{M_1^2}\frac{-3 + 4x - x^2 - 2\ln x}{4(1-x)^3} + \mathcal{O}(Q^4), \tag{705}$$

$$C_{11} = C_{22} = 2C_{12} = \frac{1}{M_1^2}\frac{11 - 18x + 9x^2 - 2x^3 + 6\ln x}{18(1-x)^4} + \mathcal{O}(Q^4), \tag{706}$$

$$C_{00} = -\frac{1}{2}B_1 - \frac{Q^2}{M_1^2}\frac{11 - 18x + 9x^2 - 2x^3 + 6\ln x}{72(1-x)^4} + \mathcal{O}(Q^4). \tag{707}$$

Defining $\overline{C} \equiv C(0, Q^2, 0; M_2^2, M_1^2, M_1^2)$,

$$\overline{C}_0 = \frac{1}{M_2^2}\left[\frac{-1 + x - \ln x}{(1-x)^2} + \frac{Q^2}{M_1^2}\frac{-1 + +x - 3x^2 - 2x^3 + 6x^2\ln x}{12x(1-x)^4}\right] + \mathcal{O}(Q^4), \tag{708}$$

$$\overline{C}_1 = \overline{C}_2 = \frac{1}{M_1^2}\frac{1 - 4x + 3x^2 - 2x^2\ln x}{4(1-x)^3}, \tag{709}$$

$$\overline{C}_{11} = \overline{C}_{22} = 2\overline{C}_{12} = \frac{1}{M_1^2}\frac{-2 + 9x - 18x^2 + 11x^3 - 6x^3\ln x}{18(1-x)^4}, \tag{710}$$

$$\overline{C}_{00} = -\frac{1}{2}\overline{B}_1 - \frac{Q^2}{M_1^2}\frac{-2 + 9x - 18x^2 + 11x^3 + 6x^3\ln x}{72(1-x)^4} + \mathcal{O}(Q^4). \tag{711}$$

It is important to note that functions C_{00} y $\overline{C}_{00}$ are ultraviolet divergent in $D = 4$ dimensions. In the limit $Q^2 = 0$ the following useful relations among two and three point functions hold

$$\overline{B}_1 + 2\overline{C}_{00} = 0 \tag{712}$$

$$-\frac{1}{4} + \frac{1}{2}\overline{B}_1 + C_{00} - \frac{x}{2}M_1^2 C_0 = 0 \tag{713}$$

$$-\frac{1}{2} + \overline{B}_1 + 6\overline{C}_{00} - xM_1^2\overline{C}_0 = \Delta_\epsilon - \ln\frac{M_1^2}{\mu^2}. \tag{714}$$

F Appendix: Four-point Functions

The functions that we used in our development are all ultraviolet finite

$$\frac{i}{16\pi^2}\{D_0, D^\mu, D^{\mu\nu}\}(args) = \int \frac{d^4q}{(2\pi)^4}\frac{\{1, q^\mu, q^\mu q^\nu\}}{(q^2-m_0^2)[(q+k_1)^2-m_1^2][(q+k_2)^2-m_2^2][(q+k_3)^2-m_3^2]}, \tag{715}$$

with $k_j = \sum_i^j p_i$ and $(args) = (p_1^2, p_2^2, p_3^2, p_4^2, (p_1+p_2)^2, (p_2+p_3)^2; m_0^2, m_1^2, m_2^2, m_3^2)$. In the limit of zero external momenta, only the following integrals are relevant

$$\frac{i}{16\pi^2}D_0 = \int \frac{d^4q}{(2\pi)^2}\frac{1}{(q^2-m_0^2)(q^2-m_1^2)(q^2-m_2^2)(q^2-m_3^2)}, \tag{716}$$

$$\frac{i}{16\pi^2}D_{00} = \frac{1}{4}\int \frac{d^4q}{(2\pi)^2}\frac{q^2}{(q^2-m_0^2)(q^2-m_1^2)(q^2-m_2^2)(q^2-m_3^2)}. \tag{717}$$

In the terms of the mass ratios $x = m_1^2/m_0^2$, $y = m_2^2/m_0^2$, $z = m_3^2/m_0^2$ the integrals above can be written as [25] [37]

$$\begin{aligned} d_0(x,y,z) \equiv m_0^4 D_0 = \Bigg[&\frac{x\ln x}{(1-x)(x-y)(x-z)} - \frac{y\ln y}{(1-y)(x-y)(y-z)} \\ &+ \frac{z\ln z}{(1-z)(x-z)(y-z)}\Bigg], \end{aligned} \tag{718}$$

$$\begin{aligned} \widetilde{d}_0(x,y,z) \equiv 4m_0^2 D_{00} = \Bigg[&\frac{x^2\ln x}{(1-x)(x-y)(x-z)} - \frac{y^2\ln y}{(1-y)(x-y)(y-z)} \\ &+ \frac{z^2\ln z}{(1-z)(x-z)(y-z)}\Bigg]. \end{aligned} \tag{719}$$

$$\widetilde{d}_0'(x,y,z) = \frac{x^2\ln x}{(1-x)(x-y)(z-x)} + \frac{y^2\ln y}{(1-y)(x-y)(z-y)} + \frac{z^2\ln z}{(1-z)(x-z)(y-z)}, \tag{720}$$

with $\widetilde{d}(x,y) = \widetilde{d}'(x,y,1)$. For two equals masses ($m_0 = m_3$) we get

$$d_0(x,y) = -\left[\frac{x\ln x}{(1-x)^2(x-y)} - \frac{y\ln y}{(1-y)^2(x-y)} + \frac{1}{(1-x)(1-y)}\right], \tag{721}$$

$$\widetilde{d}_0(x,y) = -\left[\frac{x^2\ln x}{(1-x)^2(x-y)} - \frac{y^2\ln y}{(1-y)^2(x-y)} + \frac{1}{(1-x)(1-y)}\right]. \tag{722}$$

G Appendix: Light-Heavy Four-point Functions

The form factors involved in the $\ell \to \ell'\ell''\bar{\ell}'''$ decay are given by the eqs. (354), (355) and (356).

$$F_B^{\nu_i^l \nu_j^l} = \frac{\alpha_W}{16\pi M_W^2 s_W^2} \sum_{i,j=1}^{3} \{W_{\ell i} W^\dagger_{\ell' i} W_{\ell''' j} W^\dagger_{\ell'' j} + (\ell' \leftrightarrow \ell'')\} f_B^l(y_i, y_j), \tag{723}$$

$$F_B^{\nu_i^l \chi_j^h} = \frac{\alpha_W}{16\pi M_W^2 s_W^2} \sum_{i=1}^{3} \sum_{j=7}^{9} \{W_{\ell i} W^*_{\ell' i} \theta^\dagger_{\ell''' j} \theta_{\ell'' j} + (\ell' \leftrightarrow \ell'')\} f_B^{lh}(y_i, x_j), \tag{724}$$

$$F_B^{\chi_i^h \chi_j^h} = \frac{\alpha_W}{16\pi M_W^2 s_W^2} \sum_{i,j=7}^{9} \{\theta^\dagger_{\ell i} \theta_{\ell' i} \theta^\dagger_{\ell''' j} \theta_{\ell'' j} + (\ell' \leftrightarrow \ell'')\} f_B^h(x_i, x_j), \tag{725}$$

where we have added the superscripts (l), (lh) and (h) to the f_B functions to indicate that these functions are composed of light-light, light-heavy and heavy-heavy neutrinos, respectively.
Since the masses of light neutrinos satisfy $m_i \ll M_W$, it is convenient to define the y_i variable as $y_i = \frac{m_i^2}{M_W^2}$ as in this limit $y_i \to 0$. On the other hand, the condition of the heavy neutrino masses is $M_W \ll M_j$, hence it is natural to define $x_j = \frac{M_W^2}{M_j^2}$, so the x_j variable behaves as $x_j \to 0$.

The $f_B^l(y_i, y_j)$ function is formed by the d_0 and $\bar{d}_0$ functions. Because just light neutrinos are considered in the f_B function the d_0 and $\bar{d}_0$ ones have $y_{i,j}$ as variables. Therefore, d_0 and $\bar{d}_0$ functions are given from the eqs. (721) and (722). So the $f_B^l(y_i, y_i)$ function can be written as

$$f_B^l(y_i, y_j) = \left(1 + \frac{1}{4} y_i y_j\right) \bar{d}_0(y_i, y_j) - 2 y_i y_j d_0(y_i, y_j), \tag{726}$$

with $y_{i,j} = \frac{m_{i,j}^2}{M_W^2}$ $(i, j = 1, 2, 3)$.

The $f_B^{lh}(y_i, x_j)$ function mixes light-heavy neutrinos, then it has y_i and x_j as variables. The d_0 and $\bar{d}_0$ functions defined in the Appendix C have variables which behave as $\frac{m_i^2}{M_W^2}$. The consideration on heavy neutrinos variables is $x_j = \frac{M_W^2}{M_j^2}$, though. We have to refactor them considering the y_i and x_j variables for light and heavy neutrinos respectively,

$$d_0^{lh}(y_i, x_j) = \frac{y_i x_j \, \ln y_i}{(1 - y_i)^2 (1 - y_i x_j)} + \frac{x_j^2 \, \ln x_j}{(1 - x_j)^2 (1 - y_i x_j)} + \frac{x_j}{(1 - y_i)(1 - x_j)}, \tag{727}$$

$$\bar{d}_0^{lh}(y_i, x_j) = \frac{y_i^2 x_j \, \ln y_i}{(1 - y_i)^2 (1 - y_i x_j)} + \frac{x_j \, \ln x_j}{(1 - x_j)^2 (1 - y_i x_j)} + \frac{x_j}{(1 - y_i)(1 - x_j)}, \tag{728}$$

where $y_i = m_i^2/M_W^2$ $(i = 1, 2, 3)$ and $x_j = M_W^2/M_j^2$ $(j = 1, 2, 3)$. From the equations above the $f_B^{lh}(y_i, x_j)$ function is read as follows

$$f_B^{lh}(y_i, x_j) = \left(1 + \frac{1}{4}\frac{y_i}{x_j}\right) \bar{d}_0^{lh}(y_i, x_j) - 2\frac{y_i}{x_j} d_0^{lh}(y_i, x_j). \tag{729}$$

Finally, the $f_B^h(x_i, x_j)$ function just has heavy-neutrino variables $x_{i,j} = M_W^2/M_j^2$, hence, we need to refactor the d_0 and $\bar{d}_0$ functions as

$$d_0^h(x_i, x_j) = -\left[\frac{x_i^2 x_j \, \ln x_i}{(1-x_i)^2(x_i - x_j)} - \frac{x_i x_j^2 \, \ln x_j}{(1-x_j)^2(x_i - x_j)} + \frac{x_i x_j}{(1-x_i)(1-x_j)}\right], \tag{730}$$

$$\bar{d}_0^h(x_i, x_j) = -\left[\frac{x_i x_j \, \ln x_i}{(1-x_i)^2(x_i - x_j)} - \frac{x_i x_j \, \ln x_j}{(1-x_j)^2(x_i - x_j)} + \frac{x_i x_j}{(1-x_i)(1-x_j)}\right], \tag{731}$$

with $i, j = 1, 2, 3$. Therefore, the $f_B^h(x_i, x_j)$ function is given by

$$f_B^h(x_i, x_j) = \left(1 + \frac{1}{4}\frac{1}{x_i x_j}\right) \bar{d}_0^h(x_i, x_j) - 2\frac{1}{x_i x_j} d_0^h(x_i, x_j). \tag{732}$$

For the functions which coming from LNV contributions $f_B^{(l,lh,h)-LNV}(z_i, z_j)$ (eq. (375)) we can apply the same arguments as the previous $f_B^{l,lh,h}(z_i, z_j)$, therefore

$$\begin{aligned}
f_B^{l-LNV}(y_i, y_j) &= \sqrt{y_i y_j}\left(2\bar{d}_0(y_i, y_j) - (4 + y_i y_j) d_0(y_i, y_j)\right), \\
f_B^{lh-LNV}(y_i, x_j) &= \sqrt{\frac{y_i}{x_j}}\left(2\bar{d}_0^{lh}(y_i, x_j) - (4 + \frac{y_i}{x_j}) d_0^{lh}(y_i, x_j)\right), \\
f_B^{h-LNV}(x_i, x_j) &= \frac{1}{\sqrt{x_i x_j}}\left(2\bar{d}_0^h(x_i, x_j) - \left(4 + \frac{1}{x_i x_j}\right) d_0^h(x_i, x_j)\right),
\end{aligned} \tag{733}$$

with $y_i = m_i^2/M_W^2$, m_i the mass of light neutrinos; $x_j = M_W^2/M_j^2$, M_j the mass of heavy neutrinos.

H Appendix: Hadronization tools

Within the RχT framework, bilinear light quark operators coupled to the external sources are added to the massless QCD Lagrangian:

$$\mathcal{L}_{\rm QCD} = \mathcal{L}^0_{\rm QCD} + \overline{q}\left[\gamma_\mu(v^\mu + \gamma_5 a^\mu) - (s - ip\gamma_5)\right] q, \tag{734}$$

where the auxiliary fields defined as $v^\mu = v^\mu_i \lambda^i/2$, $a^\mu = a^\mu_i \lambda^i/2$, and $s = s_i\lambda^i$, with λ^i the Gell-Mann matrices, are Hermitian matrices in the flavour space. Once the RχT action $\mathcal{L}_{\rm R\chi T}$ is fixed, we can get the hadronization of the bilinear quark current by taking the appropriate functional derivative with respect to the external fields:

$$\begin{aligned} S^i &= -\overline{q}\lambda^i q = \left.\frac{\partial \mathcal{L}_{\rm R\chi T}}{\partial s_i}\right|_{j=0}, & P^i &= \overline{q} i\gamma_5 \lambda^i q = \left.\frac{\partial \mathcal{L}_{\rm R\chi T}}{\partial p_i}\right|_{j=0}, \\ V^i_\mu &= \overline{q}\gamma_\mu \frac{\lambda^i}{2} q = \left.\frac{\partial \mathcal{L}_{\rm R\chi T}}{\partial v^\mu_i}\right|_{j=0}, & A^i_\mu &= \overline{q}\gamma_\mu\gamma_5 \frac{\lambda^i}{2} q = \left.\frac{\partial \mathcal{L}_{\rm R\chi T}}{\partial a^\mu_i}\right|_{j=0}, \end{aligned} \tag{735}$$

where $j = 0$ indicates that all external currents are set to zero.
The vector form factor from the γ contribution to the decay into two pseudoscalar mesons is driven by the electromagnetic current

$$V^{\rm em}_\mu = \sum_d^{u,d,s} Q_q \overline{q}\gamma_\mu q = V^3_\mu + \frac{1}{\sqrt{3}} V^8_\mu = J^{\rm em}_\mu, \tag{736}$$

where Q_q is the electric charge of the q quark. We get also

$$\begin{aligned} \overline{u}\gamma_\mu P_L u &= J^3_\mu + \frac{1}{\sqrt{3}} V^8_\mu + \frac{2}{\sqrt{6}} J^0_\mu, \\ \overline{d}\gamma_\mu P_L d &= -J^3_\mu + \frac{1}{\sqrt{3}} V^8_\mu + \frac{2}{\sqrt{6}} J^0_\mu, \\ \overline{s}\gamma_\mu P_L s &= -\frac{2}{\sqrt{3}} V^8_\mu + \frac{2}{\sqrt{6}} J^0_\mu, \end{aligned} \tag{737}$$

with $J^i_\mu = (V^i_\mu - A^i_\mu)/2$. The vector current contributes to an even number of pseudoscalar mesons or a vector resonance, while axial-vector current gives an odd number of pseudoscalar mesons.
In Z contribution both vector and axial-vector currents do contribute:

$$\begin{aligned} J^Z_\mu &= V^Z_\mu + A^Z_\mu, \\ V^Z_\mu &= \frac{g}{2c_W} \overline{q}\gamma_\mu \left[2 s^2_W Q_q - T^{(q)}_3\right] q, \\ A^Z_\mu &= \frac{g}{2c_W} \overline{q}\gamma_\mu\gamma_5 T^{(q)}_3 q, \end{aligned} \tag{738}$$

with Q_q (see eq. (564)) and $T_3^{(q)} = \text{diag}(1,-1,-1)/2$ the electric charge and and weak hypercharges, respectively.

H.1 $\tau \to \mu P$

The $\tau \to \mu P$ decay, in our model, is mediated only by axial-vector current (Z gauge boson), it means that $\mathcal{M}_\gamma$ does not contribute. The total amplitude for $\tau \to \mu P$ reads as

$$\mathcal{M}_{\tau\to\mu P} = \mathcal{M}_Z^P + \mathcal{M}_{\text{Box}}^P, \tag{739}$$

where $\mathcal{M}_Z^P$ is given by

$$\begin{aligned}
\mathcal{M}_Z^P &= -i\frac{g^2}{2c_W}\frac{F}{M_Z^2}C(P)\sum_j V_\ell^{j\mu *}V_\ell^{j\tau}\overline{\mu}(p')\left[\not{q}(F_L^Z P_L + F_R^Z P_R)\right]\tau(p), \\
\mathcal{M}_{\text{Box}}^P &= -ig^2 F\sum_j V_\ell^{j\mu *}V_\ell^{j\tau}B_j(P)\overline{\mu}(p')\left[\not{q}P_L\right]\tau(p),
\end{aligned} \tag{740}$$

where $Z_L = \frac{g}{c_W}(T_3^q - s_W^2 Q_q)$ and $Z_R = -\frac{g}{c_W}s_W^2 Q_q$. The hadronization of the quark bilinear in $\mathcal{M}_Z$ is determined by vector and axial-vector currents from eq. (738), which are written in terms of one P meson, it turns out to be [75]

$$\begin{aligned}
V_\mu^Z &= 0, \\
A_\mu^Z &= -\frac{g}{2c_W}F\{C(\pi^0)\partial_\mu\pi^0 + C(\eta)\partial_\mu\eta + C(\eta')\partial_\mu\eta'\},
\end{aligned} \tag{741}$$

where $F \simeq 0.0922$ GeV is the decay constant of the pion and the $C(P)$ functions are given by [75, 76]

$$\begin{aligned}
C(\pi^0) &= 1, \\
C(\eta) &= \frac{1}{\sqrt{6}}\left(\sin\theta_\eta + \sqrt{2}\cos\theta_\eta\right), \\
C(\eta') &= \frac{1}{\sqrt{6}}\left(\sqrt{2}\sin\theta_\eta - \cos\theta_\eta\right).
\end{aligned} \tag{742}$$

The box amplitude is composed by the following $B_j(P)$ factors [83]

$$\begin{aligned}
B_j(\pi^0) &= \frac{1}{2}(B_d^j - B_u^j), \\
B_j(\eta) &= \frac{1}{2\sqrt{3}}\left[(\sqrt{2}\sin\theta_\eta - \cos\theta_\eta)B_u^j + (2\sqrt{2}\sin\theta_\eta + \cos\theta_\eta)B_d^j\right], \\
B_j(\eta') &= \frac{1}{2\sqrt{3}}\left[(\sin\theta_\eta - 2\sqrt{2}\cos\theta_\eta)B_d^j - (\sin\theta_\eta + \sqrt{2}\cos\theta_\eta)B_u^j\right],
\end{aligned} \tag{743}$$

where the B_q^j functions are the form factors from box diagrams and the angle $\theta_\eta \simeq -18^\circ$.
The branching ratio reads

$$\mathrm{Br}(\tau \to \mu P) = \frac{1}{4\pi}\frac{\lambda^{1/2}(m_\tau^2, m_\mu^2, m_P^2)}{m_\tau^2 \Gamma_\tau}\frac{1}{2}\sum_{i,f}|\mathcal{M}_{\tau\to\mu P}|^2, \tag{744}$$

where $\Gamma_\tau \approx 2.267 \times 10^{-12}$ GeV and $\lambda(x,y,z) = (x+y-z)^2 - 4xy$, thus $\mathcal{M}_{\tau\to\mu P}$ is given by eq. (739). Thus,

$$\sum_{i,f}|\mathcal{M}_{\tau\to\mu P}|^2 = \frac{1}{2m_\tau}\sum_{k,l}\left[(m_\tau^2 + m_\mu^2 - m_P^2)(a_P^k a_P^{l*} + b_P^k b_P^{l*}) + 2m_\mu m_\tau (a_P^k a_P^{l*} - b_P^k b_P^{l*})\right], \tag{745}$$

with $k, l = Z, B$. Defining $\Delta_{\tau\mu} = m_\tau - m_\mu$ and $\Sigma_{\tau\mu} = m_\tau + m_\mu$ we get

$$\begin{aligned}
a_P^Z &= -\frac{g^2}{2c_W}\frac{F}{2}\frac{C(P)}{M_Z^2}\Delta_{\tau\mu}(F_L^Z + F_R^Z),\\
b_P^Z &= \frac{g^2}{2c_W}\frac{F}{2}\frac{C(P)}{M_Z^2}\Sigma_{\tau\mu}(F_R^Z - F_L^Z),\\
a_P^B &= -\frac{g^2 F}{2}\Delta_{\tau\mu}B_j(P),\\
b_P^B &= -\frac{g^2 F}{2}\Sigma_{\tau\mu}B_j(P).
\end{aligned} \tag{746}$$

H.2 $\tau \to \mu PP$

This channels are mediated by $\gamma-$, $Z-$penguins and box diagrams. Using the the electromagnetic current (eq. (736)), the electromagnetic form factor reads

$$\langle P_1(p_1)P_2(p_2)|V_\mu^{\mathrm{em}}|0\rangle = (p_1 - p_2)_\mu F_V^{P_1P_2}(Q^2), \tag{747}$$

where $Q = p_1 + p_2$ and $F_V^{P_1P_2}(Q^2)$ is steered by both $I = 1$ and $I = 0$ vector resonances. Then, the complete amplitude is given by

$$\mathcal{M}_{\tau\to\mu PP} = \mathcal{M}_\gamma^{P\overline{P}} + \mathcal{M}_Z^{P\overline{P}} + \mathcal{M}_{\mathrm{Box}}^{P\overline{P}}. \tag{748}$$

The next step is to hadronize the quark bilinears appearing in each amplitude. They turn out to be

$$\begin{aligned}
\mathcal{M}_{\gamma}^{P\overline{P}} =& \frac{e^2}{Q^2} F_V^{P_1P_2}(s)\times \\
& \sum_j V_\ell^{j\mu *} V_\ell^{j\tau} \overline{\mu}(p')[Q^2(\not{p}_q - \not{p}_{\overline{q}})F_L^\gamma(Q^2)P_L + 2im_\tau p_q^\mu \sigma_{\mu\nu} p_{\overline{q}}^\nu F_M^\gamma(Q^2)P_R]\tau(p), \\
\mathcal{M}_{Z}^{P\overline{P}} =& g^2 \frac{2s_W^2 - 1}{2c_W M_Z^2} F_V^{P_1P_2}(s) \sum_j V_\ell^{j\mu *} V_\ell^{j\tau} \overline{\mu}(p')(\not{p}_q - \not{p}_{\overline{q}})[\gamma^\mu (F_L^Z P_L + F_R^Z P_R)]\tau(p), \\
\mathcal{M}_{\text{Box}}^{P\overline{P}} =& \frac{g^2}{2} F_V^{P_1P_2}(s) \sum_j V_\ell^{j\mu *} V_\ell^{j\tau} (B_u^j - B_d^j)\overline{\mu}(p')(\not{p}_q - \not{p}_{\overline{q}})P_L\tau(p).
\end{aligned} \tag{749}$$

After computing each amplitude, we get the following branching ratio

$$\text{Br}(\tau \to \mu PP) = \frac{\kappa_{PP}}{64\pi^3 m_\tau^2 \Gamma_\tau} \int_{s_-}^{s_+} ds \int_{t_-}^{t_+} dt \frac{1}{2} \sum_{i,f} |\mathcal{M}_{\tau\to\mu PP}|^2, \tag{750}$$

where κ_{PP} is 1 for $PP = \pi^+\pi^-, K^+K^-, K^0\bar{K}^0$ and 1/2 for $PP = \pi^0\pi^0$. In terms of the momenta of the particles participating in the process, $s = (p_q + p_{\overline{q}})^2$ and $t = (p - p_{\overline{q}})^2$, so that

$$\begin{aligned}
t_-^+ &= \frac{1}{4s}\left[\left(m_\tau^2 - m_\mu^2\right)^2 - \left(\lambda^{1/2}(s, m_{P_1}^2, m_{P_2}^2) \mp \lambda^{1/2}(m_\tau^2, s, m_\mu^2)\right)^2\right], \\
s_- &= 4m_P^2, \\
s_+ &= (m_\tau - m_\mu)^2.
\end{aligned} \tag{751}$$

H.3 $\tau \to \mu V$

For these cases the branching ratio of $\tau \to \mu V$ is related with the $\tau \to \mu PP$ by trying to implement the experimental procedure as follows

$$\text{Br}(\tau \to \mu V) = \sum_{P_1,P_2} \text{Br}(\mu P_1 P_2)\Big|_V . \tag{752}$$

In the above equation the s limits are now restricted to

$$s_- = M_V^2 - \frac{1}{2}M_V\Gamma_V, \quad s_+ = M_V^2 + \frac{1}{2}M_V\Gamma_V. \tag{753}$$

Therefore, when $V = \rho, \phi$ their branching ratios are given by

$$\begin{aligned}
\text{Br}(\tau \to \mu\rho) &= \text{Br}(\tau \to \mu\pi^+\pi^-)\big|_\rho , \\
\text{Br}(\tau \to \mu\phi) &= \text{Br}(\tau \to \mu K^+K^-)\big|_\phi + \text{Br}(\tau \to \mu K^0\bar{K}^0)\big|_\phi .
\end{aligned} \tag{754}$$

I Appendix: Hadronic form factors

The vector form factors $F_V^{PP}(s)$, defined by eq. (747) , are based on two key points:

- At $s \ll M_R^2$ (being M_R a generic resonance mass), the vector form factor should match the $\mathcal{O}(p^4)$ result of χPT.
- Form factors of QCD currents should vanish for $s \gg M_R^2$.

We include energy-dependent widths for the wider resonances $\rho(770)$ and $\rho(1450)$ or constant for the narrow ones: $\omega(782)$ and $\phi(1020)$. For the $\rho(770)$ we take the definition put forward in [84]

$$\Gamma_\rho(s) = \frac{M_\rho s}{96\pi F^2}\left[\sigma_\pi^3(s)\theta(s-4m_\pi^2) + \frac{1}{2}\sigma_K^3(s)\theta(s-4m_K^2)\right], \tag{755}$$

where $\sigma_P(s) = \sqrt{1-4\frac{m_P^2}{s}}$, while $\rho(1450)$ is parameterized as follows

$$\Gamma_{\rho'}(s) = \Gamma_{\rho'}(M_{\rho'}^2)\frac{s}{M_{\rho'}^2}\left(\frac{\sigma_\pi^3(s)+\frac{1}{2}\sigma_K^3(s)\theta(s-4m_K^2)}{\sigma_\pi^3(M_{\rho'}^2)+\frac{1}{2}\sigma_K^3(M_{\rho'}^2)\theta(s-4m_K^2)}\right)\theta(s-4m_\pi^2), \tag{756}$$

with $\Gamma_{\rho'}(M_{\rho'}^2) = 400 \pm 60$ MeV [6]. We get the following expressions for the vector form factors

$$F_V^{\pi\pi}(s) = F(s)\exp\left[2Re\left(\tilde{H}_{\pi\pi}(s)\right) + Re\left(\tilde{H}_{KK}(s)\right)\right], \tag{757}$$

$$F(s) = \frac{M_\rho^2}{M_\rho^2 - s - iM_\rho\Gamma_\rho(s)}\left[1 + \left(\delta\frac{M_\omega^2}{M_\rho^2} - \gamma\frac{s}{M_\rho^2}\right)\frac{s}{M_\omega^2 - s - iM_\omega\Gamma_\omega}\right] - \frac{\gamma s}{M_{\rho'}^2 - s - iM_{\rho'}\Gamma_{\rho'}(s)}, \tag{758}$$

$$\begin{aligned} F_V^{K^+K^-}(s) =& \frac{1}{2}\frac{M_\rho^2}{M_\rho^2 - s - iM_\rho\Gamma_\rho(s)}\exp\left[2Re\left(\tilde{H}_{\pi\pi}(s)\right) + Re\left(\tilde{H}_{KK}(s)\right)\right] \\ &+ \frac{1}{2}\left[\sin^2\theta_V\frac{M_\omega^2}{M_\omega^2 - s - iM_\omega\Gamma_\omega} + \cos^2\theta_V\frac{M_\phi^2}{M_\phi^2 - s - iM_\phi\Gamma_\phi}\right]\exp\left[3Re\left(\tilde{H}_{KK}(s)\right)\right], \end{aligned} \tag{759}$$

$$\begin{aligned} F_V^{K^0\overline{K^0}}(s) =& -\frac{1}{2}\frac{M_\rho^2}{M_\rho^2 - s - iM_\rho\Gamma_\rho(s)}\exp\left[2Re\left(\tilde{H}_{\pi\pi}(s)\right) + Re\left(\tilde{H}_{KK}(s)\right)\right] \\ &+ \frac{1}{2}\left[\sin^2\theta_V\frac{M_\omega^2}{M_\omega^2 - s - iM_\omega\Gamma_\omega} + \cos^2\theta_V\frac{M_\phi^2}{M_\phi^2 - s - iM_\phi\Gamma_\phi}\right]\exp\left[3Re\left(\tilde{H}_{KK}(s)\right)\right], \end{aligned} \tag{760}$$

where we have defined the following terms

$$\begin{aligned}
\beta &= \frac{\Theta_{\rho\omega}}{3M_\rho^2}, \\
\gamma &= \frac{F_V G_V}{F^2}(1+\beta) - 1, \\
\delta &= \frac{F_V G_V}{F^2} - 1, \\
\tilde{H}_{PP}(s) &= \frac{s}{F^2} M_P(s), \\
M_P(s) &= \frac{1}{12}\left(1 - 4\frac{m_P^2}{s}\right) J_P(s) - \frac{k_P(M_\rho)}{6} + \frac{1}{288\pi^2}, \\
J_P(s) &= \frac{1}{16\pi^2}\left[\sigma_P(s) \ln\frac{\sigma_P(s)-1}{\sigma_P(s)+1} + 2\right], \\
k_P(\mu) &= \frac{1}{32\pi^2}\left(\ln\frac{m_P^2}{\mu^2} + 1\right).
\end{aligned} \tag{761}$$

The β parameter includes the contribution of the isospin breaking $\rho - \omega$ mixing through $\Theta_{\rho\omega} = -3.3 \times 10^{-3}$ GeV^2 [85]. The asymptotic constrain on the $N_C \to \infty$ vector form factor indicates $F_V G_V \simeq F^2$ [86]. We will use ideal mixing between the octet and single vector components, $\theta_V = 35^\circ$. We note that when isospin-breaking effects are turned off, the resummation of the real part of the chiral loop functions is not undertaken and the contribution from the ρ' is neglected, the well-known results from the vector-meson dominance hypothesis are recovered. More elaborated form factors are obtained using the results presented here as seeds for the input phaseshift in the dispersive formulation, see e.g. refs. [87, 88]. These refinements modify only slightly the numerical results obtained with the form factors quoted in this appendix.

References

[1] N. Arkani-Hamed, A. G. Cohen H. Georgi, Phys. Lett. B 513, 232 (2001) [arXiv:hepph/0105239].

[2] Palash B. Pal, An Introductory Course of Particle Physics, CRC Press, Taylor & Francis Group, 2015.

[3] Antonio Pich, CERN-2012-001, pp.1-50, arXiv:1201.0537v1 [hep-ph]

[4] Donald H. Perkins, Introduction to High Energy Physics, 4th Edition, Cambridge University Press, 2000.

[5] J. Lorenzo Diaz-Cruz, Rev.Mex.Fis. 65 (2019) no.5, 419-439, arXiv:1904.06878v2 [hep-ph]

[6] R.L. Workmanet al.(Particle Data Group), to be published (2022)

[7] Francis Halzen, Alan D. Martin, Quarks and Leptons: An Introductory Course In Modern Particle Physics, John Wyley and Sons.

[8] Ta-Pei Cheng and Ling-Fong Li, Gauge theory of elementary particle physics, Oxford Science Publications.

[9] Amitabha Lahiri, Palash B. Pal, A First Book of Quantum Field Theory, Narosa.

[10] Alexandra Gaviria, Robinson Longas, and Oscar Zapata,JHEP **10** (2018), 188, arXiv:1809.00655v2 [hep-ph]

[11] Andrea Lami, Ph. D. Thesis: Flavor violation of charged leptons in the Simplest Little Higgs model, Department of Physics of CINVESTAV, July 2016.

[12] Monika Blanke, Andrzej J. Buras, Anton Poschenrieder, Stefan Recksiegel, Cecilia Tarantino, Selma Uhlig and Andreas Weiler, Phys.Lett.B646:253-257,2007, [arXiv:hep-ph/0609284v1]

[13] S. T. Petcov, "The Processes $\mu \to e + \gamma, \mu \to e + \overline{e}, \nu' \to \nu + \gamma$ in the Weinberg-Salam Model with Neutrino Mixing," Sov. J. Nucl. Phys. **25** (1977), 340 [erratum: Sov. J. Nucl. Phys. **25** (1977), 698; erratum: Yad. Fiz. **25** (1977), 1336] JINR-E2-10176.

[14] G. Hernández-Tomé, G. López Castro and P. Roig, "Flavor violating leptonic decays of τ and μ leptons in the Standard Model with massive neutrinos," Eur. Phys. J. C **79** (2019) no.1, 84 [erratum: Eur. Phys. J. C **80** (2020) no.5, 438] doi:10.1140/epjc/s10052-019-6563-4 [arXiv:1807.06050 [hep-ph]].

[15] Kai-Peer O. Diener, Nucl.Phys. B697 (2004) 387-396, [arXiv:hep-ph/0403251v1]

[16] Calibbi L, Signorelli G. , Riv Nuovo Cim. (2018) 41:71.

[17] de Gouvêa A, Vogel P., arXiv:1303.4097

[18] Marciano WJ, Mori T, Roney JM., Annu Rev Nucl Part Sci. (2008) 58:315–41.

[19] R.H. Bernstein, arXiv:1901.11099v1

[20] Jasper Lukkezen, Ph. D. Thesis: Little Higgs Phenomenology, Leiden University, September 18, 2008.

[21] Tao Han, Heather E. Logan, Bob McElrath, and Lian-Tao Wang, Phys.Rev. D67 (2003) 095004, [arXiv:hep-ph/0301040v4]

[22] Jay Hubisz, Patrick Meade, Andrew Noble, Maxim Perelstein, JHEP 0601 (2006) 135 [arXiv:hep-ph/0506042v3]

[23] Jay Hubisz, Patrick Meade, Phenomenology of the Littlest Higgs with T-Parity, Phys.Rev. D71 (2005) 035016, DOI: 10.1103/PhysRevD.71.035016, [arXiv:hep-ph/0411264v3].

[24] Monika Blanke, Andrzej J. Buras, Anton Poschenrieder, Stefan Recksiegel, Cecilia Tarantino, Selma Uhlig and Andreas Weiler, Rare and CP-Violating K and B Decays in the Littlest Higgs Model with T-Parity, JHEP 0701:066,2007, DOI: 10.1088/1126-6708/2007/01/066, [arXiv:hep-ph/0610298v3].

[25] F. del Águila, J. I. Illana, M. D. Jenkins, Precise limits from lepton flavour violation processes on the Littlest Higgs model with T-parity, arXiv:0811.2891v3 [hep-ph].

[26] Hsin-Chia Cheng and Ian Low, JHEP 0408:061, 2004, [arXiv:hep-ph/0405243v3]

[27] Ian Low, T Parity and the Littlest Higgs, JHEP 0410 (2004) 067, DOI: 10.1088/1126-6708/2004/10/067, [arXiv:hep-ph/0409025v2].

[28] Jay Hubisz, Seung J. Lee, Gil Paz, The flavor of a little Higgs with T-parity, JHEP0606:041,2006, DOI: 10.1088/1126-6708/2006/06/041, [arXiv:hep-ph/0512169v1].

[29] Francisco del Aguila, Lluis Ametller, Jose Ignacio Illana, Jose Santiago, Pere Talavera, and Roberto Vega-Morales, Lepton Flavor Changing Higgs decays in the Littlest Higgs Model with T-parity, arXiv:1705.08827v3 [hep-ph].

[30] B. W. Lee and R. E. Shrock, "Natural Suppression of Symmetry Violation in Gauge Theories: Muon - Lepton and Electron Lepton Number Nonconservation," Phys. Rev. D **16** (1977), 1444 doi:10.1103/PhysRevD.16.1444.

[31] T. P. Cheng and L. F. Li, "GAUGE THEORY OF ELEMENTARY PARTICLE PHYSICS," Oxford, Uk: Clarendon (1984) 536 P. (Oxford Science Publications).

[32] P. Blackstone, M. Fael and E. Passemar, "$\tau \to \mu\mu\mu$ at a rate of one out of 10^{14} tau decays?," Eur. Phys. J. C **80** (2020) no.6, 506 doi:10.1140/epjc/s10052-020-8059-7 [arXiv:1912.09862 [hep-ph]].

[33] I. Pacheco and P. Roig, "Lepton flavor violation in the Littlest Higgs Model with T parity realizing an inverse seesaw," JHEP **02** (2022), 054, doi:10.1007/JHEP02(2022)054, [arXiv:2110.03711 [hep-ph]].

[34] Wolfram Research, Inc., Mathematica, Version 10.0, Champaign, IL (2014).

[35] B. Ruijl, T. Ueda and J. Vermaseren, "FORM version 4.2," [arXiv:1707.06453 [hep-ph]].

[36] FeynCalc version 9.2.0, V. Shtabovenko, R. Mertig and F. Orellana, "New Developments in FeynCalc 9.0", Comput. Phys. Commun., 207, 432-444, 2016, arXiv:1601.01167. R. Mertig, M. Böhm, and A. Denner, "Feyn Calc - Computer-algebraic calculation of Feynman amplitudes", Comput. Phys. Commun., 64, 345-359, 1991.

[37] Francisco del Aguila, Lluis Ametller, José Ignacio Illana, José Santiago, Pere Talavera, and Roberto Vega-Morales, The Full Lepton Flavor of the Littlest Higgs Model with T–parity, doi 10.1007/JHEP07(2019)154, arXiv:1901.07058.

[38] Hiren H. Patel, Comput. Phys. Commun. 197, 276 (2015), ePrint: arXiv:1503.01469.

[39] Francisco del Aguila, José Ignacio Illana, José María Pérez-Poyatos, and José Santiago, Inverse see–saw neutrino masses in the Littlest Higgs model with T–parity, arXiv:1910.09569v2 [hep-ph].

[40] I. Pacheco and P. Roig Garces, "New limits from lepton flavour violating processes on the Littlest Higgs model with T-parity," Rev. Mex. Fis. Suppl. **3** (2022) no.2, 1-10, doi:10.31349/SuplRevMexFis.3.020704.

[41] Hans Hettmansperger, Manfred Lindner, Werner Rodejohann, Phenomenological Consequences of sub-leading Terms in See-Saw Formulas, arXiv:1102.3432v2 [hep-ph].

[42] W. Grimus, L. Lavoura, The seesaw mechanism at arbitrary order: disentangling the small scale from the large scale, arXiv:hep-ph/0008179v2.

[43] Takaaki Nomura, Hiroshi Okada, Inverse seesaw model with large $SU(2)_L$ multiplets and natural mass hierarchy, Physics Letters B Volume 792, 10 May 2019, Pages 424-429.

[44] A. Ilakovac, A. Pilaftsis, Flavour-Violating Charged Lepton Decays in Seesaw-Type Models, Nucl.Phys. B437 (1995) 491, DOI: 10.1016/0550-3213(94)00567-X, [arXiv:hep-ph/9403398v3].

[45] Luis Fernando Alcerro Alcerro, Exploratory analysis of the lepton number violating process tt $\to$ bbll, Master Thesis, Cinvestav, 2019.

[46] A. Denner, H. Eck, O. Hahn and J. Kublbeck, Nucl. Phys. B 387, 467 (1992).

[47] J. Gluza, Marek Zralek, Feynman rules for Majorana-neutrino interactions, Physical review D: Particles and fields 45(5):1693-1700, DOI 10.1103/PhysRevD.45.1693.

[48] G. Hernández-Tomé, J. I. Illana, G. López Castro, M. Masip, P. Roig, Effects of heavy Majorana neutrinos on lepton flavor violating processes, Phys. Rev. D 101, 075020 (2020), DOI 10.1103/PhysRevD.101.075020, [arXiv:1912.13327v3 [hep-ph]].

[49] G. Hernández-Tomé, J. I. Illana and M. Masip, "The ρ parameter and $H^0 \to \ell_i \ell_j$ in models with TeV sterile neutrinos," Phys. Rev. D **102** (2020) no.11, 113006 doi:10.1103/PhysRevD.102.113006, [arXiv:2005.11234 [hep-ph]].

[50] B. Yang, J. Han and N. Liu, "Lepton flavor violating Higgs boson decay $h \to \mu\tau$ in the littlest Higgs model with T parity," Phys. Rev. D **95** (2017) no.3, 035010, doi:10.1103/PhysRevD.95.035010, [arXiv:1605.09248 [hep-ph]].

[51] F. del Aguila, L. Ametller, J. I. Illana, J. Santiago, P. Talavera and R. Vega-Morales, "Lepton Flavor Changing Higgs decays in the Littlest Higgs Model with T-parity," JHEP **08** (2017), 028, [erratum: JHEP **02** (2019), 047] doi:10.1007/JHEP08(2017)028, [arXiv:1705.08827 [hep-ph]].

[52] A. Lami and P. Roig, "$H \to \ell\ell'$ in the simplest little Higgs model," Phys. Rev. D **94** (2016) no.5, 056001 doi:10.1103/PhysRevD.94.056001, [arXiv:1603.09663 [hep-ph]].

[53] Claudio Giganti, Stéphane Lavignac, Marco Zito, Neutrino oscillations: the rise of the PMNS paradigm, arXiv:1710.00715v2 [hep-ex].

[54] V. De Romeri, M.J. Herrero, X. Marcano, F. Scarcella, Lepton flavor violating Z decays: A promising window to low scale seesaw neutrinos, Phys. Rev. D 95, 075028 (2017), DOI: 10.1103/PhysRevD.95.075028, [arXiv:1607.05257v4 [hep-ph]].

[55] R. Kitano, M. Koike and Y. Okada, Phys. Rev. D 66, 096002 (2002) Erratum: [Phys. Rev. D 76, 059902 (2007)] [hep-ph/0203110].

[56] T. Suzuki, D. F. Measday and J. P. Roalsvig, Phys. Rev. C 35, 2212 (1987).

[57] Enrique Fernández-Martínez, Josu Hernández-García, Jacobo López-Pavón, Global constraints on heavy neutrino mixing, JHEP 1608 (2016) 033, [arXiv:1605.08774v2 [hep-ph]].

[58] R. N. Mohapatra et al, Rep. Prog. Phys. 70, 1757 (2007).

[59] S. M. Bilenky, Neutrinoless double beta decay, Phys. Part. Nucl. 41, 690 (2010).

[60] Evgeny Akhmedov, Majorana neutrinos and other Majorana particles: Theory and experiment, [arXiv:1412.3320v1 [hep-ph]].

[61] Yong-Hamb Kim, Neutrinoless double beta decay experiment, [arXiv:2004.02510v1 [hep-ex]].

[62] Anupama Atre, Tao Han, Silvia Pascoli, Bin Zhang, The Search for Heavy Majorana Neutrinos, JHEP 0905:030,2009, [arXiv:0901.3589v2 [hep-ph]].

[63] G. Bélanger, F. Boudjema, D. London, H. Nadeau, Inverse Neutrinoless Double Beta Decay Revisited, Phys.Rev. D53 (1996) 6292-6301, [arXiv:hep-ph/9508317v1].

[64] Werner Rodejohann, Inverse Neutrino-less Double Beta Decay Revisited: Neutrinos, Higgs Triplets and a Muon Collider, Phys.Rev.D81:114001,2010, [arXiv:1005.2854v1 [hep-ph]].

[65] KamLAND-Zen Collaboration, *et. al.*, First Search for the Majorana Nature of Neutrinos in the Inverted Mass Ordering Region with KamLAND-Zen, arXiv:2203.02139v1 [hep-ex].

[66] Benjamin Fuks, Jonas Neundorf, Krisztian Peters, Richard Ruiz, Matthias Saimpert, Majorana Neutrinos in Same-Sign $W^{\pm}W^{\pm}$ Scattering at the LHC: Breaking the TeV Barrier, Phys. Rev. D 103, 055005 (2021), [arXiv:2011.02547v2 [hep-ph]].

[67] Gabriel López Castro, Néstor Quintero, Lepton number violation in tau lepton decays, [arXiv:1212.0037v2 [hep-ph]]

[68] Y. Miyazaki *et al.* [Belle Collab.], Search for lepton-flavor and lepton-number-violating $\tau \to \ell hh'$ decay modes, Phys. Lett. B682, (2010).

[69] A. Ilakovac, Phys. Rev. D54, 5653 (1996), Probing Lepton-number/flavour-violation in Semileptonic Tau Decays into Two Mesons , [arXiv:hep-ph/9608218].

[70] Vladimir Gribanov, Sergey Kovalenko, Ivan Schmidt, Sterile neutrinos in tau lepton decays, Nucl.Phys. B607 (2001) 355-368, DOI 10.1016/S0550-3213(01)00169-9, [arXiv:hep-ph/0102155v1].

[71] Anupama Atre, Vernon Barger, Tao Han, Upper Bounds on Lepton-number Violating Processes, Phys.Rev.D71:113014,2005, DOI 10.1103/PhysRevD.71.113014, [arXiv:hep-ph/0502163v2].

[72] Frank T. Avignone III, Steven R. Elliott, Jonathan Engel, Double Beta Decay, Majorana Neutrinos, and Neutrino Mass, Rev.Mod.Phys.80:481-516,2008, DOI 10.1103/RevModPhys.80.481, [arXiv:0708.1033v2 [nucl-ex]].

[73] D. Delepine, G. López Castro and N. Quintero, Effects of heavy Majorana neutrinos in semileptonic heavy quark decays, J.Phys.Conf.Ser. 378 (2012) 012024, DOI 10.1088/1742-6596/378/1/012024.

[74] I. Pacheco and P. Roig Garces, "Lepton Flavour Violation in Hadron Decays of the Tau Lepton within the Littlest Higgs Model with T-parity," [arXiv:2207.04085 [hep-ph]].

[75] Ernesto Arganda, María J. Herrero and Jorge Portolés, Lepton flavour violating semileptonic decays in constrained MSSM-seesaw scenarios, JHEP06(2008)079, doi: 10.1088/1126-6708/2008/06/079 , [arXiv:0803.2039v3 [hep-ph]].

[76] Tomas Husek, Kevin Monsálvez-Pozo, Jorge Portolés, Lepton-flavour violation in hadronic tau decays and $\mu - \tau$ conversion in nuclei, J. High Energ. Phys. 2021, 59 (2021). doi: 10.1007/JHEP01(2021)059, [arXiv:2009.10428v1 [hep-ph]].

[77] R. Escribano, S. Gonzalez-Solís and P. Roig, "Predictions on the second-class current decays $\tau^- \to \pi^- \eta^{(\prime)} \nu_\tau$," Phys. Rev. D **94** (2016) no.3, 034008 doi:10.1103/PhysRevD.94.034008, [arXiv:1601.03989 [hep-ph]].

[78] R. Kaiser and H. Leutwyler, "Large N(c) in chiral perturbation theory," Eur. Phys. J. C **17** (2000), 623-649, , [arXiv:hep-ph/0007101 [hep-ph]].

[79] P. Roig, A. Guevara and G. López Castro, "$VV'P$ form factors in resonance chiral theory and the $\pi - \eta - \eta'$ light-by-light contribution to the muon $g-2$," Phys. Rev. D **89** (2014) no.7, 073016, , [arXiv:1401.4099 [hep-ph]].

[80] A. Guevara, P. Roig and J. J. Sanz-Cillero, "Pseudoscalar pole light-by-light contributions to the muon $(g-2)$ in Resonance Chiral Theory," JHEP **06** (2018), 160, , [arXiv:1803.08099 [hep-ph]].

[81] M. A. Arroyo- Ureña, R. Gaitán and T. A. Valencia-Pérez, "`SpaceMath` version 1.0. A `Mathematica` package for beyond the standard model parameter space searches," [arXiv:2008. 00564 [hep-ph]].

[82] Miguel Crispim Romao, The SU(5) Grand Unification Theory Revisited, October 2011.

[83] A. Lami, J. Portolés, P. Roig, Lepton Flavour Violation in Hadron Decays of the Tau Lepton in the Simplest Little Higgs Model, Phys. Rev. D 93, 076008 (2016), doi: 10.1103/PhysRevD.93.076008, [arXiv:1601.07391v1 [hep-ph]].

[84] D. Gómez Dumm, A. Pich and J. Portolés, The hadronic off-shell width of meson resonances, Phys. Rev. D **62** (2000) 054014, doi: 10.1103/PhysRevD.62.054014, [arXiv:hepph/0003320].

[85] A. Pich and J. Portolés, Nucl. Phys. Proc. Suppl. **121** (2003) 179 [arXiv:hep-ph/0209224].

[86] G. Ecker, J. Gasser, H. Leutwyler, A. Pich and E. de Rafael, Phys. Lett. B **223** (1989) 425; F. Guerrero and A. Pich, Effective Field Theory Description of the Pion Form Factor, Phys. Lett. B **412** (1997) 382, doi: 10.1016/S0370-2693(97)01070-8, [arXiv:hep-ph/9707347].

[87] D. Gómez Dumm and P. Roig, "Dispersive representation of the pion vector form factor in $\tau \to \pi\pi\nu_\tau$ decays," Eur. Phys. J. C **73** (2013) no.8, 2528, doi:10.1140/epjc/s10052-013-2528-1 [arXiv:1301.6973 [hep-ph]].

[88] S. Gonzàlez-Solís and P. Roig, "A dispersive analysis of the pion vector form factor and $\tau^- \to K^- K_S \nu_\tau$ decay," Eur. Phys. J. C **79** (2019) no.5, 436, doi:10.1140/epjc/s10052-019-6943-9, [arXiv:1902.02273 [hep-ph]].

[89] F. del Aguila, J. I. Illana and M. D. Jenkins, "Muon to electron conversion in the Littlest Higgs model with T-parity," JHEP **09** (2010), 040, doi:10.1007/JHEP09(2010)040, [arXiv:1006.5914 [hep-ph]].

[90] E. Ramirez and P. Roig, "Lepton flavor violation within the Simplest Little Higgs model," [arXiv:2205.10420 [hep-ph]].